PNNL-37448 Rev 0
PHC-RPT-002 Rev 0

Physical and Hydraulic Properties of RCRA Borehole Samples from the Hanford Site

Final Report, Fiscal Years 2023-2024

March 2025

Mark Rockhold
Thomas Wietsma
Jonah Bartrand
Shelby Phillips
Tamas Varga
Amanda Lawter
Nancy Escobedo
Xiaoliang He
Judy Robinson

U.S. DEPARTMENT OF ENERGY

Prepared for the U.S. Department of Energy
under Contract DE-AC05-76RL01830

PACIFIC NORTHWEST NATIONAL LABORATORY
operated by
BATTELLE
for the
UNITED STATES DEPARTMENT OF ENERGY
under Contract DE-AC05-76RL01830

Printed in the United States of America

Available to DOE and DOE contractors from
the Office of Scientific and Technical Information,
P.O. Box 62, Oak Ridge, TN 37831-0062
www.osti.gov
ph: (865) 576-8401
fox: (865) 576-5728
email: reports@osti.gov

Available to the public from the National Technical Information Service
5301 Shawnee Rd., Alexandria, VA 22312
ph: (800) 553-NTIS (6847)
or (703) 605-6000
email: info@ntis.gov
Online ordering: http://www.ntis.gov

PNNL-37448 Rev 0
PHC-RPT-002 Rev 0

Physical and Hydraulic Properties of RCRA Borehole Samples from the Hanford Site

Final Report, Fiscal Years 2023-2024

March 2025

Mark Rockhold
Thomas Wietsma
Jonah Bartrand
Shelby Phillips
Tamas Varga
Amanda Lawter
Nancy Escobedo
Xiaoliang He
Judy Robinson

Prepared for
the U.S. Department of Energy
under Contract DE-AC05-76RL01830

Pacific Northwest National Laboratory
Richland, Washington 99354

Summary

Sediment from 44 core samples collected from Resource Conservation and Recovery Act (RCRA) boreholes drilled in the 200 East and 200 West areas of the Hanford Site were characterized for physical and hydraulic properties (Table S.1). Characterization data included gravimetric water contents and matric potentials, grain-size distributions, saturated hydraulic conductivity, water retention characteristics, and unsaturated hydraulic conductivity. These properties provide site-specific data and parameters that can be used in subsurface flow and contaminant transport models to assess the transport and fate of contaminants in the vadose zone and underlying aquifer systems.

The analyzed core samples come from specific areas and depth intervals at the Hanford Site that were targeted for sampling to address data gaps identified by site contractors (Khaleel 2020). X-ray computed tomography (XCT) was used to evaluate the general textural characteristics of the samples and to determine which samples to use for further physical and hydraulic property characterization. Subsequent sample selection was determined by consensus after review of the XCT images by Pacific Northwest National Laboratory, Central Plateau Cleanup Company, and INTERA staff.

XCT imaging was performed on 43 intact core samples and particle size analyses were conducted on the 44 intact samples and 3 composite core samples. The as-received matric potential, gravimetric moisture content, and dry bulk density were measured for 29, 38, and 37 core samples, respectively. Multistep outflow experiments were performed on 19 intact and 3 composite core samples. A summary of the analyses performed on each sample is provided within the report and Appendix F.

Table S.1. Summary of cores analyzed from RCRA monitoring wells.

Well Name / ID	Year Drilled	Depth Range of Core Samples Analyzed (top-bottom ft bgs)	Number of Core Samples Analyzed	Hanford Units Analyzed[(a)]	RCRA Dangerous Waste Management Unit (DWMU) [(b)]
200 EAST AREA					
699-43-44B (D0049)	2021	180.3-182.8	1	CCUg	216-B-3 Pond
299-E25-241 (D0056)	2021	40.5-252.4	4	Hf1, Hf3, CCU	216-A-29 Ditch
299-E25-242 (D0057)	2021	150-152.2	1	Hf3	216-A-29 Ditch
299-E26-82 (D0058)	2021	188.4-209.3	2	CCU	216-A-29 Ditch
299-E33-272 (D0059)	2021	29.8-272.5	7	Hf1, Hf3, CCU, CCUg	Single-Shell Tank Waste Management Area (WMA) B-BX-BY
299-E28-35 (D0060)	2021	219.7-232.6	2	CCU	Low-Level Burial Grounds WMA-1
299-E33-276 (D0061)	2021	30-264.2	8	Hf1, CCU, CCUg, HF3/CCU	Low-Level Burial Grounds WMA-1
200 WEST AREA					
299-W10-201 (D0013)	2023	51.5-224.1	7	Hf1, Hf2, CCU/CCUc, CCUc, Rwie	Low-Level Burial Grounds WMA-3
299-W10-202 (D0014)	2023	56.4-136.5	6	Hf1, Hf2, CCU, CCUc, Rwie	Low-Level Burial Grounds WMA-3
299-W10-203 (D0015)	2023	69.9-191.3	6	Hf2, CCUc, Rwie	Low-Level Burial Grounds WMA-3

(a) Details of Hanford hydrostratigraphic units and abbreviations are provided in Section 1.0 - Introduction.
(b) The DWMU was identified with the Hanford Site RCRA Groundwater Monitoring Report for 2023 (DOE/RL-2023-53, Rev. 0)

Acknowledgments

We thank Sean Sexton (formerly CPCCo), Randal Fox (CPCCo), Joy Ferry (CPCCo), and Katlin Hanson (CPCCo) for project oversight, Sabrina Hoyle (PNNL) and Michelle Snyder (PNNL) for technical reviews, and Matt Wilburn (PNNL) for technical editing. Fred Zhang, Raz Khaleel, and Sunil Mehta (all INTERA) are acknowledged for providing additional technical reviews of this report.

Acronyms and Abbreviations

bgs	below ground surface
CCU	Cold Creek Unit undifferentiated
CCUg	Cold Creek unit - gravel
CCUz	Cold Creek unit - silt
CPCCo	Central Plateau Cleanup Company
DBD	dry bulk density
EMSL	Environmental Molecular Sciences Laboratory
FIO	For Information Only
GMC	gravimetric moisture content
Hf1	Hanford formation - unit 1
Hf2	Hanford formation - unit 2
Hf3	Hanford formation - unit 3
ID	identification
K	hydraulic property measurements
Ksat	saturated hydraulic conductivity
MP	matric potential
MS	multistep
O	outflow
P	pressure
PNNL	Pacific Northwest National Laboratory
PSA	particle size analysis
PSD	particle size distribution
RCRA	Resource Conservation and Recovery Act
Rlm	Ringold Formation lower mud unit
Rtf	Ringold Formation member of Taylor Flat
Rwia	Ringold Formation member of Wooded Island - unit A
Rwie	Ringold Formation member of Wooded Island - unit E
STOMP	Subsurface Transport Over Multiple Phases
STOMP-WA	water-air mode of the Subsurface Transport Over Multiple Phases simulator
Kunsat	unsaturated hydraulic conductivity
XCT	X-ray computed tomography

Contents

Figures

Tables

1.0 Introduction

The Hanford Site is a former plutonium production site located in southeastern Washington State. The Central Plateau is a 75 square mile (~194 km^2) area located in the middle of the Hanford Site that includes the 200 East and West areas where most of the former nuclear material production activities were concentrated. Residual sources of contamination from these activities exist in the vadose zone and continue to impact groundwater. Site remediation and waste cleanup efforts on the Central Plateau are ongoing.

The sediments at the Hanford Site are highly variable. They have been categorized into four main hydro stratigraphic units which are used in the Hanford geologic framework model. The units that make up the vadose zone and unconfined aquifer system in the 200 Areas are shown in Figure 1. From youngest to oldest, these include the Hanford formation sediments (Hf1, Hf2 and Hf3), which are associated with cataclysmic floods during the Pleistocene from ancestral Lake Missoula. The Hf1 and Hf3 units tend to be coarser and more permeable than the Hf2 unit. The Cold Creek Formation is subdivided into the undifferentiated CCU unit, the calcic CCUc unit, and a gravel-dominated CCUg unit, which are of fluvial origin. The Ringold Formation is divided into the Taylor Flat member - Rtf, Unit E - Rwie, the lower mud - Rlm, and Unit A – Rwia. The Ringold Formation includes alluvial and aeolian deposits and paleosols.

In fiscal years 2023 and 2024, sediment from 25 individual core samples collected from Resource Conservation and Recovery Act (RCRA) boreholes drilled in the 200 East Area and 19 core samples collected from boreholes drilled in the 200 West Area were characterized for physical and hydraulic properties. Sample selection was based on the need for vadose zone hydraulic property data defined by site contractors (Khaleel 2020) and sample quality, which was evaluated by both visual inspection and X-ray computed tomography (XCT) of intact (as collected) core samples. All samples used in this study were collected from the vadose zone, above the regional water table. In the 200 West Area the water table is generally located at an elevation that is within the Rwie unit. In the 200 East Area, the water table is located at the bottom of the Hf3 unit or top of the CCU unit (see Figure 1). In the 200 East Area, nine individual cores were combined into three composite samples consisting of three individual cores each. Physical properties included dry bulk density and porosity. Hydraulic properties included saturated hydraulic conductivity and water retention characteristics. Physical and hydraulic properties are needed to support subsurface flow and transport modeling efforts used for risk assessment and remedial decision-making.

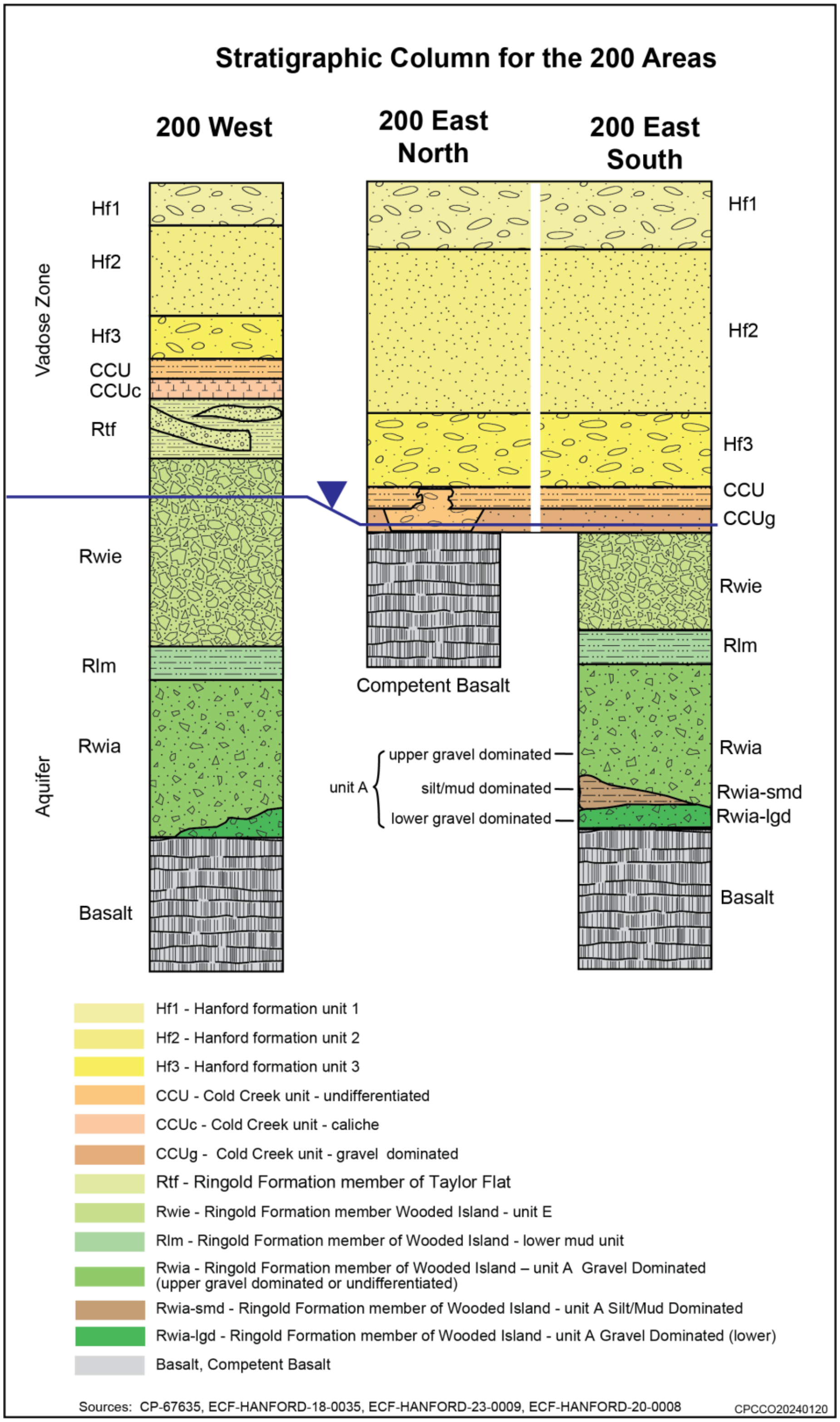

Figure 1. Generalized Hanford Site stratigraphy and differences between 200 West and 200 East Areas (sources noted in figure).

This report is organized as follows. Section 1.0 (this section) summarizes project objectives and provides an overview of the site and geologic formations from which samples were collected. Section 2.0 describes the methods used for the analyses. Section 3.0 shows the locations of boreholes where cores samples were collected that were analyzed as part of this study and provides details about each core and the physical and hydraulic property measurements that were collected. Section 4.0 presents results and discussion. Summary and conclusions are presented in Section 5.0, followed by a section on quality assurance, and references.

The appendices provide the following information:

- Appendix A: X-ray computed (XCT) tomography images of intact core samples.
- Appendix B and Appendix C: Physical property characterization information, including sieve data and particle size distribution plots.
- Appendix D: Hydraulic property characterization information, including fitted water retention curves, model parameters, and plots of quasi-static water retention data from the multi-step outflow experiments.
- Appendix E: Hydraulic property characterization results from inverse modeling of dynamic multi-step outflow experiments.
- Appendix F: Summary table of characterization data collected for each core sample.

The data produced for this report are available electronically on request.

2.0 Methods

This section summarizes the methods that were used to generate physical and hydraulic properties and parameters that are presented in this report.

2.1 X-Ray Computed Tomography

Intact cores from different hydrostratigraphic units of interest were selected and imaged using an X-ray computed tomography (XCT) system. The imaging results helped guide selection of specific core samples that were used for physical and hydraulic property characterization in the laboratory. The XCT system is housed in the Environmental Molecular Sciences Laboratory (EMSL) on the Pacific Northwest National Laboratory (PNNL) campus in Richland, WA.

Whole core imaging was performed for screening purposes to determine when cores contained excessive amounts of gravel and cobbles that could make hydraulic measurements more difficult, as opposed to performing higher-resolution scans over smaller regions to quantify porosity and pore topology (Wildenschild and Sheppard 2013). The nominal resolution of the XCT system is ~1/1000 of the field of view, which is nominally the largest sample dimension. The intact cores were ~150 mm long and ~9.53 cm in diameter, so the resolution of the whole core XCT images was ~0.15 mm. This resolution was deemed sufficient for imaging of individual gravel and larger-sized particles, as well as defects and voids, within the intact core samples. Appendix A presents selected XCT image slices for core samples that were characterized.

2.2 Matric Potential and Gravimetric Moisture Content

Acquired data included matric potential and gravimetric water content for subsamples of the intact (as-received) sediments. Matric potential is a measure of the capillary and adsorptive forces that attract and bind water to sediment particles and can be used to determine gradients and/or flow directions. Gravimetric water content can aid in identifying regions of finer texture and/or areas with different recharge or discharge rates.

Two different methods were used for determining as-received matric potential and moisture content. The initial method for determining matric potential (applied only to a subset of the 200 East Area cores) used moisture adsorption onto dried filter papers, coupled with a calibration curve derived from reference solutions of KCl with known water activities, to estimate the matric potential of the bulk core. The procedure was as follows: (1) remove one end cap from the Lexan liner and loosen top layer of soil so that a dry filter paper can be placed within the soil volume; (2) place a dry piece of filter paper between two other pieces of dry filter paper to prevent soil from adhering to the inner piece and bury the entire assembly in the core end; (3) reseal the core and allow the entire system to equilibrate (allow 7 days); (4) determine the mass of moisture absorbed by the inner filter paper piece as a relative fraction of the dry mass of the paper; (5) compare this number to the calibration curve to estimate the soil matric potential. See ASTM D5298-16, *Standard Test Method for Measurement of Soil Potential (Suction) Using Filter Paper*, for a more detailed procedure and how the calibration curve is derived.

The second procedure (applied to most 200 East Area cores and all composite and 200 West Area cores) to determine the as-received state of the samples consisted of the following steps: (1) for each core, the end caps on the Lexan liners were removed and a small (6-7 g) subsample was collected from each end, followed by putting the end caps back on the Lexan liner; (2) each collected sample was placed in the sample cup of the WP4C instrument (Meter Group, Pullman, WA) for measurement of water activity; (3) after the instrument had stabilized and a measurement was recorded, the sediment samples were subsequently weighed, oven dried at 110 °C for 48 hours, and then reweighed to determine gravimetric water contents. The WP4C instrument determines the dew point, or relative humidity of the air above a sample, in a sealed chamber using a chilled mirror method. Measured water activities are used to calculate matric potentials, which are paired with the water contents determined from the difference between the initial and the air- or oven-dried sample weights.

Subsamples were also collected from multiple (4-7) locations/elevations within each core sample at the end of each multistep (MS) outflow experiment (Section 2.4.1) to obtain additional matric potential and gravimetric water content data pairs for drier conditions. Samples collected closer to the bottom of each core are expected to be wetter than those collected closer to the top due to their proximity to the water-saturated porous plate at the bottom of the core. Measurements were made with the WP4C instrument on samples collected immediately after the MS outflow experiments were stopped, as well as on samples that were allowed to air-dry for several hours. Volumetric water contents were determined by multiplying the gravimetric water contents by the dry bulk densities of the core samples. The volumetric water content and matric potential data pairs obtained using the WP4C instrument were combined with data from the MS experiments for estimating water retention parameters.

2.3 Hydraulic Properties

Hydraulic property characterization provides parameters for vadose zone flow modeling and was performed on core samples in the laboratory under both water-saturated and unsaturated conditions. Owing to the potentially contaminated nature of some of the sediment cores, hydraulic property characterization was performed in a laboratory in the PNNL 331 Building, which is equipped and authorized for work with radioactive materials. The standard size of the Lexan liners in which the intact cores were received is 6 in. tall and either 3.75 or 4 in. nominal diameter. The photo (Figure 2) shows the 4-in. nominal diameter Lexan liner (right) with end caps. Intact cores that were out-of-round required custom collars to be fitted for the sample holder. Several samples were identified for which measurements of physical and hydraulic properties on intact cores were desired, but the samples were too coarse and/or the Lexan liners were not completely full. Therefore, selected cores were composited and repacked in a larger (8-in.-diameter) sample holder, shown on the left in Figure 2. The larger sample holder and the end caps for the MS outflow experiments were custom fabricated in PNNL's EMSL machine shop.

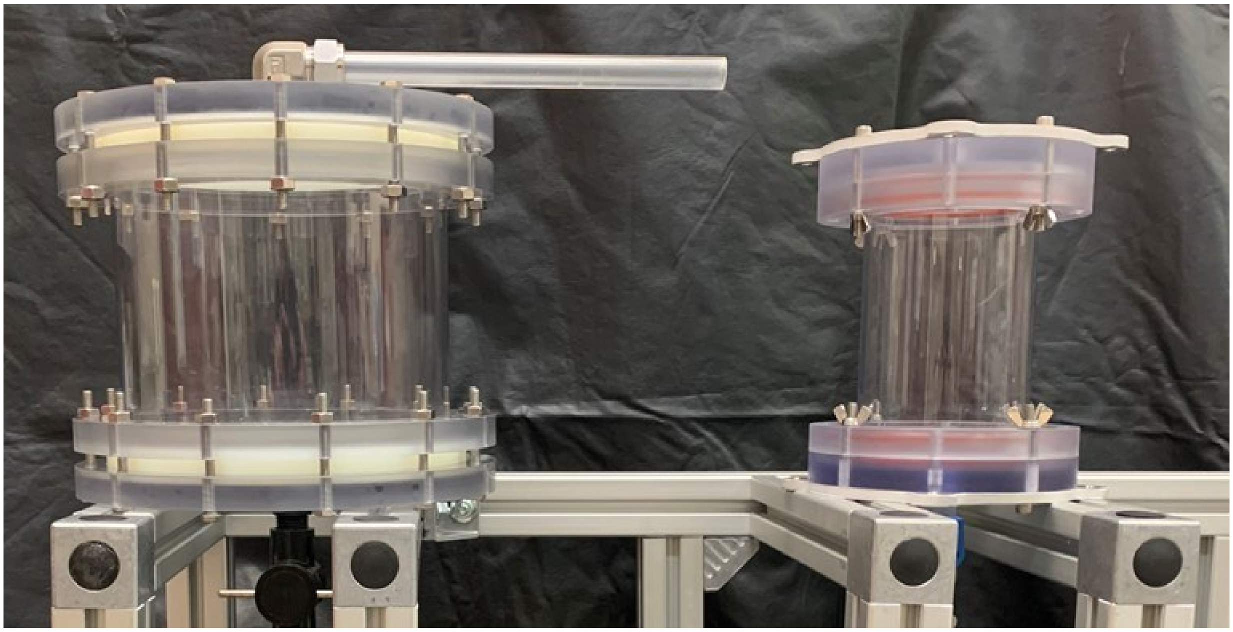

Figure 2. Sample holders for larger (8-in-diam) core used for composite, repacked sediments (left) and standard size (4-in-diam) core (right)

2.3.1 Saturated Hydraulic Conductivity

The Ksat, of a porous medium can be determined in the laboratory using constant head, falling head, and constant flux (a.k.a. steady flow) methods. Wietsma at al. (2009) developed an experimental apparatus for automated measurement of Ksat using any or all these methods (Figure 3). According to Reynolds and Elrick (2002), the range of Ksat that can be determined using the constant head method is about 10^0 to 10^{-5} cm s^{-1} and the range of Ksat that can be determined using the falling head method is about 10^{-4} to 10^{-7} cm s^{-1}. Use of modern pressure transducers and data acquisition software allows these ranges to be expanded. In theory, the constant flux method is applicable for any value of Ksat.

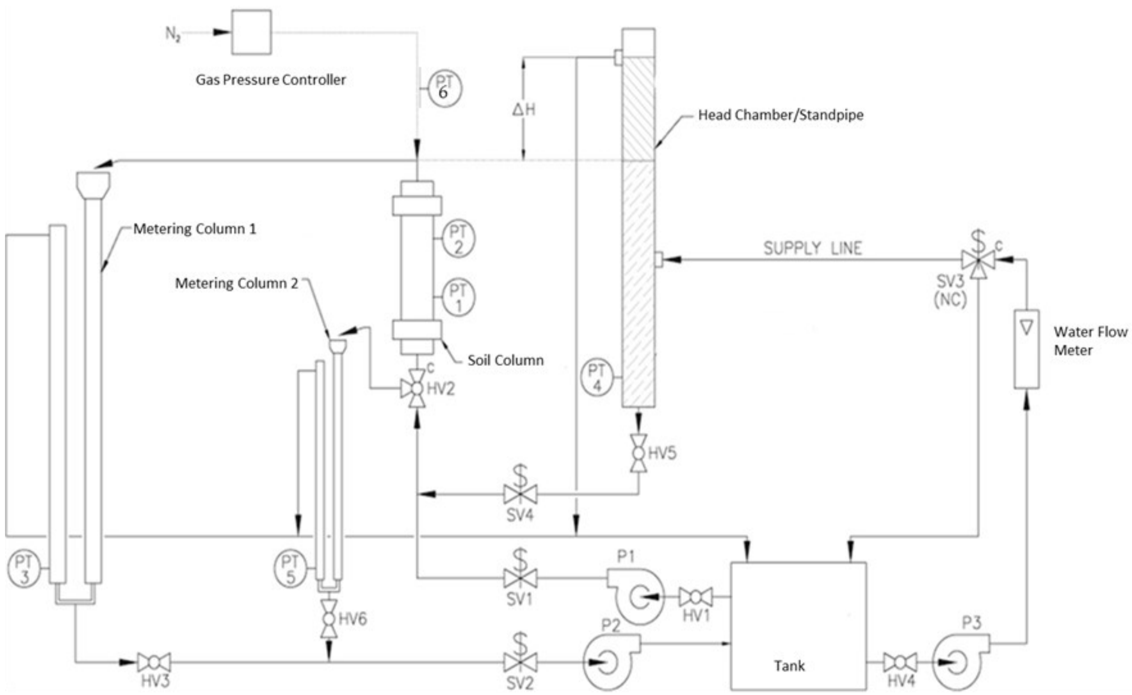

Figure 3. Schematic drawing of the experimental system used for determining saturated hydraulic conductivity with pressure transducers (PT1-PT6), pumps (P1-P5), solenoid valves (SV1-SV2), and manual valves (HV1-HV5).

The falling head method was used for characterization of the sediment core samples reported here. The constant head method was not used because it usually requires larger volumes of water, which would have to be treated and disposed of as radioactive waste. The following sections describe the measurements and calculations used to determine K_s using these methods.

2.3.2 Falling Head Method

For the falling head method, the column conducts water according to a decreasing head in a standpipe with cross-sectional area A_s [L^2]. The parameter K_s is computed according to the following equation:

$$K_s = \left(\frac{A_s L_c}{A_c \Delta t}\right) ln\left(\frac{H_1}{H_2}\right) \tag{1}$$

where L_c [L] is the length of the porous media in the column, Δt [T] is the time for the hydraulic head to fall from level H_1 to level H_2 [L], and A_c [L^2] is the cross-sectional area. With reference to Figure 3, H_1 and H_2 are the logged, time-stamped, digital pressure (head) readings of PT4 at two different times whose difference is Δt. The parameters A_s, L_c, and A_c were all measured using a steel tape measure.

2.3.3 Constant Flux Method

For the constant flux method, a 0.01 M $CaCl_2$ solution is injected at a specified rate while hydraulic head measurements are obtained by pressure transducers connected to tensiometers at two or more internal locations. The K_s values obtained using this method represent the zone between the two locations where the hydraulic heads are measured, according to the following equation:

$$K_s = \frac{QL_p}{A_c \Delta H_p} \quad (1)$$

where L_p [L] and ΔH_p [L] are the distance and hydraulic head difference, respectively, between the two locations where the hydraulic head data are obtained, Q [L^3 T^{-1}] is the observed flow rate, and A_c is the column cross-sectional area [L^2]. With reference to Figure 3, pump P1 imposes a flow rate, and time-stamped pressure dates are logged from pressure transducers PT1, PT2, and PT3. The observed flow rate Q is the logged digital pressure reading from PT3, converted to volume, as a function of time. The volume is V= ($\pi r^2 h$)*2, where r is the radius of metering column 1, h is the pressure reading of PT3 in units of cm of water, and the value is multiplied by 2 because metering column 1 is made of two standpipes with an identical radius. The volume conversion method was validated with a Type A graduated cylinder, and the parameters L_p and A_c were measured with a steel tape measure.

2.4 Water Retention and Unsaturated Hydraulic Conductivity

Several laboratory methods are available for determining water retention characteristics of variably saturated porous media. These include the hanging water column, pressure plate extraction, and chilled mirror hygrometer-based methods (Dane and Hopmans 2002). The hanging water column method is usually applicable to soil moisture tensions up to ~300 cm of water, while the pressure plate extraction methods are typically used for an intermediate range of soil moisture tensions, ranging from ~500 cm up to ~15,000 cm of water, depending on the bubbling pressures of the porous plates. The chilled mirror hygrometer method applies to higher tensions. A WP4C Soil Water Potential meter was used in the study (Meter Group, Pullman, WA). This instrument has a reported range of 0 to -300 MPa and an accuracy of +/- 0.05 MPa from 0 to -5 MPa, and 1% from -5 to -300 MPa.

Water retention and unsaturated hydraulic conductivity for variably saturated conditions can also be obtained simultaneously using the MS outflow method (Hopmans et al. 2002) that was used in the current study, which covers a range from 0 to ~700 cm of soil moisture tension.

Figure 4 shows a more detailed schematic of a soil-filled column, or intact core sample. For determination of K_s, acrylic endcaps are typically fitted with perforated support plates. For MS outflow experiments, a porous ceramic plate is typically used on the bottom end of the core. The core is also instrumented with tensiometers attached to pressure transducers for measurement of aqueous pressures. The 5-mm-diam porous ceramic cups and 10-cm-long tensiometer shafts (model M0131510 for TEROS 31 and T5 tensiometers) used in these experiments were obtained from Meter Group (Pullman, WA).

The pressure transducers used in this study (Heise DXD) were calibrated by a calibration facility operated by Energy Northwest (A2LA certificate number: 2724.01). The transducer accuracy is 0.02% of full scale. The transducers that were used have a compound range of -700 to + 700 cm, so their accuracy is 1400 x 0.02% = 0.28 cm, or ~0.3 cm. Tensiometer data were collected, logged, and displayed continuously during multistep outflow experiments using LabView™ software. Monitoring of the displayed data allowed for intervention in the experiments if any problems with the tensiometers were obvious. Typically, if a tensiometer appeared to be failing (leaking), the experiment would either be stopped, repairs made or tensiometers replaced, the core re-saturated, and the experiment restarted from the beginning. In some cases, if the experiment was near completion before tensiometer failure, it was either continued as-is or stopped and the experiment terminated prematurely without starting over. Tensiometer data that were obviously bad were not used for parameter estimation.

Placement of tensiometers in intact cores can be problematic. If the cores contain large fractions of coarse material, the porous ceramic cups on the tensiometers may have poor contact with the sediment (or rocks) and can be easily cracked during emplacement. Once installed, the tensiometer tubes are sealed to the core liner using a custom O-ring and clamp system. The bubbling pressure of the porous ceramic cups and porous plates used in the MS outflow experiments for the standard-size (~4-in.-diam) cores analyzed in this study was ~1,000 cm of water.

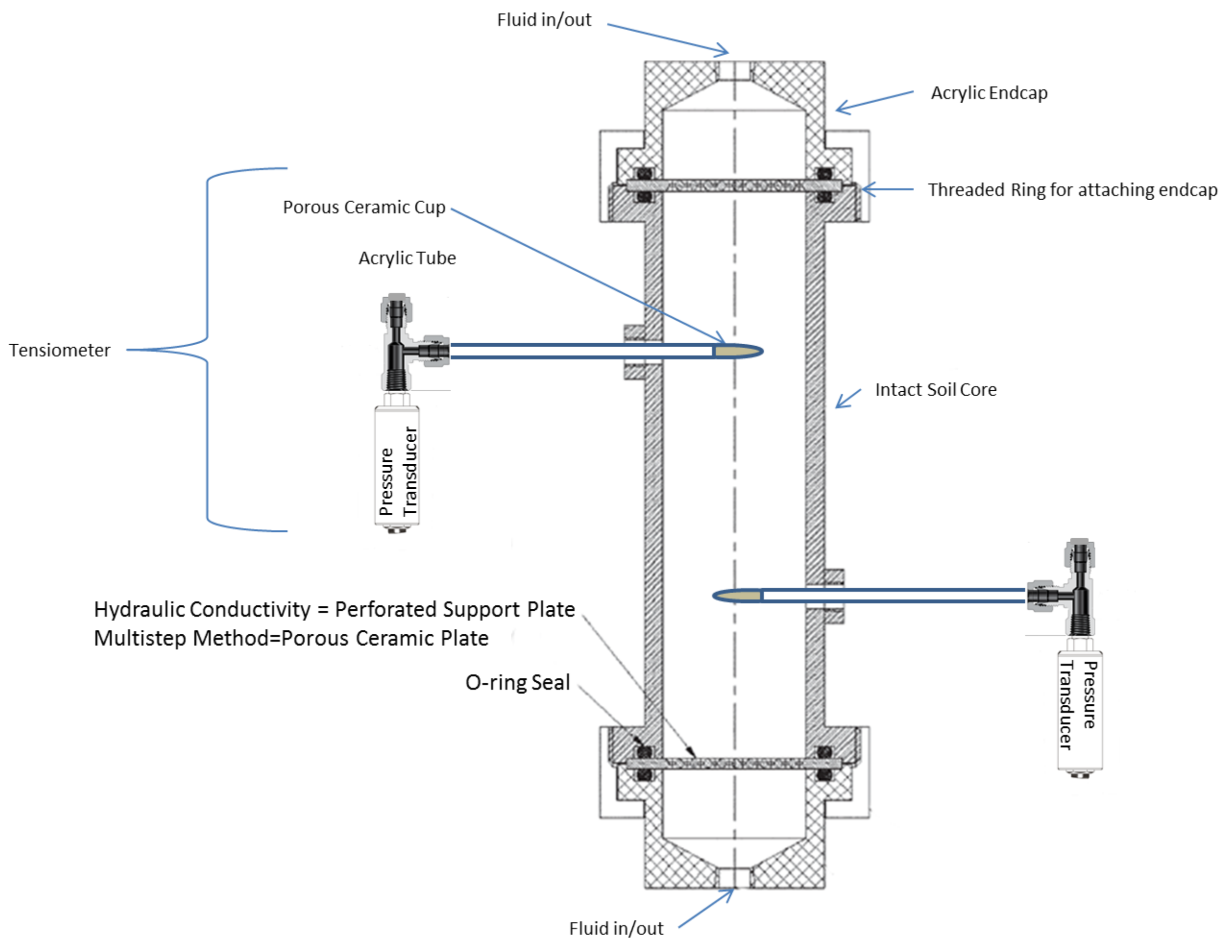

Figure 4. Schematic of a column or sediment-filled core sample used for multistep outflow experiments.

2.4.1 Multistep Outflow Method

The MS outflow method is a standard method for determination of soil hydraulic properties (Hopmans et al. 2002). The experimental procedure is performed as follows. After the intact core sample is mounted in the experimental apparatus, the core is initially saturated with de-aired water from the bottom up to minimize entrapped air. The porous plate at the bottom of the core and the bottom endcap are completely water-filled and are attached to a water-filled outflow line. The end of the outflow line is positioned so that the drip point is at the same elevation as the top of the sediment in the column. The top endcap is then attached and connected to a gas flow line. At this point, the core should be gas tight.

With the outflow line positioned as described, the lower boundary condition for the soil column is a fixed aqueous pressure, equal to the height of the sediment-filled column. The upper boundary condition is set to a prescribed gas pressure (initially atmospheric) using a gas pressure controller. With reference to 0, gas pressure is measured at PT6, and aqueous pressures are measured at PT1 and PT2. Gas pressure is increased incrementally, and the cumulative water outflow volume and changes in aqueous pressures are measured as a function of time. Gas pressure is typically increased when the water outflow has ceased and the aqueous pressures have stabilized for the current gas pressure step. An MS outflow experiment is usually terminated when negligible outflow is observed after a prolonged period at relatively higher gas pressure.

The air-entry pressure of the porous plate at the bottom of the core is nominally ~1,000 cm, so this is the maximum gas pressure that could theoretically be applied before the system was no longer gas-tight. However, pressures this high are rarely used to maintain a safety factor in case the bubbling pressure of the plates is lower than advertised. In practice, the maximum air pressure applied to the top of the columns is usually ~700 cm. MS outflow experiments on intact cores are often terminated earlier than planned due to air leaks. Air leaks are not uncommon when MS outflow experiments are performed on intact sediment cores due to the stresses experienced by the Lexan core liners during drilling. The high temperature and pressure conditions that develop during drilling can make the Lexan liners brittle and susceptible to cracking, and the cracks may open when the core liner is pressurized. When obvious air leaks do occur, attempts are usually made to seal the leak with marine-grade epoxy. The core is then re-saturated and the experiment is repeated.

2.4.2 Parameter Estimation

Hydraulic parameters can be estimated from MS outflow experimental data in several different ways. The most common approach is to numerically simulate the experiment and to use non-linear parameter estimation to determine hydraulic parameters, using measured outflow and pressure data as observations (Eching and Hopmans 1993a; Eching et al. 1994). In this inverse parameter estimation approach, the dynamic experiment is simulated repeatedly as parameters are adjusted iteratively to minimize the differences between measured and simulated outflow volumes and water pressures. Most inverse parameter estimation methods used for estimating hydraulic parameters from MS outflow data have used a single-phase flow equation, known as the Richards equation (Richards 1931), for solving the forward flow problem (Kool and Parker 1988; Eching and Hopmans 1993a,b; Eching et al. 1994; Tuli et al. 2001).

For the current study, the water-air operational mode of the STOMP (Subsurface Transport Over Multiple Phases) simulator (White and Oostrom 2006), referred to as STOMP-WA, was used in conjunction with the well-known parameter estimation software PEST (Doherty 2016). STOMP-WA solves coupled mass conservation equations for both aqueous (water) and gas (air) phases under isothermal conditions. PEST can use several different parameter estimation algorithms, including the Levenberg-Marquardt method (Levenberg 1944; Marquardt 1963), which was used in the current study.

STOMP-WA is well-suited for simulating the type of MS outflow experiment described here since the boundary conditions used in the experiment can be accurately prescribed for the simulator. No liquid water moves across the top boundary of the core sample, and the bottom of the core sample sits on a water-saturated porous plate through which air cannot pass (unless the air-entry pressure of the plate is exceeded). Therefore, Dirichlet-type boundary conditions of fixed aqueous pressure and prescribed gas pressures are specified for the bottom and top of the model domain, respectively. Neumann-type zero-flux boundary conditions are specified for the aqueous and gas phases at the top and bottom of the domain, respectively.

Intact and repacked core samples are typically modeled as uniform porous media. Nonuniformities in a core sample, and/or poor contact between the porous cups of the tensiometers and sediments contained within the intact core, can result in behavior that may be inconsistent with what would generally be expected for uniform porous media. Therefore, the use of only outflow data for observations in inverse parameter estimation may be necessary in some cases, if both observed pressure and outflow responses cannot be well matched by model results, or if tensiometers fail or exhibit spurious or unexpected behavior during an MS outflow experiment. However, owing to the well-constrained boundary conditions used in the experimental setup, and the use of a two-phase flow simulator, outflow data alone are expected to yield reliable parameter estimates.

An alternative to using inverse modeling for parameter estimation is to use the prescribed gas pressures and measured aqueous pressures from the MS experiment to calculate capillary pressures, and the measured outflow volumes and volume of water remaining at the end of the experiment to calculate average water contents as a function of time. The average water contents and capillary pressures at selected times (end of each pressure step, just prior to increasing gas pressure) can then be paired and fitted to estimate parameters for any water retention model of interest. This approach implicitly assumes that quasi-static conditions are reached just prior to a change in gas pressures.

The multistep outflow method is a standard method. Another standard method (not used here) is the pressure-plate extraction method, which relies on subjecting a sample that is placed on a porous ceramic plate to increasing gas pressure that displaces water from the sample. The experimentalist determines when the sample has come to equilibrium by periodically weighing it. When weight changes are considered negligibly small, the sample is moved to a different porous plate with higher bubbling pressure and the process is continued with higher pressure. The same principle is applied during the multistep outflow experiments to determine when gas pressures are increased but based on cumulative water outflow. For a given pressure step, when outflow has ceased or the rate is considered low enough, gas pressure is increased. The data points collected just prior to (a few seconds before) an increase in gas pressure are used as the “quasi-static” data. These data are essentially equivalent to what would be obtained from a pressure plate method, but at lower pressures. A plot of applied air pressure and cumulative outflow volume vs time is shown in Figure 5 to illustrate how applied air pressures are typically increased during multistep outflow experiments after outflow at a given pressure step has become very small or negligible.

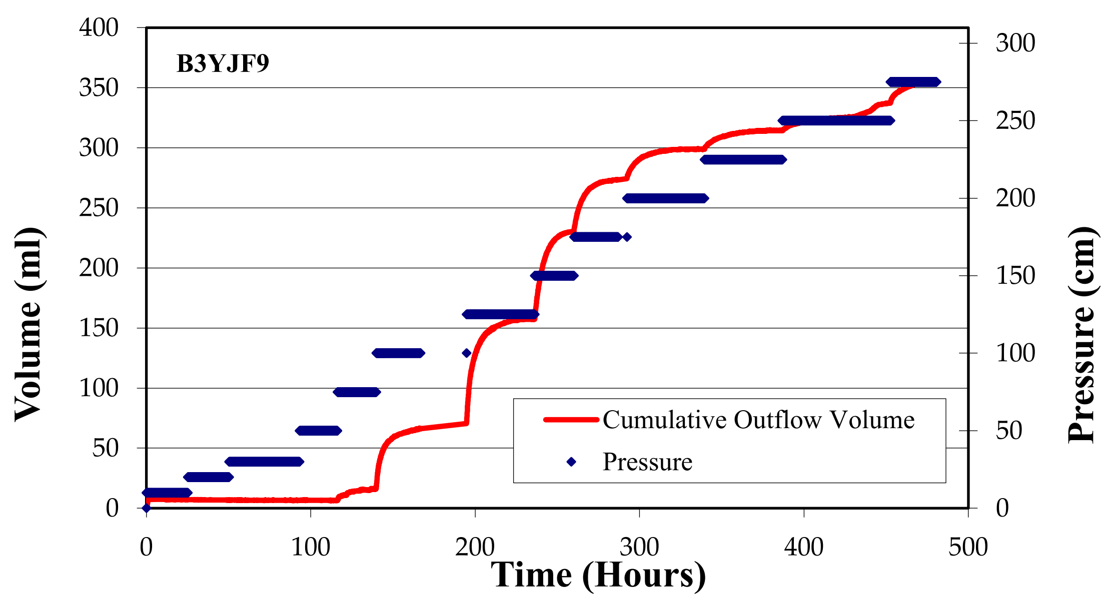

Figure 5. Air pressure step sequence and corresponding cumulative outflow volume for multistep outflow experiment performed on intact core sample B3YJF9 from the 200 East Area.

2.4.2.1 Water Retention Functions and Unsaturated Hydraulic Conductivity Models

Many different functions and models have been proposed for representing the water retention characteristics and unsaturated hydraulic conductivity of porous media. The water retention functions of van Genuchten (1980) and Brooks and Corey (1964) are the most popular owing to their relative simplicity and accuracy in representing measured water retention characteristics. The van Genuchten (1980) model can be written as

$$S_e(h) = [1 + (\alpha h)^n]^{-m} \tag{1}$$

where:

S_e = effective saturation = $\frac{\theta - \theta_r}{\theta_s - \theta_r}$; $0 \le S_e \le 1$
h = soil-moisture tension [L]
α = curve-fitting parameter related to the inverse of the air-entry pressure [L^{-1}]
n, m = curve-fitting parameters related to the pore size distribution; m = 1-1/n is often assumed [-]
θ_r = residual water content [-]
θ_s = saturated water content [-].

The van Genuchten hydraulic conductivity relationship, based on the Mualem (1976) hydraulic conductivity model with the restriction that $m = 1 - 1/n$, can be written as

$$K(S_e) = K_s S_e^l \left[1 - \left(1 - S_e^{1/m}\right)^m\right]^2 \tag{2}$$

where K_s is the saturated hydraulic conductivity and l is a pore-interaction term that is typically assumed to be equal to 1/2 if only K_s and water retention data are available (Mualem 1976).

The Brooks-Corey model may be written as

$$S_e(h) = \left(\frac{h_b}{h}\right)^l \; if \; h \ge h_b$$
$$S_e(h) = 1 \; otherwise. \tag{3}$$

where λ is a pore-size distribution parameter that affects the slope of the water retention function, and h_b is the air-entry (a.k.a. bubbling) pressure. The Brooks-Corey function can be combined with the Burdine (1953) or Mualem (1976) relative permeability models to yield

$$K(S_e) = K_s S_e^{2+ l+2/l} \tag{4}$$

where it is typically assumed that the pore-interaction term ℓ = 1/2 and 1 for the Mualem and Burdine models, respectively.

Eqs. (1) and (2) are the most-commonly used hydraulic property functions for vadose zone materials, followed by Eqs. (3) and (4). Note that the Brooks-Corey water retention model [Eq. (3)] is sometimes preferred over the van Genuchten model [Eq. (1)] if a porous medium has relatively uniform particle and pore sizes that result in a sharp or abrupt decrease in aqueous saturation from a fully water-saturated condition after a distinct air-entry pressure is exceeded.

Porous media can also have multi-modal pore size distributions that manifest multi-modal water retention characteristics. Such characteristics can be represented using multiple, van Genuchten-type subcurves, S_{e_i}

$$S_e = \frac{\theta - \theta_r}{\theta_s - \theta_r} = \sum_{i=1}^{k} w_i S_{e_i} \tag{5}$$

where

$$S_{e_i} = [1 + (\alpha_i h)^{n_i}]^{-m_i} \tag{6}$$

and $\sum w_i = 1$ (Durner 1994). Priesack and Durner (2006) developed closed-form expressions for multi-modal unsaturated hydraulic conductivity functions based on the van Genuchten-Mualem relationships.

Parameter estimates are provided in this report for water retention curves that are fit using (1) the quasi-static MS outflow water retention data only, (2) the quasi-static MS outflow water retention data plus the WP4C data, and (3) the dynamic MS outflow data without WP4C data. The most appropriate parameters will depend on the application, but the following should be considered.

Water retention characteristics in the drier range of soil moisture conditions that are measured using the WP4C instrument typically have a log-linear character that should align with but follow a somewhat different trajectory than the water retention data for wetter conditions that are obtained from the MS outflow experiments. Webb (2000) developed a simple analytical extension to augment standard water retention functions that accounts for the log-linear character of water retention data in the drier ranges of soil moisture conditions. This extension, which is implemented in the STOMP simulator, typically uses a value of soil moisture tension or capillary pressure of 10^7 cm and a corresponding volumetric water content of 0.0 as one end of the log-linear extension. The other end is determined as the point of contact of a tangent line of the log-linear function to the standard water retention curve. The tangent point is determined using an iterative procedure implemented in the STOMP simulator. The use of this method is triggered when the keyword “Webb” is present on the Saturation function card of the input file used for STOMP. The Webb extension allows for approximating the character of water retention data in the dry range, as well as the data representing wetter conditions that are obtained using the MS outflow method that are represented using standard Brooks-Corey or van Genuchten functions, without having or fitting dry-end data.

If the soil or hydrogeologic unit being represented in a model is near the ground surface, such that it can experience a wide range of moisture conditions, then parameters obtained using options 1or 3 should be used with the Webb extension, or option 2 can be used with or without the Webb extension. If the hydrogeologic unit is located below the water table or in the capillary fringe region, such that it never gets very dry, then options 1 or 3 may be preferred, without the Webb extension. Parameter estimates obtained using option 3 have historically been considered the gold standard, or most accurate, over the range of pressures that typically occur in the MS outflow experiments. Further discussion on specific recommendations for selection of hydraulic parameters is provided in Section 4.2.4.

2.5 Physical Properties

After laboratory MS outflow experiments were terminated, the acrylic endcaps on the intact core samples were removed and the sediment contained in the cores was removed and dried in a convection oven for

24 hours at 105 °C. Physical properties, including porosity, dry bulk density, particle density, and particle size distribution, were then determined as described below.

2.5.1 Total Porosity

The total porosity of the intact cores was estimated by converting the mass of water remaining in the sediments at the end of the MS outflow experiment to a volume, adding the volume of water that flowed out of the column during the experiment, and dividing by the bulk volume of core sample occupied by sediment. This calculation assumes that the sediment is fully water-saturated at the beginning of an MS outflow experiment, with no excess water ponded on top of the sediment. The porosity calculated in this way is an *apparent* total porosity, rather than the true total porosity that exists in situ, owing to potential sample disturbance during core sampling.

The XCT images for most of the intact cores indicate some degree of sample disturbance that created small cracks or a small amount of void space around the walls of the Lexan liner and sometimes around the ends of the columns. Outflow data from many of the analyzed cores showed some evidence of "wall effects," wherein a relatively small volume of water drained from the cores in the first pressure step, even for relatively fine-textured materials. Although the cores were collected intact, some sample disturbance inevitably occurs during drilling and sampling, and this is expected.

Total porosity, ϕ, can also be estimated from bulk and particle densities using

$$\emptyset = 1 - \frac{\rho_b}{\rho_s} \tag{1}$$

where ρ_b and ρ_s are the dry bulk density [M L^{-3}] and particle density [M L^{-3}], respectively. Dry bulk density was determined for the whole cores. Particle density was not directly determined for this study, but it generally falls within a relatively narrow range (e.g., 2.6 to 2.8 g cm^{-3}) for Hanford sediments (Rockhold et al. 1993). Particle density is typically measured on a subsample of the <2 mm size fraction of the sediments. Differences between porosity calculated using Eq. (1) and porosity calculated as the sum of the water volume drained plus water volume remaining in the column at the end of an MS experiment divided by core volume can often be attributed, in part, to differences in the particle density of the bulk sediment, versus the measured particle density for subsamples from the <2 mm size fraction.

2.5.2 Dry Bulk Density

The dry bulk density, ρ_b [M L^{-3}], is defined as

$$\rho_b = \frac{M_s}{V_b} \tag{1}$$

where M_s is the dry mass of solids and V_b is the bulk volume occupied by the solids. Particle density was calculated as the total mass of dry sediment contained in the Lexan core liner divided by the volume of core liner. For all samples used in this study, the inside diameter of the Lexan core liners was 8.89 cm. The nominal length of the core liners was 15 cm.

2.5.3 Particle Density

Particle density, ρ_s [M L^{-3}], is defined as

$$\rho_s = \frac{M_s}{V_s} \tag{1}$$

where M_s is the dry mass of solid particles and V_s is the volume of the particles. Particle density was determined on subsamples of the <2 mm size fraction of sediments from the core samples using the pycnometer method (Flint and Flint 2002).

2.5.4 Particle Size Distribution

The particle size distribution can be correlated with other properties of interest (e.g. hydraulic, sorption) and can aid in facies delineation and stratigraphic correlations. Particle size distribution was determined using two methods: (1) mechanical sieving (Gee and Or 2002) and (2) laser light scattering (ASTM D4464-15).

2.5.4.1 Sieve Analysis

Sieving was performed on air-dried, bulk sediment. If a core sample was selected for MS outflow experiments, grain size analyses were performed after completion of those experiments. Grain size analyses were also performed on other selected samples that were not used in MS outflow experiments. Sieve sizes of 2.5, 1.25, 3/4, and 5/16 in., and #5 and #10 sieves, were used, which correspond to sizes of 64, 32, 19, 8, 4, and 2 mm, respectively.

2.5.4.2 Laser Light Scattering Method

The laser light scattering method was used on subsamples collected from the catch pan at the bottom of the sieve stack (<2 mm size fraction) using ASTM D4464-15, 2009. Three replicates of each sample were used, with each replicate being measured three times. Data generated by the sieve and laser light scattering methods were combined to determine the complete particle size distributions for the bulk sediments. The standard deviation reported is averaged across multiple standard deviations.

3.0 RCRA Borehole Sampling Locations

This section defines where samples were collected in the 200 East and West areas, how core samples were selected for further evaluation, and which characterization methods were applied to each core sample.

The locations of the opportunistic samples from RCRA boreholes where core samples were received is shown in Figure 6. For 200 East samples, Central Plateau Cleanup Company (CPCCo) provided Pacific Northwest National Laboratory (PNNL) with a single core from a given split-spoon sample interval for evaluation and potential characterization. For 200 West, either single or multiple cores were provided from a split-spoon sample interval. Multiple cores provided an opportunity to select the highest quality core for intact core analysis from which one core was selected for characterization from a given split-spoon sample interval. Where multiple cores were not available, the sample provided was evaluated.

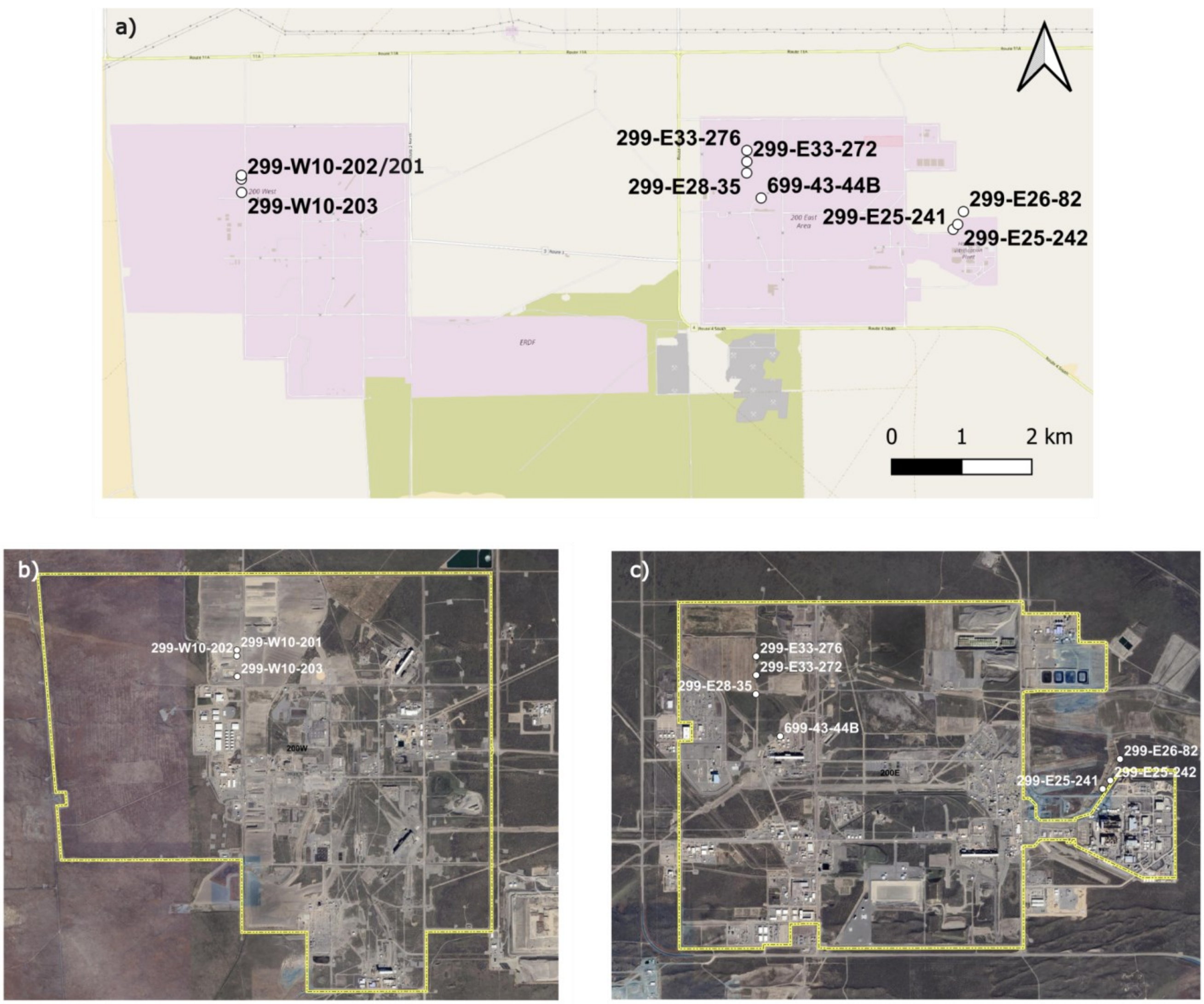

Figure 6. 200 East and West areas showing a) locations of boreholes, b) aerial photographic image of 200 West Area with borehole locations, and c) aerial photographic image of 200 East with borehole

locations. Core samples were collected from these boreholes and analyzed for physical and hydraulic properties.

3.1 Core Selection

Drilling at Hanford is usually done using several methods, including Becker hammer, resonant sonic, air-rotary, and cable-tool. The core liners that are used in split-spoon core samplers are typically made from Lexan and have a diameter of 4 in. However, in some cases, the drilling contractor used stainless-steel and/or 3.75-in.-diameter core liners. After sampling, the core liners are typically removed from the sampler, end caps are placed on the ends of the cores (nominal length is 6 in.), and the ends are then taped shut to prevent loss of sediment or moisture from the core samples. The cores are then labeled, cooled to ≤6 °C and transferred to the PNNL 331 Building for further analyses. Upon delivery, cores are inspected for defects and heat damage and stored at ≤6 °C until used.

The original intent of the RCRA core characterization effort was to obtain physical and hydraulic properties on intact cores to represent in situ conditions as closely as possible. However, because of the nature of well drilling, it is not always guaranteed that good quality core samples will be obtained. Measurements associated with multistep (MS) outflow experiments, which are used to estimate parameters representing water retention characteristics and unsaturated hydraulic conductivity, require the use of tensiometers that are inserted into the cores through holes that are drilled into the core. Tensiometer placement can be problematic in very coarse samples or samples that do not completely fill the entire Lexan liner (see Section 2.4.1). PNNL initially excluded some samples for further testing if the core liners were not sufficiently full; otherwise, XCT imaging was generally performed on the cores.

XCT imaging was performed on selected cores to assess sample quality and to determine if a core should be further characterized. Final core selection for intact hydraulic characterization was determined based on inspection of XCT images. Figure 7 shows examples of the wide variety of sediment textures of these samples. The first two samples on the left (Figure 7a-b) were selected for further characterization of the intact core material. The sample shown in Figure 7c was identified as a formation for which there is a data gap. Since the sample consists of very large cobbles, and is not well-packed, it was combined with sediment from adjacent core samples of the same formation into a larger composite sample in a custom-built core assembly. Additional criteria for composite sample selection included textural similarity (judged qualitatively by XCT or quantitatively by particle size distribution data) and close spatial proximity (same well, same formation, and samples close to each other, if possible). Final selections for the cores used to build the composite core samples were made in consultation with CPCCo and INTERA staff. Appendix A presents XCT images for cores that were analyzed.

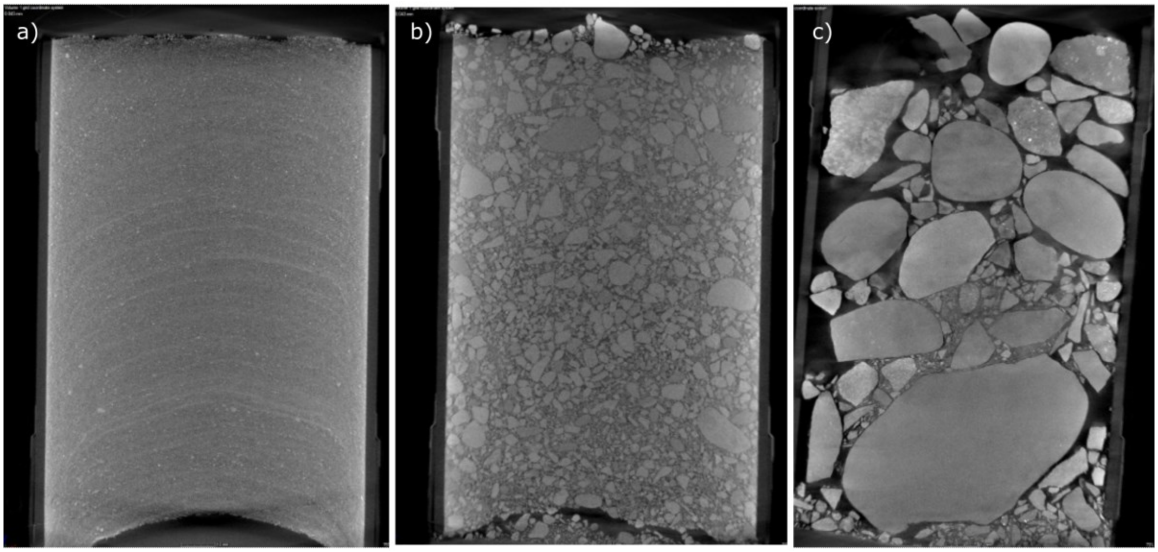

Figure 7. XCT images of three intact Hanford sediment core samples from the 200 East Area. Sample IDs are, from left to right, B41802 (Hf1 unit), and B3YJH1 (CCUg unit), and B41807 (Hf3 unit).

3.1.1 Core Processing and Measurements

Cores were characterized using the decision-making logic described in Figure 8. After XCT imaging, a determination was made whether measurements should be taken on the intact core samples, used for physical property measurements, or if a sample should be combined with others to develop a composite core sample.

Gravimetric moisture content (GMC) and matric potential (MP) were measured on small subsamples of the intact cores in their as-received condition. This was followed by hydraulic property measurements (K), including saturated hydraulic conductivity (Ksat) (Section 2.3.1), and water retention and unsaturated hydraulic conductivity (Kunsat) from multi-step (MS) outflow experiments (Section 2.4.1). MP measurements were also collected on subsamples of core materials after the completion of the MS experiment to obtain lower water contents than could be collected during the MS experiments. MP values at the drier conditions were determined using a WP4C water activity meter by Meter Group (Pullman, WA). Dry bulk density (DBD) was estimated by measuring the mass of oven-dried soil after completion of the MS experiments and dividing by the volume of the sediment-filled column (Section 2.5.2). Particle size analysis (PSA) (Section 2.5.4) was performed after completion of the hydraulic property measurements.

Intact cores that were combined into a composite core first had GMC, MP, and PSA data collected on material from the individual cores. After combining the sediment from these cores, measurements of K, DBD, and PSA were made on the composite sample.

Some cores were not selected for intact or composite core characterization. In this case, a combination of GMC, MP, DBD, or PSA data were collected for the sediments – hydraulic property measurements were not made. Table 1 and Table 2 list the core sample identification numbers and the analyses that were performed on different core samples from the 200 East and West areas. The formation identification information in these tables was provided by CPCCo when the core samples were transferred to PNNL. A summary table listing the types of characterization data collected for each core sample is provided in Appendix F.

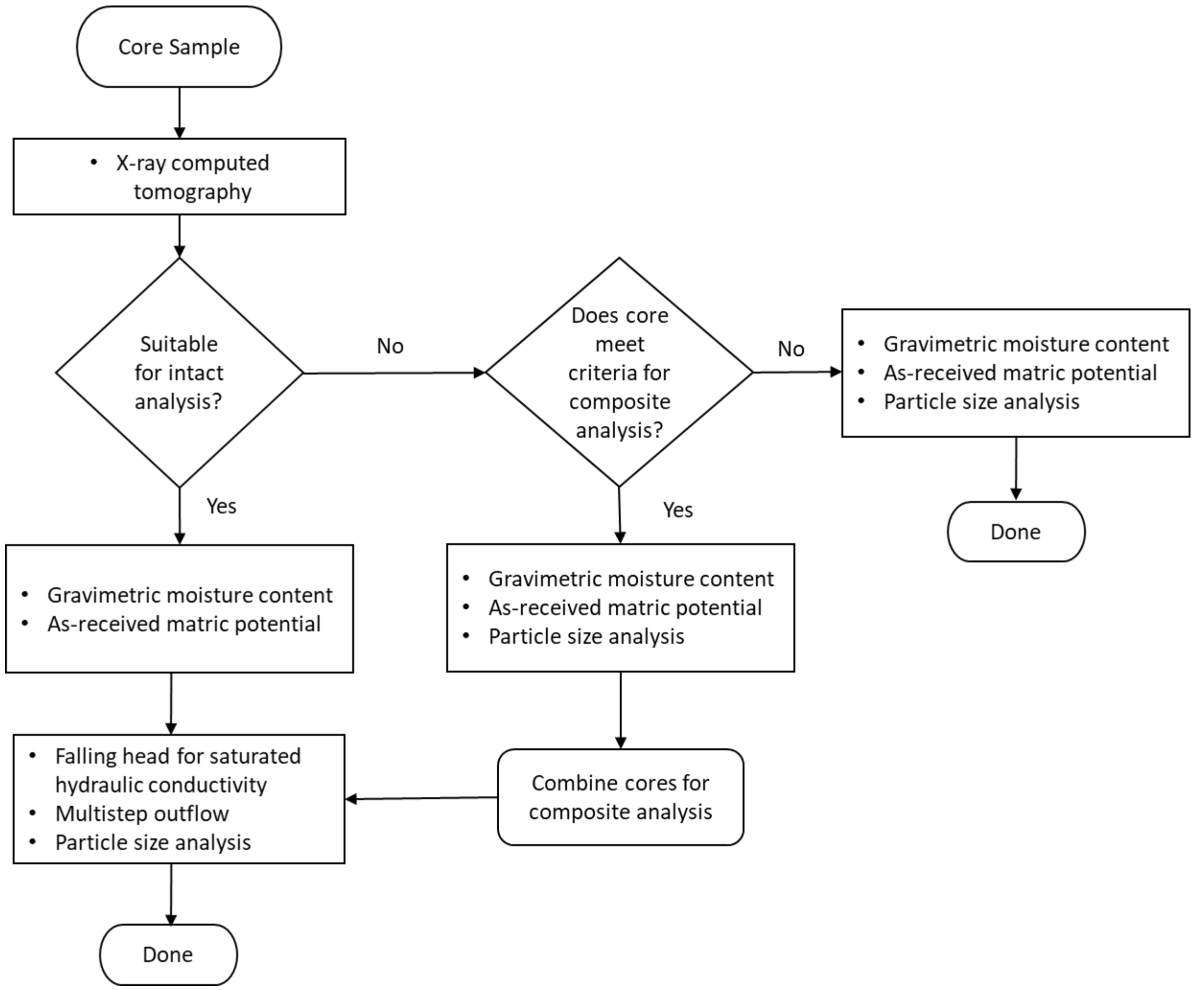

Figure 8. Logic diagram showing sequence of core sample analyses. This is a generalized diagram – actual analyses performed on each core are presented in Table 1. Refer to the 2.0 for descriptions of each method.

Table 1. 200 East core samples for RCRA borehole/well sample characterization.

Borehole ID	Well Name	Sample ID	Sample Interval bgs Top (ft)	Sample Interval bgs Bottom (ft)	Formation	Analyses Performed
D0049	699-43-44B	B40DC4	180.3	182.8	CCUg	MP, GMC, DBD, PSA
D0056	299-E25-241	B41802	40.5	42.7	Hf1	MP, GMC, DBD, K, PSA
D0056	299-E25-241	B41806[1]	159.5	161.7	Hf3	MP, GMC, DBD, PSA
D0056	299-E25-241	B41807[1]	199.5	201.7	Hf3	MP, GMC, PSA
D0056	299-E25-241	B41809	250.2	252.4	CCU	MP, GMC, DBD, PSA
D0057	299-E25-242	B41868[1]	150	152.2	Hf3	MP, GMC, PSA
D0058	299-E26-82	B418C0	188.4	190.6	CCU	MP, GMC, DBD, PSA
D0058	299-E26-82	B418C2	207.1	209.3	CCU	MP, GMC, DBD, PSA
D0059	299-E33-272	B3YK00[2]	270	272.5	CCUg	MP, GMC, PSA
D0059	299-E33-272	B3YJY6	209.4	211.9	Hf3	DBD, K, PSA
D0059	299-E33-272	B3YJY7	219.5	222	CCU	DBD, K, PSA
D0059	299-E33-272	B3YJY8[2]	230	232.5	CCUg	MP, GMC, PSA
D0059	299-E33-272	B3YJY9[2]	249.8	252.3	CCUg	MP, GMC, PSA
D0059	299-E33-272	B3YJX6	29.8	32.3	Hf1	MP, GMC, PSA
D0059	299-E33-272	B3YJY5	199.6	202.1	Hf3	MP, GMC, DBD, K, PSA
D0060	299-E28-35	B3YJX1	219.7	222.2	CCU	MP, GMC, DBD, PSA
D0060	299-E28-35	B3YJX2	230.1	232.6	CCU	DBD, K, PSA
D0061	299-E33-276	B3YJD8	30	32.5	Hf1	MP, GMC, PSA
D0061	299-E33-276	B3YJD9	40	42.5	Hf1	MP, GMC, DBD, PSA
D0061	299-E33-276	B3YJF9	199.7	202.2	CCU	DBD, K, PSA
D0061	299-E33-276	B3YJH0	209.6	212.1	CCUg	DBD, K, PSA
D0061	299-E33-276	B3YJH1[3]	219.7	222.2	CCUg	MP, GMC, DBD, PSA
D0061	299-E33-276	B3YJH2[3]	240	242.5	CCUg	MP, GMC, DBD, PSA
D0061	299-E33-276	B3YJH3[3]	261.7	264.2	CCUg	MP, GMC, DBD, PSA
D0061	299-E33-276	B3YJF8	189.8	192.3	Hf3/CCU	MP, GMC, DBD, PSA
D0056 D0057	299-E25-241 299-E25-242	Composite1 (B41806, B41807, B41868)	159.5 199.5 150	161.7 201.7 152.2	Hf3	DBD, K, PSA
D0059	299-E33-272	Composite2 (B3YK00, B3YJY8, B3YJY9)	270 230 249.8	272.5 232.5 252.3	CCUg	DBD, K, PSA
D0061	299-E33-276	Composite3 (B3YJH1, B3YJH2, B3YJH3)	219.7 240 261.7	222.2 242.5 264.2	CCUg	DBD, K, PSA

bgs is below ground surface; CCU is undifferentiated Cold Creek Unit; CCUg is Cold Creek Unit gravels; Hf1 is Hanford formation - unit 1; Hf3 is Hanford formation - unit 3.

Table 2. 200 West core samples for RCRA borehole/well sample characterization.

Borehole ID	Well Name	Sample ID	Designation in Split Spoon	Sample Interval bgs Top (ft)	Sample Interval bgs Bottom (ft)	Formation	Analyses
D0013	299-W10-201	B488V3	A	51.5	52	Hf1	MP, GMC, PSA
D0013	299-W10-201	B488V7	C	95.6	96.1	Hf2	MP, GMC, K, DBD, PSA
D0013	299-W10-201	B488Y1	H	117	117.5	CCU/CCUc	MP, GMC, PSA
D0013	299-W10-201	B488Y3	G	122.5	123	CCUc	MP, GMC, K, DBD, PSA
D0013	299-W10-201	B488Y4	C	124.5	125	CCUc	MP, GMC, K, DBD, PSA
D0013	299-W10-201	B488W5	D	138	138.5	Rwie	MP, GMC, K, DBD, PSA
D0013	299-W10-201	B488W7	B	223.6	224.1	Rwie	MP, GMC, K, DBD, PSA
D0014	299-W10-202	B488X2	B	56.4	56.9	Hf1	MP, GMC, PSA
D0014	299-W10-202	B48N72	B	100.2	N/A	Hf2	MP, GMC, K, DBD, PSA
D0014	299-W10-202	B48N73	B	114.9	115.4	CCU	MP, GMC, K, DBD, PSA
D0014	299-W10-202	B48N74	I	116	121	CCU	MP, K, DBD, PSA
D0014	299-W10-202	B48N76	H	122	122.5	CCUc	MP, GMC, K, DBD, PSA
D0014	299-W10-202	B48N79	B	136	136.5	Rwie	MP, GMC, K, DBD, PSA
D0015	299-W10-203	B48ND9	B	70.9	71.4	Hf2	MP, GMC, K, DBD, PSA
D0015	299-W10-203	B48ND9	D	69.9	70.4	Hf2	MP, GMC, DBD, PSA
D0015	299-W10-203	B48NF4	C	114.5	115	Hf2	MP, GMC, K, DBD, PSA
D0015	299-W10-203	B48NH0	H	122	122.5	CCUc	MP, GMC, K, DBD, PSA
D0015	299-W10-203	B48NH0	I	121.5	122	CCUc	MP, GMC, K, DBD, PSA
D0015	299-W10-203	B48NH7	C	190.8	191.3	Rwie	MP, GMC, DBD, PSA

bgs is below ground surface; CCU is undifferentiated Cold Creek Unit; CCUc is Cold Creek Unit caliche; Hf1 is Hanford formation - unit 1; Hf2 is Hanford formation - unit 2; Hf3 is Hanford formation - unit 3.

4.0 Results and Discussion

4.1 Physical Property Analyses

Grain size distribution data provide information about the grain size and sorting characteristics of the sediments and can be related to or correlated with other soil properties of interest. They may also be used for other purposes, such as helping to identify stratigraphic contacts between boreholes. The core samples that were characterized for this study exhibited a wide range of sediment textures reflecting the heterogeneous nature of the subsurface. For example, the gravel contents of the samples ranged from less than 1% to ~95%; sand contents ranged from ~3% to 90%; silt contents ranged from ~1% to ~86%; and clay contents ranged from 0% to ~19%. Dry bulk densities ranged from 1.52 to 2.24 g/cm^3, with higher values (> 2.0 g/cm3) generally indicating denser materials, like gravel. Folk-Wentworth textural classifications ranged from sandy silt to gravel. Appendix B and Appendix C provide sieve results and particle size distribution plots, respectively. Associated formation designations are provided in Tables 1 and 2.

When calculating the DBD, the core liner was generally assumed to be full. Cores with excessive voids as determined by visual examination of XCT images were generally excluded from hydraulic property measurements and DBD calculations due to inaccurate volume determinations.

Table 3 and Table 4 summarize the sample grain size distribution results for 200 East and 200 West, respectively, obtained using a combination of sieving and laser PSA. Each sample was measured in triplicate and each replicate was measured three times. The standard deviation across the triplicates was averaged by taking the square root of the quantity sum of squares of the individual standard deviations divided by the sample size, which was 3 in this case.

XCT imaging was performed on all core samples listed in this report except for sample B3YJF8 (Hf/CCU), which was designated for physical property analysis. This sample was adjacent to core sample B3YJF9 (CCU), which was chosen for physical and hydraulic property analysis. The XCT images for sample B3YJF8 were assumed to be like sample B3YJF9.

Table 3. Summary of particle size analysis results for 200 East Area samples.

Sample ID	Particle Size Analysis % Gravel (> 2 mm)	% Sand (63 µm-2 mm)	% Silt (63-4 µm)	% Clay (< 4 µm)	Dry Bulk Density (g/cm^3)	Soil Texture Folk/Wentworth Classification
B40DC4	61.68	17.66 ± 1.05	17.58 ± 0.87	3.09 ± 0.18	1.894	Muddy gravel
B41802	0.59	89.86 ± 0.75	9.56 ± 0.75	0.00 ± 0.00	1.579	Slightly gravelly sandy mud
B41806[(a)]	84.97	12.50 ± 1.18	2.36 ± 1.07	0.16 ± 0.11	1.998	Gravel
B41807[(a)]	95.14	3.48 ± 0.50	1.25 ± 0.44	0.12 ± 0.06	N/A	Gravel
B41809	87.81	8.71 ± 1.36	3.10 ± 1.17	0.38 ± 0.19	2.189	Gravel
B41868[(a)]	94.7	3.65 ± 0.76	1.48 ± 0.66	0.17 ± 0.09	N/A	Gravel
B418C0	81.69	15.00 ± 1.22	3.14 ± 1.13	0.17 ± 0.08	2.325	Gravel
B418C2	89.54	6.68 ± 1.37	3.50 ± 1.26	0.29 ± 0.11	2.137	Gravel
B3YK00[(b)]	73.42	16.25 ± 3.04	9.28 ± 2.68	1.05 ± 0.37	N/A	Muddy sandy gravel
B3YJY6	26.63	68.64 ± 0.87	4.20 ± 0.68	0.53 ± 0.19	1.892	Gravelly sand
B3YJY7	5.46	53.91 ± 8.62	29.66 ± 6.20	10.97 ± 2.42	1.990	Gravelly muddy sand
B3YJY8[(b)]	64.97	28.32 ± 1.91	5.95 ± 1.61	0.76 ± 0.30	N/A	Muddy sandy gravel
B3YJY9[(b)]	73.53	14.23 ± 2.78	11.43 ± 2.58	0.82 ± 0.20	N/A	Muddy sandy gravel
B3YJX6	45.9	27.62 ± 4.03	23.98 ± 3.45	2.50 ± 0.59	N/A	Muddy sandy gravel
B3YJY5	33.99	60.16 ± 2.66	5.54 ± 2.40	0.32 ± 0.27	1.845	Sandy gravel
B3YJX1	0.15	45.52 ± 13.03	35.58 ± 8.33	18.75 ± 4.70	2.150	Slightly gravelly sandy mud
B3YJX2	24.88	39.76 ± 5.10	27.78 ± 3.88	7.58 ± 1.22	1.959	Gravelly muddy sand
B3YJD8	69.11	27.19 ± 0.74	3.45 ± 0.67	0.26 ± 0.08	N/A	Muddy sandy gravel
B3YJD9	68.00	27.99 ± 1.07	3.79 ± 0.98	0.22 ± 0.09	2.194	Muddy sandy gravel
B3YJF9	1.07	71.84 ± 0.48	26.76 ± 0.48	0.33 ± 0.00	1.465	Slightly gravelly muddy sand
B3YJH0	30.96	31.60 ± 12.60	31.14 ± 10.41	6.31 ± 2.25	1.896	Muddy gravel
B3YJH1[(c)]	59.2	30.44 ± 4.67	9.58 ± 4.22	0.78 ± 0.44	2.143	Muddy sandy gravel
B3YJH2[(c)]	71.08	21.17 ± 2.68	7.00 ± 2.32	0.75 ± 0.37	2.379	Muddy sandy gravel
B3YJH3[(c)]	41.1	26.00 ± 10.49	21.44 ± 6.77	11.46 ± 3.73	2.416	Muddy gravel
B3YJF8	8.47	51.48 ± 10.32	30.98 ± 7.74	9.08 ± 2.58	1.860	Gravelly muddy sand
Composite1 (B41806, B41807, B41868)	92.79	5.52±1.40	1.64±1.18	0.22±0.23	1.802	Gravel
Composite2 (B3YK00, B3YJY8, B3YJY9)	71.69	18.80±2.33	8.15±1.90	1.36±0.44	2.284	Muddy sandy gravel
Composite3 (B3YJH1, B3YJH2, B3YJH3)	58.22	23.4±7.42	13.66±5.30	4.72±2.13	2.076	Muddy sandy gravel

(a) Used for Composite 1
(b) Used for Composite 2
(c) Used for Composite 3

Table 4. Summary of particle size analysis results for 200 West Area samples.

Sample ID and Interval	Particle Size Analysis				Dry Bulk Density (g/cm^3)	Soil Texture
	% Gravel (> 2 mm)	% Sand (63 µm-2 mm)	% Silt (63-4 µm)	% Clay (< 4 µm)		Folk/Wentworth Classification
B488V3-A	84.39	10.80 ± 2.49	4.65 ± 2.37	0.16 ± 0.12	N/A	Gravel
B488V7-C	2.9	79.22 ± 2.62	17.57 ± 2.54	0.31 ± 0.08	1.836	Slightly gravelly muddy sand
B488Y1-H	24.15	51.86 ± 4.13	23.51 ± 3.99	0.48 ± 0.14	N/A	Gravelly muddy sand
B488Y3-G	1.21	81.64 ± 2.62	16.67 ± 2.50	0.49 ± 0.11	1.686	Slightly gravelly muddy sand
B488Y4-C	7.62	66.02 ± 1.64	25.23 ± 1.57	1.13 ± 0.08	1.637	Gravelly muddy sand
B488W5-D	1.39	86.59 ± 2.10	10.56 ± 1.64	1.45 ± 0.51	1.931	Slightly gravelly muddy sand
B488W7-B	39.54	36.88 ± 5.10	22.44 ± 4.78	1.14 ± 0.32	1.969	Muddy sandy gravel
B488X2-B	64.9	30.40 ± 2.09	4.42 ± 1.90	0.28 ± 0.19	N/A	Muddy sandy gravel
B48N72-B	3.51	79.95 ± 3.66	16.27 ± 3.54	0.27 ± 0.13	2.004	Slightly gravelly muddy sand
B48N73-B	0	11.47 ± 1.11	86.49 ± 1.31	2.04 ± 0.71	1.766	Sandy silt
B48N74-I	18.68	39.10 ± 5.79	41.15 ± 5.61	1.07 ± 0.19	2.094	Gravelly mud
B48N76-H	1.64	74.09 ± 3.34	23.85 ± 3.25	0.41 ± 0.10	1.932	Slightly gravelly muddy sand
B48N79-B	4.43	82.26 ± 3.56	10.14 ± 2.54	3.17 ± 1.03	1.895	Slightly gravelly muddy sand
B48ND9-B	20.97	74.09 ± 2.26	4.85 ± 2.13	0.10 ± 0.13	1.858	Gravelly sand
B48ND9-D	46.62	44.34 ± 2.21	8.59 ± 2.06	0.45 ± 0.16	2.180	Muddy sandy gravel
B48NF4-C	0	44.51 ± 2.83	54.46 ± 2.81	1.04 ± 0.06	1.828	Sandy silt
B48NH0-H	0	19.73 ± 1.20	77.31 ± 1.21	2.96 ± 0.06	1.705	Sandy silt
B48NH0-I	0.14	29.12 ± 4.00	68.48 ± 3.79	2.26 ± 0.21	1.571[1]	Slightly gravelly sandy mud
B48NH7-C	71.85	17.18 ± 2.06	9.76 ± 1.80	1.21 ± 0.27	2.336	Muddy sandy gravel

Table 5 and Table 6 summarize the as-received MPs, determined using a WP4C water activity meter, and the GMC, determined by oven drying and weighing the sediments. MP is a measure of the energy status of the soil, representing the capillary and adsorptive forces that attract and bind water to soil particles. MP measurements were collected using the WP4C instrument by either subsampling soil from the core or using the filter paper method. Subsamples were collected from the top and bottom of each core. Where the filter paper method was used, only one MP measurement was collected. The filter paper method was superseded by the WP4C method to avoid unnecessarily disturbing the intact cores. Sample cores used in composites have as-received MP and GMC reported individually in the tables. The as-received gravimetric water contents of the core samples ranged from 0.8% to ~11.3%.

[1] Core B48NH0-I was partially full and did not occupy the entirety of liner volume at time of receipt. See Appendix A, Section A.2.18. The length of liner that was empty was not recorded for this sample, so when calculating DBD, it was assumed the sample occupied the entire volume of the liner. Therefore, the reported value should be considered a lower bound to the true value.

Table 5. As-received matric potential (MP) and gravimetric moisture content (GMC) for 200 East Area samples.

Sample ID	Matric Potential (MPa) Top of Core	Matric Potential (MPa) Bottom of Core	Matric Potential (MPa) Average[(a)]	Gravimetric Moisture Content (%)
B40DC4	-0.25	-0.28	-0.27	2.4
B41802	0.01	0.13	0.07	9.7
B41806 [(b), (c)]	-0.02	-	-	1.5
B41807 [(b), (c)]	0	-	-	1.1
B41809	0.01	0.02	0.02	2.9
B41868 [(b), (c)]	-0.03	-	-	1.9
B418C0	0.06	0.07	0.07	5.9
B418C2	0.04	0.05	0.05	3.0
B3YK00 [(b), (c)]	-0.03	-	-	1.6
B3YJY8 [(b), (c)]	-0.01	-	-	1.9
B3YJY9 [(b), (c)]	-0.07	-	-	1.8
B3YJX6	-7.76	-4.09	-5.93	2.2
B3YJY5	-0.86	-0.78	-0.82	2.5
B3YJX1	-72.7	-77.22	-74.96	0.8
B3YJD8	-0.38	-0.47	-0.43	2.4
B3YJD9	-0.77	-0.86	-0.82	2.6
B3YJH1[(b), (c)]	-0.05	-	-	3.1
B3YJH2 [(b), (c)]	-0.2	-	-	1.5
B3YJH3 [(b), (c)]	-1556.7	-	-	0.8
B3YJF8	-8.98	-	-	11.3

(a) Average MPa values are an arithmetic mean of the top and bottom soil samples.
(b) This sample was used in a composite sample.
(c) The filter paper method was used to measure matric potential. For most of these cores, only one measurement was taken.

Table 6. As-received matric potential (MP) and gravimetric moisture content (GMC) for 200 West Area samples.

Sample ID and Interval	Matric Potential (MPa)			Gravimetric Moisture Content (%)
	Top of Core	Bottom of Core	Average[(a)]	
B488V3-A	-2.96	-4.10	-3.53	0.8
B488V7-C	-0.04	-0.02	-0.03	5.9
B488Y1-H	-1.26	-0.64	-0.95	13.7
B488Y3-G	-2.81	-0.74	-1.78	5.1
B488Y4-C	-1.07	-0.79	-0.93	7.6
B488W5-D	-0.01	0.00	-0.01	8.8
B488W7-B	-2.67	-1.99	-2.33	4.6
B488X2-B	-0.19	-0.38	-0.29	2.9
B48N72-B	0.12	0.08	0.10	9.1
B48N73-B	-0.09	-0.07	-0.08	18.9
B48N74-I	-0.27	-0.10	-0.19	-
B48N76-H	-0.93	-0.67	-0.80	3.0
B48N79-B	-34.02	-40.01	-37.02	1.3
B48ND9-B	-0.20	-0.08	-0.14	4.4
B48ND9-D	-0.37	-0.11	-0.24	3.6
B48NF4-C	-0.20	-0.01	-0.11	8.8
B48NH0-H	0.00	0.05	0.03	16.3
B48NH0-I	-0.35	-0.31	-0.33	11.9
B48NH7-C	0.14	0.05	0.10	4.8

(a) Average MPa values are an arithmetic mean of the top and bottom soil samples.

4.2 Hydraulic Property Analysis

This section reports the results from hydraulic property measurements and associated parameter estimates. Results are provided only for samples that had hydraulic property measurements (refer to Table 1 and Table 2).

4.2.1 Saturated Hydraulic Conductivity (Ksat)

The Ksat of intact and repacked composite cores were determined using the falling head method (Section 2.3.2). Ksat is a measure of the rate at which water can move through sediments under fully water-saturated conditions, such as below the water table or possibly during past discharges of wastewater to cribs and trenches. Measurements were performed in triplicate, and two different reference head values were used in replicates. The means and standard deviations of the saturated hydraulic conductivity values reported in Table 7 and Table 8 represent the six falling head tests that were performed on each sample. The reported mean values of saturated hydraulic conductivity range from 4.20E-7 to 9.73E-1 cm/s.

Hydraulic property measurements were performed primarily on intact core samples. However, the very coarse nature of the some of the sampled intervals required the use of larger, custom-developed core holders into which the sediments from multiple Lexan liners were combined, and hydraulic property measurements were performed on the composite sediments (Table 7; composite 1, composite 2, and composite 3) for these coarser materials. Combining and homogenizing sediments from multiple intact core samples disturbs any structure that existed in the intact samples but allows for measurements to be made on these coarser materials that would not be possible otherwise. It is also expected that for the very coarse sediments, the Ksat values determined using the larger sample sizes should be more representative of field behavior.

Table 7. Saturated hydraulic conductivities Ksat (all units are cm/s) for 200 East Area samples.

Sample ID	Replicate 1[(a)]		Replicate 2[(a)]		Replicate 3[(a)]		Mean	Std Dev
B41802	3.74E-03	3.68E-03	3.71E-03	3.65E-03	3.67E-03	3.61E-03	3.68E-03	4.59E-05
B3YJY6	2.81E-02	2.84E-02	2.68E-02	2.72E-02	2.70E-02	2.81E-02	2.76E-02	6.66E-04
B3YJY7	5.49E-05	5.39E-02	5.36E-05	5.24E-05	5.35E-05	5.23E-05	5.34E-05	9.78E-07
B3YJY5	3.83E-02	3.77E-02	3.80E-02	3.74E-02	3.80E-02	3.75E-02	3.78E-02	3.37E-04
B3YJX2	3.58E-06	3.53E-06	3.70E-06	3.69E-06	3.91E-06	3.90E-06	3.72E-06	1.59E-07
B3YJF9	9.50E-04	9.44E-04	9.49E-04	9.25E-04	9.42E-04	9.21E-04	9.38E-04	1.24E-05
B3YJH0	1.17E-05	1.14E-05	1.13E-05	1.12E-05	1.15E-05	1.10E-05	1.13E-05	2.49E-07
Composite1 (B41806, B41807, B41868)	9.00E-01	1.03E+00	9.07E-01	1.02E+00	9.29E-01	1.06E+00	9.73E-01	6.92E-02
Composite 2 (B3YK00, B3YJY8, B3YJY9)	6.92E-01	7.83E-01	7.17E-01	8.31E-01	6.63E-01	6.87E-01	7.29E-01	6.48E-02
Composite3 (B3YJH1, B3YJH2, B3YJH3)	6.61E-02	7.61E-02	8.29E-02	9.16E-02	9.10E-02	1.01E-01	8.47E-02	1.24E-02

(a) Hydraulic conductivities were calculated with respect to an upper and lower reference head, the values of which varied by core.

Table 8. Saturated hydraulic conductivities Ksat (all units are cm/s) for 200 West Area samples.

Sample ID and Interval	Replicate 1[(a)]		Replicate 2[(a)]		Replicate 3[(a)]		Mean	Std Dev
B488V7-C	1.00E-04	9.79E-05	1.01E-04	9.95E-05	1.03E-04	1.01E-04	1.00E-04	1.59E-06
B488Y3-G	6.40E-03	6.09E-03	5.81E-03	5.61E-03	5.56E-03	5.42E-03	5.81E-03	3.72E-04
B488Y4-C	1.32E-04	1.29E-04	1.28E-04	1.26E-04	1.27E-04	1.24E-04	1.28E-04	2.61E-06
B488W5-D	3.69E-05	3.60E-05	3.47E-05	3.34E-05	3.38E-05	3.26E-05	3.46E-05	1.63E-06
B488W7-B	2.01E-04	1.94E-04	1.85E-04	1.79E-04	1.76E-04	1.72E-04	1.85E-04	1.09E-05
B48N72-B	1.47E-05	1.44E-05	1.46E-05	1.42E-05	1.44E-05	1.40E-05	1.44E-05	2.31E-07
B48N73-B	4.22E-07	4.06E-07	4.30E-07	4.20E-07	4.25E-07	4.15E-07	4.20E-07	8.19E-09
B48N74-I	1.75E-05	1.73E-05	1.79E-05	1.77E-05	1.82E-05	1.81E-05	1.78E-05	3.48E-07
B48N76-H	3.62E-04	3.59E-04	3.57E-04	3.53E-04	3.56E-04	3.53E-04	3.57E-04	3.68E-06
B48N79-B	8.90E-04	8.29E-04	8.00E-04	7.63E-04	7.56E-04	7.22E-04	7.93E-04	6.01E-05
B48ND9-B	1.11E-02	1.09E-02	1.07E-02	1.06E-02	1.06E-02	1.06E-02	1.07E-02	1.89E-04
B48NF4-C	1.76E-05	1.74E-05	1.75E-05	1.73E-05	1.77E-05	1.75E-05	1.75E-05	1.46E-07
B48NH0-H	3.02E-04	2.97E-04	3.00E-04	2.95E-04	2.97E-04	2.93E-04	2.97E-04	3.29E-06
B48NH0-I	1.27E-04	1.24E-04	1.24E-04	1.22E-04	1.21E-04	1.19E-04	1.23E-04	2.87E-06

(a) Hydraulic conductivities were calculated with respect to an upper and lower reference head, the values of which varied by core.

4.2.2 Water Retention Characteristics

MS outflow experiments (Section 2.4.1) were performed on selected intact cores (refer to Table 1 and Table 2) and three composite cores of repacked sediments from the 200 East Area to determine water retention characteristics under quasi-static conditions and to estimate hydraulic properties from the dynamic pressure and outflow data. The van Genuchten (1980) and Brooks and Corey (1964) water retention models were used to fit the quasi-static data from each sample using the Excel solver to estimate model parameters. Quasi-static data for each core sample consisted of the water retention data from the MS outflow experiments and a combination of the MS data plus data from subsamples of the cores that were collected under drier conditions after the end of the experiments using a WP4C water activity meter (MS+WP4C). Therefore, van Genuchten and Brooks and Corey model fits are provided for the datasets (MS and MS+WP4C), resulting in two sets of parameters for each water retention model. Appendix D provides plots of the quasi-static water retention data and model fits for 200 East and West area core samples.

The most appropriate set of parameters, based on fits to the MS or combined MS+WP4C data sets, will depend on the application. For near-surface water balance modeling of Hanford waste sites, for which drier conditions usually prevail, the parameters representing the fits to the combined MS+WP4C data should generally be preferrable. For deep vadose zone or aquifer sediments that are relatively moist, or water saturated, either set of parameters may suffice. The fits to the MS data alone tend to be slightly better than the fits to the combined MS+WP4C data sets owing to some scatter in the WP4C data.

The θ_s values given in Table 9 to Table 12 are smaller for some samples than the values of porosity calculated from the total volume of water contained in the saturated samples and their sample volume, due to corrections made to account for apparent wall effects. Specifically, early in the experiments, if the tensiometers indicated that the cores were still fully water-saturated, but outflow was occurring, it was assumed that this outflow was a result of sampling-induced disturbance that created void space and gravity drainage along the walls of the core, rather than from pores within the sediment. The volumes of water ascribed to wall flow were generally small but were omitted from the water outflow volumes that were used as observational data, resulting in θ_s values that are typically lower (1% to 3%) than the values of porosity calculated from the total volume of water contained in the saturated samples and their sample volume.

4.2.2.1 Brooks-Corey Water Retention Parameters

Table 9 and Table 10 show the best-fit Brooks-Corey model water retention parameters for intact and composite core samples from the 200 East and West areas. For the Brooks-Corey model, when only the MS data were used, the air-entry pressures, h_b, for the samples ranged from ~4 to ~203 cm. When the combined MS+WP4C data were used, the air-entry pressures for the samples ranged from ~4 to ~300 cm. Using the MS+WP4C data usually resulted in smaller fitted values of the residual water content, θ_r. In all cases, the saturated water content values, θ_s, were fixed rather than fitted. The parameters resulting from fitting the quasi-static retention data for the combined MS+WP4C datasets are generally expected to be more broadly useful, relative to the parameters from fitting the quasi-static MS data only, since the MS+WP4C data cover a wider range of conditions.

Table 9. Brooks-Corey model parameters fit to quasi-static water retention data from multistep (MS) and combined MS+WP4C measurements for 200 East Area samples.

	MS			MS+WP4C			
Sample ID	h_b (cm)	λ	θ_r	h_b (cm)	λ	θ_r	θ_s[(a)]
B41802	28.9717	1.6416	0.0871	26.717	1.162	0.0614	0.3834
B3YJY6	8.2357	0.9823	0.0894	6.3233	0.3996	0.0254	0.2979
B3YJY7	41.2956	0.0788	0.0000	25.3495	0.0591	0	0.2749
B3YJY5	7.7073	0.874	0.0713	5.2544	0.4531	0.0299	0.2915
B3YJX2	46.1428	0.1325	0.0000	145.1033	0.3183	0	0.2258
B3YJF9	82.0183	1.1155	0.0000	82.2033	1.223	0.0247	0.4483
B3YJH0	153.2695	0.2303	0.0000	142.8235	0.2446	0	0.2947
Composite 1 (B41806, B41807, B41868)	N/A	N/A	N/A	N/A	N/A	N/A	N/A
Composite 2 (B3YK00, B3YJY8, B3YJY9)	3.9664	0.1800	0.0000	3.9223	0.1884	0.0076	0.2022
Composite 3 (B3YJH1, B3YJH2, B3YJH3)	9.2253	0.1789	0.0000	10.1324	0.1904	0.0000	0.2805

(a) θ_s was fixed to account for apparent wall effects that were observed in the MS data for some samples.

Table 10. Brooks-Corey model parameters fit to quasi-static data from multistep (MS) and combined MS +WP4C measurements for 200 West Area samples.

Sample ID and Interval	MS			MS+WP4C			θ_s[(a)]
	h_b (cm)	λ	θ_r	h_b (cm)	λ	θ_r	
B488V7-C	33.0299	0.9652	0.0832	43.2639	1.2744	0.0640	0.2804
B488Y3-G	18.6873	0.9034	0.0685	14.7993	0.5112	0.0149	0.3401
B488Y4-C	46.0113	0.2898	0.0000	51.0470	0.3319	0.0000	0.3889
B488W5-D	8.3465	0.3421	0.0511	8.1284	0.2288	0.0000	0.2215
B488W7-B	47.3414	0.2095	0.0000	49.9149	0.2215	0.0000	0.3207
B48N72-B	38.2761	0.9026	0.0978	27.4785	0.3268	0.0125	0.2608
B48N73-B	202.8454	0.0996	0.0000	300.1572	0.1920	0.0000	0.3800
B48N74-I	117.7514	0.4855	0.0000	118.9426	0.5593	0.0335	0.3701
B48N76-H	12.3084	0.2407	0.0000	13.4616	0.2561	0.0000	0.2672
B48N79-B	15.8058	0.9009	0.0779	9.5535	0.3554	0.0148	0.2597
B48ND9-B	9.9055	0.9475	0.0747	5.7536	0.3635	0.0215	0.2518
B48NF4-C	107.2766	0.3581	0.0000	198.6818	1.2084	0.0627	0.3884
B48NH0-H	19.4986	0.0818	0.0000	97.0913	0.2282	0.0000	0.3938
B48NH0-I	23.3461	0.1724	0.0000	25.3171	0.1837	0.0000	0.4244

(a) θ_s was fixed to account for apparent wall effects that were observed in the MS data for some samples.

4.2.2.2 van-Genuchten Water Retention Parameters

Table 11 and Table 12 present the fitted van Genuchten model parameters for 200 East and West area core samples. The 200 East Area Composite 1 sample was omitted from parameter estimation using quasi-static data because, due to its very coarse nature, nearly half of the water contained in the core drained before the tensiometers indicated that the core was unsaturated.

Appendix D shows comparisons of the van Genuchten and Brooks-Corey model fits to the quasi-static water retention data for each of the core samples. In general, both models provide good fits to the water retention data. The Brooks-Corey model tends to provide somewhat better fits if the sediment has a distinct air-entry pressure, and the van Genuchten model tends to provide better fits if the sediment drains more gradually with increasing pressure.

Table 11. van-Genuchten model parameters assuming quasi-static conditions for multistep (MS) and combined MS+WP4C measurements for 200 East Area samples.

Sample ID	MS			MS+WP4C			θ_s[a]
	α (1/cm)	n	θ_r	α (1/cm)	n	θ_r	
B41802	0.0245	3.8686	0.0965	0.0249	2.926	0.0714	0.3834
B3YJY6	0.054	2.9247	0.0956	0.1614	1.3818	0.0231	0.2979
B3YJY7	0.0085	1.1247	0.0000	0.0265	1.0899	0.0666	0.2749
B3YJY5	0.0853	2.2186	0.0770	0.1701	1.4628	0.0296	0.2915
B3YJX2	0.0085	1.8492	0.1395	0.0043	1.3517	0.0000	0.2258
B3YJF9	0.0084	4.8447	0.1182	0.0078	3.2601	0.0298	0.4483
B3YJH0	0.0026	2.2049	0.1284	0.0028	1.3383	0.0019	0.2947
Composite 1 (B41806, B41807, B41868)	N/A	N/A	N/A	N/A	N/A	N/A	N/A
Composite 2 (B3YK00, B3YJY8, B3YJY9)	0.1487	1.2327	0.0143	0.1540	1.2366	0.0184	0.2022
Composite 3 (B3YJH1, B3YJH2, B3YJH3)	0.0330	1.2886	0.0000	0.0404	1.2580	0.0005	0.2805

(a) θ_s was fixed to account for wall effects that were observed in the MS data for some samples.

Table 12. van-Genuchten model parameters assuming quasi-static conditions for multistep (MS) and combined MS+WP4C measurements for 200 West Area samples.

Sample ID and Interval	MS			MS+WP4C			θ_s[a]
	α (1/cm)	n	θ_r	α (1/cm)	n	θ_r	
B488V7-C	0.0191	2.7719	0.0971	0.0251	1.5378	0.0207	0.2804
B488Y3-G	0.0342	2.4434	0.0817	0.0474	1.6072	0.0194	0.3401
B488Y4-C	0.0101	1.7306	0.1078	0.0086	1.5080	0.0078	0.3889
B488W5-D	0.0628	1.6075	0.0759	0.0860	1.2513	0.0000	0.2215
B488W7-B	0.0069	1.3922	0.0000	0.0085	1.3577	0.0220	0.3207
B48N72-B	0.0159	2.7369	0.1110	0.0229	1.4030	0.0182	0.2608
B48N73-B	0.0026	3.1851	0.3214	0.0009	1.2861	0.0000	0.3800
B48N74-I	0.0046	3.2775	0.1472	0.0040	2.1185	0.0459	0.3701
B48N76-H	0.0473	1.2890	0.0000	0.0415	1.3238	0.0058	0.2672
B48N79-B	0.0420	2.3239	0.0846	0.0795	1.3915	0.0165	0.2597
B48ND9-B	0.0604	2.5731	0.0808	0.1589	1.3662	0.0210	0.2518
B48NF4-C	0.0048	2.5485	0.1672	0.0042	1.6826	0.0279	0.3884
B48NH0-H	0.0177	1.1243	0.0000	0.0054	1.2839	0.0000	0.3938
B48NH0-I	0.0193	1.4234	0.1405	0.0190	1.2867	0.0491	0.4244

(a) θ_s was fixed to account for wall effects that were observed in the MS data for some samples.

4.2.3 Unsaturated Hydraulic Conductivity (Kunsat)

The results in the previous section represent the water retention characteristics of the core samples for quasi-static conditions. These water retention parameters can be used together with the experimentally determined Ksat values and theoretical relative permeability models, such as those developed by Mualem (1976) and Burdine (1956), to estimate Kunsat. Alternatively, transient outflow and capillary pressure data obtained from the MS outflow experiments can be used in conjunction with a flow simulator to estimate hydraulic parameters by inverse modeling. In this study, the water-air mode of the Subsurface Transport Over Multiple Phases simulator (White and Oostrom 2006), referred to as STOMP-WA, was used to simulate the MS outflow experiments and PEST (Doherty 2016) was used for parameter estimation.

Input files for STOMP-WA were developed to be consistent with measured physical properties (i.e., density and porosity) and dimensions (i.e., lengths and cross-sectional areas) of the core samples used in the experiments. Upper and lower boundary conditions were specified to correspond with the gas pressures that were applied to the tops of the columns, and to the aqueous pressures that were maintained at the bottoms of the columns during the experiments, respectively. Each MS outflow experiment used a porous plate at the bottom of the core, which was accounted for in the model setup. The Ksat values of the porous plates were independently measured, and their values were specified in the STOMP-WA input files. Observation locations for output of simulated capillary pressures were specified to correspond with the locations of tensiometers in the core samples. Flux plane output was also specified for the bottom boundary of the model domain for comparisons to water outflow data from the experiments.

Table 13 and Table 14 list the van Genuchten α, n, θ_r and θ_s parameters determined by inverse modeling of the MS outflow experiments for intact and repacked composite core samples from the 200 East and West areas, respectively. STOMP-WA uses the residual saturation, S_r (= θ_r/θ_s), instead of θ_r, so the latter were computed from the estimated values of S_r and porosity or saturated water content, θ_s. The parameters θ_s and the Ksat were fixed at their independently determined values. The parameters listed in Table 13 and Table 14 differ somewhat from those that were determined by fitting the quasi-static water retention data (Tables 11 and 12), as expected, since the inverse modeling uses the dynamic data and pressure controls that were applied during the experiments.

Appendix E shows results for the simulated and observed water outflow and aqueous pressure. For all the samples, inverse modeling was performed first using both the capillary pressure data from the two tensiometers in each core and the outflow data as observational data. In some cases, observed and simulated results did not match well for all variables, so inverse modeling was repeated using only the observed outflow data. The boundary conditions used in the experiments are well prescribed and constrained, so using only the outflow data for observations is still expected to yield reasonable parameter estimates. In Table 13 and Table 14, the column labeled as “Data” indicates if the observation data included both capillary pressure and outflow data (P+O) or just outflow data (O).

Each experiment was modeled as a homogeneous porous medium with uniform properties. Mismatches between observed and simulated results are assumed to be attributable primarily to sample heterogeneities. If a sample is highly heterogeneous, which most are (see Appendix A), some discrepancies between observed and simulated results should be expected.

Table 13. Hydraulic parameters estimated by inverse modeling for the van Genuchten (1980) water retention model and Mualem (1976) relative permeability model for 200 East Area samples. P+O = capillary pressure + outflow data, O = outflow data only.

Sample ID	Data	α (1/cm)	n (-)	θ_r (-)	θ_s[a] (-)	K_{sat}[a](cm/s)
B41802	P+O	0.0142	1.7664	0.0000	0.3834	3.68E-3
B3YJY6	P+O	0.0132	1.7998	0.0116	0.2979	2.76E-2
B3YJY7	P+O	0.0069	1.3037	0.1100	0.2749	5.34E-5
B3YJY5	P+O	0.0112	1.7171	0.0000	0.2915	3.78E-2
B3YJX2	P+O	0.0055	1.7322	0.0903	0.2258	3.72E-6
B3YJF9	P+O	0.0082	3.9574	0.0824	0.4483	9.39E-4
B3YJH0	P+O	0.0028	1.4079	0.0017	0.2947	1.14E-5
Composite 1 (B41806, B41807, B41868)	O	1.1994	2.0040	0.0025	0.2816	9.73E-1
Composite 2 (B3YK00, B3YJY8, B3YJY9)	O	0.1330	1.2956	0.0039	0.2022	7.29E-1
Composite 3 (B3YJH1, B3YJH2, B3YJH3)	P+O	0.0235	1.3946	0.0000	0.2805	8.47E-2

(a) θ_s was fixed to account for wall effects that were observed in the MS data for some samples, and Ks was fixed at independently determined values.

Table 14. Hydraulic parameters estimated by inverse modeling for the van Genuchten (1980) water retention model and Mualem (1976) relative permeability model for 200 West Area samples. P+O = capillary pressure + outflow data, O = outflow data only.

Sample ID and Interval	Data	α (1/cm)	n (-)	θ_r (-)	θ_s[(a)] (-)	K_{sat}[(a)](cm/s)
B488V7-C	O	0.0205	2.0000	0.0600	0.2830	1.00E-4
B488Y3-G	O	0.0331	2.3761	0.0602	0.3460	5.82E-3
B488Y4-C	P+O	0.0061	1.6123	0.0028	0.3920	1.28E-4
B488W5-D	O	0.0845	1.7963	0.0013	0.2480	3.46E-5
B488W7-B	P+O	0.0049	1.5181	0.0003	0.3210	1.85E-4
B48N72-B	O	0.0188	2.0000	0.0642	0.2630	1.44E-5
B48N73-B	P+O	0.0013	1.5000	0.0427	0.3880	4.20E-7
B48N74-I	P+O	0.0041	1.8742	0.0047	0.3790	1.78E-5
B48N76-H	O	0.0375	1.4277	0.0000	0.2740	3.57E-4
B48N79-B	O	0.0402	2.0900	0.0681	0.2610	7.93E-4
B48ND9-B	P+O	0.0480	1.4521	0.0097	0.2670	1.08E-2
B48NF4-C	P+O	0.0047	1.6428	0.0192	0.4110	1.75E-5
B48NH0-H	P+O	0.0141	1.2910	0.1313	0.4090	2.97E-4
B48NH0-I	P+O	0.0086	1.3882	0.0000	0.4350	1.23E-4

(a) θ_s was fixed to account for wall effects that were observed in the MS data for some samples, and Ks was fixed at independently determined values.

4.2.4 Recommendations for Hydraulic Parameter Selection

For Hanford Site vadose zone flow and transport modeling applications, the parameters listed in Tables 13 and 14 are recommended. These parameters were generated by inverse modeling of the MS outflow experiments. The parameters listed in Tables 11 and 12 provide alternative parameter estimates that are based on fitting quasi-static water retention data from the combined MS+WP4C data sets. The parameters in Tables 11-14 represent the van Genuchten (1980) and Mualem (1976) models which are the most commonly used water retention and relative permeability models for Hanford Site flow and transport modeling applications.

5.0 Summary and Conclusions

The objectives of this study were to characterize the physical and hydraulic properties of sediment samples collected from Resource Conservation and Recovery Act (RCRA) boreholes drilled in the 200 East and 200 West areas of the Hanford. The analyzed core samples come from specific areas and depth intervals at the Hanford Site that were targeted for sampling to address data gaps identified by site contractors (Khaleel 2020).

X-ray computed tomography (XCT) was used to evaluate the general textural characteristics of the samples and to determine which samples to use for further physical and hydraulic property characterization. Subsequent sample selection was determined by consensus after review of the XCT images by PNNL, CPCCo, and INTERA staff.

The sediments characterized in this effort represent a very wide variety of materials. Characterization data that were generated included gravimetric water contents and matric potentials, grain-size distributions, saturated hydraulic conductivity, water retention characteristics, and unsaturated hydraulic conductivity. Sediment textures ranged from cobble and gravel to sandy silt. Saturated hydraulic conductivity values ranged over six orders of magnitude, from 9.73E-1 to 4.2E-7 cm/s, and porosities ranged from ~0.2 to ~0.45. Hydraulic property measurements were performed primarily on intact core samples. However, the very coarse nature of some of the sampled intervals required the use of larger, custom-developed core holders into which the sediments from multiple Lexan liners were combined. Hydraulic property measurements were performed on the composite sediments for these coarser materials.

The physical and hydraulic properties generated for this study provide site-specific data and parameters that can be used in subsurface flow and contaminant transport models to assess the transport and fate of contaminants in the vadose zone and underlying aquifer systems. The hydraulic parameters listed in Tables 13 and 14 are recommended for general Hanford Site flow and transport modeling applications.

6.0 Quality Assurance

This work was performed in accordance with the PNNL Nuclear Quality Assurance Program (NQAP). The NQAP complies with the DOE Order 414.1D, *Quality Assurance*. The NQAP uses NQA-1-2012, *Quality Assurance Requirements for Nuclear Facility Application*, as its consensus standard and NQA-1-2012, Subpart 4.2.1 as the basis for its graded approach to quality.

7.0 References

ASTM D4464-15, 2009. *Standard Test Method for Particle Size Distribution of Catalytic Materials by Laser Light Scattering*. ASTM International, West Conshohocken, PA. www.astm.org.

Brooks RH and AT Corey. 1964. "Hydraulic properties of porous media." *Hydrol. Pap. 3*, Colorado State University, Fort Collins.

Burdine NT. 1953. "Relative permeability calculations from pore-size distribution data." *Trans. Amer. Inst. Mining Met. Petrol. Eng*., 198, 71–77, 1953.

Dane JH and JW Hopmans. 2002. "Water Retention and Storage." In Dane JH and GC Top (eds.), *Methods of Soil Analysis, Part 4, Physical Methods*. Book Series No. 5. Soil Science Society of America, Madison, WI. pp. 671-796.

DOE Order 414.1D, *Quality Assurance*. U.S. Department of Energy, Washington, D.C.

Doherty J. 2016. *PEST – Model-Independent Parameter Estimation, User Manual Part 1: PEST, SENSAN, and Global Optimizers*. Sixth Edition, Watermark Numerical Computing, Australia.

Durner W. 1994. "Hydraulic conductivity estimation for soils with heterogeneous pore structure." *Water Resour. Res*. 30:211-223.

Eching SO and JW Hopmans. 1993a. "Optimization of hydraulic functions from transient outflow and soil water pressure data." *Soil Sci. Soc. Am. J.* 57:1167-1175.

Eching SO and JW Hopmans. 1993b. *Inverse solution of unsaturated soil hydraulic functions from transient outflow and soil water pressure data*. Land, Air and Water Resources Report No. 100021, University of California, Davis.

Eching SO, JW Hopmans, and O Wendroth. 1994. "Unsaturated hydraulic conductivity from transient multi-step outflow and soil water pressure data." *Soil Sci. Soc. Am. J.* 58:687-695.

Flint AL and LE Flint. 2002. "Porosity". In Dane JH and GC Topp G.C (eds), *Methods of Soil Analysis, Part 4, Physical Methods*. Book Series No. 5. Soil Science Society of America, Madison, WI, pp. 241-254.

Gee GW and D Or. 2002. "Particle-Size Analysis." In Dane JH and GC Top (eds.), *Methods of Soil Analysis, Part 4, Physical Methods*. Book Series No. 5. Soil Science Society of America, Madison, WI. pp. 201-228.

Hopmans JW, J Simunek, N Romano, and W Durner. 2002. "Inverse Methods." In JH Dane and CT Topp (eds.), *Methods of Soil Analysis Part 4 Physical Methods*. Soil Science Society of America, Madison, WI. pp. 963-1008.

Khaleel, R. 2020. Vadose Zone Flow and Transport Parameters Data Package for the Hanford Site Composite Analysis. CP-63883 Rev 0, CH2MHill Plateau Remediation Company, Richland, WA.

Kool JB and JC Parker. 1988. "Analysis of the inverse problem for transient unsaturated flow." *Water Resour. Res.* 24:817-830.

Levenberg K. 1944. "A method for the solution of certain non-linear problems in least squares." *Quart. Appl. Math*. 2(2):164-168.

Marquardt DW. 1963. "An algorithm for least-squares estimation of nonlinear parameters." *J. Soc. Indust. Appl. Math.* 11(2):431-441.

Mualem Y. 1976. "A new model for predicting the hydraulic conductivity of unsaturated porous media." *Water Resour. Res.* 12(3):513-522.

NQA-1-2012, *Quality Assurance Requirements for Nuclear Facility Application*. American Society of Mechanical Engineers, New York, NY.

Priesack E and W Durner. 2006. "Closed-form expression for multi-modal unsaturated hydraulic conductivity function." *Vadose Zone J.* 5:121-124.

Reynolds WD and DE Elrick. 2002. "Constant Head Soil Core (Tank) Method.", In JH Dane and G Clarke Topp (eds.), *Methods of Soil Analysis, Part 4 – Physical Methods*. Soil Science Society of America, Madison, WI. pp. 804-808.

Richards LA. 1931. "Capillary conduction of liquids through porous mediums." *Physics* 1(5), pp. 318-333.

Rockhold ML, MJ Fayer, and PR Heller. 1993. *Physical and Hydraulic Properties of Sediments and Engineered Materials Associated with Grouted Double-Shell Tank Waste Disposal at Hanford*. PNL-8813, Pacific Northwest Laboratory, Richland, WA.

Rockhold ML, FA Spane, TW Wietsma, DR Newcomer, RE Clayton, I Demirkanli, DL Saunders, MJ Truex, MM Valenta-Snyder, and CJ Thompson. 2018. *Physical and Hydraulic Properties of Sediments from the 200-DV-1 Operable Unit*. PNNL-27846, Pacific Northwest National Laboratory, Richland, WA.

Springer SD. 2020. *Central Plateau Vadose Zone Geoframework*. ECF-HANFORD-18-0035, Rev. 0, CH2M Hill Plateau Remediation Company, Richland, WA.

Tuli A, MA Denton, JW Hopmans, T Harter, and JL MacIntyre. 2001. *Multi-Step Outflow Experiment: From Soil Preparation to Parameter Estimation*. Land, Air and Water Resources Report No. 100037, University of California, Davis.

van Genuchten M Th. 1980. "A closed-form equation for predicting the unsaturated hydraulic conductivity of unsaturated soils." *Soil Sci. Soc. Am. J* 44:892-898.

Webb SW. 2000. "A simple extension of two-phase characteristic curves to include the dry region." *Water Resour. Res*. 36(6):1425-1430. https://doi.org/10.1029/2000WR900057.

White MD and M Oostrom. 2006. *STOMP – Subsurface Transport Over Multiple Phases, Version 4.0 User's Guide*. PNNL-15782, Pacific Northwest National Laboratory, Richland, WA.

Wietsma TW, M Oostrom, MA Covert, TA Queen, and MJ Fayer. 2009. "An automated tool for three types of hydraulic conductivity laboratory measurements." *Soil Sci. Soc. Am. J.* 73(2):466-470.

Wildenschild D and AP Sheppard. 2013. "X-ray imaging and analysis techniques for quantifying pore-scale structure and processes in subsurface porous medium systems." *Adv. Water Resour*. 51:217-246.

Appendix A – XCT Images

This appendix shows X-ray computed tomography (XCT) images for each of the cores listed in Table 1 and Table 2 of the main report. Hundreds of images were collected for each core as side and top views. For each core, three images are shown: (1) a center slice through the long axis of the core, (2) a top view 1/3 of the way up from the bottom of the core, and (3) a top view 2/3 of the way up from the bottom of the core.

A.1 200 East Cores

A.1.1 B40DC4 (D0049 / 180.3-182.8 ft bgs / CCUg)

a) B40DC4_side_view_0665

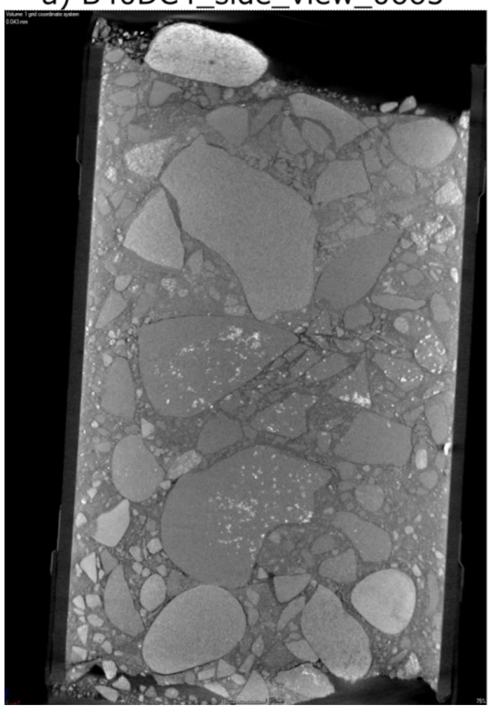

b) B40DC4_top_view_0641

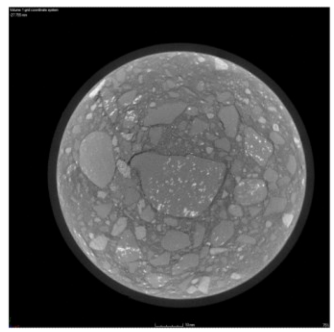

c) B40DC4_top_view_1282

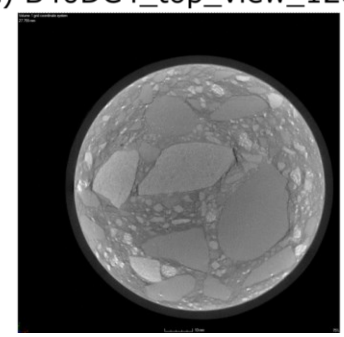

A.1.2 B41802 (D0056 / 40.5-42.7 ft bgs / Hf1)

a) B41802_side_view_00000674

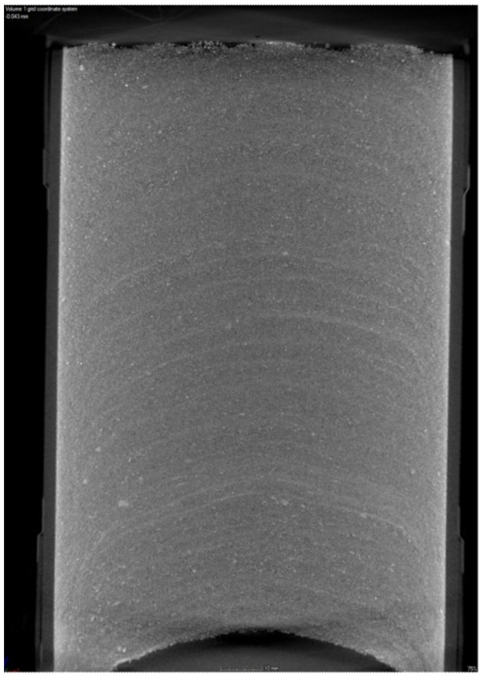

b) B41802_top_view_0628

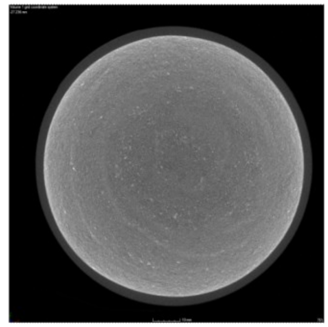

c) B41802_top_view_1256

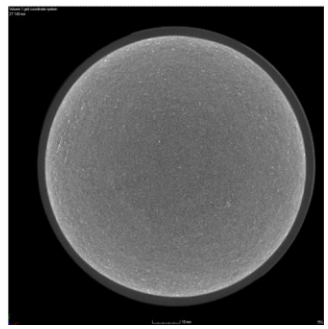

A.1.3 B41806 (D0056 / 159.5-161.7 ft bgs / Hf3)

a) B41806_side_view0659

b) B41806_Top_view_0622

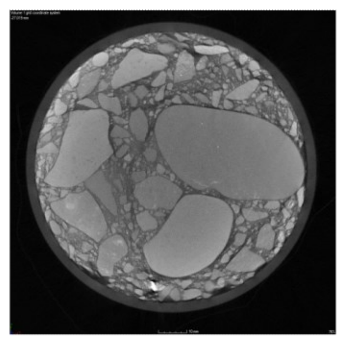

c) B41806_Top_view_1245

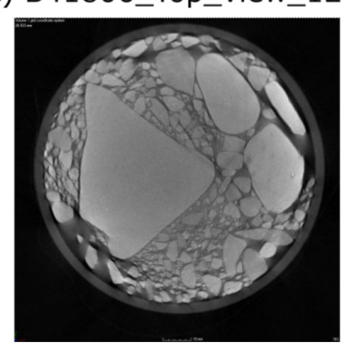

A.1.4 B41807 (D0056 / 199.5-201.7 ft bgs / Hf3)

a) B41807_side_view_0680

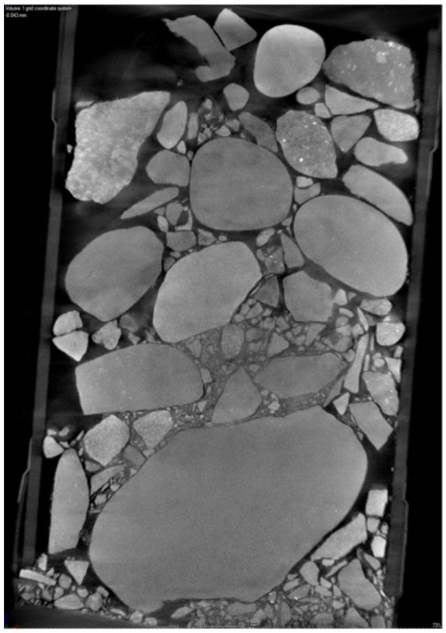

b) B41807_top_view_0652

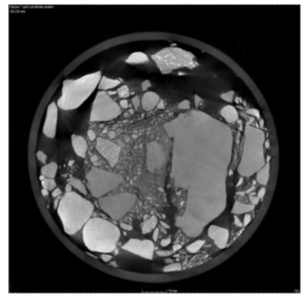

c) B41807_top_view_1304

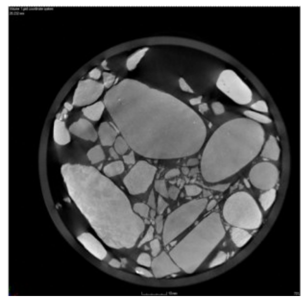

A.1.5 B41809 (D0056 / 250.2-252.4 ft bgs / CCU)

a) B41809_side_0662

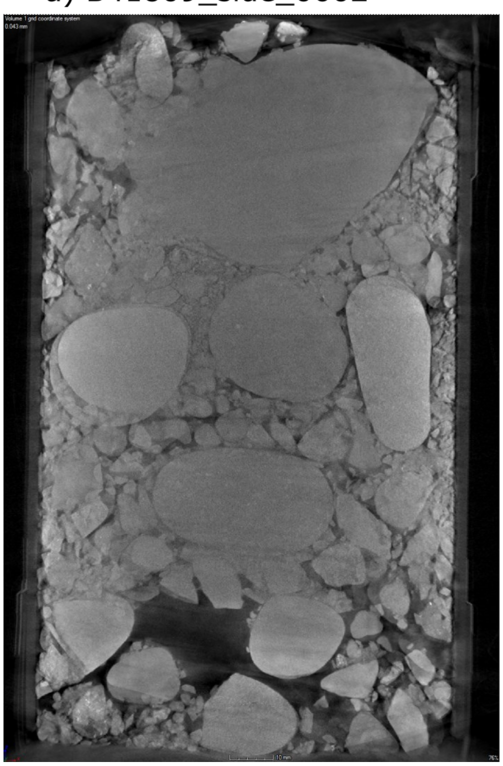

b) B41809_top_0662

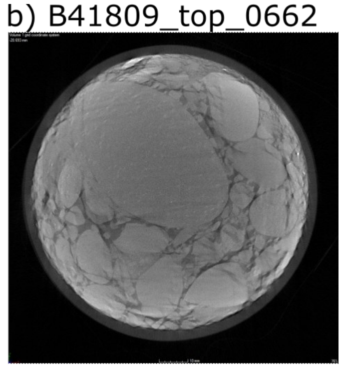

c) B41809_top_1324

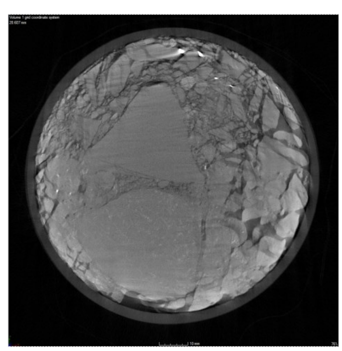

A.1.6 B41868 (D0057 / 150-152.2 ft bgs / Hf3)

a) B41868_Side_view_0674

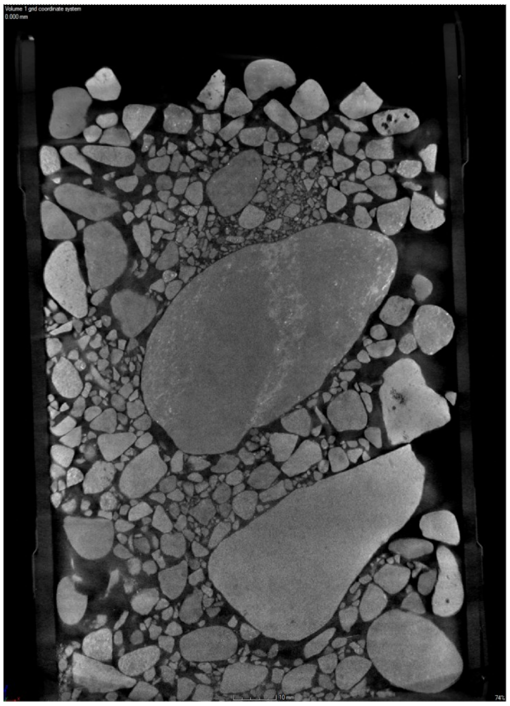

b) B41868_Top_view_0624

c) B41868_Top_view_1248

A.1.7 B418C0 (D0058 / 188.4-190.6 ft bgs / CCU)

a) B418C0_side_0690

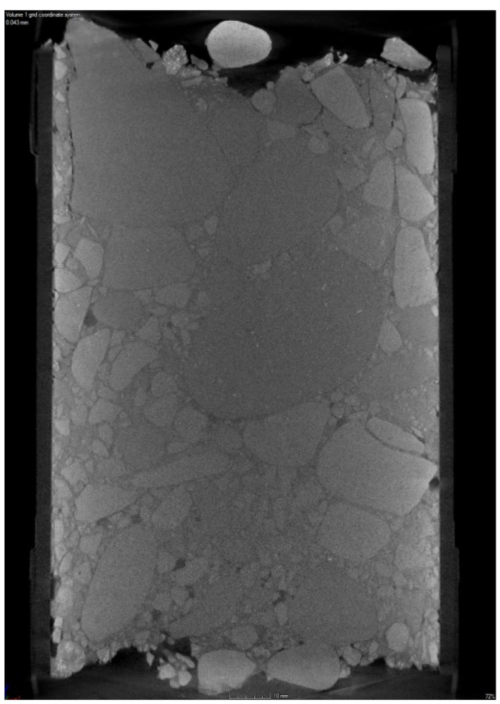

b) B418C0_top_0650

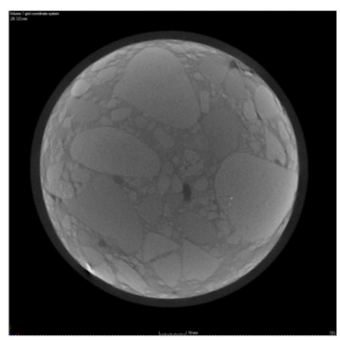

c) B418C0_top_1299

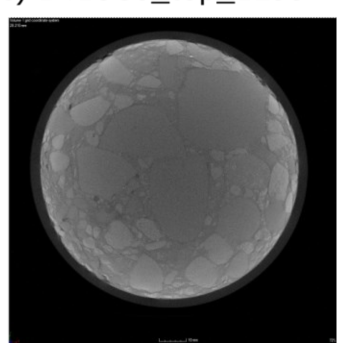

A.1.8 B418C2 (D0058 / 207.1-209.3 ft bgs / CCU)

a) B418C2_side_0755

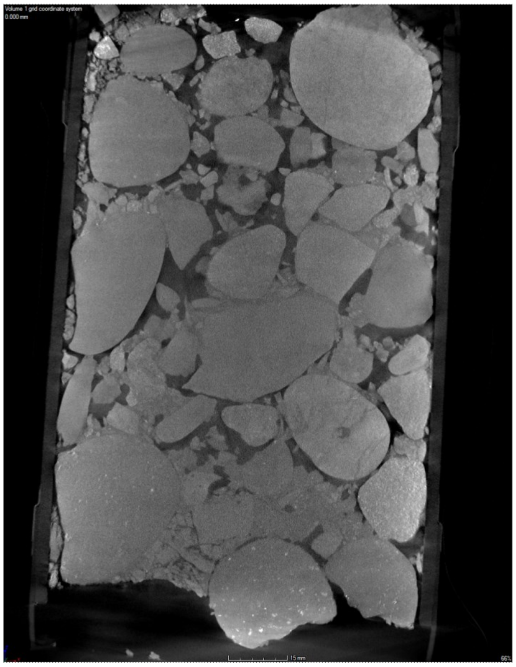

b) B418C2_top_0650

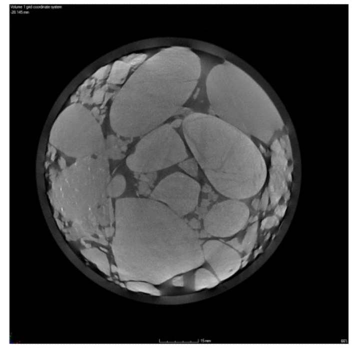

c) B418C2_top_1300

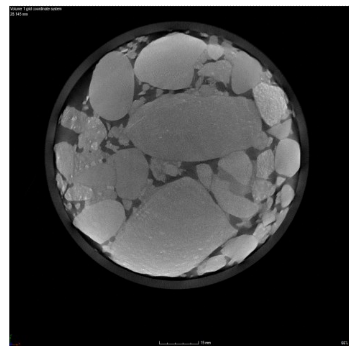

A.1.9 B3YK00 (D0059 / 270-272.5 ft bgs / CCUg)

a) B3YK00_side_0686

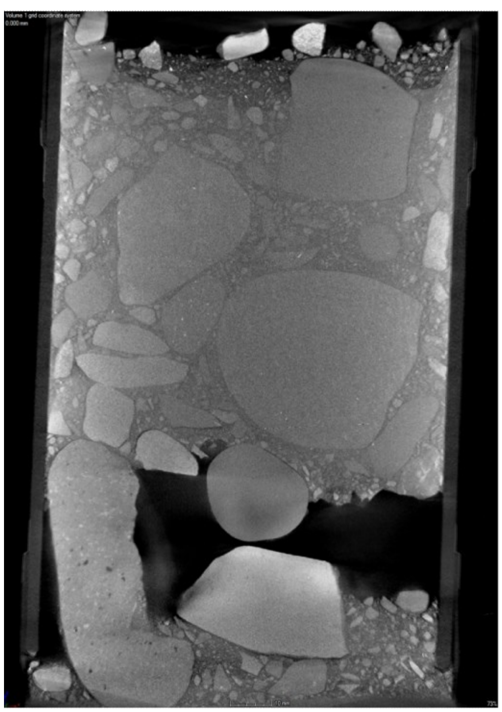

b) B3YK00_top_0644

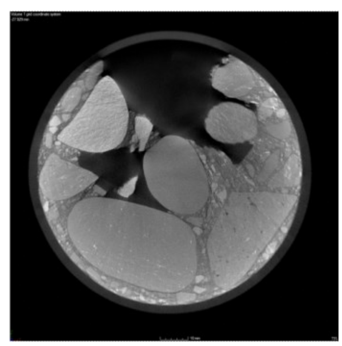

c) B3YK00_top_1289

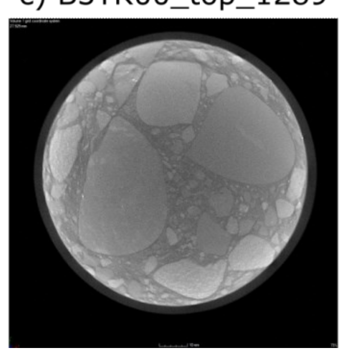

A.1.10 B3YJY6 (D0059/ 209.4- 211.9 ft bgs / Hf3)

a) B3YJY6_side_0669

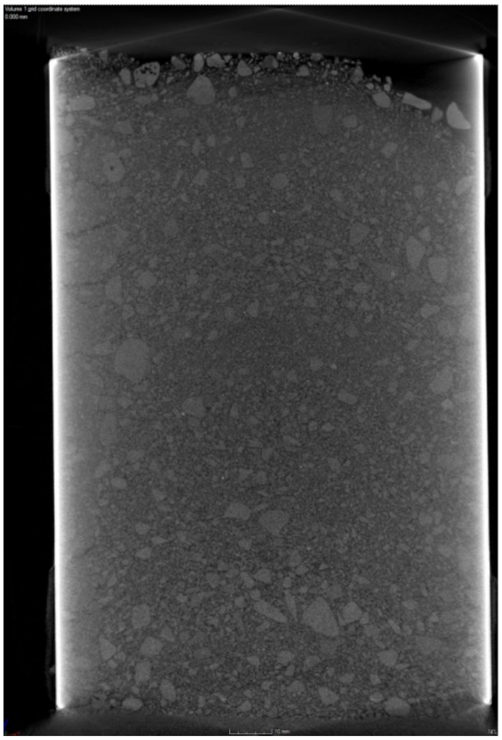

b) B3YJY6_top_0666

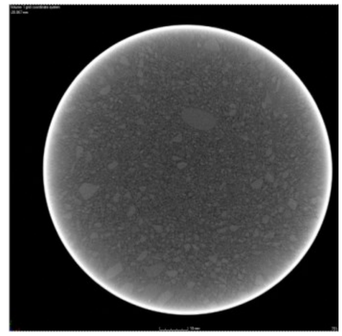

c) B3YJY6_top_1333

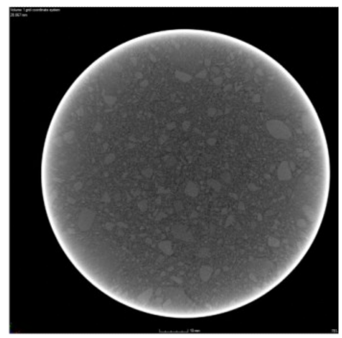

A.1.11 B3YJY7 (D0059/ 219.5- 222 ft bgs / CCU)

a) B3YJY7_side_0696

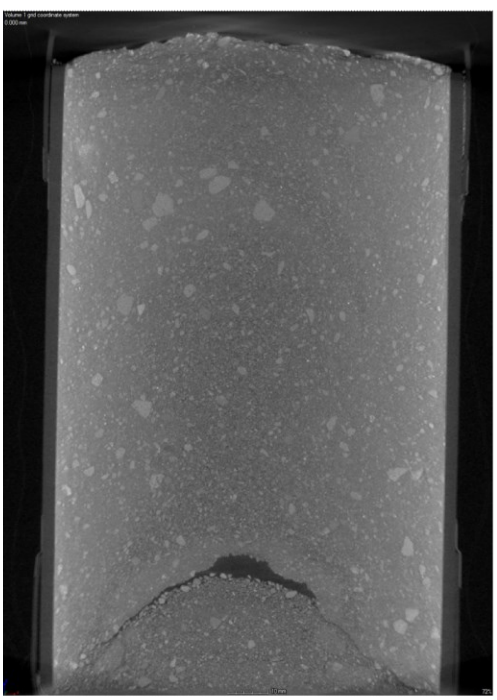

b) B3YJY7_top_0648

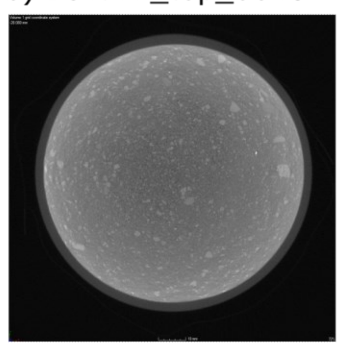

c) B3YJY7_top_1295

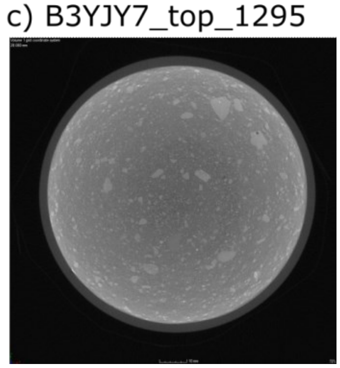

A.1.12 B3YJY8 (D0059/ 230- 232.5 ft bgs / CCUg)

a) B3YJY8_side_0694

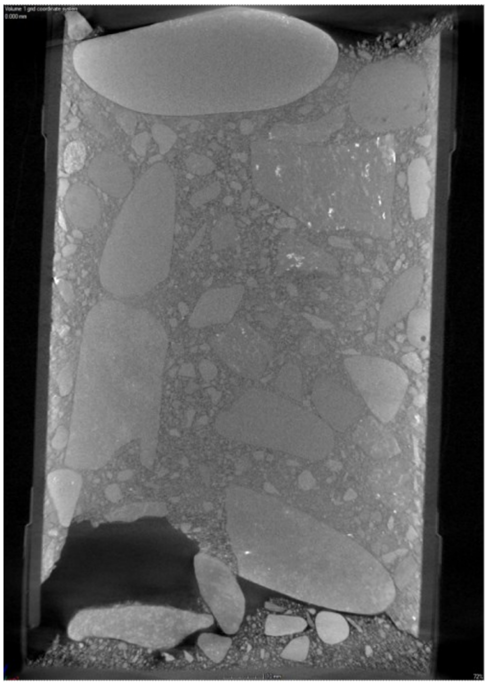

b) B3YJY8_top_0654

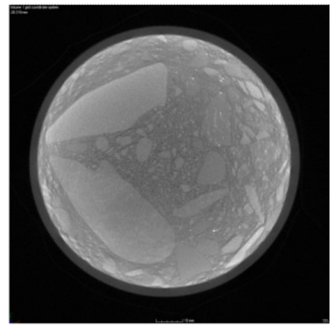

c) B3YJY8_top_1308

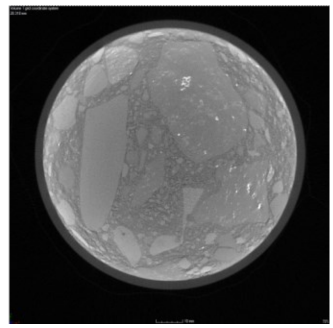

A.1.13 B3YJY9 (D0059/ 249.8- 252.3 ft bgs / CCUg)

a) B3YJY9_side_0696

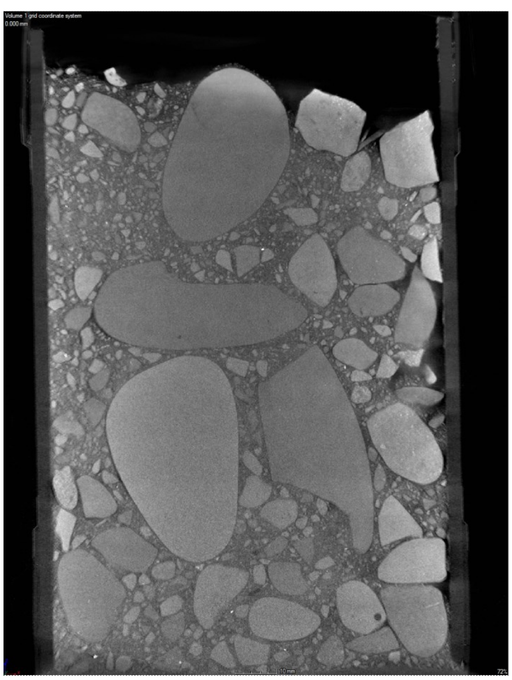

b) B3YJY9_top_0612

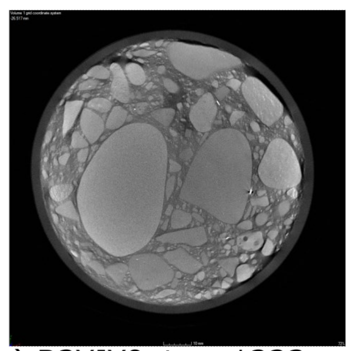

c) B3YJY9_top_1223

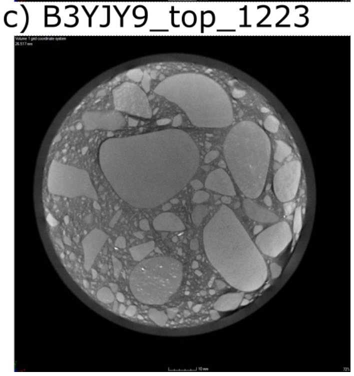

A.1.14 B3YJX6 (D0059/ 29.8- 32.3 ft bgs / Hf1)

a) B3YJX6_side_0668

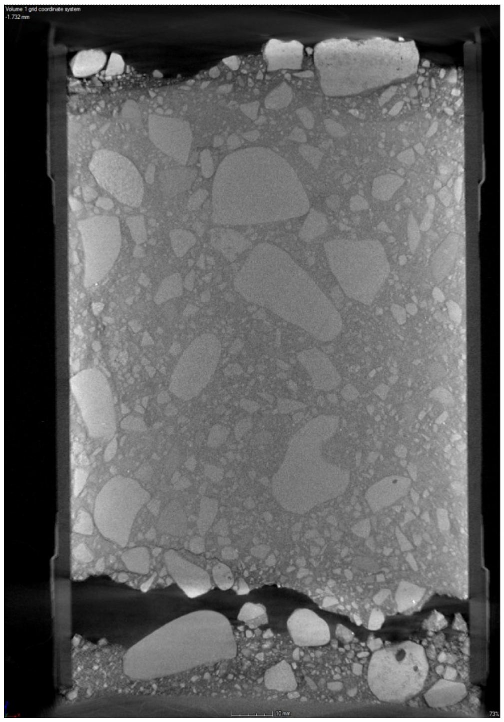

b) B3YJX6_top_0659

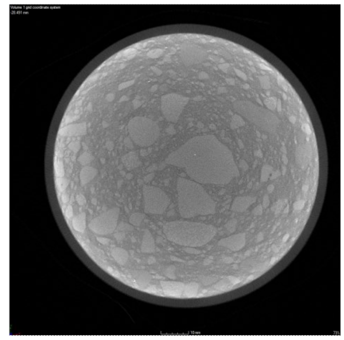

c) B3YJX6_top_1317

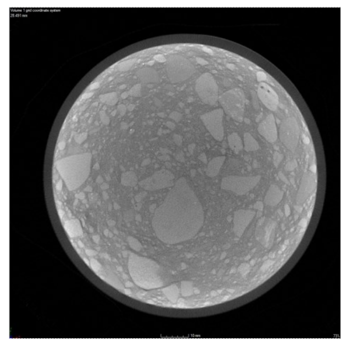

A.1.15 B3YJY5 (D0059/ 199.6- 202.1 ft bgs / Hf3)

a) B3YJY5_side_0678

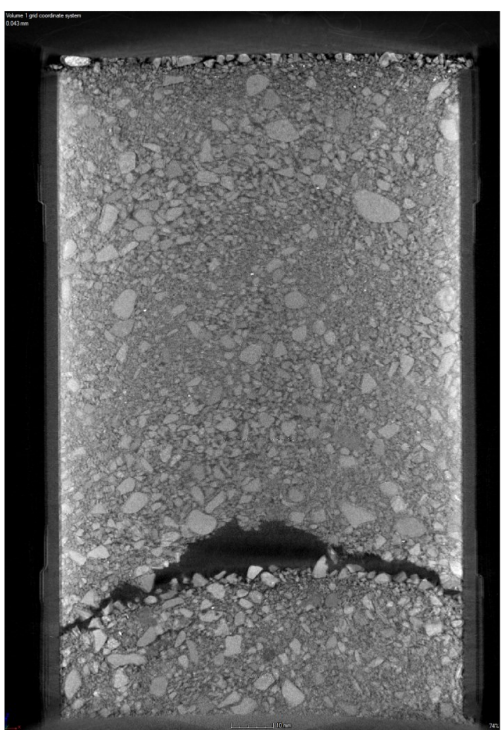

b) B3YJY5_top_0654

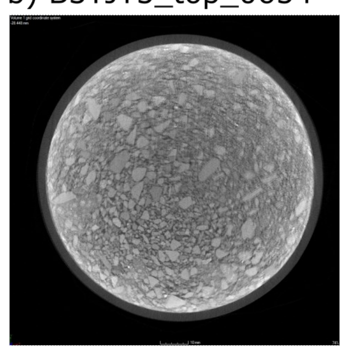

c) B3YJY5_top_1309

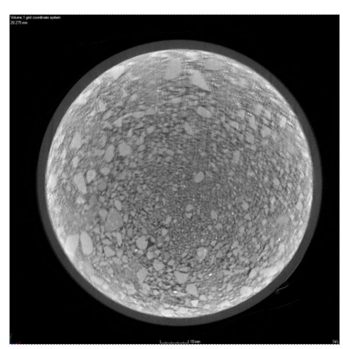

A.1.16 B3YJX1 (D0060/ 219.7- 222.2 ft bgs / CCU)

a) B3YJX1_side_0655

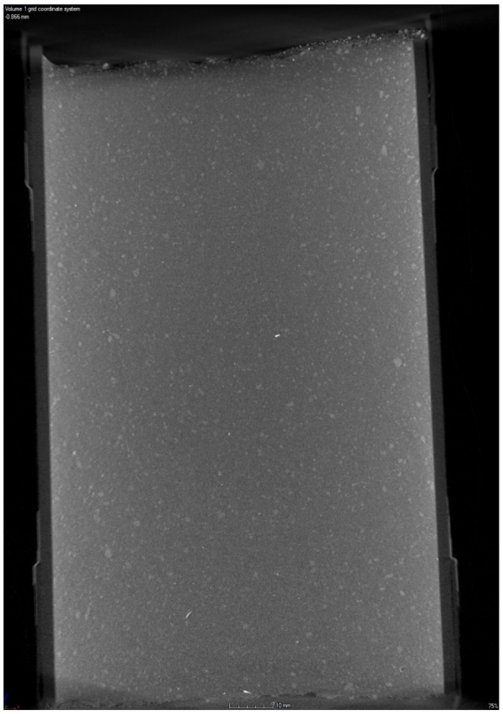

b) B3YJX1_top_0636

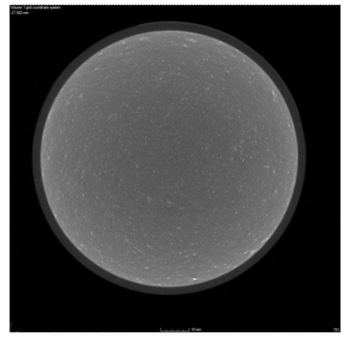

c) B3YJX1_top_1272

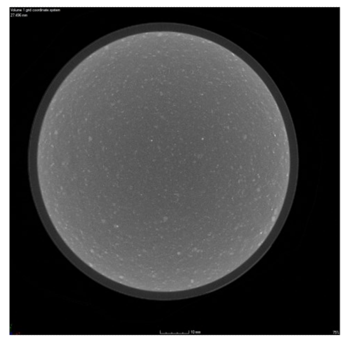

A.1.17 B3YJX2 (D0060/ 230.1- 232.6 ft bgs / CCU)

a) B3YJX2_side_0720

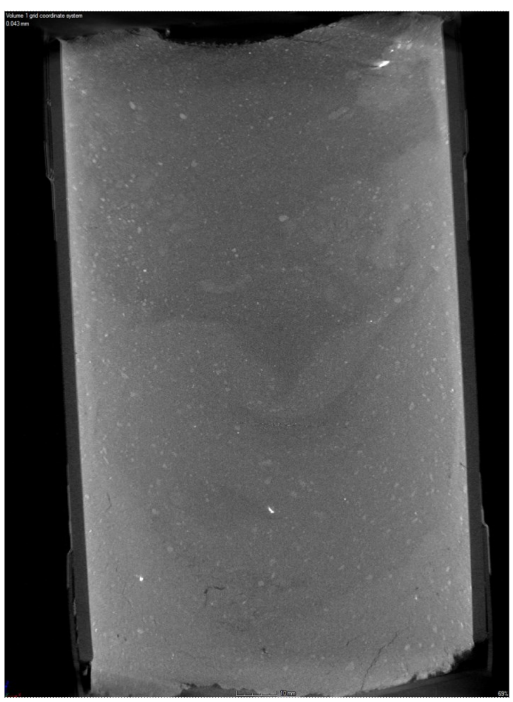

b) B3YJX2_top_0654

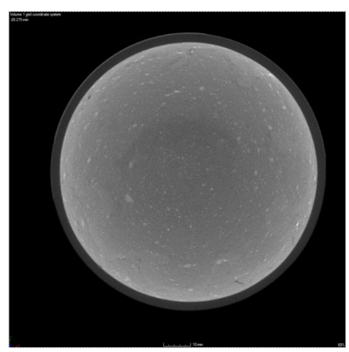

c) B3YJX2_top_1307

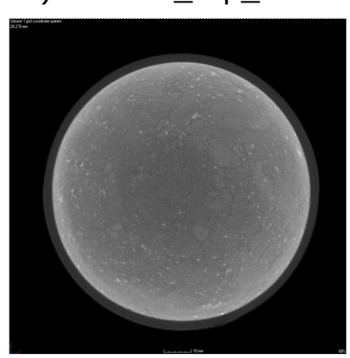

A.1.18 B3YJD8 (D0061/ 30- 32.5 ft bgs / Hf1)

a) B3YJD8_side_0694

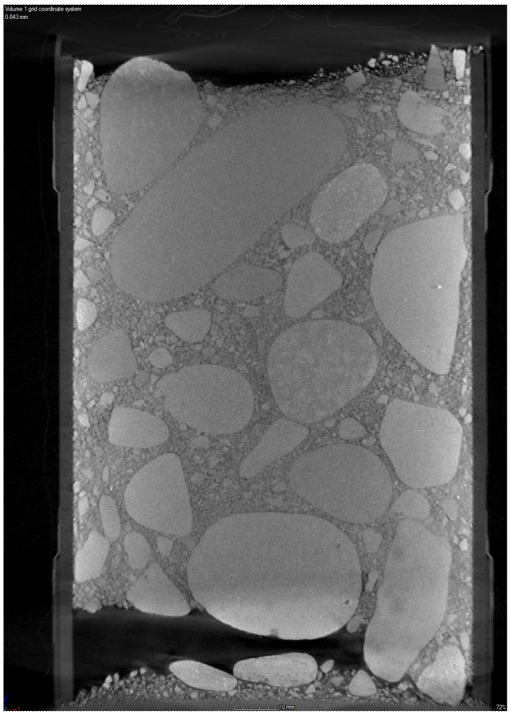

b) B3YJD8_top_0647

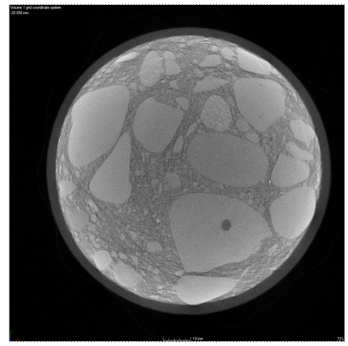

c) B3YJD8_top_1295

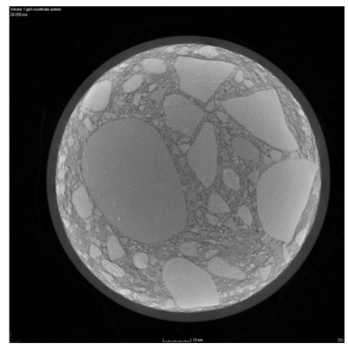

A.1.19 B3YJD9 (D0061/ 40- 42.5 ft bgs / Hf1)

a) B3YJD9_side_0686

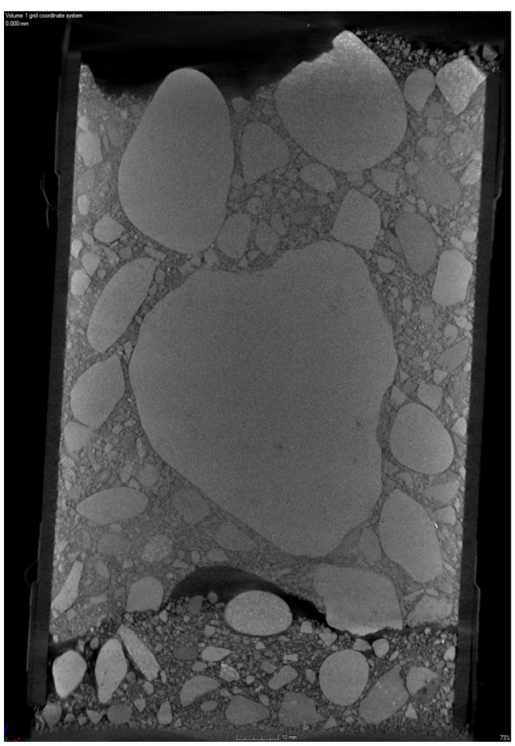

b) B3YJD9_top_0660

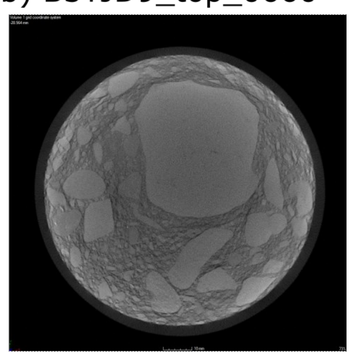

c) B3YJD9_top_1320

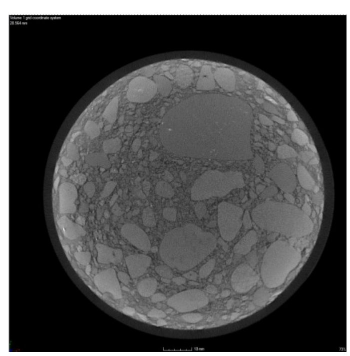

A.1.20 B3YJF9 (D0061 199.7- 202.2 ft bgs / CCU)

a) B3FJF9_side_0673

b) B3YJF9_top_0666

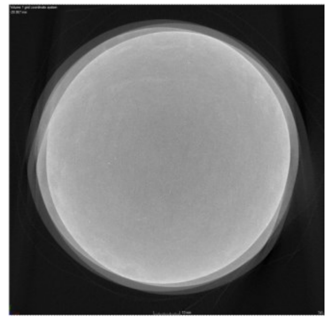

c) B3YJF9_top_1333

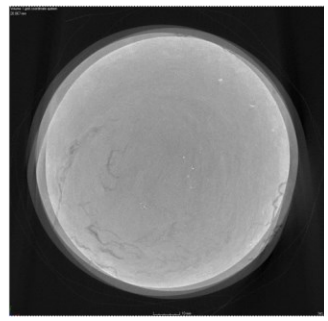

A.1.21 B3YJH0 (D0061 209.6- 212.1 ft bgs / CCUg)

a) B3YJH0_side_0655

b) B3YJH0_top_0641

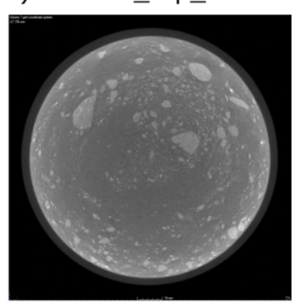

c) B3YJH0_top_1282

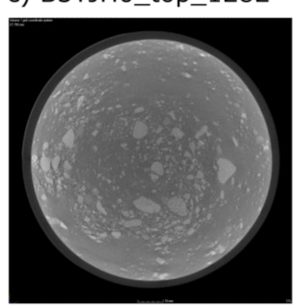

A.1.22 B3YJH1 (D0061 219.7- 222.2 ft bgs / CCUg)

a) B3YJH1_side_0700

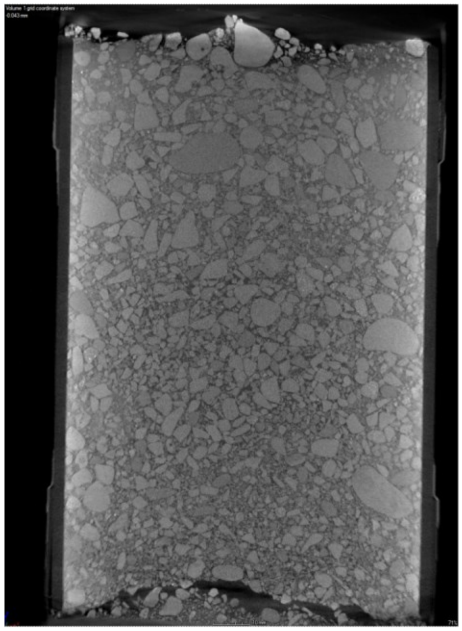

b) B3YJH1_top_0644

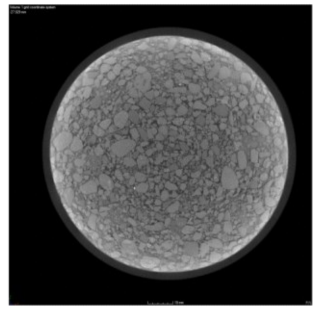

c) B3YJH1_top_1289

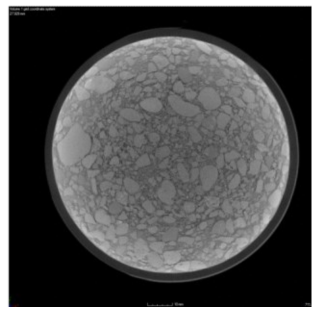

A.1.23 B3YJH2 (D0061 240- 242.5 ft bgs / CCUg)

a)B3YJH2_side_0700

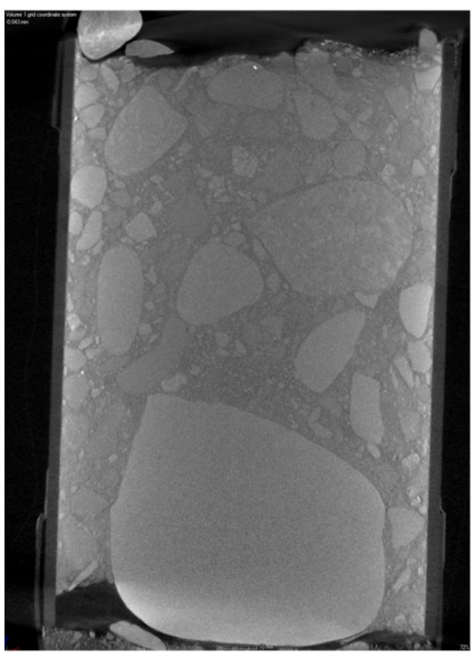

b) B3YJH2_top_0637

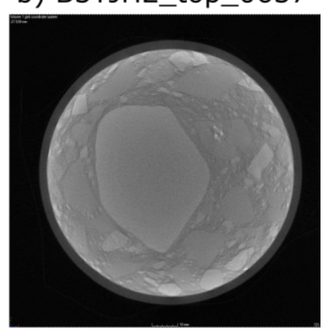

c) B3YJH2_top_1273

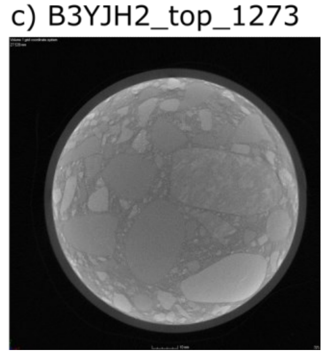

A.1.24 B3YJH3 (D0061 261.7- 264.2 ft bgs / CCUg)

a) B3YJH3_side_0737

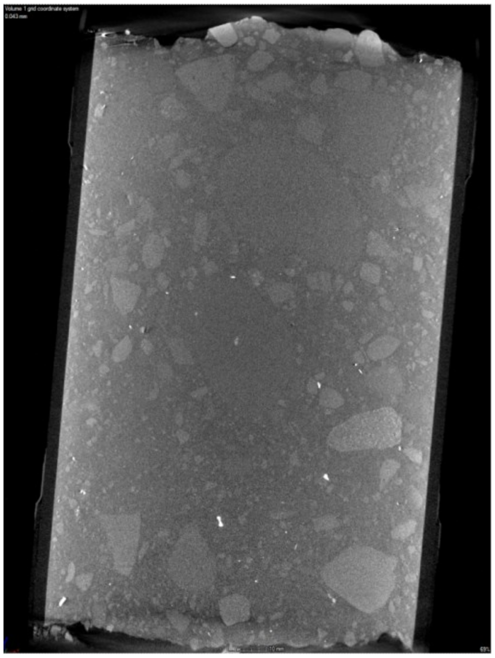

b) B3YJH3_top_0646

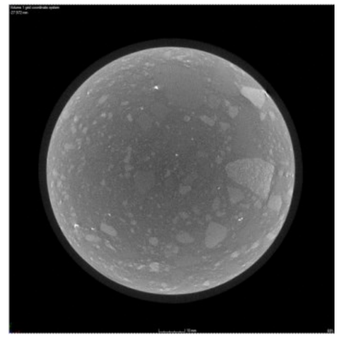

c) B3YJH3_top_1292

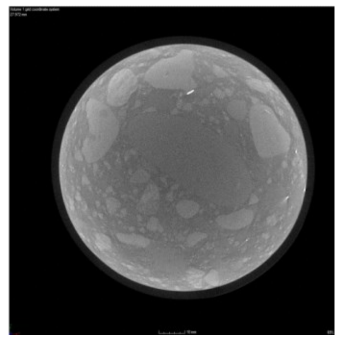

A.2 200 West Cores

A.2.1 B488V3-A (D0013 51.5- 52 ft bgs / Hf1)

a) B488V3_side_view_0796

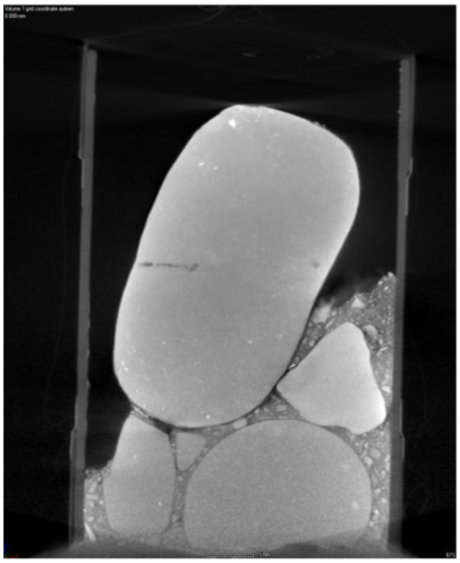

b) B488V3_top_view_0666

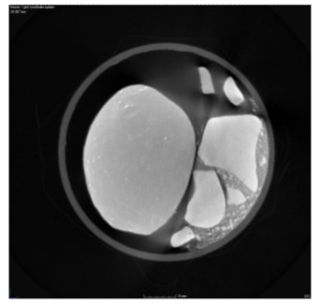

c) B488V3_top_view_1333

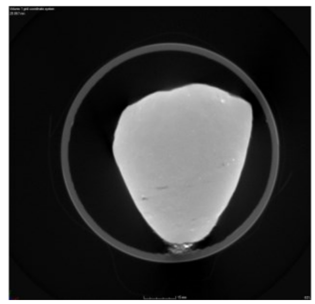

A.2.2 B488V7-C (D0013 95.6- 96.1 ft bgs / Hf2)

a) B488V7_side_view_0680

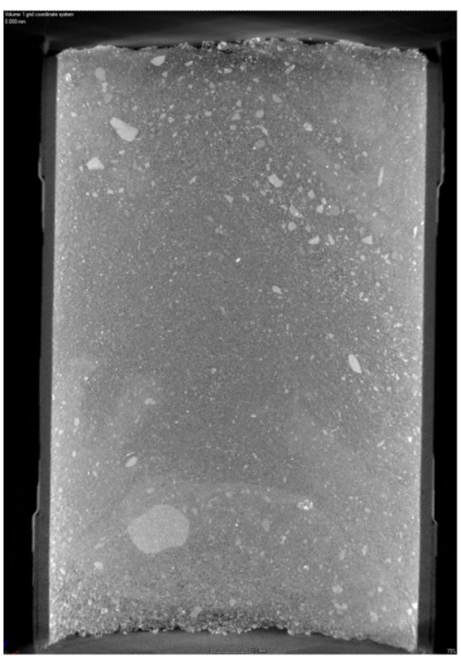

b) B488V7_top_view_0645

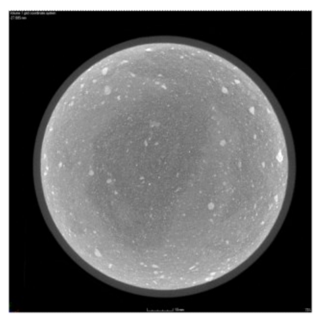

c) B488V7_top_view_1289

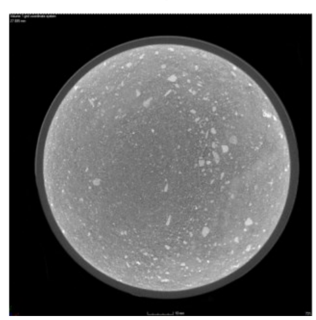

A.2.3 B488Y1-H (D0013 117- 117.5 ft bgs / CCU/CCUc)

a) B488Y1_side_view_0762

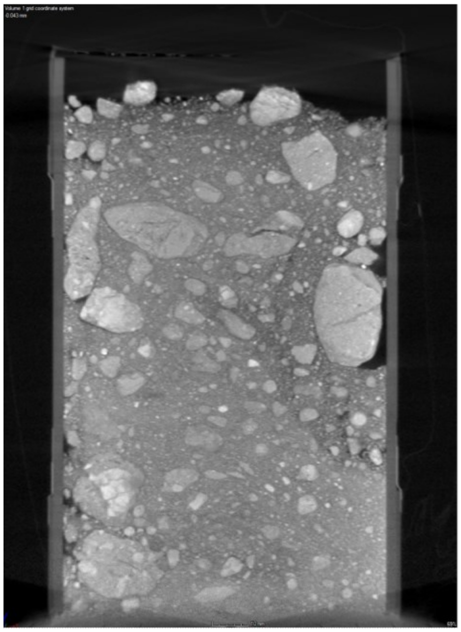

b) B488Y1_top_view_0666

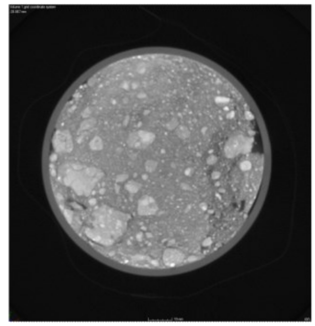

c) B488Y1_top_view_1333

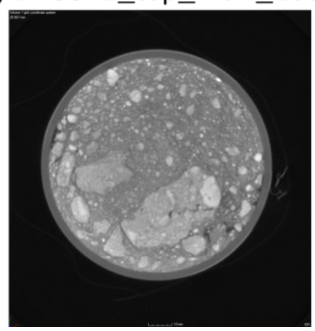

A.2.4 B488Y3-G (D0013 122.5- 123 ft bgs / CCUc)

a) B488Y3_side_view_0721

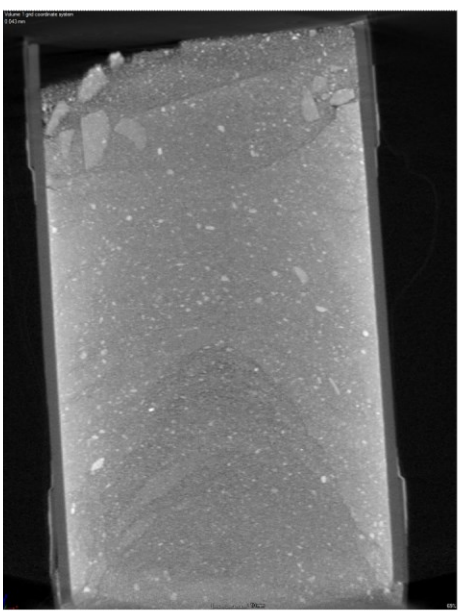

b) B488Y3_top_view_0636

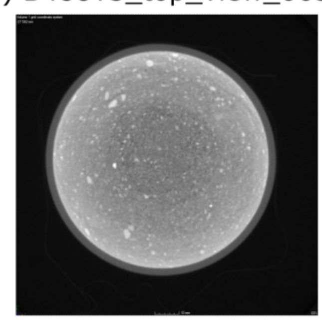

c) B488Y3_top_view_1272

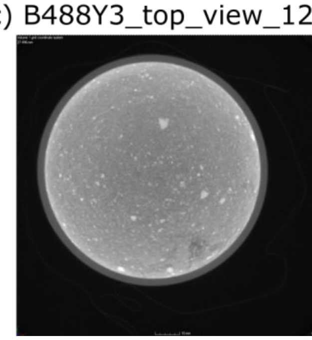

A.2.5 B488Y4-C (D0013 124.5- 125 ft bgs / CCUc)

a) B488Y4_side_view_0623

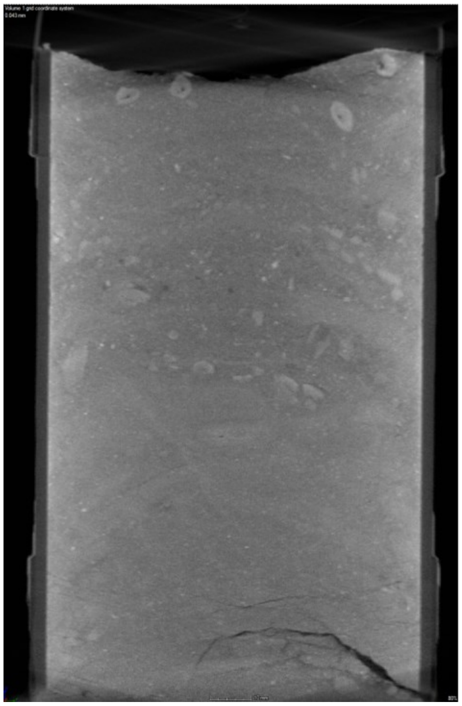

b) B488Y4_top_view_0644

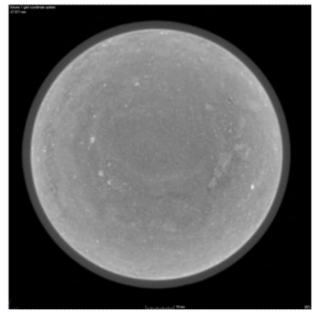

c) B488Y4_top_view_1289

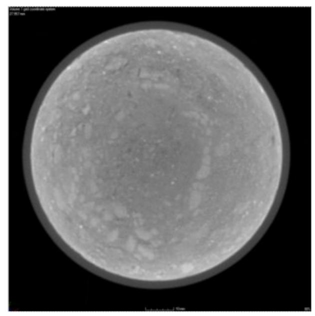

A.2.6 B488W5-D (D0013 138- 138.5 ft bgs / Rwie)

a) B488W5_side_view_0697

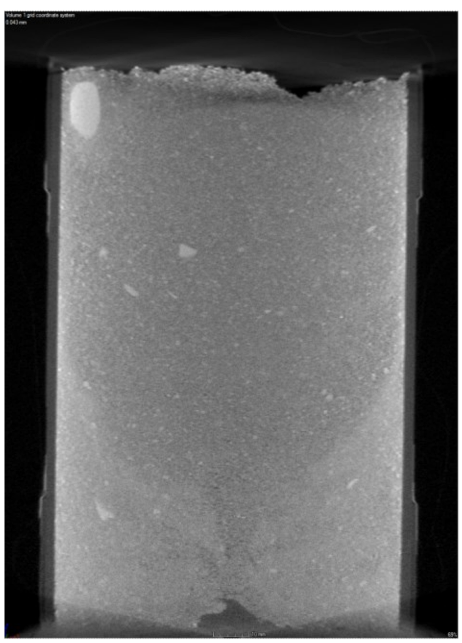

b) B488W5_top_view_0666

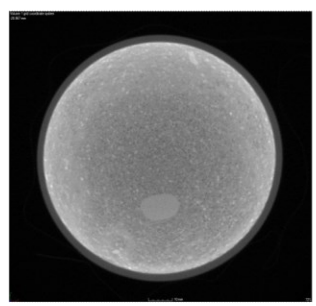

c) B488W5_top_view_1333

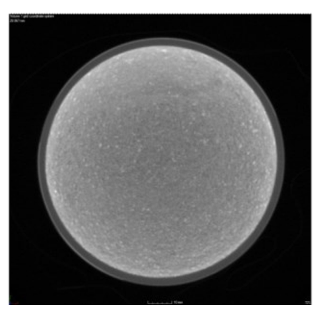

A.2.7 B488W7-B (D0013 223.6- 224.1 ft bgs / Rwie)

a) B488W7_side_view_0688

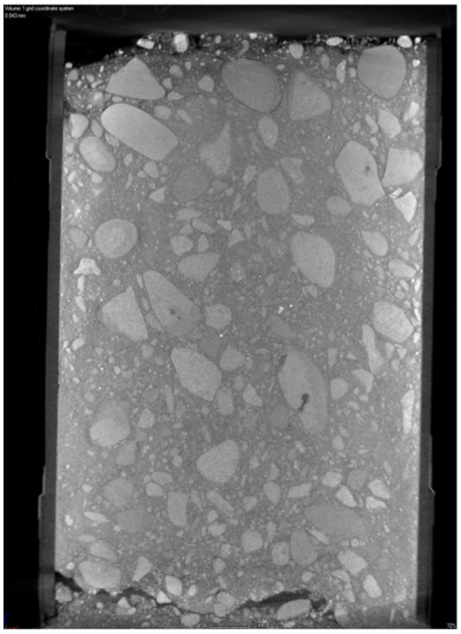

b) B488W7_top_view_0633

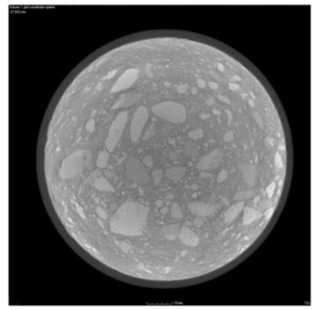

c) B488W7_top_view_1267

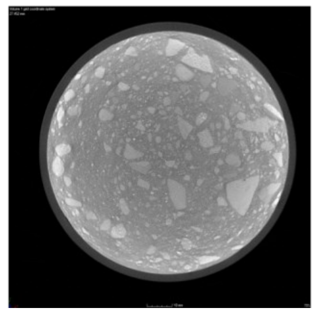

A.2.8 B488X2-B (D0014 56.4- 56.9 ft bgs / Hf1)

a) B488X2_side_view_0674

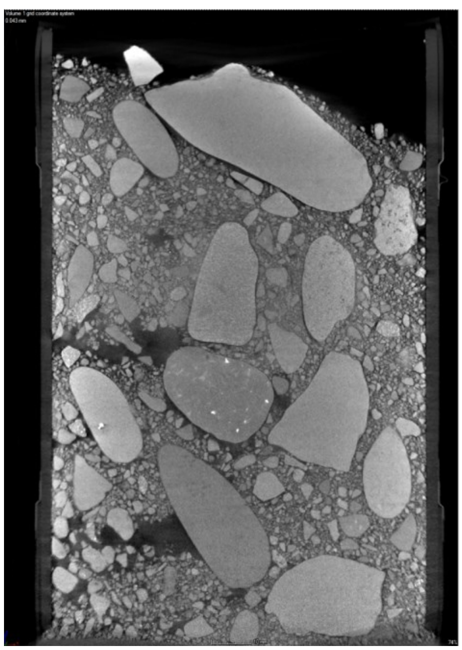

b) B488X2_top_view_0627

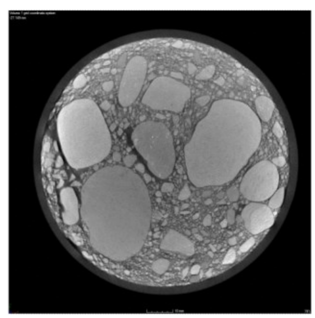

c) B488X2_top_view_1254

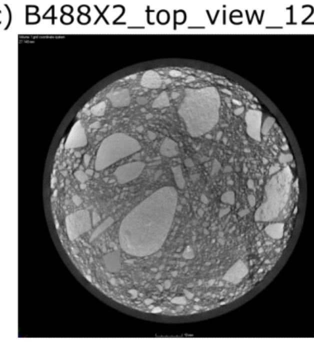

A.2.9 B48N72-B (D0014 N/A- 100.2 ft bgs / Hf2)

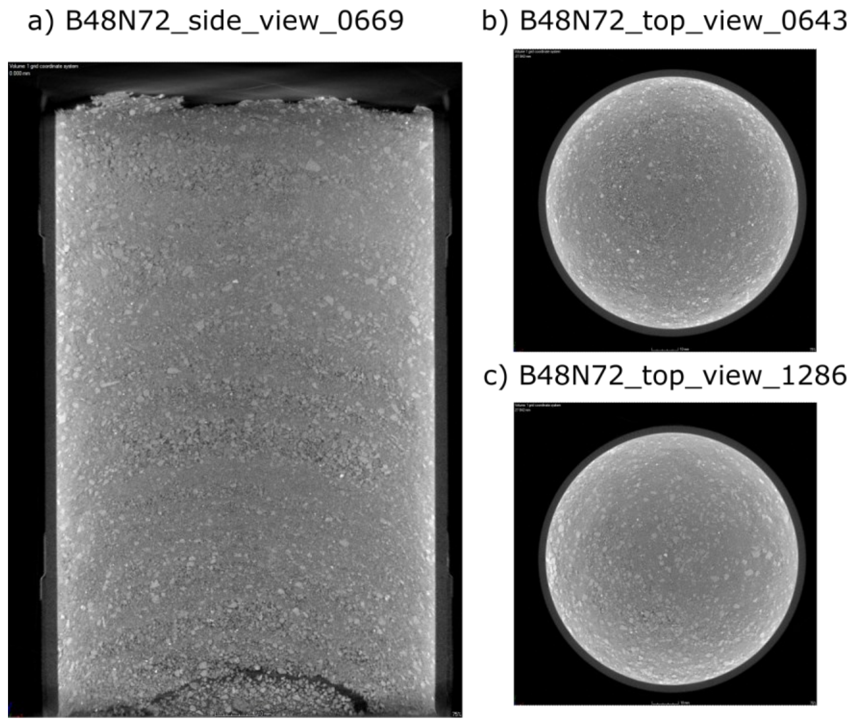

A.2.10 B48N73-B (D0014 114.9- 115.4 ft bgs / CCU)

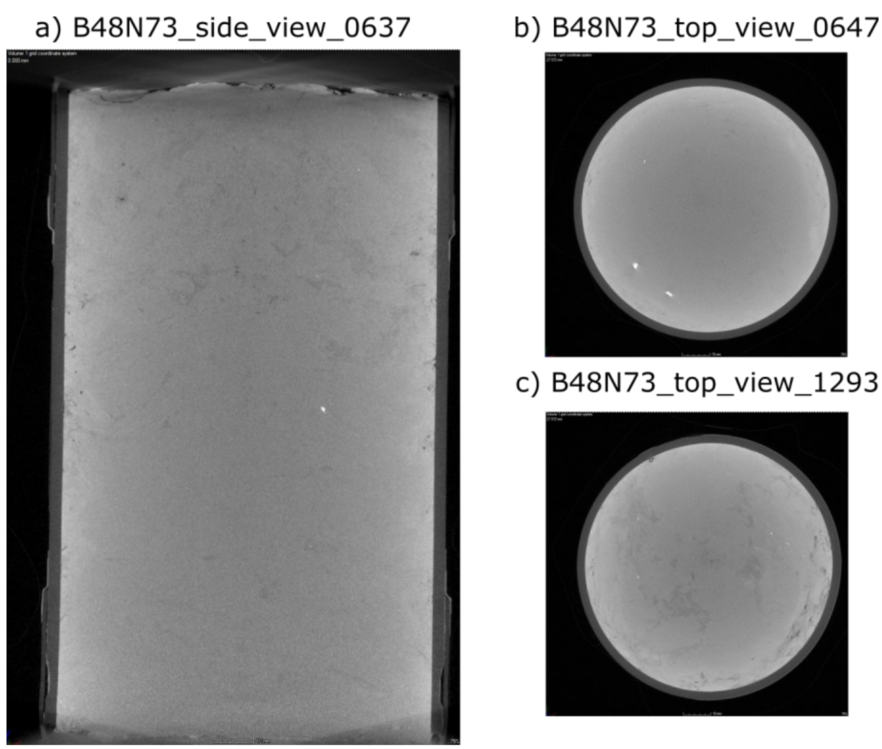

A.2.11 B48N74-I (D0014 116- 121 ft bgs / CCU)

a) B48N74_side_view_0719

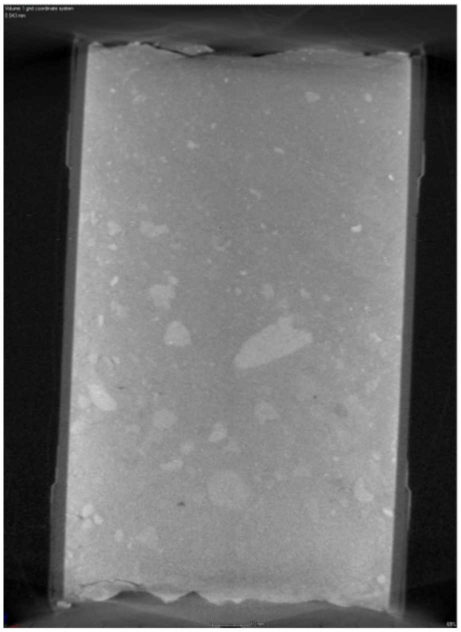

b) B48N74_top_view_0666

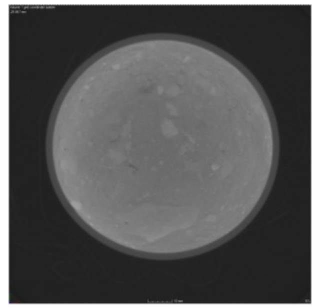

c) B48N74_top_view_1333

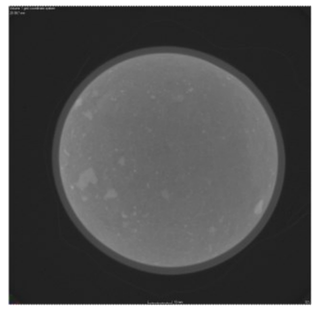

A.2.12 B48N76-H (D0014 122- 122.5 ft bgs / CCUc)

a) B48N76_side_view_0652

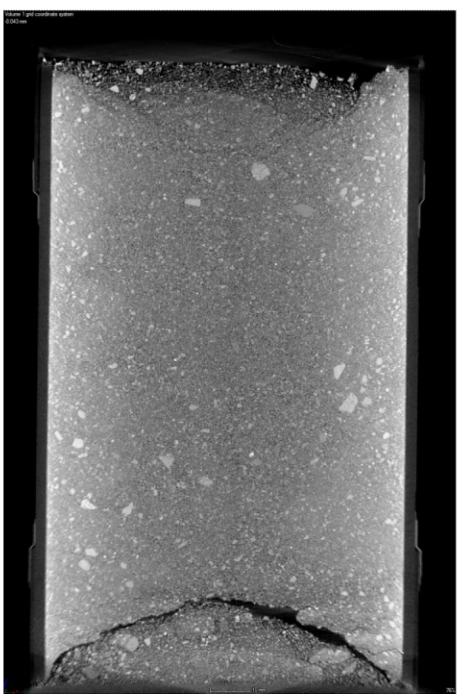

b) B48N76_top_view_0658

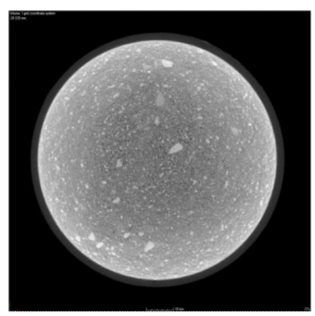

c) B48N76_top_view_1317

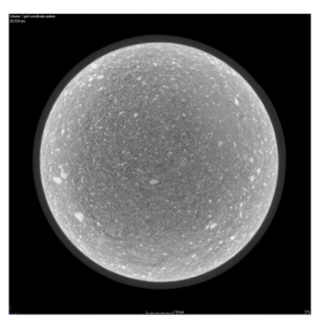

A.2.13 B48N79-B (D0014 136- 136.5 ft bgs / Rwie)

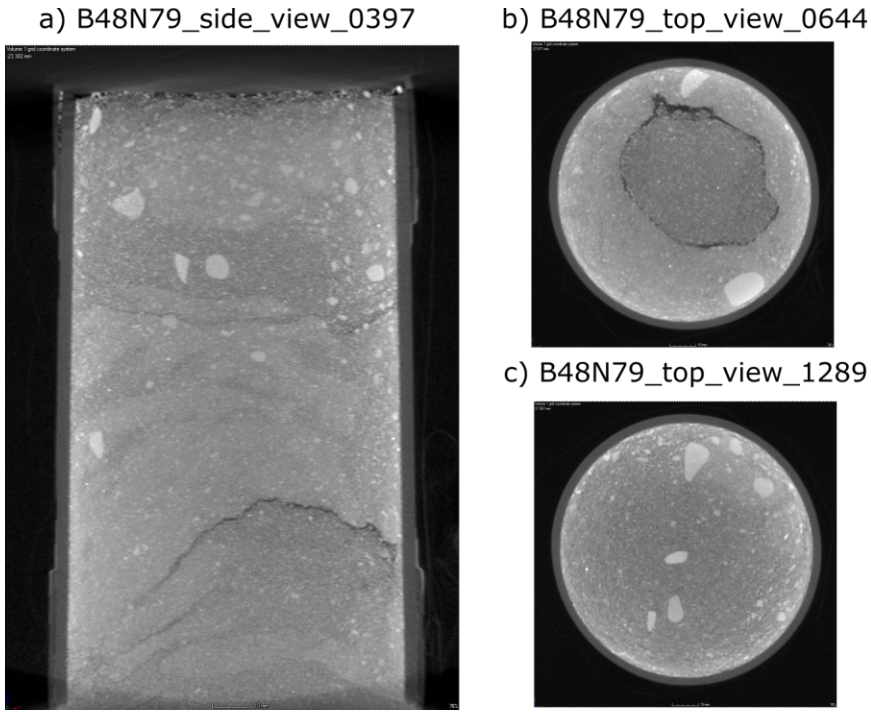

A.2.14 B48ND9-B (D0015 70.9- 71.4 ft bgs / Hf2)

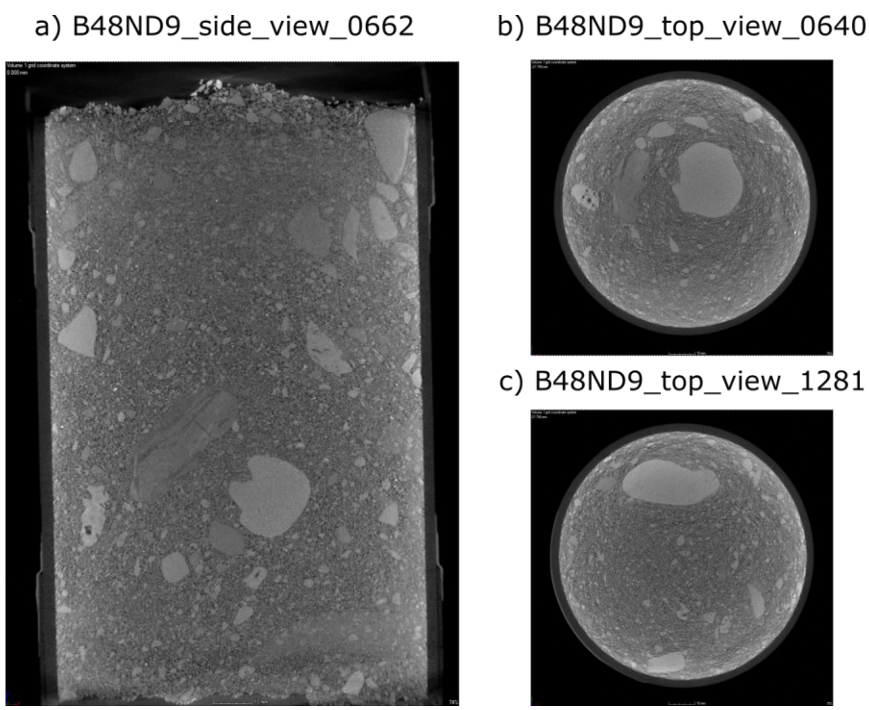

A.2.15 B48ND9-D (D0015 69.9- 70.4 ft bgs / Hf2)

a) B48ND9-D_side_view_0662

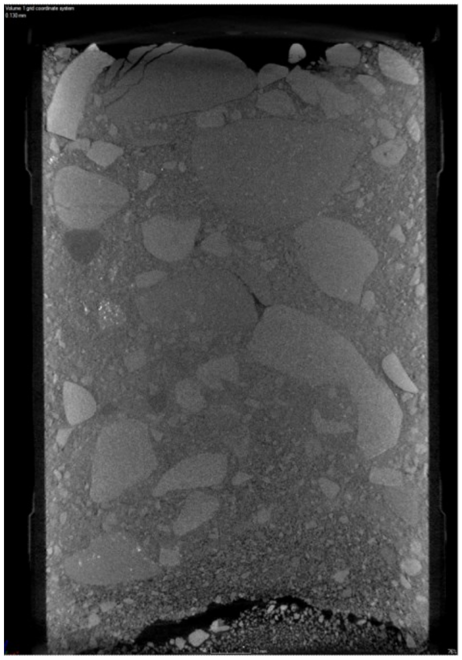

b) B48ND9-D_top_view_0631

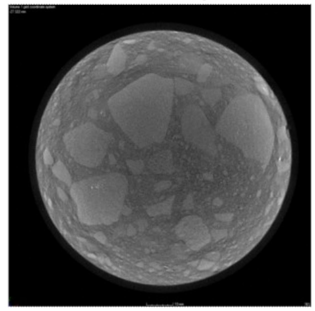

c) B48ND9-D_top_view_1262

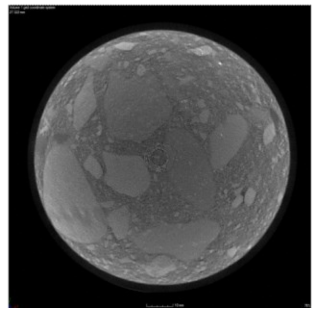

A.2.16 B48NF4-C (D0015 114.5-115 ft bgs / Hf2)

a) B48NF4-C_side_view_0628

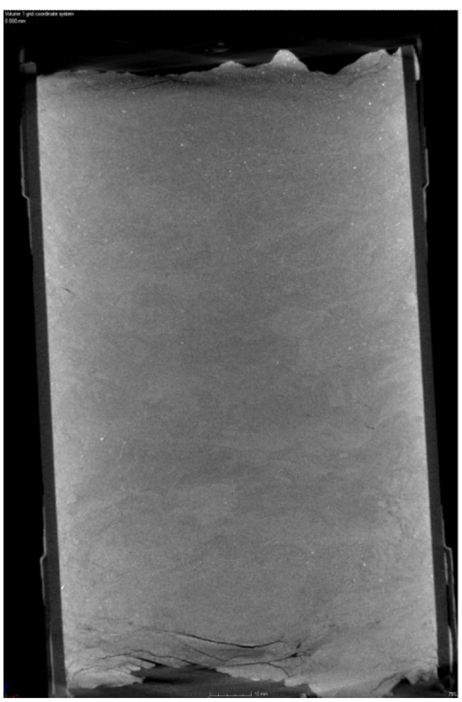

b) B48NF4-C_top_view_0639

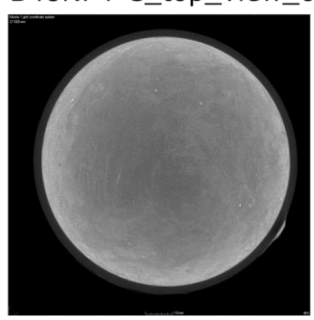

c) B48NF4-C_top_view_1278

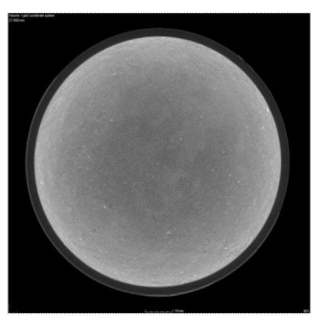

A.2.17 B48NH0-H (D0015 122- 122.5 ft bgs / CCUc)

a) B48NH0-H_side_view_0623

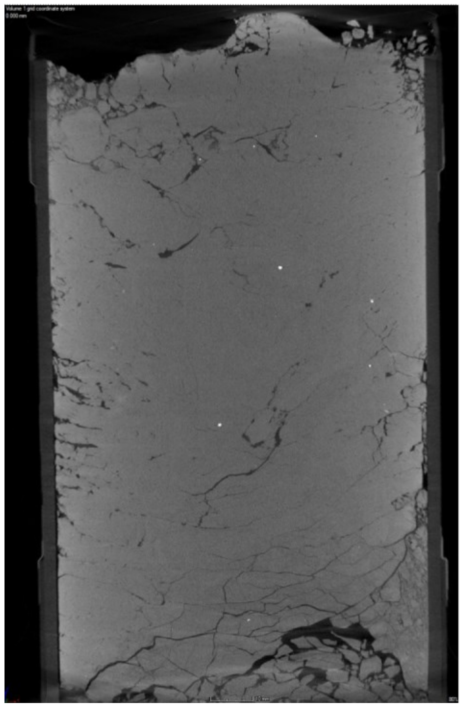

b) B48NH0-H_top_view_0641

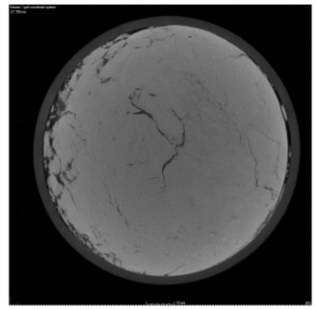

c) B48NH0-H_top_view_1283

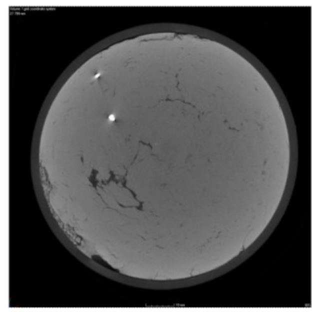

A.2.18 B48NH0-I (D0015 121.5- 122 ft bgs / CCUc)

a) B48NH0-I_side_view_0625

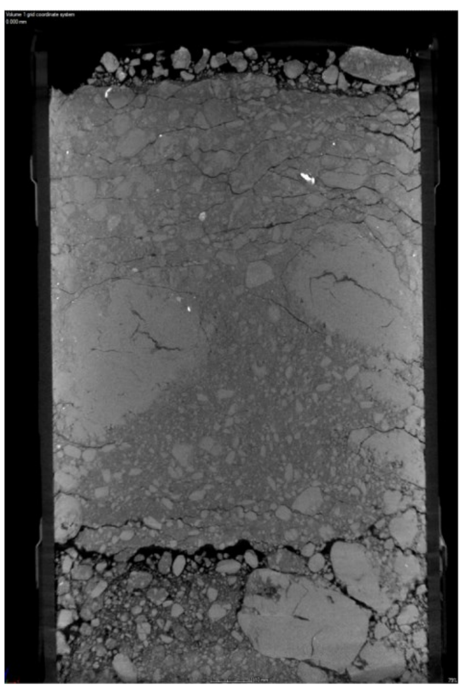

b) B48NH0-I_top_view_0622

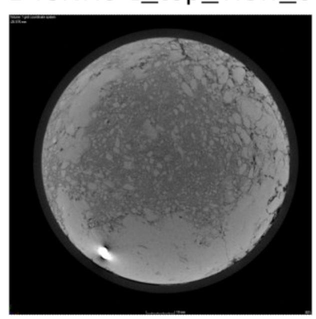

c) B48NH0-I_top_view_1245

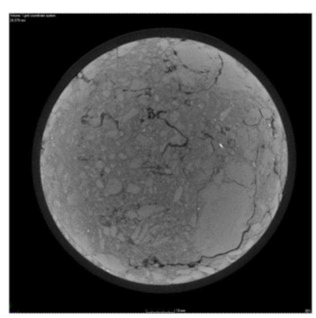

A.2.19 B48NH7-C (D0015 190.8- 191.3 ft bgs / Rwie)

a) B48NH7-C_side_view_0662

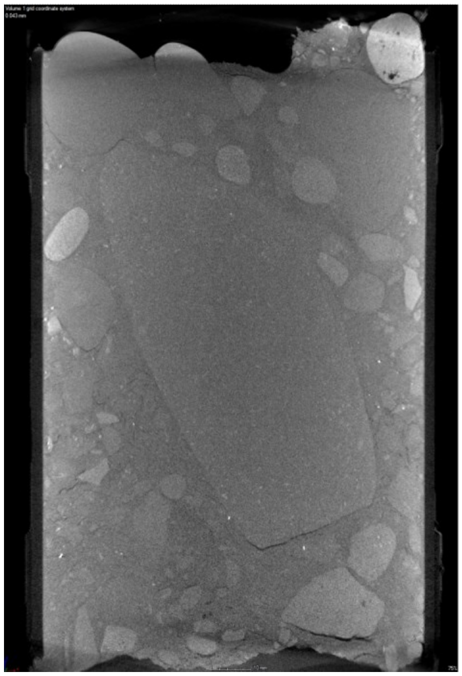

b) B48NH7-C_top_view_0650

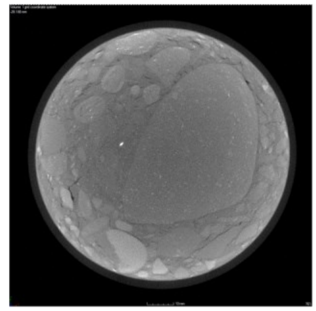

c) B48NH7-C_top_view_1301

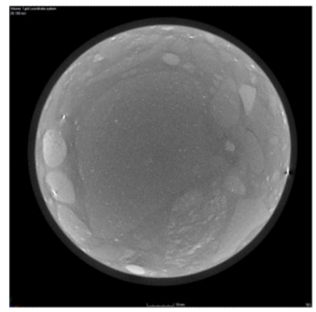

Appendix B – Sieve Results

This appendix contains tabulated sieve data for core samples from the Hanford 200 East and West areas.

B.1 200 East

		Sieve sizes (in mm then inch or mesh)						
		63	31.5	19	8	4	2	<2
Sample ID	**sediment (dry) sieved (kg)**	2.5"	1.25"	3/4"	5/16"	5	10	pan
sieve tares		0.501	0.549	0.468	0.526	0.475	0.399	0.372
B40DC4	2.049	0.501	0.693	0.839	0.867	0.693	0.590	1.158
		Sieve sizes (in mm then inch or mesh)						
		63	31.5	19	8	4	2	<2
		2.5"	1.25"	3/4"	5/16"	5	10	pan
	Soil wt	0.00	0.14	0.37	0.34	0.22	0.19	0.79
	Soil fraction	0.00	0.07	0.18	0.17	0.11	0.09	0.38
	% passing	100%	93%	75%	58%	48%	38%	0%

		Sieve sizes (in mm then inch or mesh)						
		63	31.5	19	8	4	2	<2
Sample ID	**sediment (dry) sieved (kg)**	2.5"	1.25"	3/4"	5/16"	5	10	pan
sieve tares		0.500	0.549	0.468	0.526	0.475	0.399	0.372
B41802	1.708	0.500	0.549	0.468	0.526	0.480	0.404	2.070
		Sieve sizes (in mm then inch or mesh)						
		63	31.5	19	8	4	2	<2
		2.5"	1.25"	3/4"	5/16"	5	10	pan
	Soil wt	0.00	0.00	0.00	0.00	0.01	0.01	1.70
	Soil fraction	0.00	0.00	0.00	0.00	0.00	0.00	0.99
	% passing	100%	100%	100%	100%	100%	99%	0%

		Sieve sizes (in mm then inch or mesh)						
		63	31.5	19	8	4	2	<2
Sample ID	**sediment (dry) sieved (kg)**	2.5"	1.25"	3/4"	5/16"	5	10	pan
sieve tares		0.500	0.549	0.468	0.526	0.475	0.399	0.372
B41806	2.170	0.500	1.161	0.801	0.852	0.766	0.680	0.698
		Sieve sizes (in mm then inch or mesh)						
		63	31.5	19	8	4	2	<2
		2.5"	1.25"	3/4"	5/16"	5	10	pan
	Soil wt	0.00	0.61	0.33	0.33	0.29	0.28	0.33
	Soil fraction	0.00	0.28	0.15	0.15	0.13	0.13	0.15
	% passing	100%	72%	56%	41%	28%	15%	0%

Sample ID	sediment (dry) sieved (kg)	Sieve sizes (in mm then inch or mesh)						
		63	31.5	19	8	4	2	<2
		2.5"	1.25"	3/4"	5/16"	5	10	pan
sieve tares		0.500	0.549	0.468	0.526	0.475	0.399	0.372
B41807	2.038	0.871	0.697	1.076	1.067	0.654	0.490	0.471
		Sieve sizes (in mm then inch or mesh)						
		63	31.5	19	8	4	2	<2
		2.5"	1.25"	3/4"	5/16"	5	10	pan
	Soil wt	0.37	0.15	0.61	0.54	0.18	0.09	0.10
	Soil fraction	0.18	0.07	0.30	0.27	0.09	0.04	0.05
	% passing	82%	75%	45%	18%	9%	5%	0%

Sample ID	sediment (dry) sieved (kg)	Sieve sizes (in mm then inch or mesh)						
		63	31.5	19	8	4	2	<2
		2.5"	1.25"	3/4"	5/16"	5	10	pan
sieve tares		0.500	0.549	0.468	0.526	0.475	0.399	0.372
B41809	2.360	0.500	1.205	0.888	1.119	0.713	0.566	0.660
		Sieve sizes (in mm then inch or mesh)						
		63	31.5	19	8	4	2	<2
		2.5"	1.25"	3/4"	5/16"	5	10	pan
	Soil wt	0.00	0.66	0.42	0.59	0.24	0.17	0.29
	Soil fraction	0.00	0.28	0.18	0.25	0.10	0.07	0.12
	% passing	100%	72%	54%	29%	19%	12%	0%

Sample ID	sediment (dry) sieved (kg)	Sieve sizes (in mm then inch or mesh)						
		63	31.5	19	8	4	2	<2
		2.5"	1.25"	3/4"	5/16"	5	10	pan
sieve tares		0.500	0.549	0.468	0.526	0.475	0.399	0.372
B41868	1.793	0.500	0.925	0.496	1.241	0.864	0.590	0.467
		Sieve sizes (in mm then inch or mesh)						
		63	31.5	19	8	4	2	<2
		2.5"	1.25"	3/4"	5/16"	5	10	pan
	Soil wt	0.00	0.38	0.03	0.72	0.39	0.19	0.10
	Soil fraction	0.00	0.21	0.02	0.40	0.22	0.11	0.05
	% passing	100%	79%	77%	38%	16%	5%	0%

		Sieve sizes (in mm then inch or mesh)						
		63	31.5	19	8	4	2	<2
Sample ID	**sediment (dry) sieved (kg)**	2.5"	1.25"	3/4"	5/16"	5	10	pan
sieve tares		0.500	0.549	0.468	0.526	0.475	0.399	0.372
B418C0	2.506	0.500	0.911	0.853	1.261	0.785	0.655	0.831
		Sieve sizes (in mm then inch or mesh)						
		63	31.5	19	8	4	2	<2
		2.5"	1.25"	3/4"	5/16"	5	10	pan
	Soil wt	0.00	0.36	0.39	0.74	0.31	0.26	0.46
	Soil fraction	0.00	0.14	0.15	0.29	0.12	0.10	0.18
	% passing	100%	86%	70%	41%	28%	18%	0%

		Sieve sizes (in mm then inch or mesh)						
		63	31.5	19	8	4	2	<2
Sample ID	**sediment (dry) sieved (kg)**	2.5"	1.25"	3/4"	5/16"	5	10	pan
sieve tares		0.500	0.549	0.468	0.526	0.475	0.399	0.372
B418C2	2.302	0.500	1.189	1.040	1.057	0.658	0.535	0.613
		Sieve sizes (in mm then inch or mesh)						
		63	31.5	19	8	4	2	<2
		2.5"	1.25"	3/4"	5/16"	5	10	pan
	Soil wt	0.00	0.64	0.57	0.53	0.18	0.14	0.24
	Soil fraction	0.00	0.28	0.25	0.23	0.08	0.06	0.10
	% passing	100%	72%	47%	24%	16%	10%	0%

		Sieve sizes (in mm then inch or mesh)						
		63	31.5	19	8	4	2	<2
Sample ID	**sediment (dry) sieved (kg)**	2.5"	1.25"	3/4"	5/16"	5	10	pan
sieve tares		0.500	0.549	0.468	0.526	0.475	0.399	0.372
B3YK00	2.265	0.500	1.284	0.781	0.833	0.649	0.530	0.973
		Sieve sizes (in mm then inch or mesh)						
		63	31.5	19	8	4	2	<2
		2.5"	1.25"	3/4"	5/16"	5	10	pan
	Soil wt	0.00	0.74	0.31	0.31	0.17	0.13	0.60
	Soil fraction	0.00	0.32	0.14	0.14	0.08	0.06	0.27
	% passing	100%	68%	54%	40%	32%	27%	0%

		Sieve sizes (in mm then inch or mesh)						
		63	31.5	19	8	4	2	<2
Sample ID	**sediment (dry) sieved (kg)**	2.5"	1.25"	3/4"	5/16"	5	10	pan
sieve tares		0.500	0.549	0.468	0.526	0.475	0.399	0.372
B3YJY6	2.055	0.500	0.549	0.468	0.561	0.674	0.712	1.879
		Sieve sizes (in mm then inch or mesh)						
		63	31.5	19	8	4	2	<2
		2.5"	1.25"	3/4"	5/16"	5	10	pan
	Soil wt	0.00	0.00	0.00	0.04	0.20	0.31	1.51
	Soil fraction	0.00	0.00	0.00	0.02	0.10	0.15	0.73
	% passing	100%	100%	100%	98%	89%	73%	0%

		Sieve sizes (in mm then inch or mesh)						
		63	31.5	19	8	4	2	<2
Sample ID	**sediment (dry) sieved (kg)**	2.5"	1.25"	3/4"	5/16"	5	10	pan
sieve tares		0.500	0.549	0.468	0.526	0.475	0.399	0.372
B3YJY7	2.181	0.500	0.549	0.468	0.53	0.517	0.472	2.433
		Sieve sizes (in mm then inch or mesh)						
		63	31.5	19	8	4	2	<2
		2.5"	1.25"	3/4"	5/16"	5	10	pan
	Soil wt	0.00	0.00	0.00	0.00	0.04	0.07	2.06
	Soil fraction	0.00	0.00	0.00	0.00	0.02	0.03	0.94
	% passing	100%	100%	100%	100%	98%	95%	0%

		Sieve sizes (in mm then inch or mesh)						
		63	31.5	19	8	4	2	<2
Sample ID	**sediment (dry) sieved (kg)**	2.5"	1.25"	3/4"	5/16"	5	10	pan
sieve tares		0.500	0.549	0.468	0.526	0.475	0.399	0.372
B3YJY8	2.517	0.500	1.277	0.763	0.842	0.619	0.552	1.254
		Sieve sizes (in mm then inch or mesh)						
		63	31.5	19	8	4	2	<2
		2.5"	1.25"	3/4"	5/16"	5	10	pan
	Soil wt	0.00	0.73	0.30	0.32	0.14	0.15	0.88
	Soil fraction	0.00	0.29	0.12	0.13	0.06	0.06	0.35
	% passing	100%	71%	59%	47%	41%	35%	0%

Sample ID	sediment (dry) sieved (kg)	Sieve sizes (in mm then inch or mesh)						
		63	31.5	19	8	4	2	<2
		2.5"	1.25"	3/4"	5/16"	5	10	pan
sieve tares		0.500	0.549	0.468	0.526	0.475	0.399	0.372
B3YJY9	1.905	0.500	0.849	0.723	1.046	0.668	0.528	0.875

		Sieve sizes (in mm then inch or mesh)						
		63	31.5	19	8	4	2	<2
B3YJY9		2.5"	1.25"	3/4"	5/16"	5	10	pan
	Soil wt	0.00	0.30	0.26	0.52	0.19	0.13	0.50
	Soil fraction	0.00	0.16	0.13	0.27	0.10	0.07	0.26
	% passing	100%	84%	71%	44%	33%	27%	0%

Sample ID	sediment (dry) sieved (kg)	Sieve sizes (in mm then inch or mesh)						
		63	31.5	19	8	4	2	<2
		2.5"	1.25"	3/4"	5/16"	5	10	pan
sieve tares		0.501	0.549	0.468	0.526	0.475	0.399	0.372
B3YJX6	2.199	0.501	0.549	0.608	0.877	0.729	0.662	1.56

		Sieve sizes (in mm then inch or mesh)						
		63	31.5	19	8	4	2	<2
B3YJX6		2.5"	1.25"	3/4"	5/16"	5	10	pan
	Soil wt	0.00	0.00	0.14	0.35	0.25	0.26	1.19
	Soil fraction	0.00	0.00	0.06	0.16	0.12	0.12	0.54
	% passing	100%	100%	94%	78%	66%	54%	0%

Sample ID	sediment (dry) sieved (kg)	Sieve sizes (in mm then inch or mesh)						
		63	31.5	19	8	4	2	<2
		2.5"	1.25"	3/4"	5/16"	5	10	pan
sieve tares		0.500	0.549	0.468	0.526	0.475	0.399	0.372
B3YJY5	1.937	0.500	0.549	0.468	0.561	0.656	0.841	1.65

		Sieve sizes (in mm then inch or mesh)						
		63	31.5	19	8	4	2	<2
B3YJY5		2.5"	1.25"	3/4"	5/16"	5	10	pan
	Soil wt	0.00	0.00	0.00	0.04	0.18	0.44	1.28
	Soil fraction	0.00	0.00	0.00	0.02	0.09	0.23	0.66
	% passing	100%	100%	100%	98%	89%	66%	0%

		Sieve sizes (in mm then inch or mesh)						
		63	31.5	19	8	4	2	<2
Sample ID	**sediment (dry) sieved (kg)**	2.5"	1.25"	3/4"	5/16"	5	10	pan
sieve tares		0.500	0.549	0.468	0.526	0.475	0.399	0.372
B3YJX1	2.024	0.500	0.549	0.468	0.526	0.475	0.402	2.394
		Sieve sizes (in mm then inch or mesh)						
		63	31.5	19	8	4	2	<2
		2.5"	1.25"	3/4"	5/16"	5	10	pan
	Soil wt	0.00	0.00	0.00	0.00	0.00	0.00	2.02
	Soil fraction	0.00	0.00	0.00	0.00	0.00	0.00	1.00
	% passing	100%	100%	100%	100%	100%	100%	0%

		Sieve sizes (in mm then inch or mesh)						
		63	31.5	19	8	4	2	<2
Sample ID	**sediment (dry) sieved (kg)**	2.5"	1.25"	3/4"	5/16"	5	10	pan
sieve tares		0.500	0.549	0.468	0.527	0.475	0.399	0.372
B3YJX2	2.139	0.500	0.549	0.651	0.707	0.593	0.451	1.981
		Sieve sizes (in mm then inch or mesh)						
		63	31.5	19	8	4	2	<2
		2.5"	1.25"	3/4"	5/16"	5	10	pan
	Soil wt	0.00	0.00	0.18	0.18	0.12	0.05	1.61
	Soil fraction	0.00	0.00	0.09	0.08	0.06	0.02	0.75
	% passing	100%	100%	91%	83%	78%	75%	0%

		Sieve sizes (in mm then inch or mesh)						
		63	31.5	19	8	4	2	<2
Sample ID	**sediment (dry) sieved (kg)**	2.5"	1.25"	3/4"	5/16"	5	10	pan
sieve tares		0.500	0.549	0.468	0.526	0.475	0.399	0.372
B3YJD8	2.262	0.501	0.885	0.877	1.041	0.614	0.565	1.072
		Sieve sizes (in mm then inch or mesh)						
		63	31.5	19	8	4	2	<2
		2.5"	1.25"	3/4"	5/16"	5	10	pan
	Soil wt	0.00	0.34	0.41	0.52	0.14	0.17	0.70
	Soil fraction	0.00	0.15	0.18	0.23	0.06	0.07	0.31
	% passing	100%	85%	67%	44%	38%	31%	0%

		Sieve sizes (in mm then inch or mesh)						
		63	31.5	19	8	4	2	<2
Sample ID	**sediment (dry) sieved (kg)**	2.5"	1.25"	3/4"	5/16"	5	10	pan
sieve tares		0.500	0.549	0.468	0.526	0.475	0.399	0.372
	2.370	0.500	1.085	0.627	1.023	0.693	0.602	1.131
		Sieve sizes (in mm then inch or mesh)						
		63	31.5	19	8	4	2	<2
B3YJD9		2.5"	1.25"	3/4"	5/16"	5	10	pan
	Soil wt	0.00	0.54	0.16	0.50	0.22	0.20	0.76
	Soil fraction	0.00	0.23	0.07	0.21	0.09	0.09	0.32
	% passing	100%	77%	71%	50%	41%	32%	0%

		Sieve sizes (in mm then inch or mesh)						
		63	31.5	19	8	4	2	<2
Sample ID	**sediment (dry) sieved (kg)**	2.5"	1.25"	3/4"	5/16"	5	10	pan
sieve tares		0.500	0.549	0.468	0.526	0.475	0.399	0.372
	1.593	0.500	0.549	0.468	0.526	0.476	0.415	1.947
		Sieve sizes (in mm then inch or mesh)						
		63	31.5	19	8	4	2	<2
B3YJF9		2.5"	1.25"	3/4"	5/16"	5	10	pan
	Soil wt	0.00	0.00	0.00	0.00	0.00	0.02	1.58
	Soil fraction	0.00	0.00	0.00	0.00	0.00	0.01	0.99
	% passing	100%	100%	100%	100%	100%	99%	0%

		Sieve sizes (in mm then inch or mesh)						
		63	31.5	19	8	4	2	<2
Sample ID	**sediment (dry) sieved (kg)**	2.5"	1.25"	3/4"	5/16"	5	10	pan
sieve tares		0.500	0.549	0.468	0.526	0.475	0.399	0.361
	2.059	0.500	0.620	0.614	0.647	0.596	0.575	1.788
		Sieve sizes (in mm then inch or mesh)						
		63	31.5	19	8	4	2	<2
B3YJH0		2.5"	1.25"	3/4"	5/16"	5	10	pan
	Soil wt	0.00	0.07	0.15	0.12	0.12	0.18	1.43
	Soil fraction	0.00	0.03	0.07	0.06	0.06	0.09	0.69
	% passing	100%	97%	89%	84%	78%	69%	0%

		Sieve sizes (in mm then inch or mesh)						
		63	31.5	19	8	4	2	<2
Sample ID	**sediment (dry) sieved (kg)**	2.5"	1.25"	3/4"	5/16"	5	10	pan
sieve tares		0.500	0.549	0.468	0.526	0.475	0.399	0.372
B3YJH1	2.327	0.500	0.549	0.48	0.663	1.021	1.081	1.321
		Sieve sizes (in mm then inch or mesh)						
		63	31.5	19	8	4	2	<2
		2.5"	1.25"	3/4"	5/16"	5	10	pan
	Soil wt	0.00	0.00	0.01	0.14	0.55	0.68	0.95
	Soil fraction	0.00	0.00	0.01	0.06	0.23	0.29	0.41
	% passing	100%	100%	99%	94%	70%	41%	0%

		Sieve sizes (in mm then inch or mesh)						
		63	31.5	19	8	4	2	<2
Sample ID	**sediment (dry) sieved (kg)**	2.5"	1.25"	3/4"	5/16"	5	10	pan
sieve tares		0.500	0.549	0.468	0.526	0.475	0.399	0.372
B3YJH2	2.583	0.500	1.192	0.75	1.052	0.692	0.567	1.119
		Sieve sizes (in mm then inch or mesh)						
		63	31.5	19	8	4	2	<2
		2.5"	1.25"	3/4"	5/16"	5	10	pan
	Soil wt	0.00	0.64	0.28	0.53	0.22	0.17	0.75
	Soil fraction	0.00	0.25	0.11	0.20	0.08	0.07	0.29
	% passing	100%	75%	64%	44%	35%	29%	0%

		Sieve sizes (in mm then inch or mesh)						
		63	31.5	19	8	4	2	<2
Sample ID	**sediment (dry) sieved (kg)**	2.5"	1.25"	3/4"	5/16"	5	10	pan
sieve tares		0.500	0.549	0.468	0.526	0.475	0.399	0.372
B3YJH3	2.624	0.500	0.674	0.617	0.903	0.685	0.617	1.918
		Sieve sizes (in mm then inch or mesh)						
		63	31.5	19	8	4	2	<2
		2.5"	1.25"	3/4"	5/16"	5	10	pan
	Soil wt	0.00	0.13	0.15	0.38	0.21	0.22	1.55
	Soil fraction	0.00	0.05	0.06	0.14	0.08	0.08	0.59
	% passing	100%	95%	90%	75%	67%	59%	0%

		Sieve sizes (in mm then inch or mesh)						
		63	31.5	19	8	4	2	<2
Sample ID	**sediment (dry) sieved (kg)**	2.5"	1.25"	3/4"	5/16"	5	10	pan
sieve tares		0.500	0.549	0.468	0.526	0.475	0.399	0.372
B3YJF8	2.020	0.500	0.549	0.468	0.527	0.5	0.544	2.221
		Sieve sizes (in mm then inch or mesh)						
		63	31.5	19	8	4	2	<2
		2.5"	1.25"	3/4"	5/16"	5	10	pan
	Soil wt	0.00	0.00	0.00	0.00	0.03	0.15	1.85
	Soil fraction	0.00	0.00	0.00	0.00	0.01	0.07	0.92
	% passing	100%	100%	100%	100%	99%	92%	0%

B.2 200 East Composites

		Sieve sizes (in mm then inch or mesh)						
		63	31.5	19	8	4	2	<2
Sample ID	**sediment (dry) sieved (kg)**	2.5"	1.25"	3/4"	5/16"	5	10	pan
sieve tares		0.500	0.549	0.469	0.526	0.475	0.399	0.372
Composite 1	5.922	1.226	1.451	1.341	2.097	1.337	0.932	0.827
		Sieve sizes (in mm then inch or mesh)						
		63	31.5	19	8	4	2	<2
		2.5"	1.25"	3/4"	5/16"	5	10	pan
	Soil wt	0.73	0.90	0.87	1.57	0.86	0.53	0.46
	Soil fraction	0.12	0.15	0.15	0.27	0.15	0.09	0.08
	% passing	88%	73%	58%	31%	17%	8%	0%

		Sieve sizes (in mm then inch or mesh)						
		63	31.5	19	8	4	2	<2
Sample ID	**sediment (dry) sieved (kg)**	2.5"	1.25"	3/4"	5/16"	5	10	pan
sieve tares		0.500	0.549	0.468	0.526	0.475	0.399	0.375
Composite 2	6.531	0.500	2.402	1.280	1.653	0.984	0.780	2.221
		Sieve sizes (in mm then inch or mesh)						
		63	31.5	19	8	4	2	<2
		2.5"	1.25"	3/4"	5/16"	5	10	pan
	Soil wt	0.00	1.85	0.81	1.13	0.51	0.38	1.85
	Soil fraction	0.00	0.28	0.12	0.17	0.08	0.06	0.28
	% passing	100%	72%	59%	42%	34%	28%	0%

		Sieve sizes (in mm then inch or mesh)						
		63	31.5	19	8	4	2	<2

Sample ID	sediment (dry) sieved (kg)	2.5"	1.25"	3/4"	5/16"	5	10	pan
sieve tares		0.500	0.549	0.468	0.526	0.475	0.399	0.375
Composite 3	7.470	1.000	0.816	1.013	1.495	1.490	1.452	3.497
		Sieve sizes (in mm then inch or mesh)						
		63	31.5	19	8	4	2	<2
		2.5"	1.25"	3/4"	5/16"	5	10	pan
	Soil wt	0.50	0.27	0.55	0.97	1.02	1.05	3.12
	Soil fraction	0.07	0.04	0.07	0.13	0.14	0.14	0.42
	% passing	93%	90%	82%	69%	56%	42%	0%

B.3 200 West

		Sieve sizes (in mm then inch or mesh)								
		75	50	31.5	25	19	8	4	2	<2
Sample ID	sediment (dry) sieved (kg)	3"	2"	1.5"	1"	3/4"	5/16"	5	10	pan
sieve tares		0.478	0.445	0.500	0.578	0.564	0.522	0.501	0.472	0.360
B488V3	1.569	1.320	0.445	0.682	0.756	0.564	0.560	0.545	0.518	0.606
		Sieve sizes (in mm then inch or mesh)								
		75	50	31.5	25	19	8	4	2	<2
		3"	2"	1.5"	1"	3/4"	5/16"	5	10	pan
	Soil wt	0.84	0.00	0.18	0.18	0.00	0.04	0.04	0.05	0.25
	Soil fraction	0.54	0.00	0.12	0.11	0.00	0.02	0.03	0.03	0.16
	% passing	46%	46%	35%	23%	23%	21%	18%	15%	0%

		Sieve sizes (in mm then inch or mesh								
		75	50	31.5	25	19	8	4	2	<2
Sample ID	sediment (dry) sieved (kg)	3"	2"	1.5"	1"	3/4"	5/16"	5	10	pan
sieve tares		0.478	0.445	0.499	0.578	0.564	0.521	0.501	0.472	0.360
B488V7	1.964	0.478	0.445	0.499	0.578	0.564	0.528	0.509	0.514	2.270
		Sieve sizes (in mm then inch or mesh)								
		75	50	31.5	25	19	8	4	2	<2
		3"	2"	1.5"	1"	3/4"	5/16"	5	10	pan
	Soil wt	0.00	0.00	0.00	0.00	0.00	0.01	0.01	0.04	1.91
	Soil fraction	0.00	0.00	0.00	0.00	0.00	0.00	0.00	0.02	0.97
	% passing	100%	100%	100%	100%	100%	100%	99%	97%	0%

		Sieve sizes (in mm then inch or mesh								
		75	50	31.5	25	19	8	4	2	<2
Sample ID	sediment (dry) sieved (kg)	3"	2"	1.5"	1"	3/4"	5/16"	5	10	pan
sieve tares		0.478	0.445	0.500	0.578	0.564	0.522	0.501	0.472	0.360
B488Y1	1.087	0.478	0.445	0.500	0.578	0.596	0.583	0.575	0.569	1.189
		Sieve sizes (in mm then inch or mesh)								
		75	50	31.5	25	19	8	4	2	<2
		3"	2"	1.5"	1"	3/4"	5/16"	5	10	pan

	Soil wt	0.00	0.00	0.00	0.00	0.03	0.06	0.07	0.10	0.83
	Soil fraction	0.00	0.00	0.00	0.00	0.03	0.06	0.07	0.09	0.76
	% passing	100%	100%	100%	100%	97%	91%	85%	76%	-1%

		Sieve sizes (in mm then inch or mesh)								
		75	50	31.5	25	19	8	4	2	<2
Sample ID	**sediment (dry) sieved (kg)**	3"	2"	1.5"	1"	3/4"	5/16"	5	10	pan
sieve tares		0.478	0.445	0.499	0.578	0.468	0.522	0.501	0.473	0.376
B488Y3	1.573	0.478	0.445	0.499	0.578	0.468	0.522	0.504	0.489	1.929
		Sieve sizes (in mm then inch or mesh)								
		75	50	31.5	25	19	8	4	2	<2
		3"	2"	1.5"	1"	3/4"	5/16"	5	10	pan
	Soil wt	0.00	0.00	0.00	0.00	0.00	0.00	0.00	0.02	1.55
	Soil fraction	0.00	0.00	0.00	0.00	0.00	0.00	0.00	0.01	0.99
	% passing	100%	100%	100%	100%	100%	100%	100%	99%	0%

		Sieve sizes (in mm then inch or mesh)								
		75	50	31.5	25	19	8	4	2	<2
Sample ID	**sediment (dry) sieved (kg)**	3"	2"	1.5"	1"	3/4"	5/16"	5	10	pan
sieve tares		0.478	0.445	0.499	0.578	0.563	0.522	0.502	0.472	0.360
B488Y4	1.549	0.478	0.445	0.499	0.578	0.563	0.552	0.536	0.526	1.791
		Sieve sizes (in mm then inch or mesh)								
		75	50	31.5	25	19	8	4	2	<2
		3"	2"	1.5"	1"	3/4"	5/16"	5	10	pan
	Soil wt	0.00	0.00	0.00	0.00	0.00	0.03	0.03	0.05	1.43
	Soil fraction	0.00	0.00	0.00	0.00	0.00	0.02	0.02	0.03	0.92
	% passing	100%	100%	100%	100%	100%	98%	96%	92%	0%

		Sieve sizes (in mm then inch or mesh)								
		75	50	31.5	25	19	8	4	2	<2
Sample ID	**sediment (dry) sieved (kg)**	3"	2"	1.5"	1"	3/4"	5/16"	5	10	pan
sieve tares		0.478	0.445	0.499	0.578	0.564	0.522	0.501	0.473	0.360
B488W5	2.080	0.478	0.445	0.499	0.578	0.564	0.537	0.506	0.482	2.411
		Sieve sizes (in mm then inch or mesh)								
		75	50	31.5	25	19	8	4	2	<2
		3"	2"	1.5"	1"	3/4"	5/16"	5	10	pan
	Soil wt	0.00	0.00	0.00	0.00	0.00	0.02	0.01	0.01	2.05
	Soil fraction	0.00	0.00	0.00	0.00	0.00	0.01	0.00	0.00	0.99
	% passing	100%	100%	100%	100%	100%	99%	99%	99%	0%

		Sieve sizes (in mm then inch or mesh)								
		75	50	31.5	25	19	8	4	2	<2
Sample ID	**sediment (dry) sieved (kg)**	3"	2"	1.5"	1"	3/4"	5/16"	5	10	pan
sieve tares		0.478	0.445	0.499	0.578	0.468	0.522	0.501	0.472	0.376
B488W7	2.145	0.478	0.445	0.499	0.578	0.488	0.912	0.760	0.650	1.671
		Sieve sizes (in mm then inch or mesh)								
		75	50	31.5	25	19	8	4	2	<2
		3"	2"	1.5"	1"	3/4"	5/16"	5	10	pan
	Soil wt	0.00	0.00	0.00	0.00	0.02	0.39	0.26	0.18	1.30
	Soil fraction	0.00	0.00	0.00	0.00	0.01	0.18	0.12	0.08	0.60
	% passing	100%	100%	100%	100%	99%	81%	69%	61%	0%

		Sieve sizes (in mm then inch or mesh)								
		75	50	31.5	25	19	8	4	2	<2
Sample ID	**sediment (dry) sieved (kg)**	3"	2"	1.5"	1"	3/4"	5/16"	5	10	pan
sieve tares		0.478	0.445	0.500	0.578	0.564	0.522	0.501	0.472	0.360
B488X2	1.930	0.478	0.445	0.741	0.775	0.707	0.806	0.672	0.695	1.041
		Sieve sizes (in mm then inch or mesh)								
		75	50	31.5	25	19	8	4	2	<2
		3"	2"	1.5"	1"	3/4"	5/16"	5	10	pan
	Soil wt	0.00	0.00	0.24	0.20	0.14	0.28	0.17	0.22	0.68
	Soil fraction	0.00	0.00	0.12	0.10	0.07	0.15	0.09	0.12	0.35
	% passing	100%	100%	88%	77%	70%	55%	46%	35%	0%

		Sieve sizes (in mm then inch or mesh)								
		75	50	31.5	25	19	8	4	2	<2
Sample ID	**sediment (dry) sieved (kg)**	3"	2"	1.5"	1"	3/4"	5/16"	5	10	pan
sieve tares		0.478	0.445	0.499	0.578	0.563	0.522	0.501	0.472	0.361
B48N72	2.134	0.478	0.445	0.499	0.578	0.563	0.522	0.501	0.547	2.423
		Sieve sizes (in mm then inch or mesh)								
		75	50	31.5	25	19	8	4	2	<2
		3"	2"	1.5"	1"	3/4"	5/16"	5	10	pan
	Soil wt	0.00	0.00	0.00	0.00	0.00	0.00	0.00	0.08	2.06
	Soil fraction	0.00	0.00	0.00	0.00	0.00	0.00	0.00	0.04	0.97
	% passing	100%	100%	100%	100%	100%	100%	100%	96%	0%

		Sieve sizes (in mm then inch or mesh)								
		75	50	31.5	25	19	8	4	2	<2
Sample ID	**sediment (dry) sieved (kg)**	3"	2"	1.5"	1"	3/4"	5/16"	5	10	pan
sieve tares		0.478	0.445	0.499	0.578	0.468	0.522	0.502	0.473	0.376
B48N73	1.645	0.478	0.445	0.499	0.578	0.468	0.522	0.502	0.473	2.021
		Sieve sizes (in mm then inch or mesh)								
		75	50	31.5	25	19	8	4	2	<2
		3"	2"	1.5"	1"	3/4"	5/16"	5	10	pan
	Soil wt	0.00	0.00	0.00	0.00	0.00	0.00	0.00	0.00	1.65
	Soil fraction	0.00	0.00	0.00	0.00	0.00	0.00	0.00	0.00	1.00
	% passing	100%	100%	100%	100%	100%	100%	100%	100%	0%

		Sieve sizes (in mm then inch or mesh)								
		75	50	31.5	25	19	8	4	2	<2
Sample ID	**sediment (dry) sieved (kg)**	3"	2"	1.5"	1"	3/4"	5/16"	5	10	pan
sieve tares		0.478	0.445	0.499	0.578	0.468	0.521	0.502	0.472	0.376
B48N74	1.802	0.478	0.445	0.499	0.578	0.494	0.625	0.629	0.551	1.843
		Sieve sizes (in mm then inch or mesh)								
		75	50	31.5	25	19	8	4	2	<2
		3"	2"	1.5"	1"	3/4"	5/16"	5	10	pan
	Soil wt	0.00	0.00	0.00	0.00	0.03	0.10	0.13	0.08	1.47
	Soil fraction	0.00	0.00	0.00	0.00	0.01	0.06	0.07	0.04	0.81
	% passing	100%	100%	100%	100%	99%	93%	86%	81%	0%

		Sieve sizes (in mm then inch or mesh)								
		75	50	31.5	25	19	8	4	2	<2
Sample ID	**sediment (dry) sieved (kg)**	3"	2"	1.5"	1"	3/4"	5/16"	5	10	pan
sieve tares		0.478	0.445	0.500	0.578	0.564	0.522	0.501	0.473	0.360
B48N76	1.825	0.478	0.445	0.500	0.578	0.564	0.523	0.505	0.498	2.155
		Sieve sizes (in mm then inch or mesh)								
		75	50	31.5	25	19	8	4	2	<2
		3"	2"	1.5"	1"	3/4"	5/16"	5	10	pan
	Soil wt	0.00	0.00	0.00	0.00	0.00	0.00	0.00	0.03	1.80
	Soil fraction	0.00	0.00	0.00	0.00	0.00	0.00	0.00	0.01	0.98
	% passing	100%	100%	100%	100%	100%	100%	100%	98%	0%

		Sieve sizes (in mm then inch or mesh)								
		75	50	31.5	25	19	8	4	2	<2
Sample ID	**sediment (dry) sieved (kg)**	3"	2"	1.5"	1"	3/4"	5/16"	5	10	pan
sieve tares		0.478	0.445	0.499	0.578	0.468	0.522	0.502	0.473	0.376
B48N79	2.054	0.478	0.445	0.499	0.578	0.468	0.544	0.527	0.517	2.338
		Sieve sizes (in mm then inch or mesh)								
		75	50	31.5	25	19	8	4	2	<2
		3"	2"	1.5"	1"	3/4"	5/16"	5	10	pan
	Soil wt	0.00	0.00	0.00	0.00	0.00	0.02	0.03	0.04	1.96
	Soil fraction	0.00	0.00	0.00	0.00	0.00	0.01	0.01	0.02	0.96
	% passing	100%	100%	100%	100%	100%	99%	98%	96%	0%

		Sieve sizes (in mm then inch or mesh)								
		75	50	31.5	25	19	8	4	2	<2
Sample ID	**sediment (dry) sieved (kg)**	3"	2"	1.5"	1"	3/4"	5/16"	5	10	pan
sieve tares		0.478	0.445	0.499	0.578	0.563	0.522	0.501	0.473	0.361
B48ND9-B	1.988	0.478	0.445	0.499	0.674	0.593	0.623	0.563	0.601	1.933
		Sieve sizes (in mm then inch or mesh)								
		75	50	31.5	25	19	8	4	2	<2
		3"	2"	1.5"	1"	3/4"	5/16"	5	10	pan
	Soil wt	0.00	0.00	0.00	0.10	0.03	0.10	0.06	0.13	1.57
	Soil fraction	0.00	0.00	0.00	0.05	0.02	0.05	0.03	0.06	0.79
	% passing	100%	100%	100%	95%	94%	89%	85%	79%	0%

		Sieve sizes (in mm then inch or mesh)								
		75	50	31.5	25	19	8	4	2	<2
Sample ID	**sediment (dry) sieved (kg)**	3"	2"	1.5"	1"	3/4"	5/16"	5	10	pan
sieve tares		0.478	0.445	0.499	0.578	0.563	0.521	0.501	0.472	0.361
B48ND9-D	2.341	0.478	0.445	0.499	0.842	0.756	0.812	0.652	0.663	1.609
		Sieve sizes (in mm then inch or mesh)								
		75	50	31.5	25	19	8	4	2	<2
		3"	2"	1.5"	1"	3/4"	5/16"	5	10	pan
	Soil wt	0.00	0.00	0.00	0.26	0.19	0.29	0.15	0.19	1.25
	Soil fraction	0.00	0.00	0.00	0.11	0.08	0.12	0.06	0.08	0.53
	% passing	100%	100%	100%	89%	80%	68%	62%	53%	0%

		Sieve sizes (in mm then inch or mesh)								
		75	50	31.5	25	19	8	4	2	<2
Sample ID	**sediment (dry) sieved (kg)**	3"	2"	1.5"	1"	3/4"	5/16"	5	10	pan
sieve tares		0.478	0.445	0.499	0.578	0.468	0.521	0.502	0.472	0.376
B48NF4	1.718	0.478	0.445	0.499	0.578	0.468	0.521	0.502	0.472	2.095

		Sieve sizes (in mm then inch or mesh)								
		75	50	31.5	25	19	8	4	2	<2
B48NF4		3"	2"	1.5"	1"	3/4"	5/16"	5	10	pan
	Soil wt	0.00	0.00	0.00	0.00	0.00	0.00	0.00	0.00	1.72
	Soil fraction	0.00	0.00	0.00	0.00	0.00	0.00	0.00	0.00	1.00
	% passing	100%	100%	100%	100%	100%	100%	100%	100%	0%

		Sieve sizes (in mm then inch or mesh)								
		75	50	31.5	25	19	8	4	2	<2
Sample ID	**sediment (dry) sieved (kg)**	3"	2"	1.5"	1"	3/4"	5/16"	5	10	pan
sieve tares		0.478	0.445	0.499	0.578	0.468	0.521	0.502	0.472	0.376
B48NH0-H	1.595	0.478	0.445	0.499	0.578	0.468	0.521	0.502	0.472	1.966

		Sieve sizes (in mm then inch or mesh)								
		75	50	31.5	25	19	8	4	2	<2
B48NH0-H		3"	2"	1.5"	1"	3/4"	5/16"	5	10	pan
	Soil wt	0.00	0.00	0.00	0.00	0.00	0.00	0.00	0.00	1.59
	Soil fraction	0.00	0.00	0.00	0.00	0.00	0.00	0.00	0.00	1.00
	% passing	100%	100%	100%	100%	100%	100%	100%	100%	0%

		Sieve sizes (in mm then inch or mesh)								
		75	50	31.5	25	19	8	4	2	<2
Sample ID	**sediment (dry) sieved (kg)**	3"	2"	1.5"	1"	3/4"	5/16"	5	10	pan
sieve tares		0.478	0.445	0.499	0.578	0.468	0.521	0.501	0.472	0.360
B48NH0-I	1.449	0.478	0.445	0.499	0.578	0.468	0.521	0.501	0.474	1.804

		Sieve sizes (in mm then inch or mesh)								
		75	50	31.5	25	19	8	4	2	<2
B48NH0-I		3"	2"	1.5"	1"	3/4"	5/16"	5	10	pan
	Soil wt	0.00	0.00	0.00	0.00	0.00	0.00	0.00	0.00	1.44
	Soil fraction	0.00	0.00	0.00	0.00	0.00	0.00	0.00	0.00	1.00
	% passing	100%	100%	100%	100%	100%	100%	100%	100%	0%

		Sieve sizes (in mm then inch or mesh)								
		75	50	31.5	25	19	8	4	2	<2
Sample ID	**sediment (dry) sieved (kg)**	3"	2"	1.5"	1"	3/4"	5/16"	5	10	pan
sieve tares		0.478	0.445	0.499	0.578	0.563	0.521	0.501	0.472	0.361
B48NH7	2.591	0.478	1.021	0.499	0.752	0.710	1.060	0.750	0.643	1.088

		Sieve sizes (in mm then inch or mesh)								
		75	50	31.5	25	19	8	4	2	<2
B48NH7		3"	2"	1.5"	1"	3/4"	5/16"	5	10	pan
	Soil wt	0.00	0.58	0.00	0.17	0.15	0.54	0.25	0.17	0.73
	Soil fraction	0.00	0.22	0.00	0.07	0.06	0.21	0.10	0.07	0.28
	% passing	100%	78%	78%	71%	65%	45%	35%	28%	0%

Appendix C – Particle Size Distribution (PSD) Plots

The following plots show data obtained using 1) laser light scattering method (PSD) for sediment passing a 2-mm sieve (< 2 mm) and 2) sieve method (PSD Sieve) for sediment > 2 mm. Cumulative distributions are also shown for the PSD sieve data (Cumulative PSD) and the PSD Sieve data (Cumulative PSD Sieve).

C.1 200 East

C.1.1 B40DC4

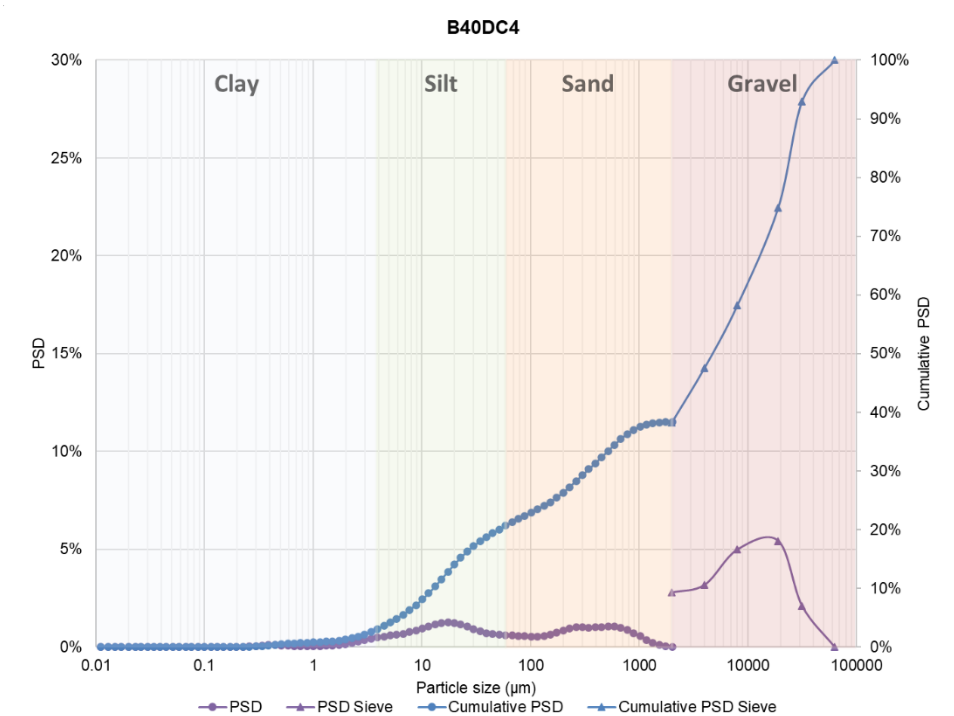

C.1.2 B41802

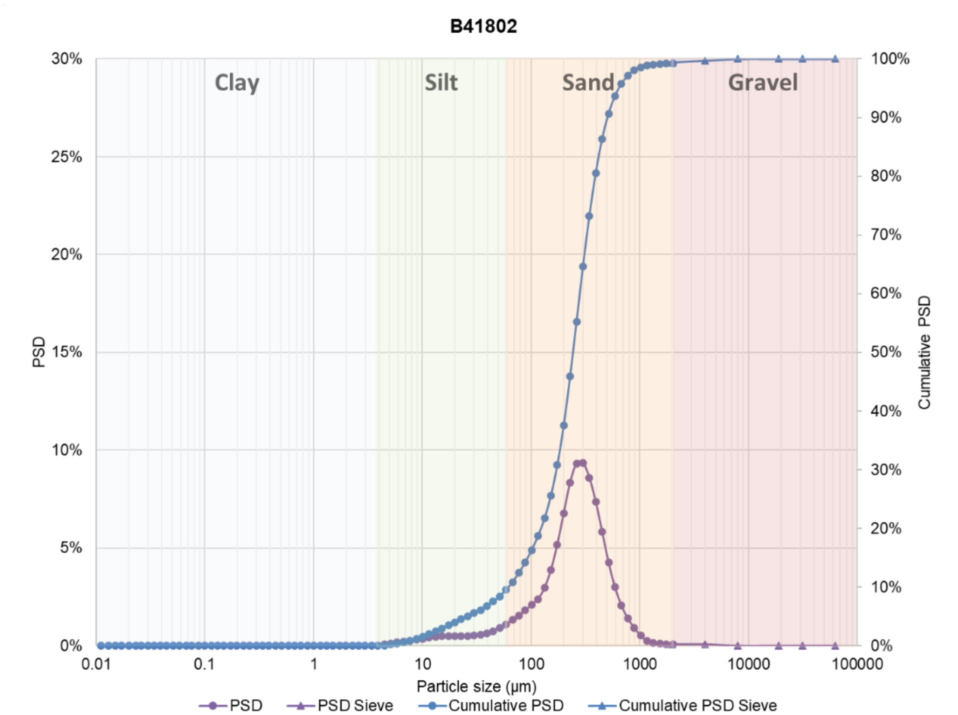

C.1.3 B41806

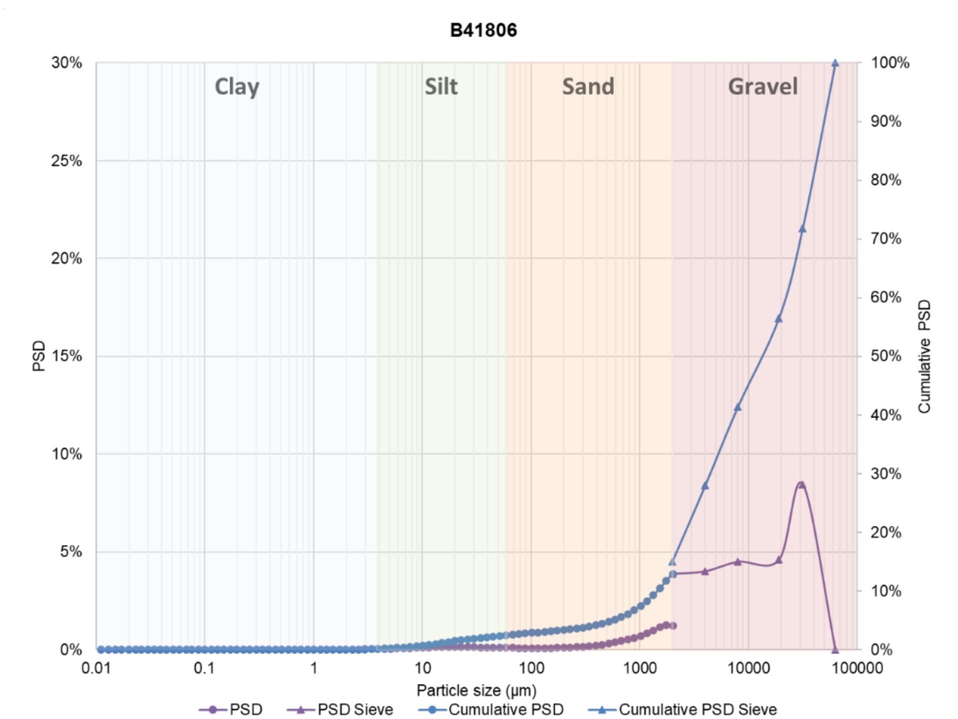

C.1.4 B41807

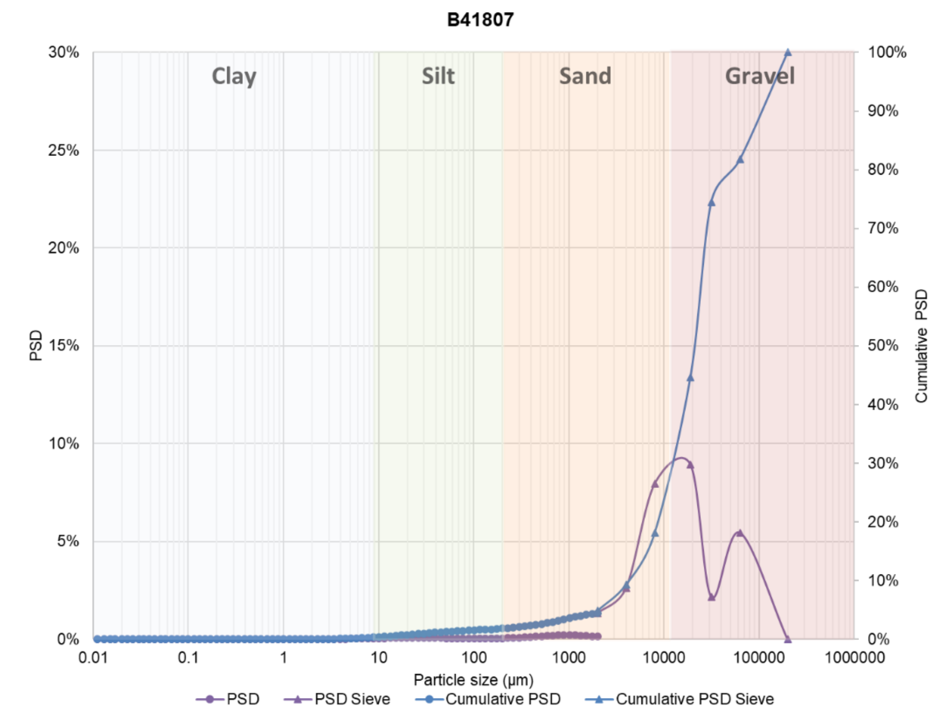

C.1.5 B41809

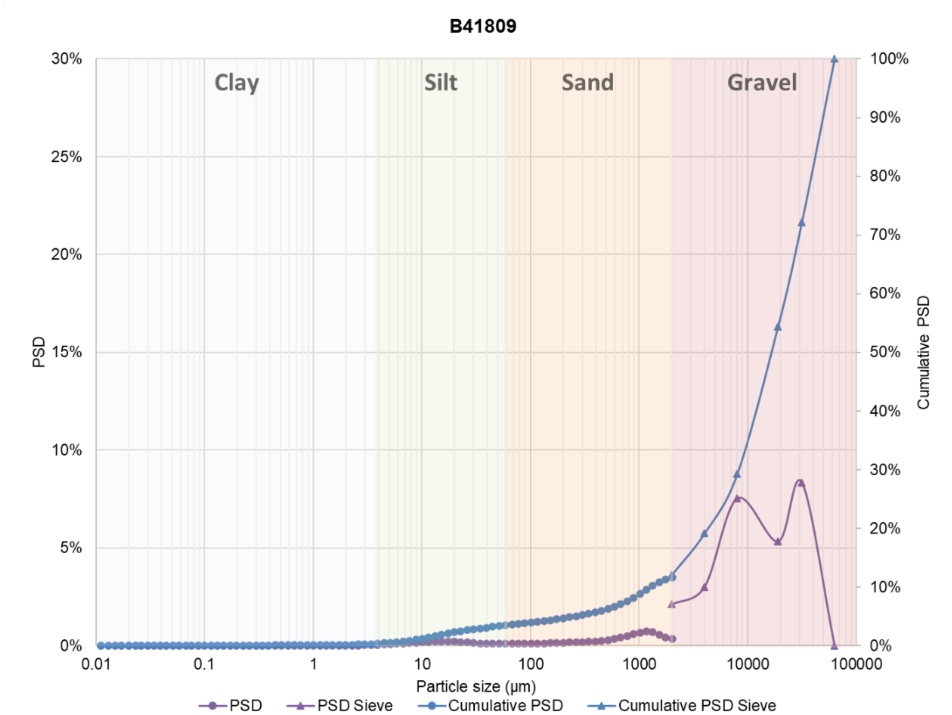

C.1.6 B41868

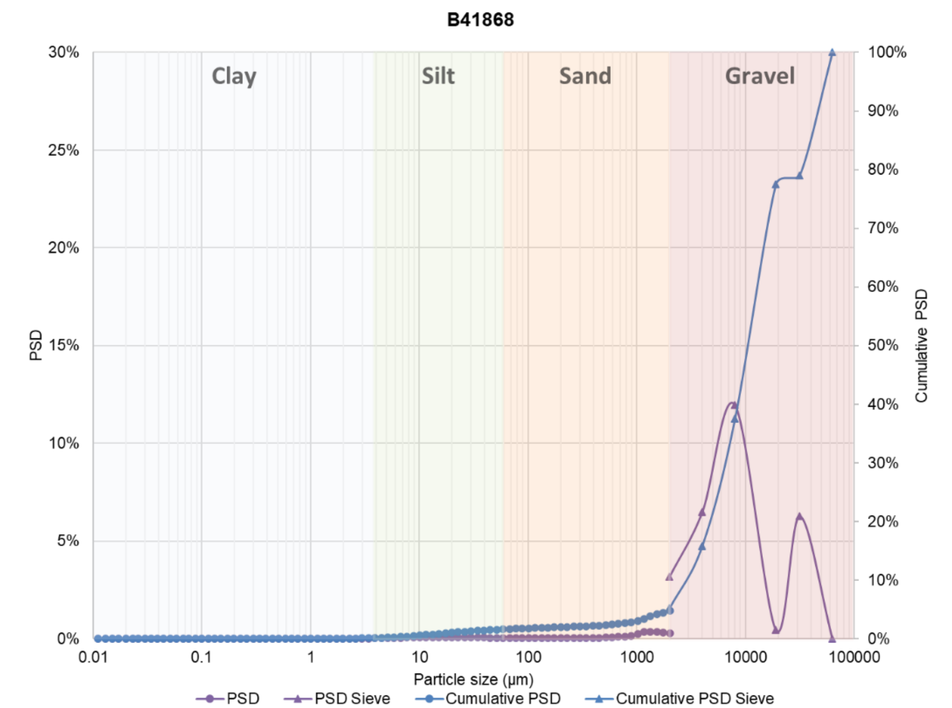

C.1.7 B418C0

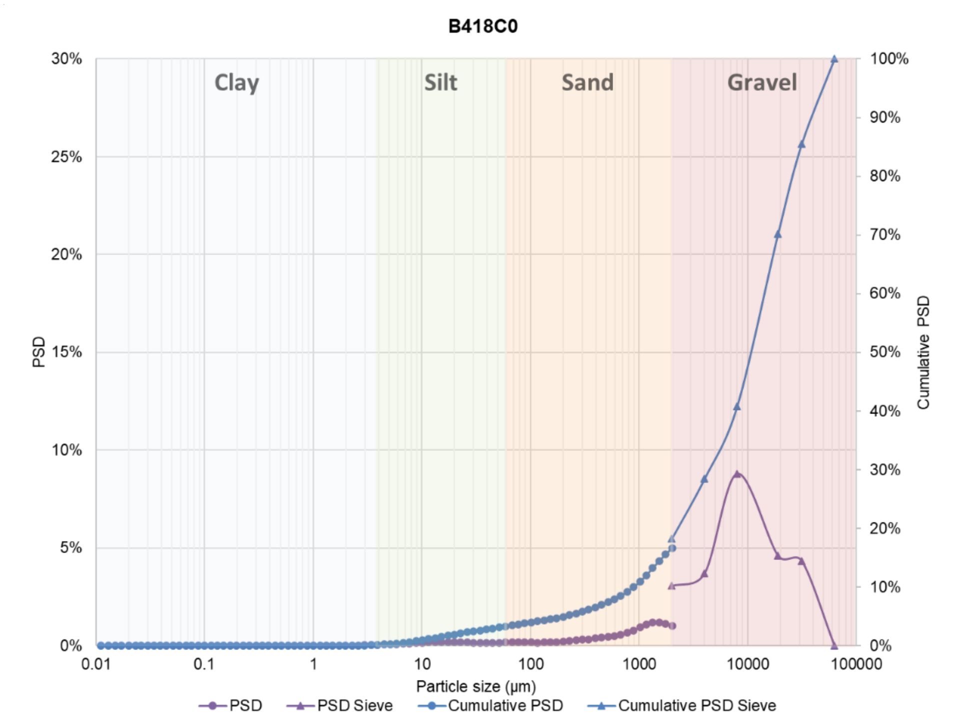

C.1.8 B418C2

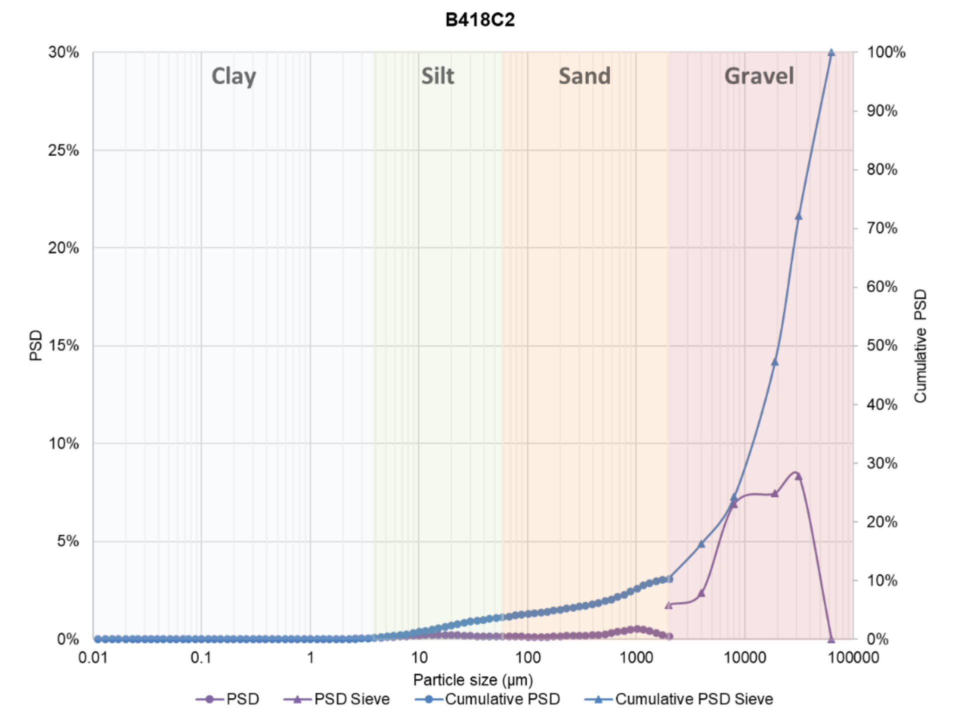

C.1.9 B3YK00

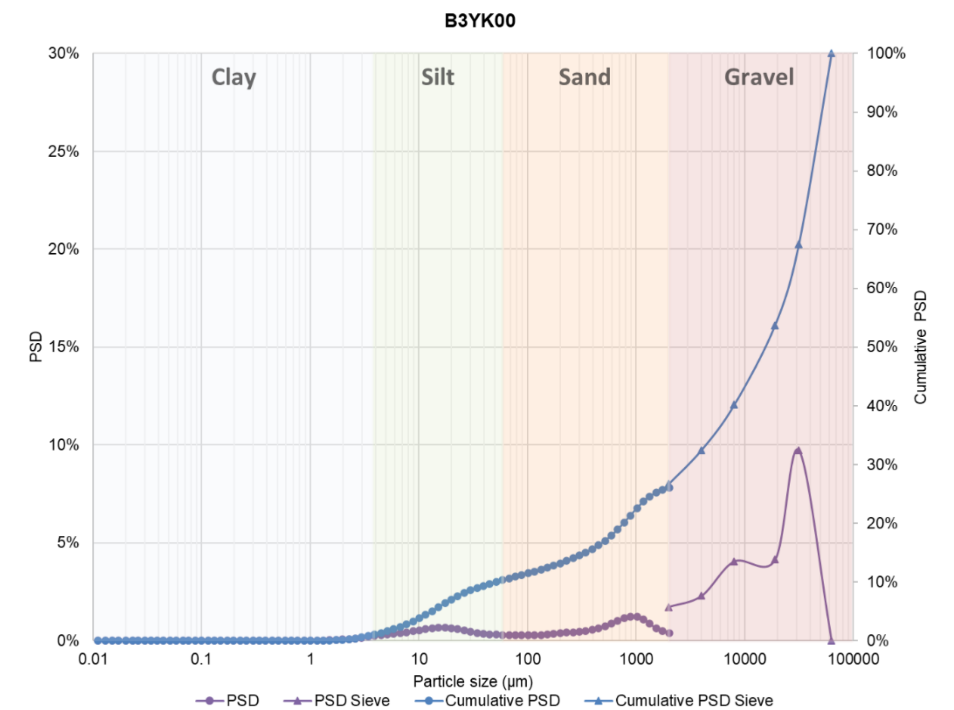

C.1.10 B3YJY6

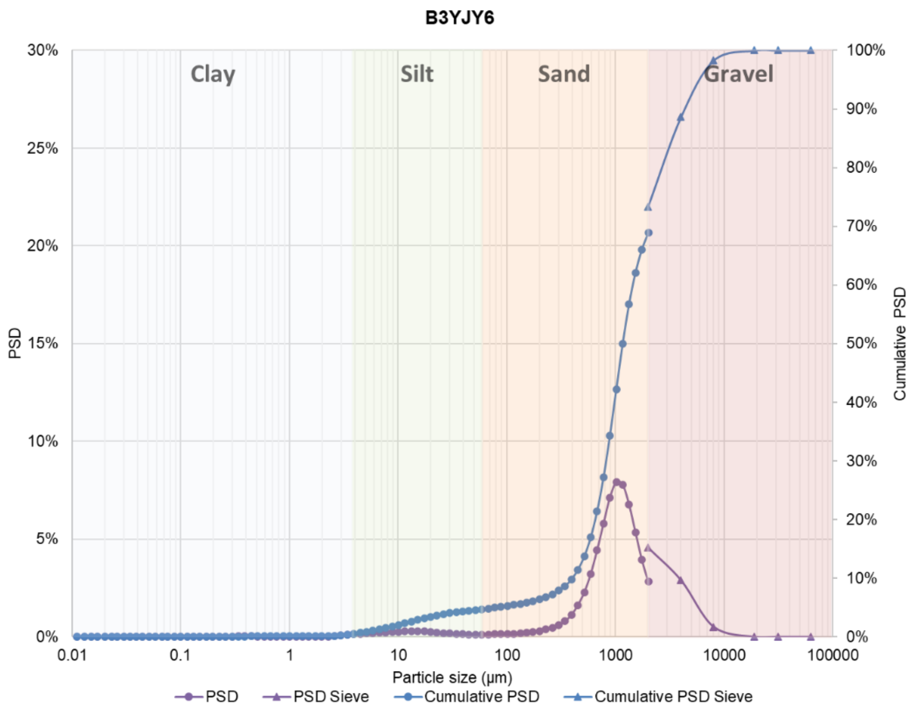

C.1.11 B3YJY7

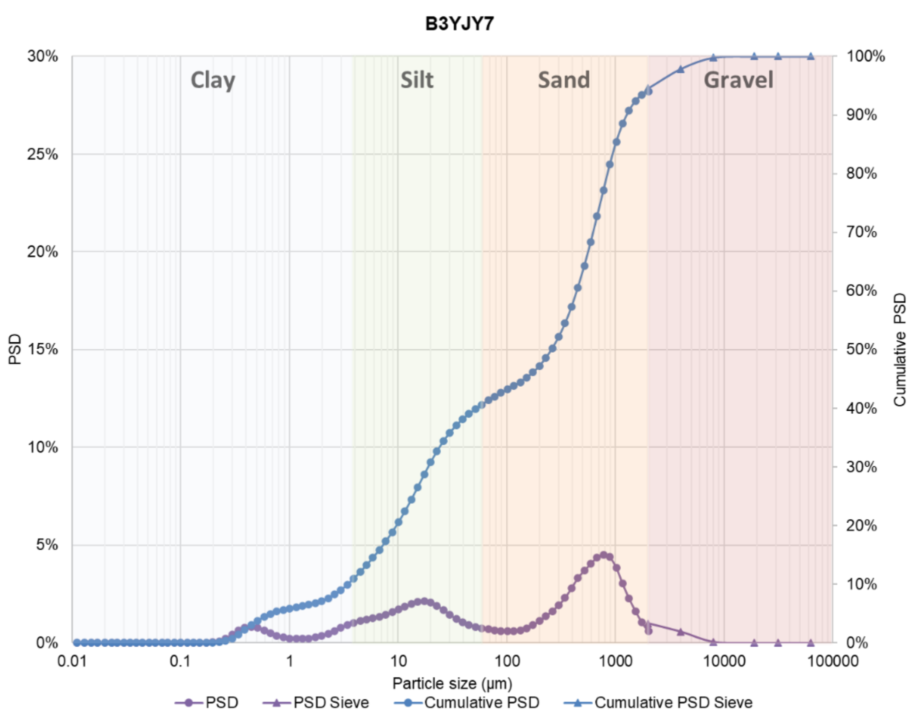

C.1.12 B3YJY8

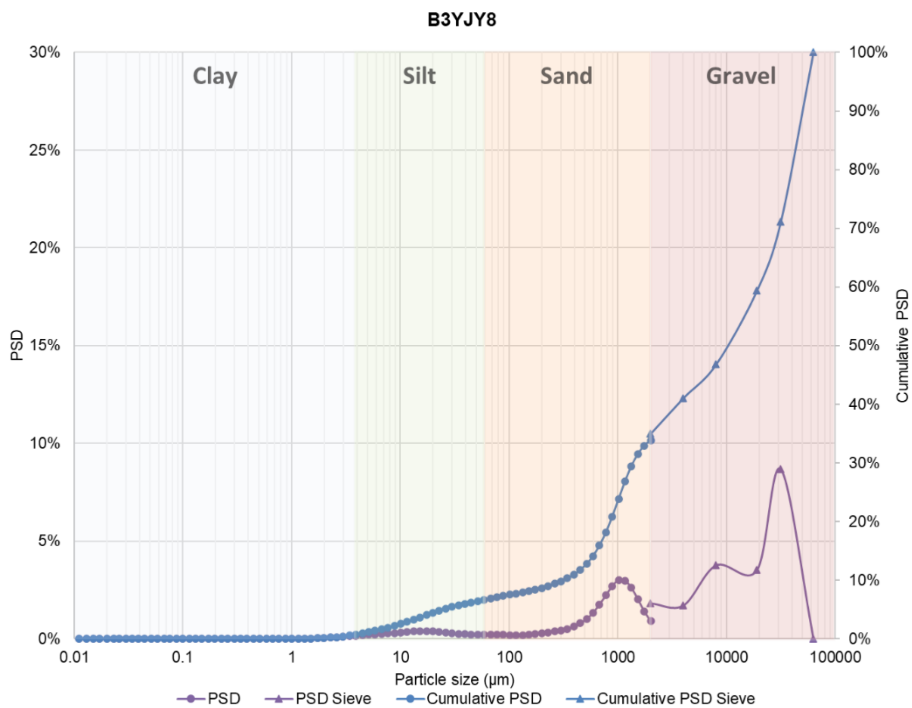

C.1.13 B3YJY9

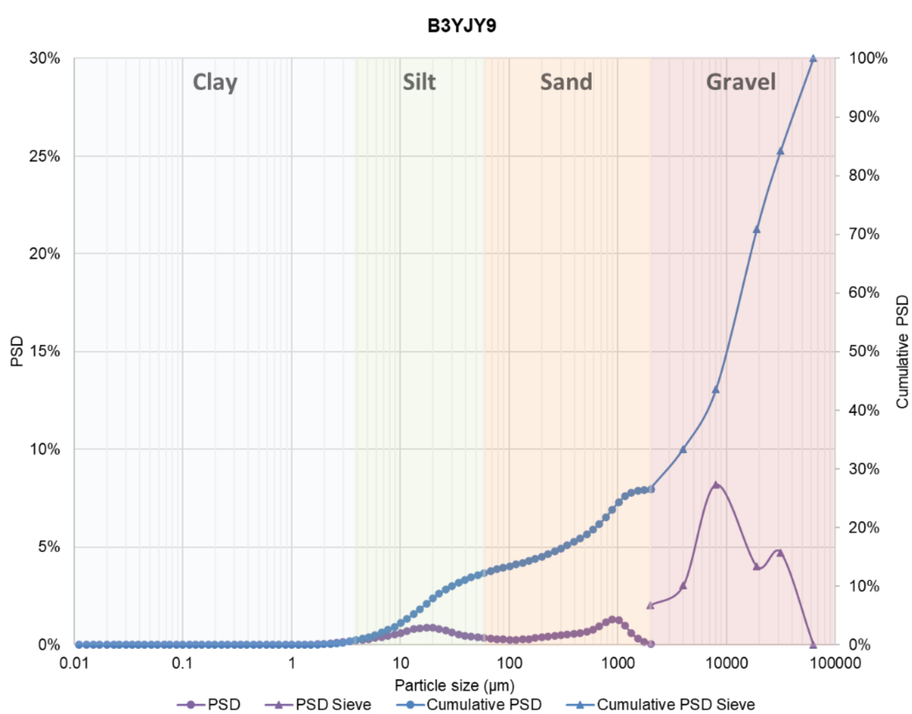

C.1.14 B3YJX6

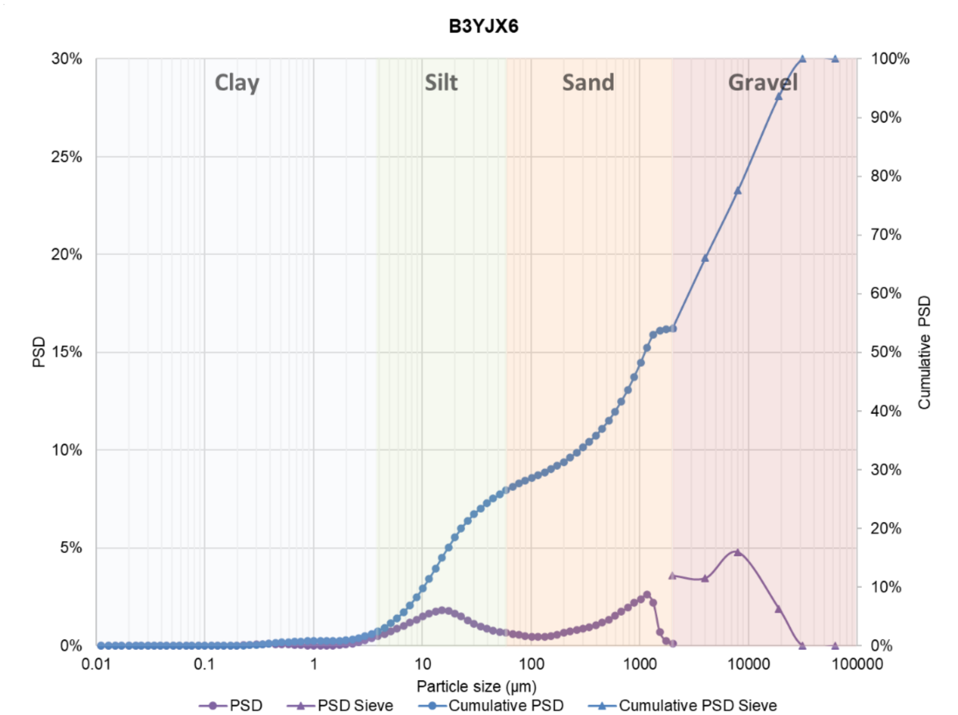

C.1.15 B3YJY5

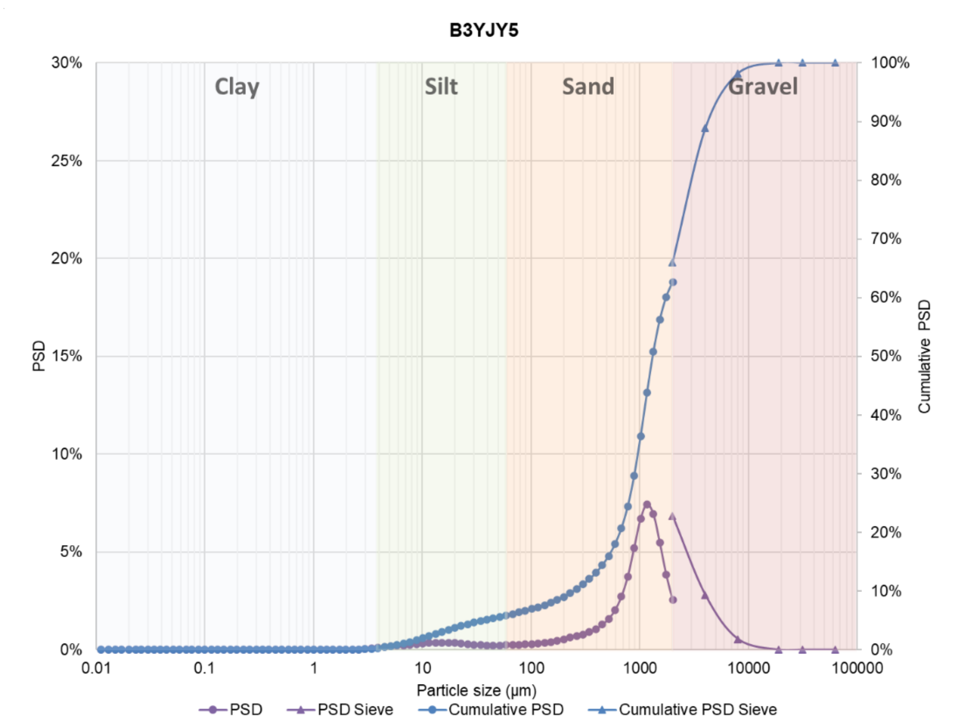

C.1.16 B3YJX1

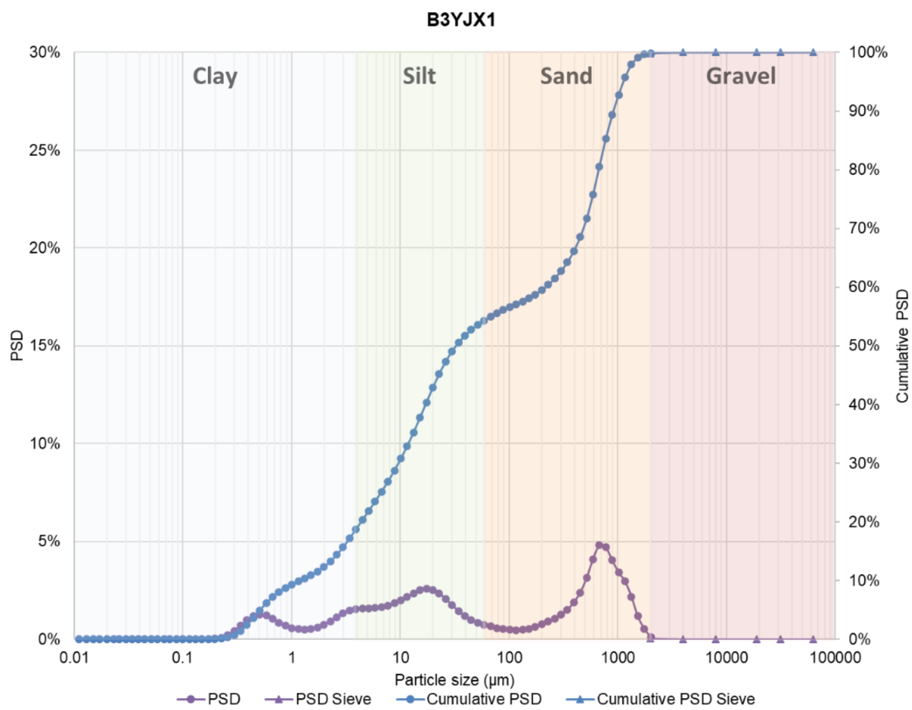

C.1.17 B3YJX2

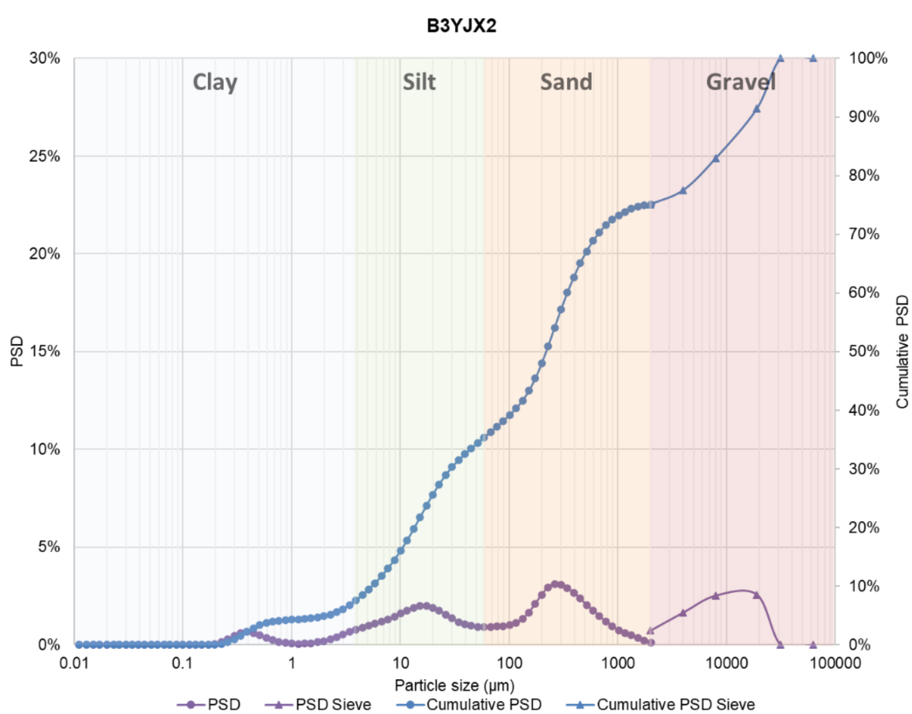

C.1.18 B3YJD8

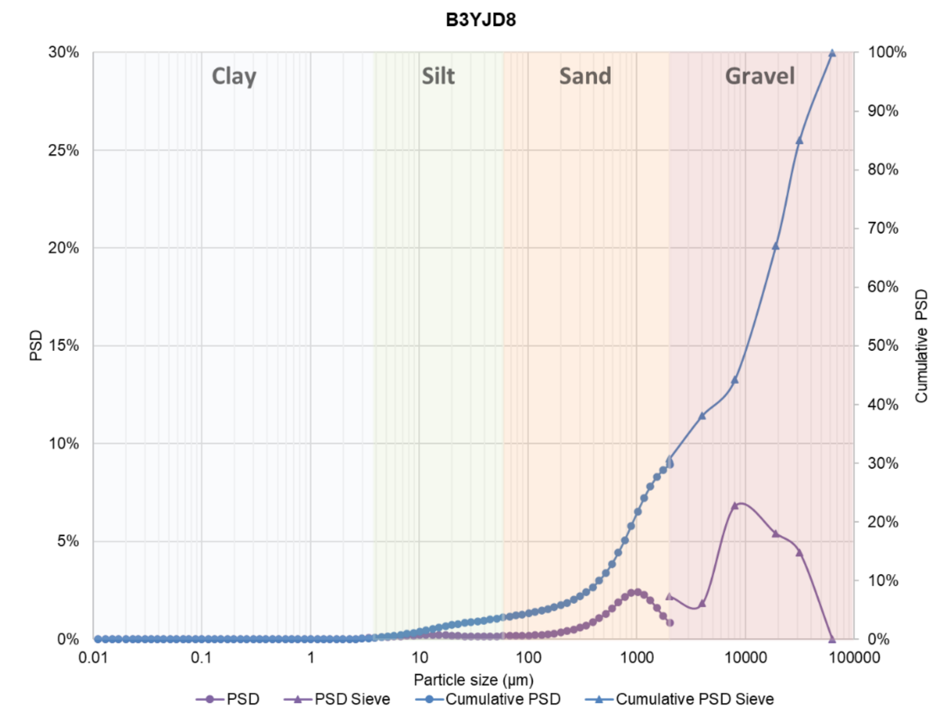

C.1.19 B3YJD9

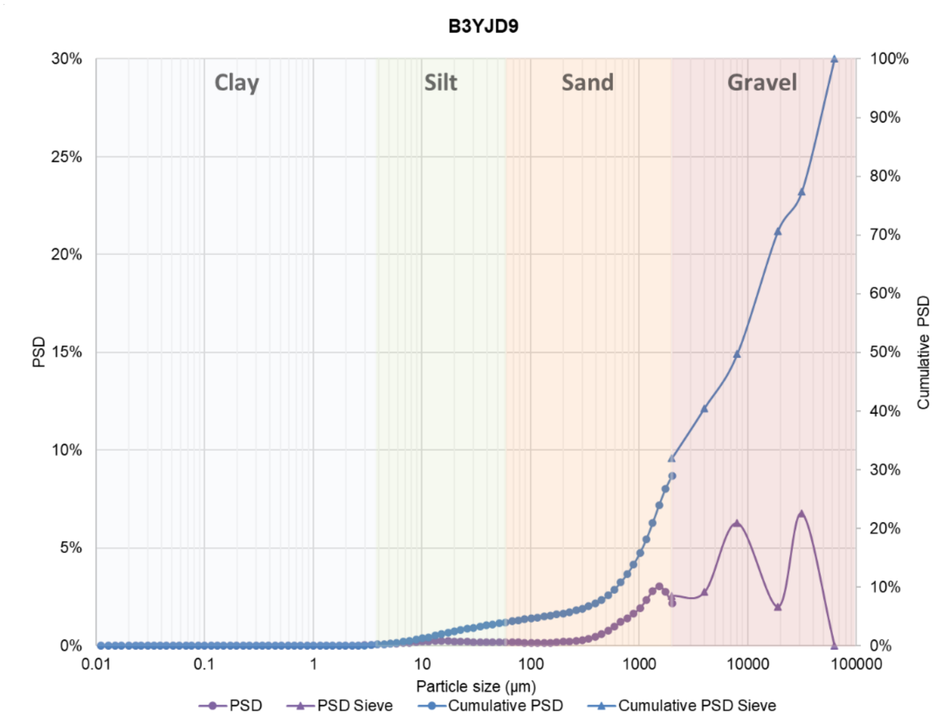

C.1.20 B3YJF9

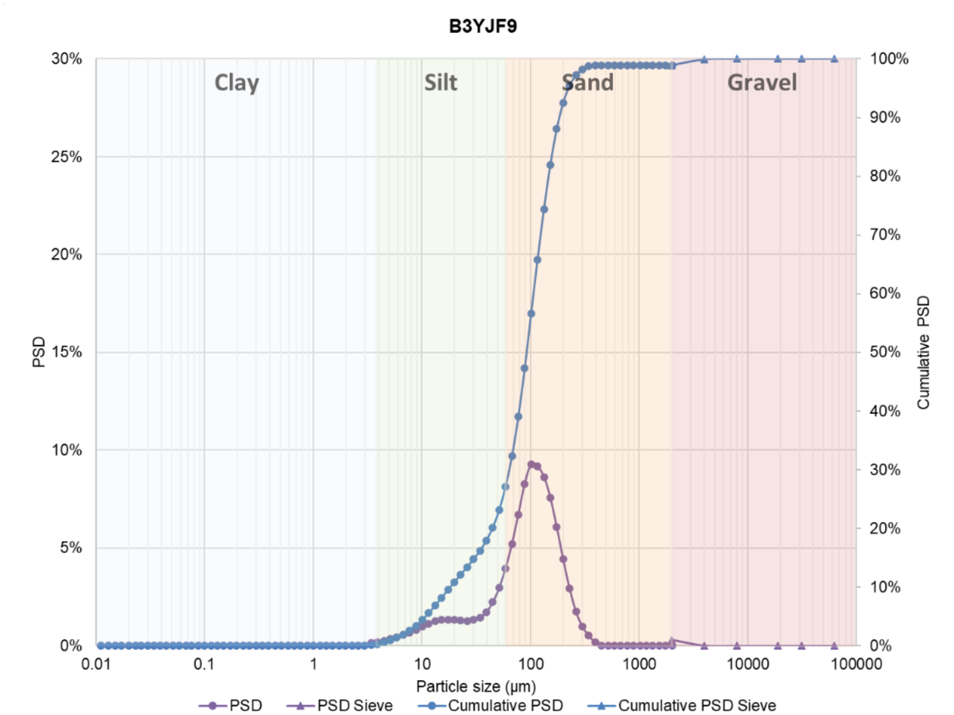

C.1.21 B3YJH0

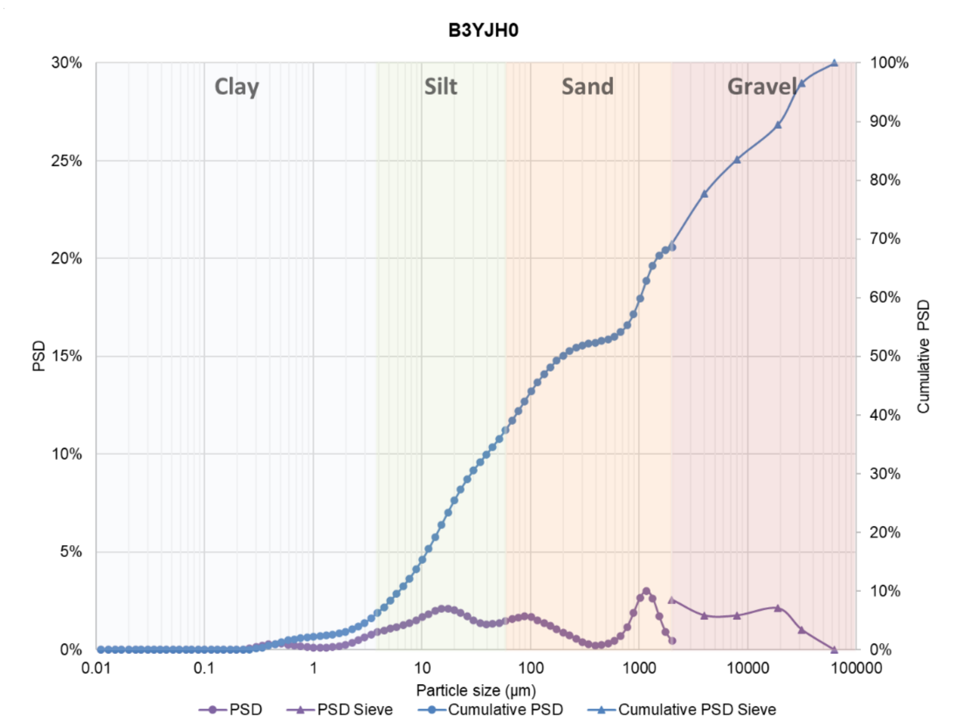

C.1.22 B3YJH1

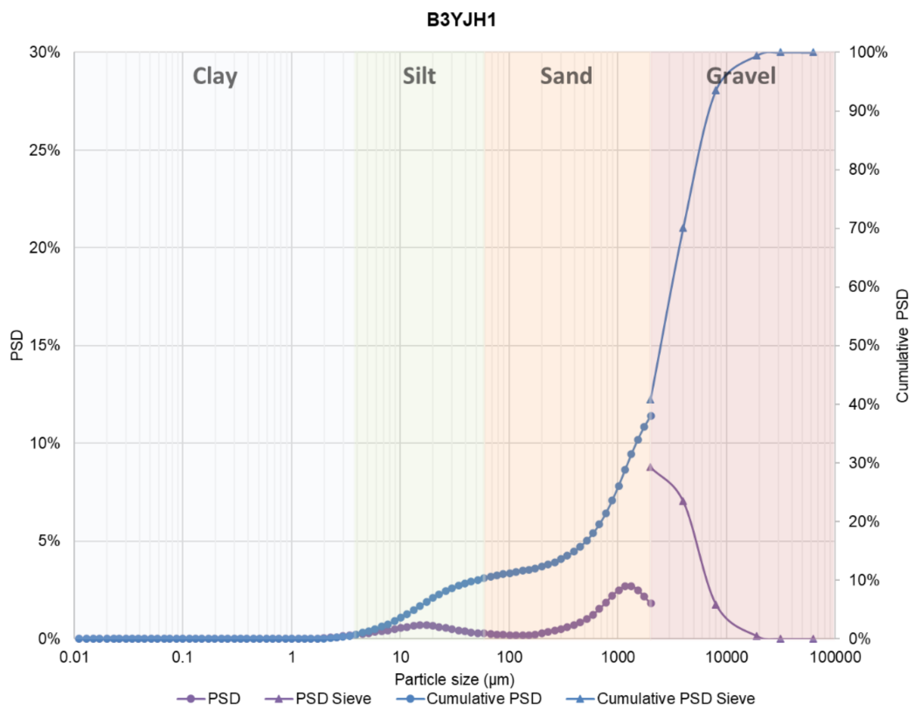

C.1.23 B3YJH2

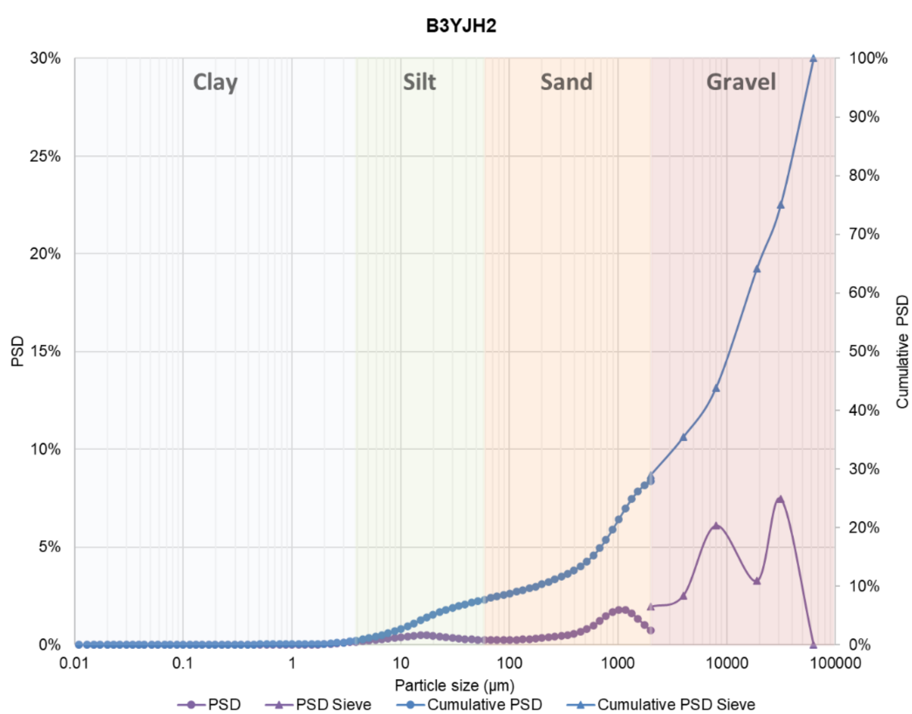

C.1.24 B3YJH3

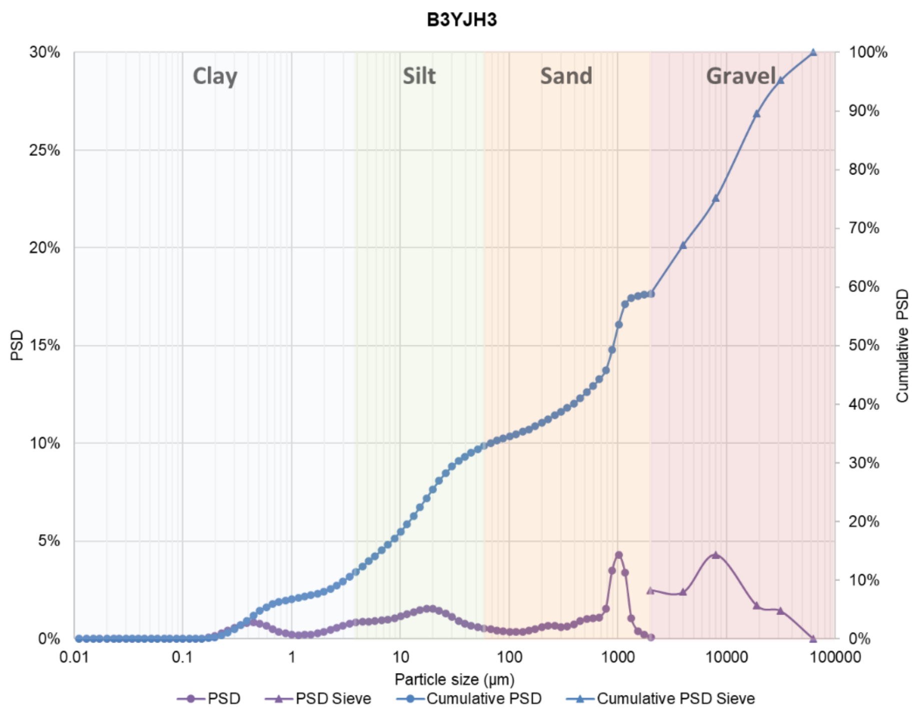

C.1.25 B3YJF8

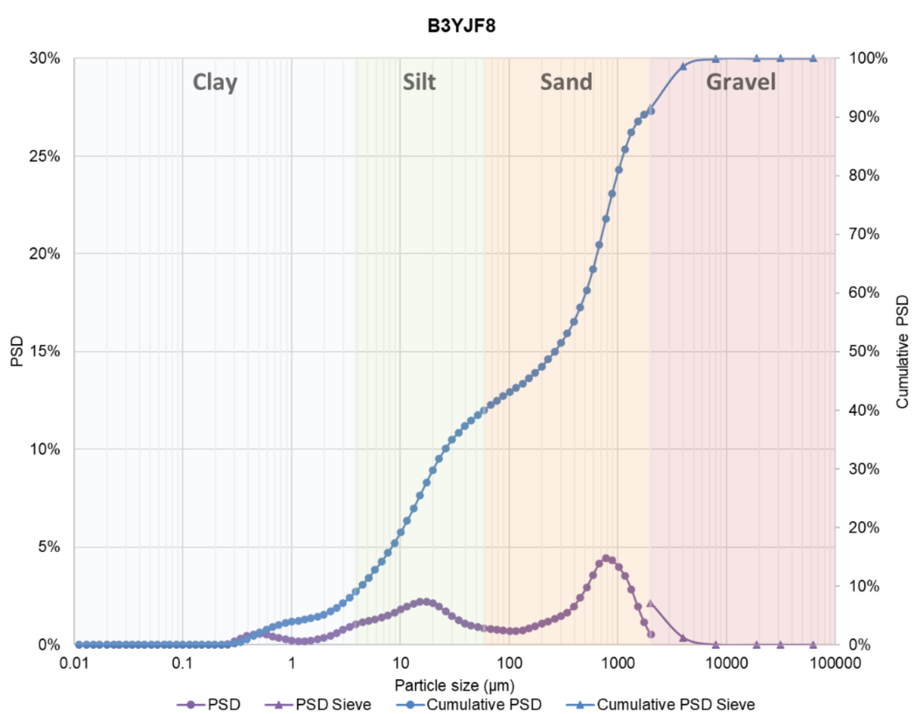

C.2 200 East Composites

C.2.1 Composite 1

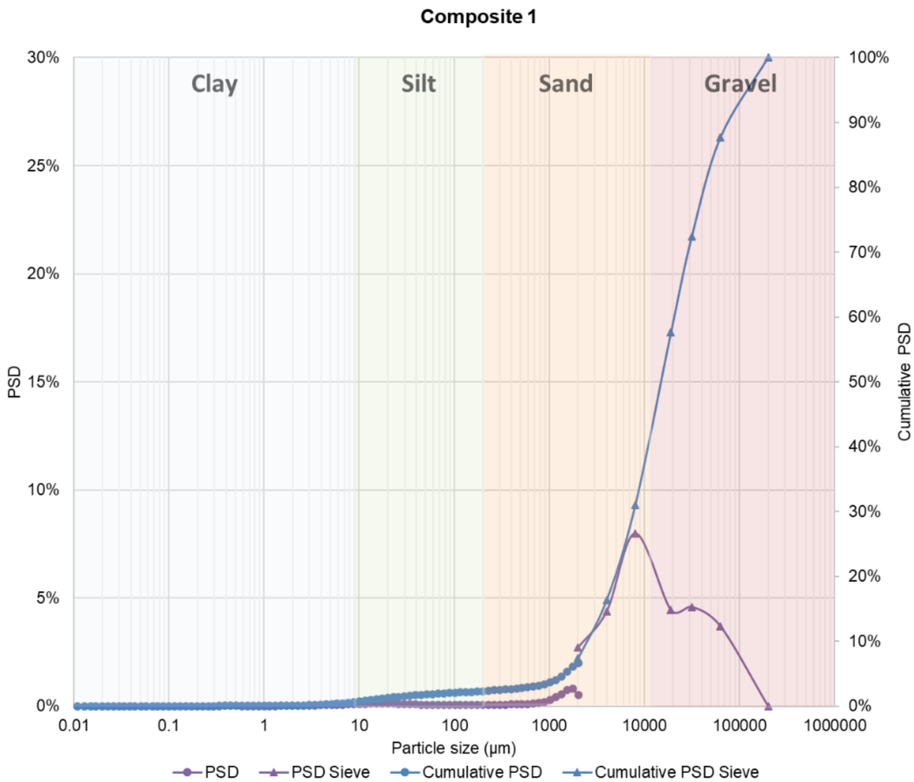

C.2.2 Composite 2

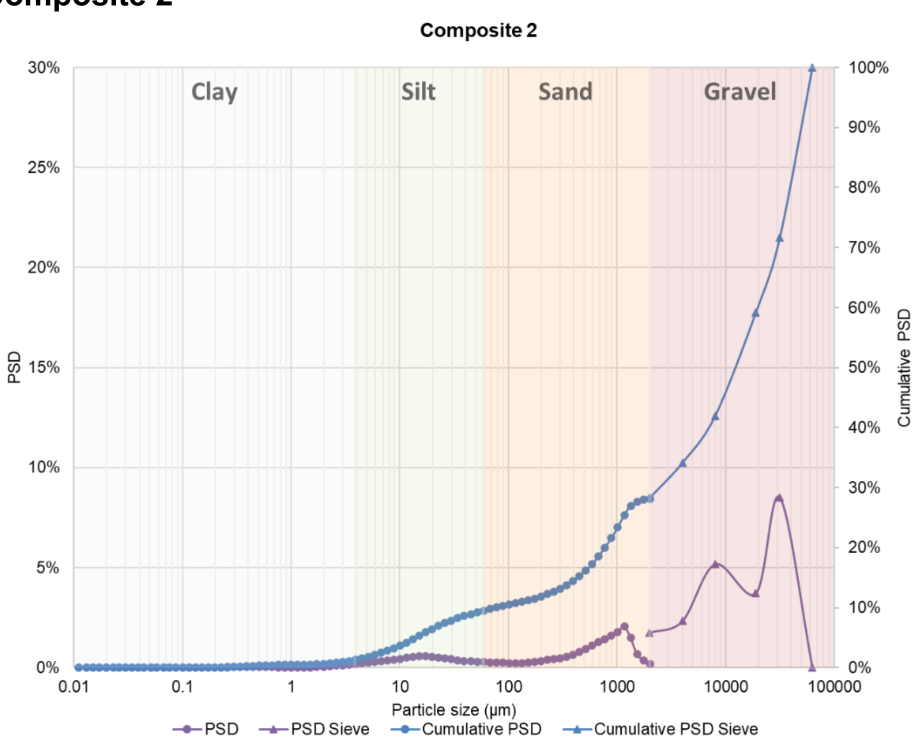

C.2.3 Composite 3

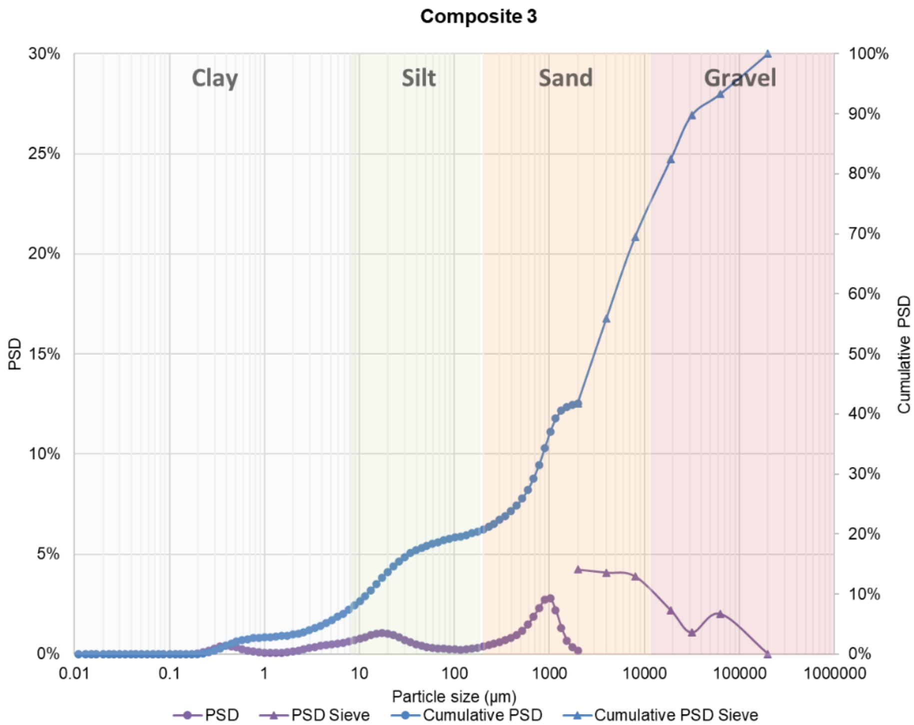

C.3 200 West

C.3.1 B488V3

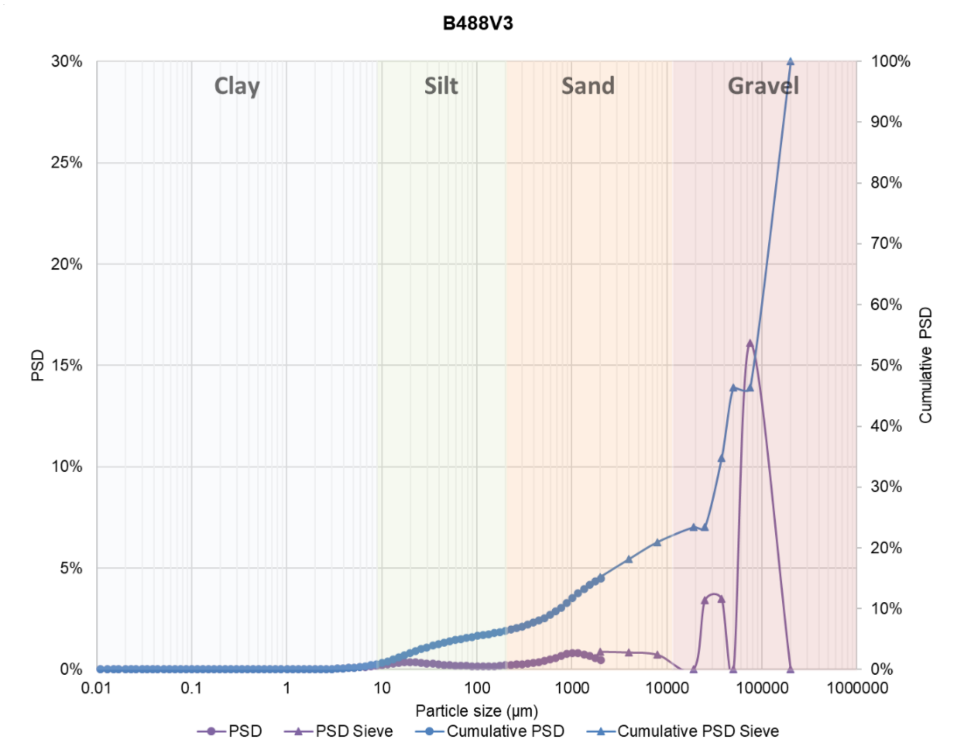

C.3.2 B488V7

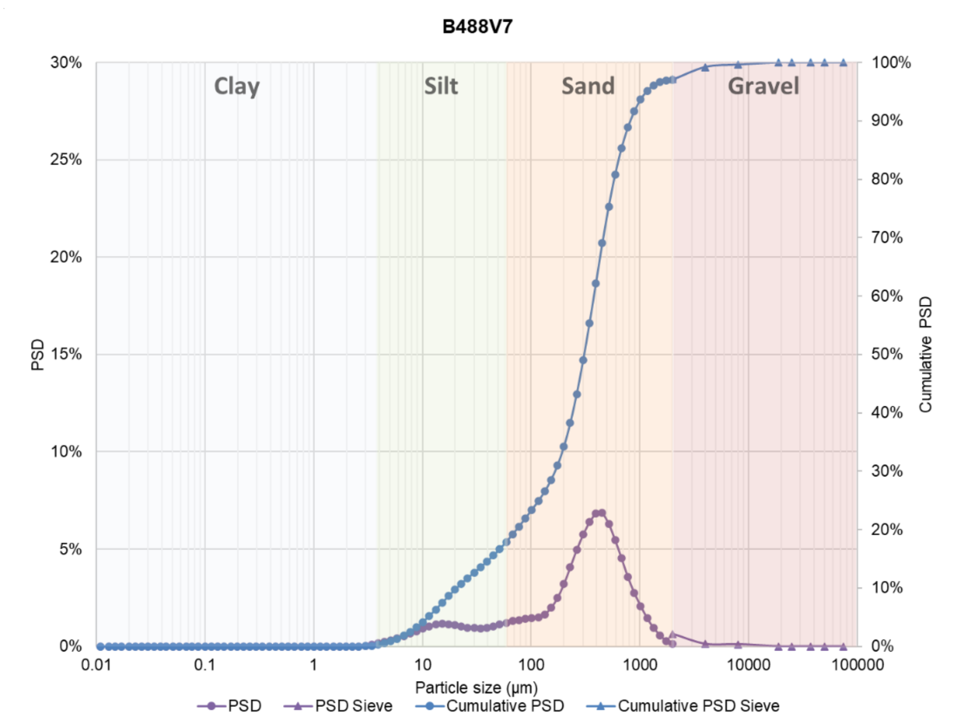

C.3.3 B488Y1

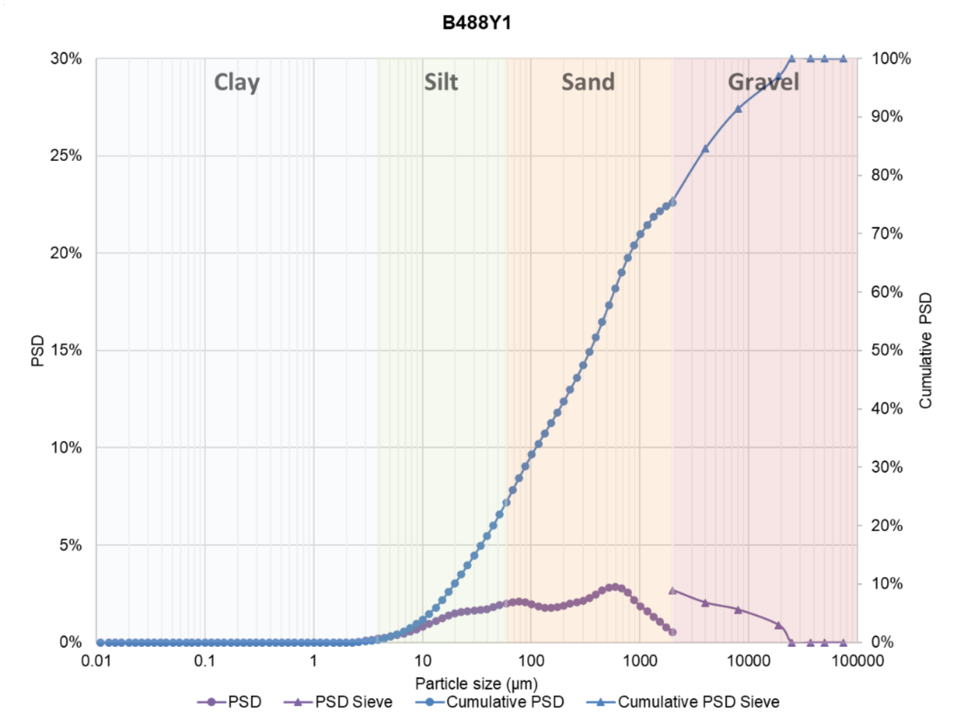

C.3.4 B488Y3

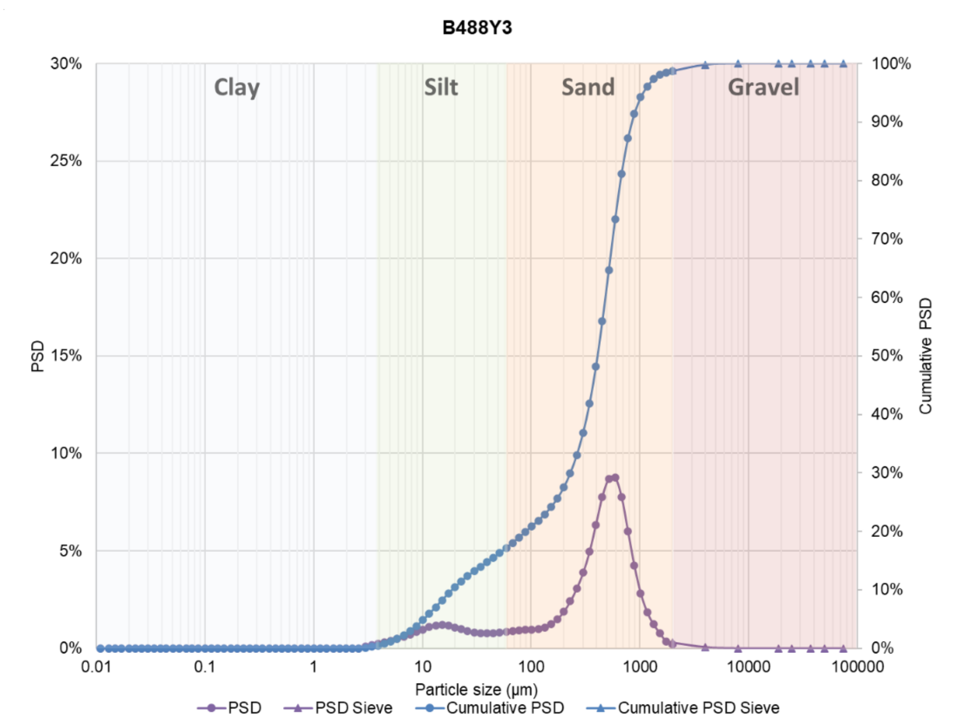

C.3.5 B488Y4

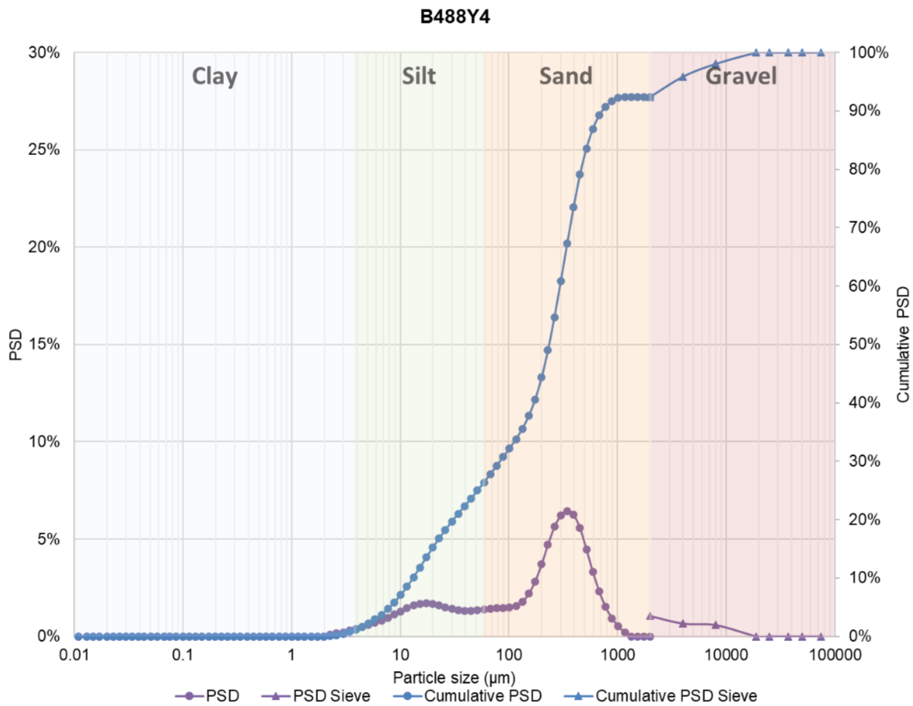

C.3.6 B488W5

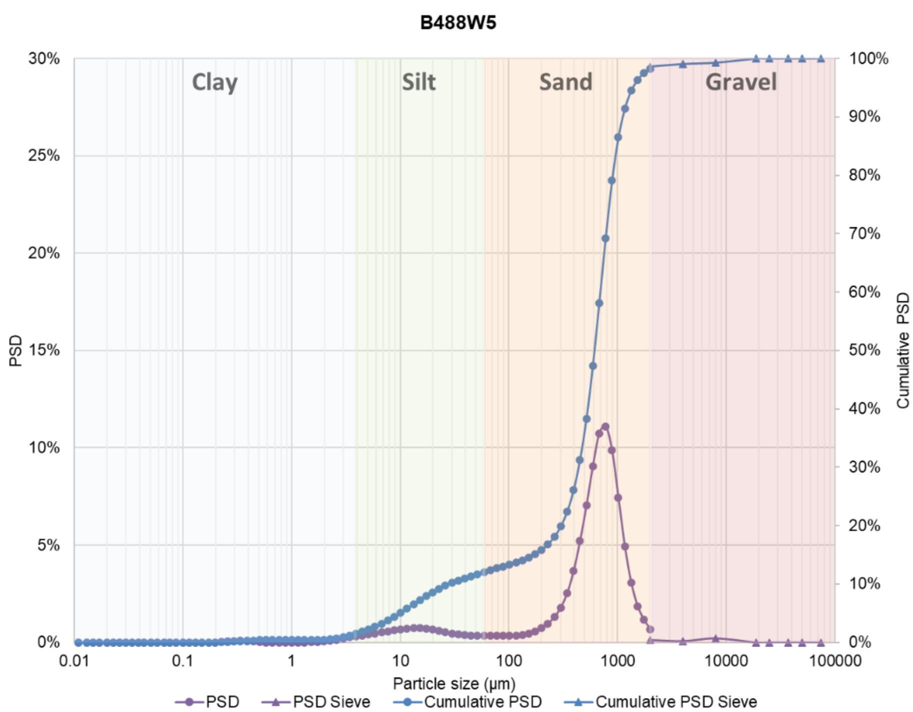

C.3.7 B488W7

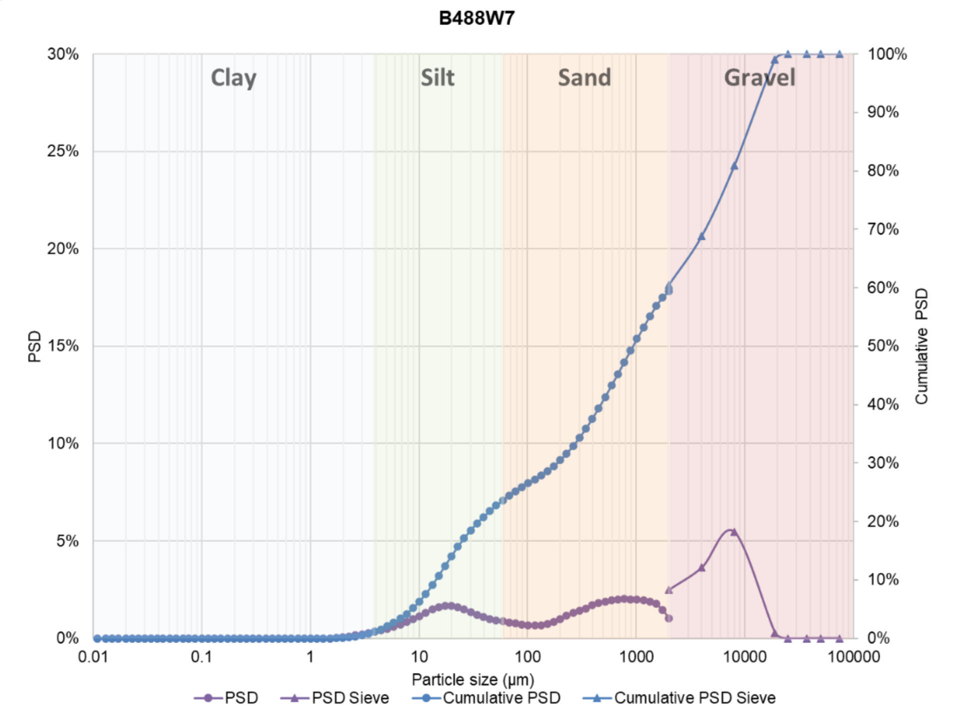

C.3.8 B488X2

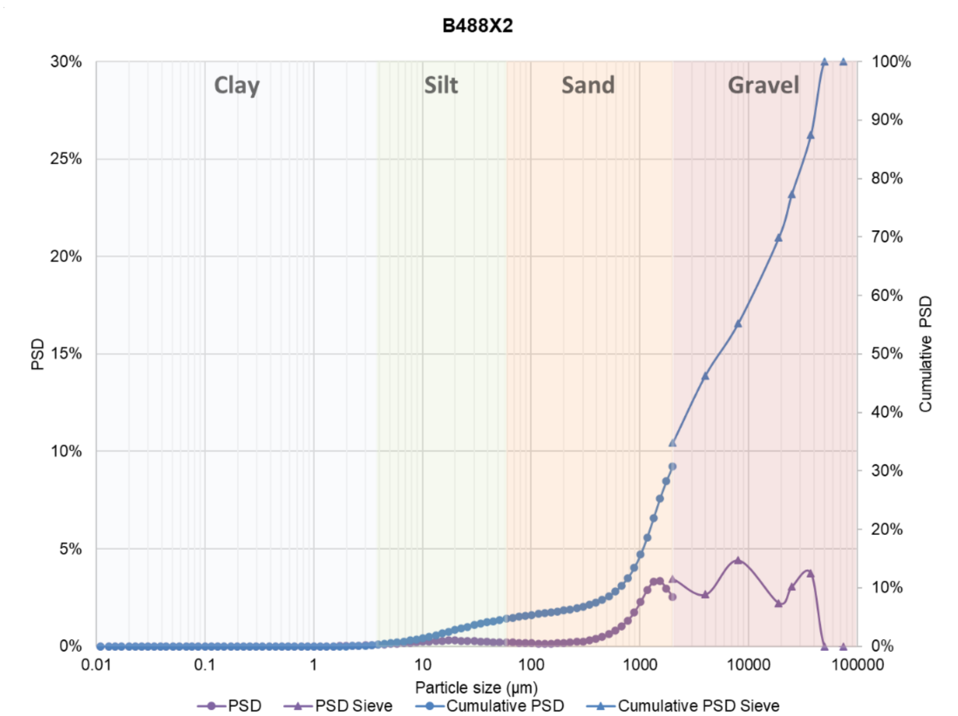

C.3.9 B48N72

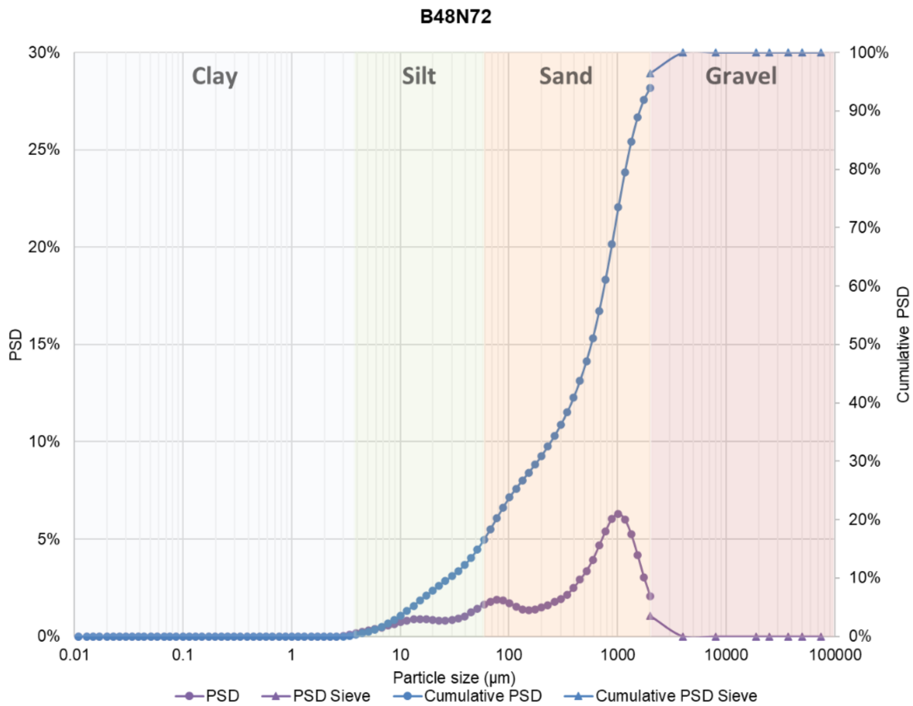

C.3.10 B48N73

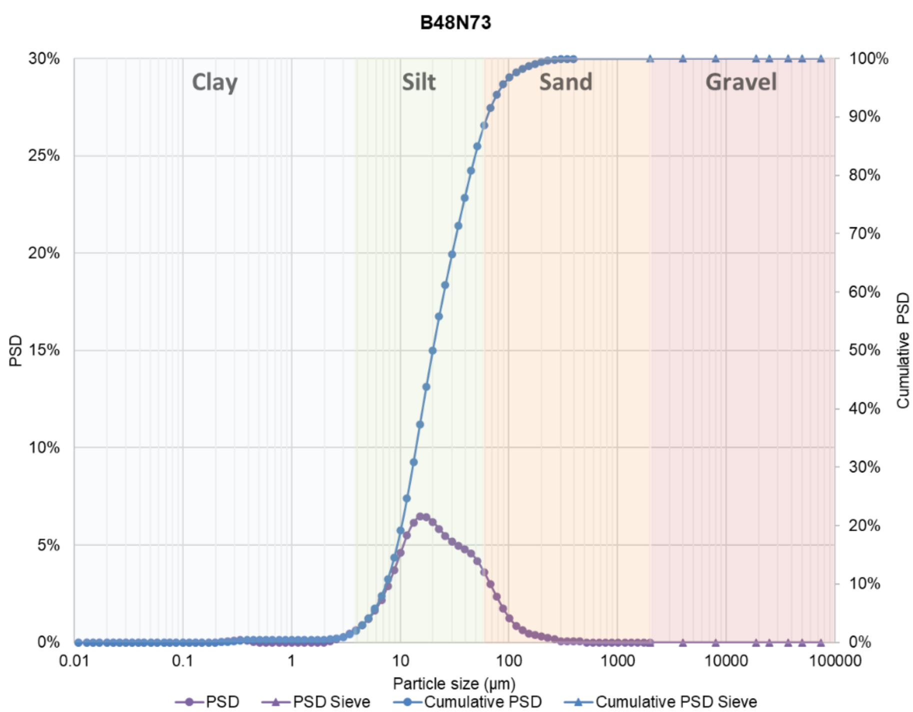

C.3.11 B48N74

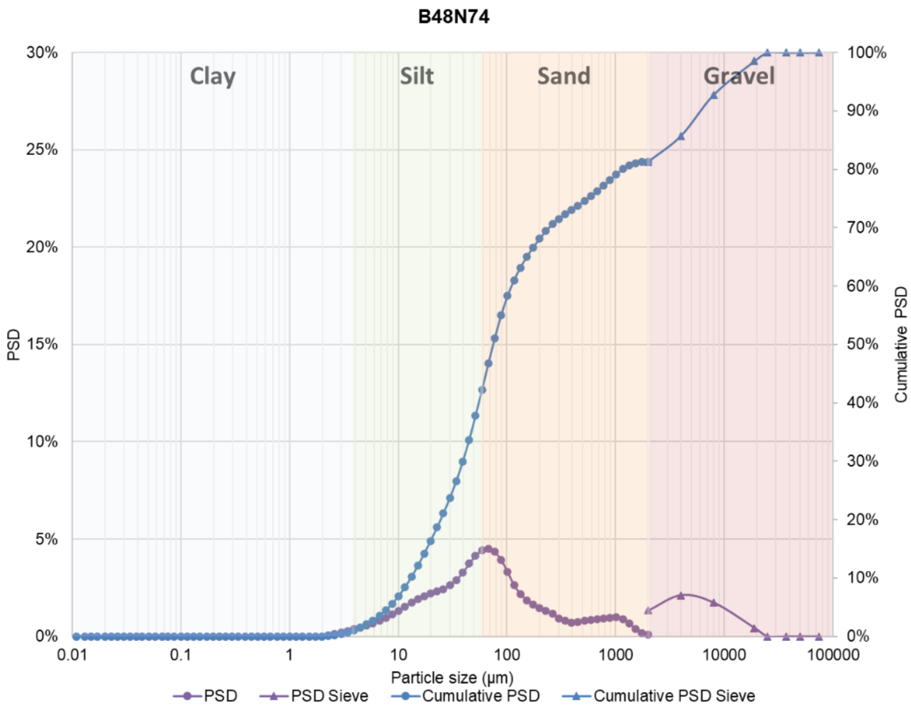

C.3.12 B48N76

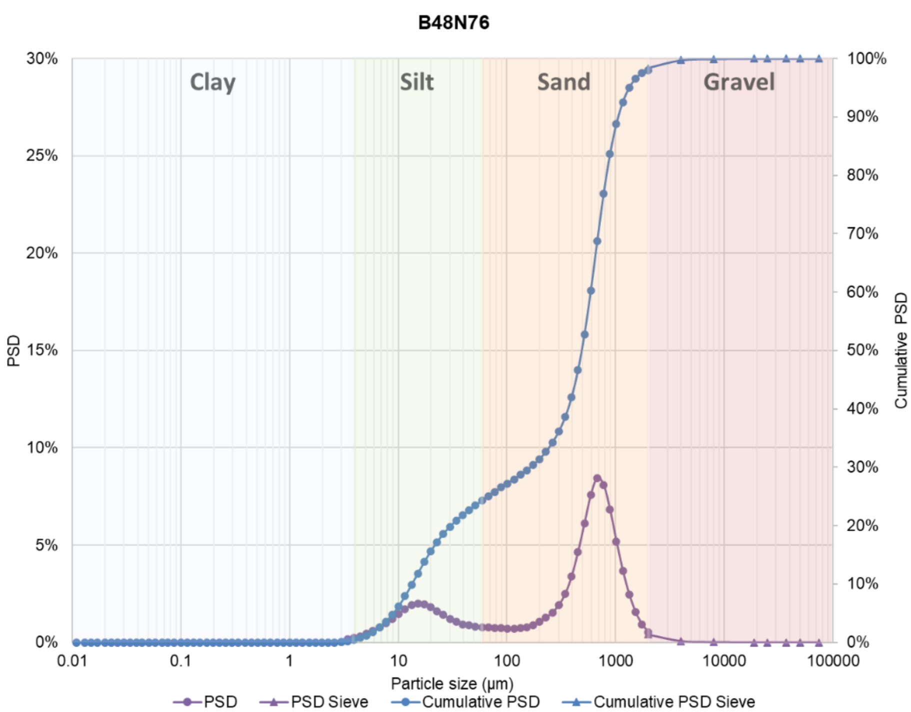

C.3.13 B48N79

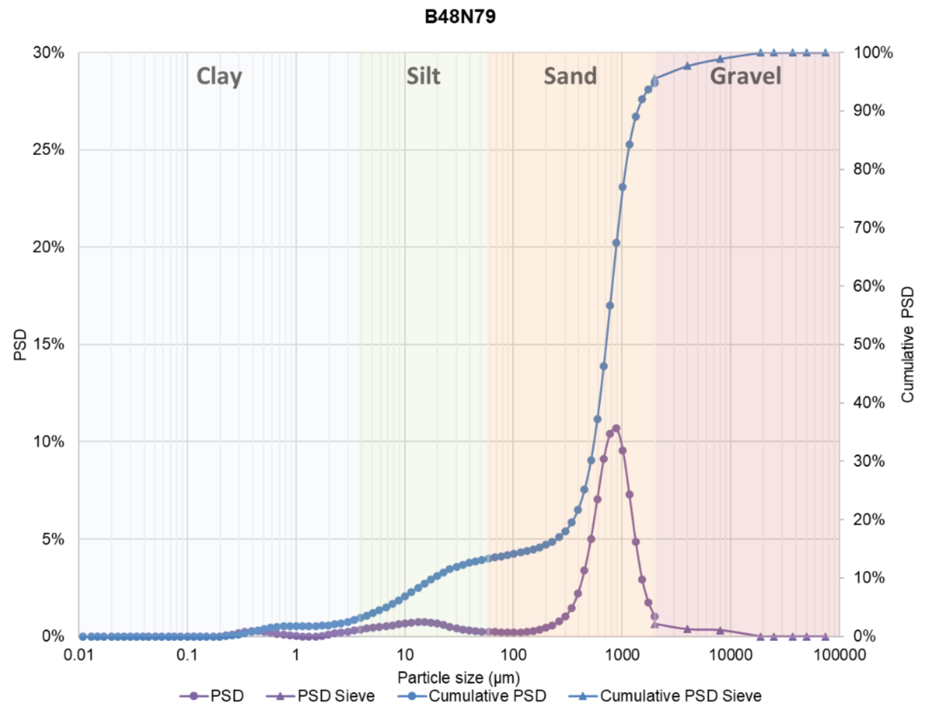

C.3.14 B48ND9-B

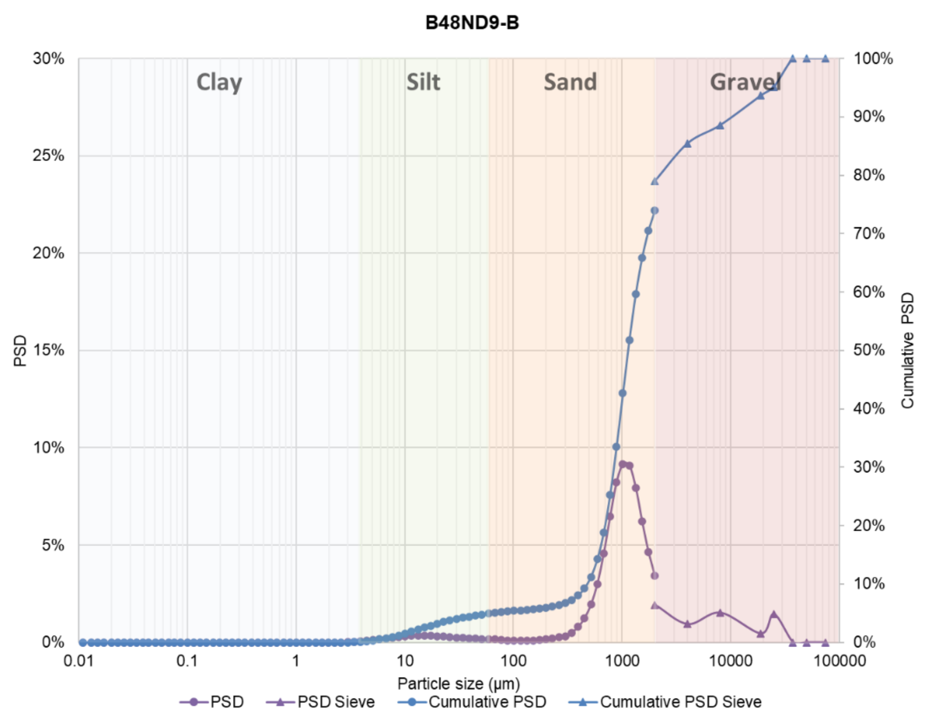

C.3.15 B48ND9-D

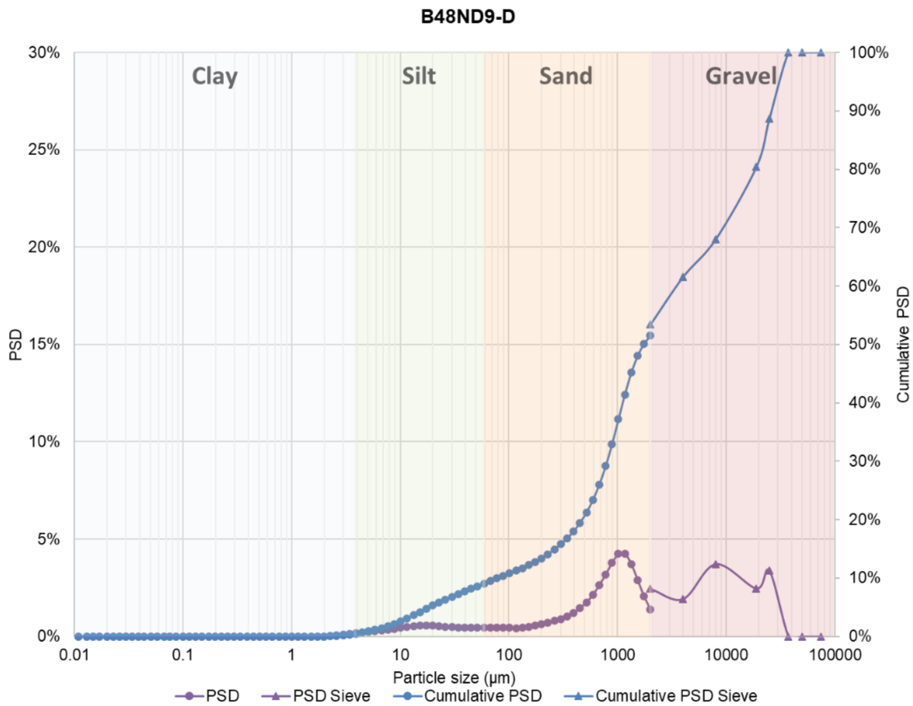

C.3.16 B48NF4

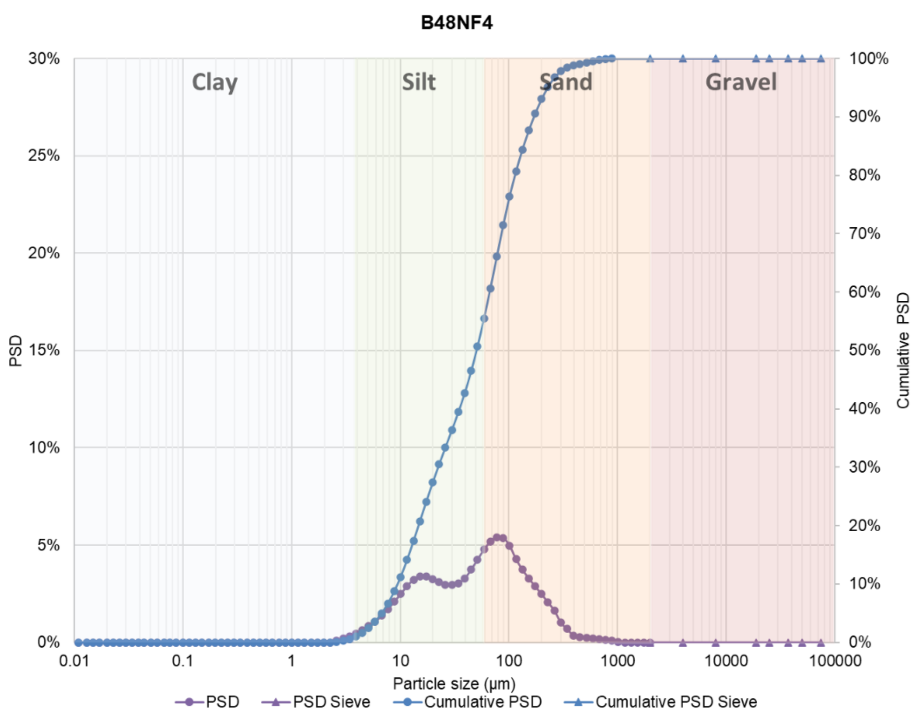

C.3.17 B48NH0-H

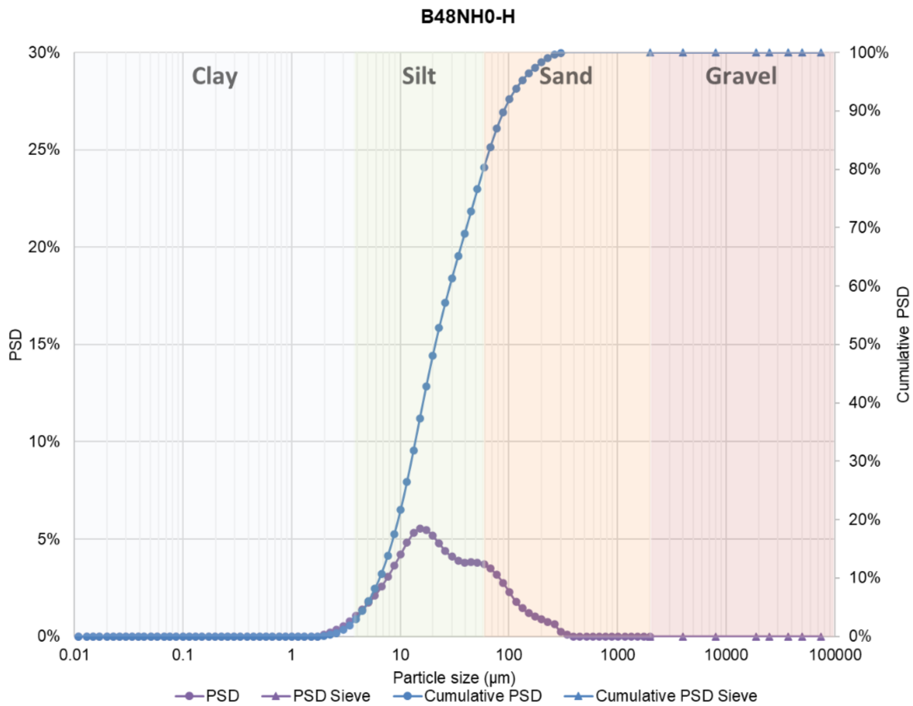

C.3.18 B48NH0-I

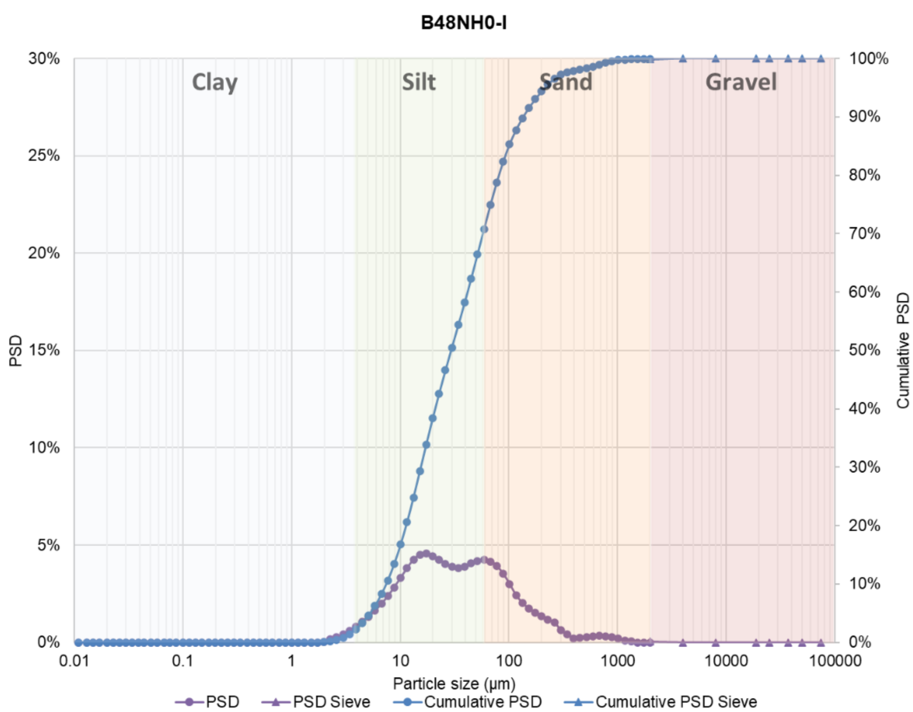

C.3.19 B48NH7

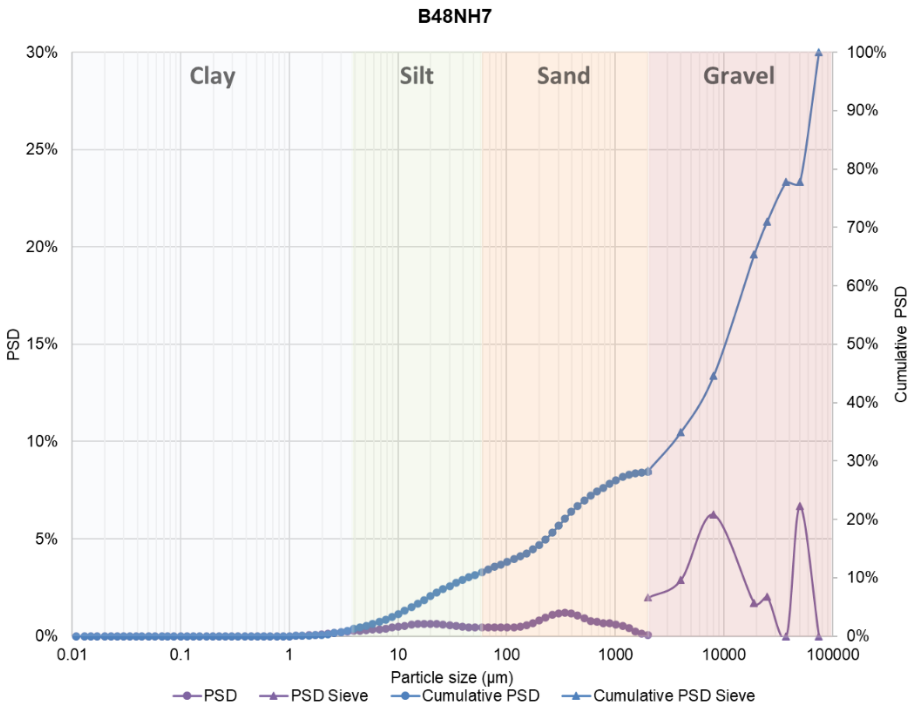
B48NH7
Clay
Silt
Sand
Gravel
30%
25%
20%
15%
10%
5%
0%
PSD
100%
90%
80%
70%
60%
50%
40%
30%
20%
10%
0%
Cumulative PSD
0.01
0.1
1
10
100
1000
10000
100000
Particle size (µm)
PSD
PSD Sieve
Cumulative PSD
Cumulative PSD Sieve

Appendix D – Quasi-Static Water Retention Data and Curve Fits

This appendix contains plots of quasi-static water retention data and fitted van Genuchten (1980) and Brooks-Corey (1964) functions and associated parameters.

D.1 200 East

D.1.1 B41802

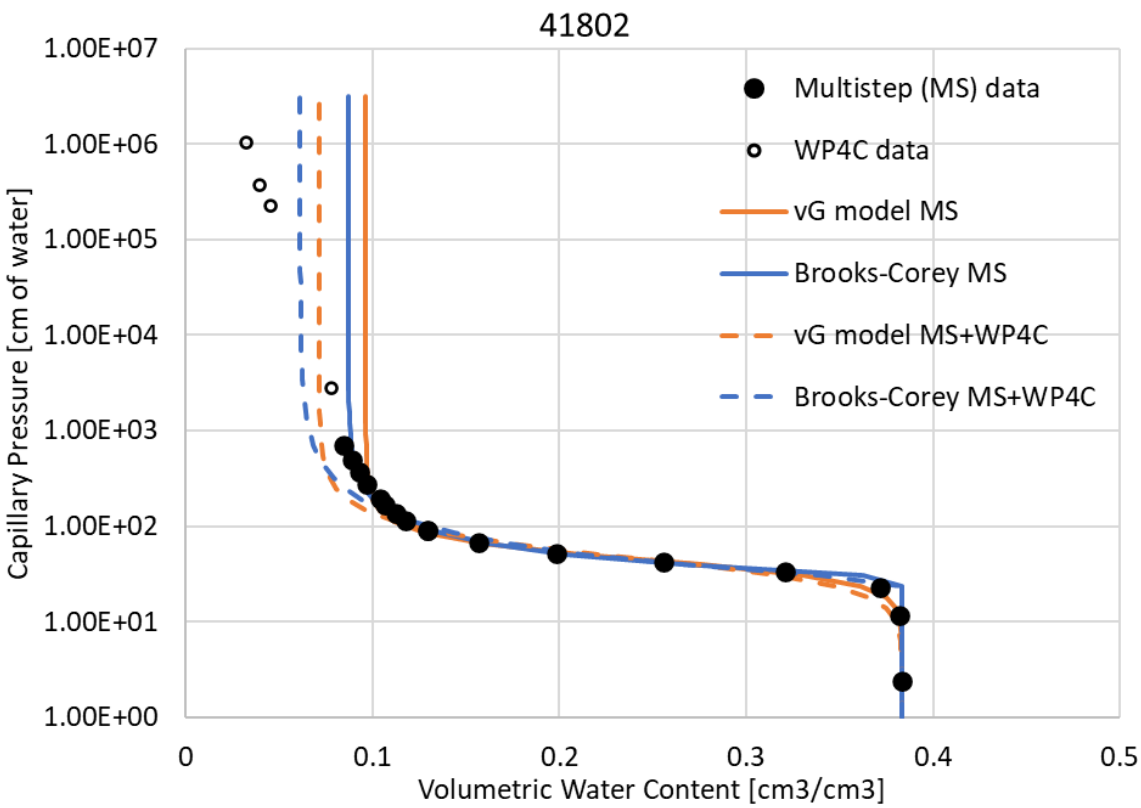

Model fits			
vG			
	alpha (1/cm)	n	theta_r
Multistep (MS)	0.0245	3.8686	0.0965
MS+WP4C	0.0249	2.9260	0.0714
Brooks-Corey			
	hb (cm)	lambda	theta_r
Multistep (MS)	28.9717	1.6416	0.0871
MS+WP4C	26.7170	1.1620	0.0614

D.1.2 B3YJY6

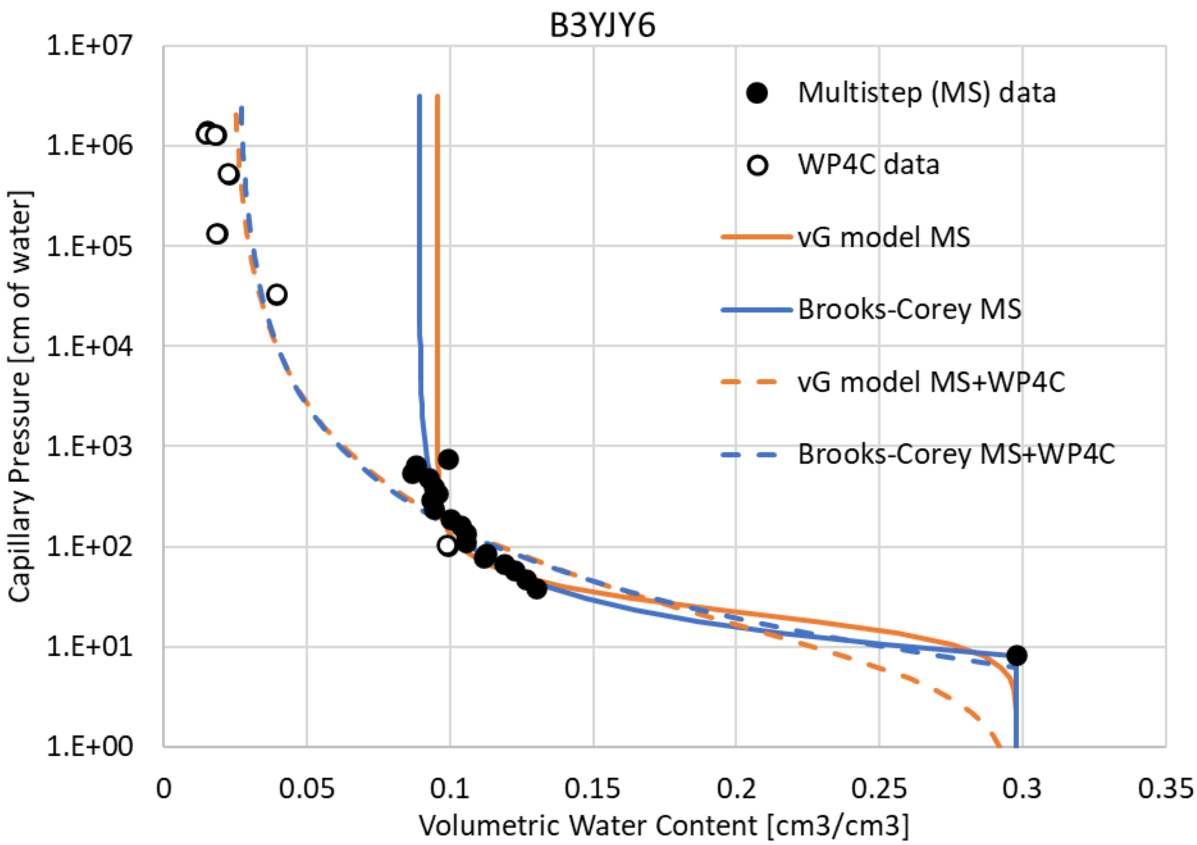

Model fits			
vG			
	alpha (1/cm)	n	theta_r
Multistep (MS)	0.0540	2.9247	0.0956
MS+WP4C	0.1614	1.3818	0.0231
Brooks-Corey			
	hb (cm)	lambda	theta_r
Multistep (MS)	8.2357	0.9823	0.0894
MS+WP4C	6.3233	0.3996	0.0254

D.1.3 B3YJY7

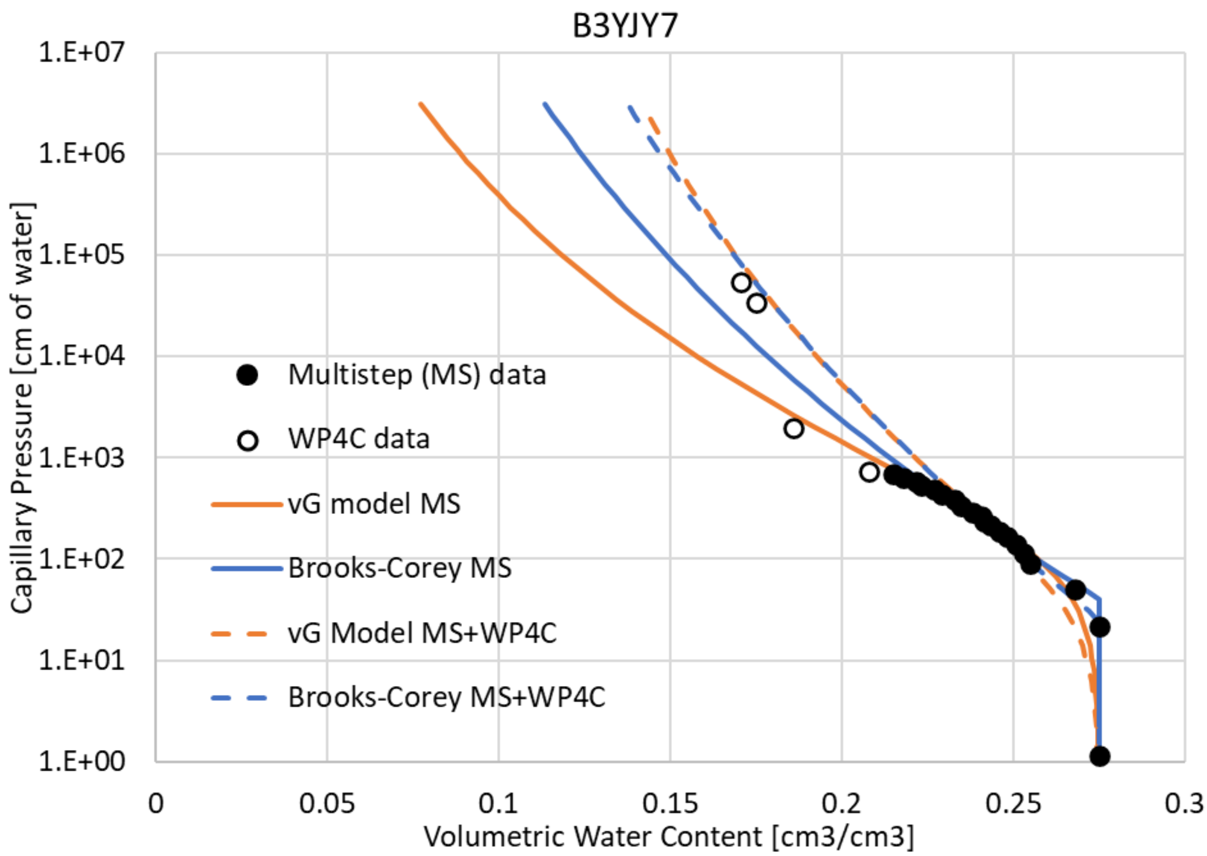

Model fits			
	vG		
	alpha (1/cm)	n	theta_r
Multistep (MS)	0.0085	1.1247	0.0000
MS+WP4C	0.0265	1.0899	0.0666
	Brooks-Corey		
	hb (cm)	lambda	theta_r
Multistep (MS)	41.2956	0.0788	0.0000
MS+WP4C	25.3495	0.0591	0.0000

D.1.4 B3YJY5

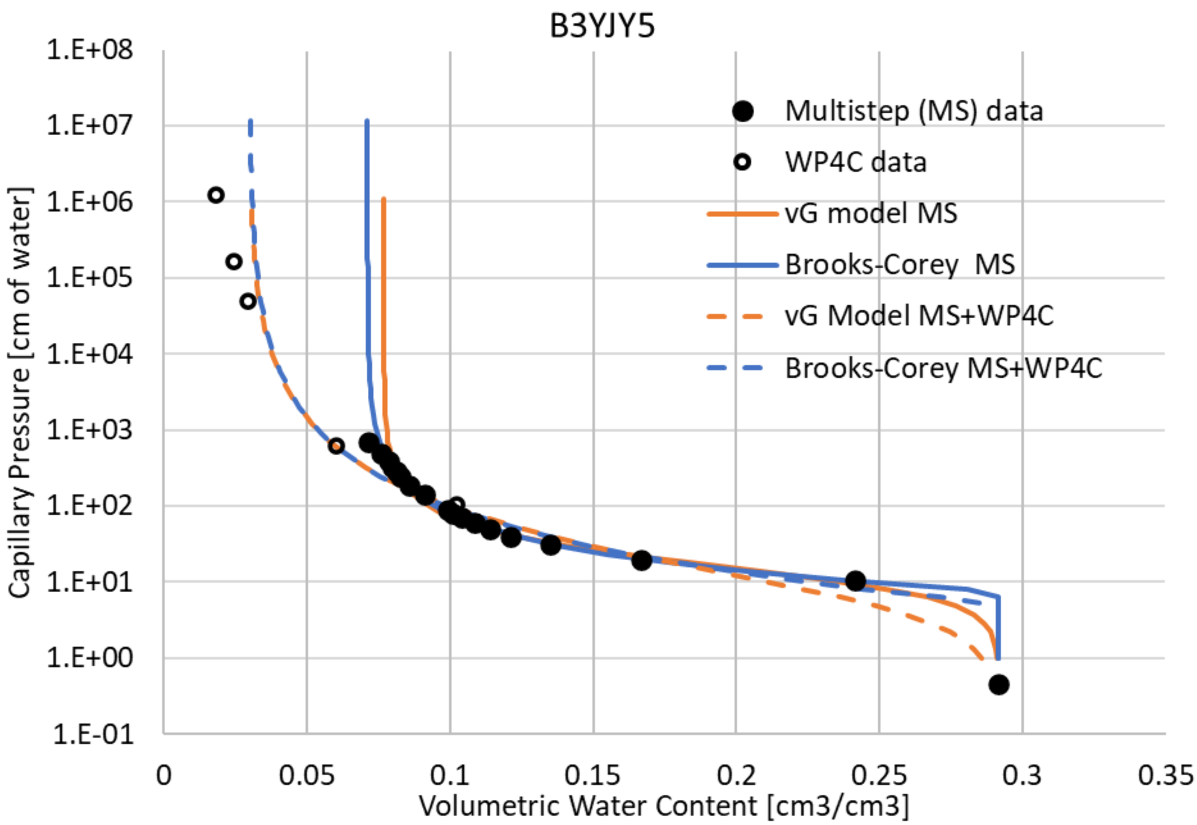

Model fits			
vG			
	alpha (1/cm)	n	theta_r
Multistep (MS)	0.0853	2.2186	0.0770
MS+WP4C	0.1701	1.4628	0.0296
Brooks-Corey			
	hb (cm)	lambda	theta_r
Multistep (MS)	7.7073	0.8740	0.0713
MS+WP4C	5.2544	0.4531	0.0299

D.1.5 B3YJX2

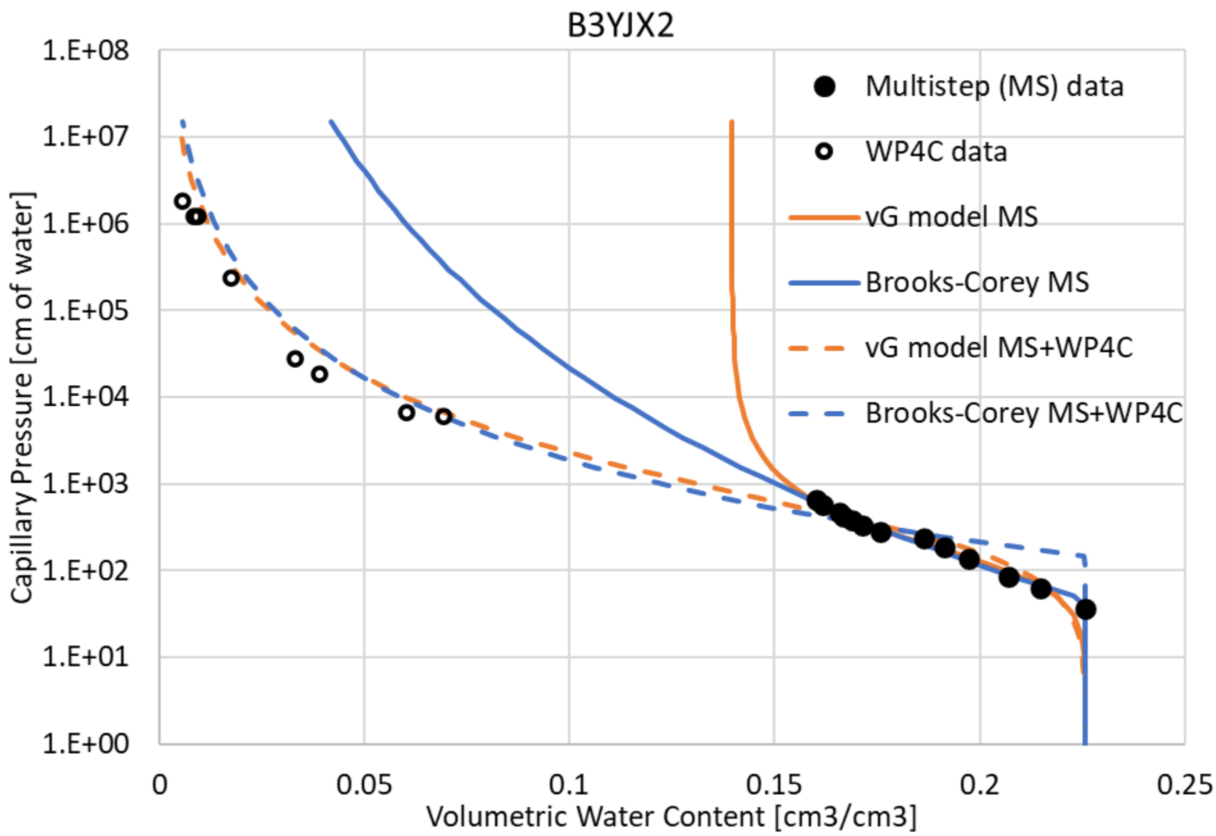

Model fits			
vG			
	alpha (1/cm)	n	theta_r
Multistep (MS)	0.0085	1.8492	0.1395
MS+WP4C	0.0043	1.3517	0.0000
Brooks-Corey			
	hb (cm)	lambda	theta_r
Multistep (MS)	46.1428	0.1325	0.0000
MS+WP4C	145.1033	0.3183	0.0000

D.1.6 B3YJF9

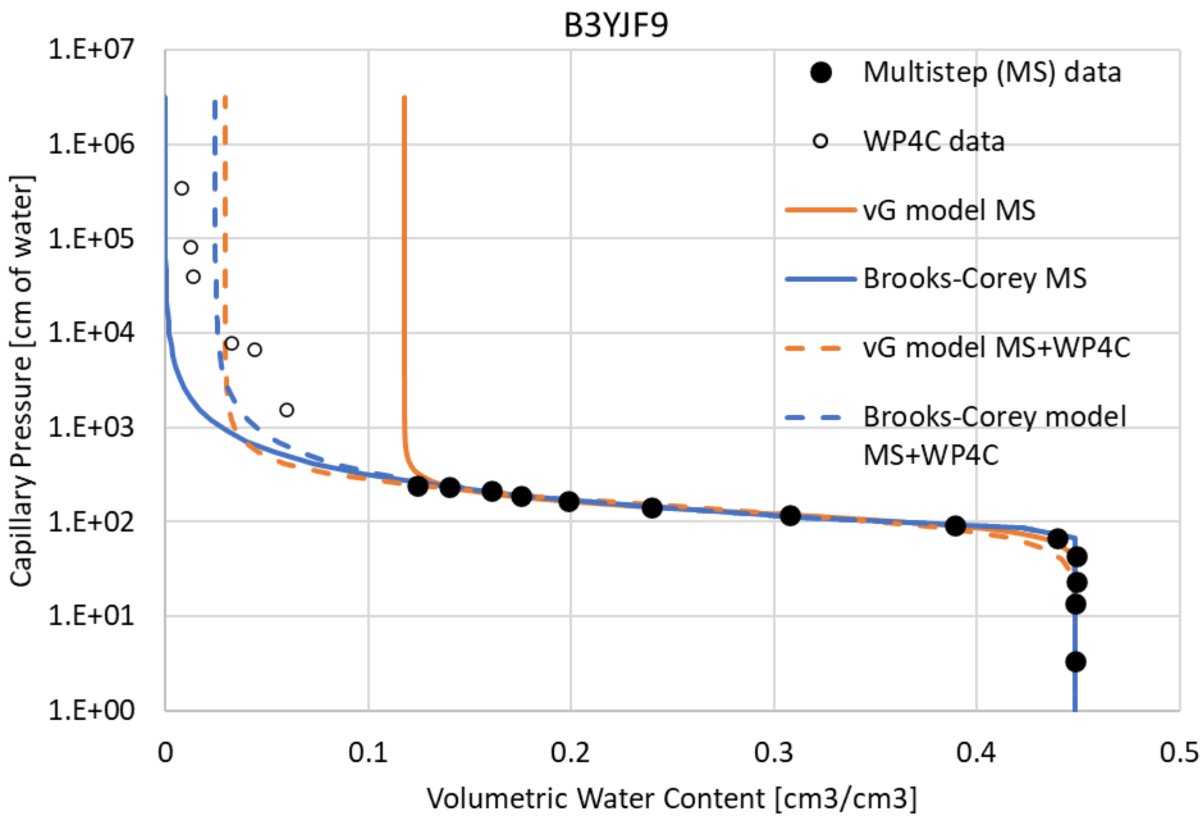

Model fits			
vG			
	alpha (1/cm)	n	theta_r
Multistep (MS)	0.0084	4.8447	0.1182
MS+WP4C	0.0078	3.2601	0.0298
Brooks-Corey			
	hb (cm)	lambda	theta_r
Multistep (MS)	82.0183	1.1155	0.0000
MS+WP4C	82.2033	1.2230	0.0247

D.1.7 B3YJH0

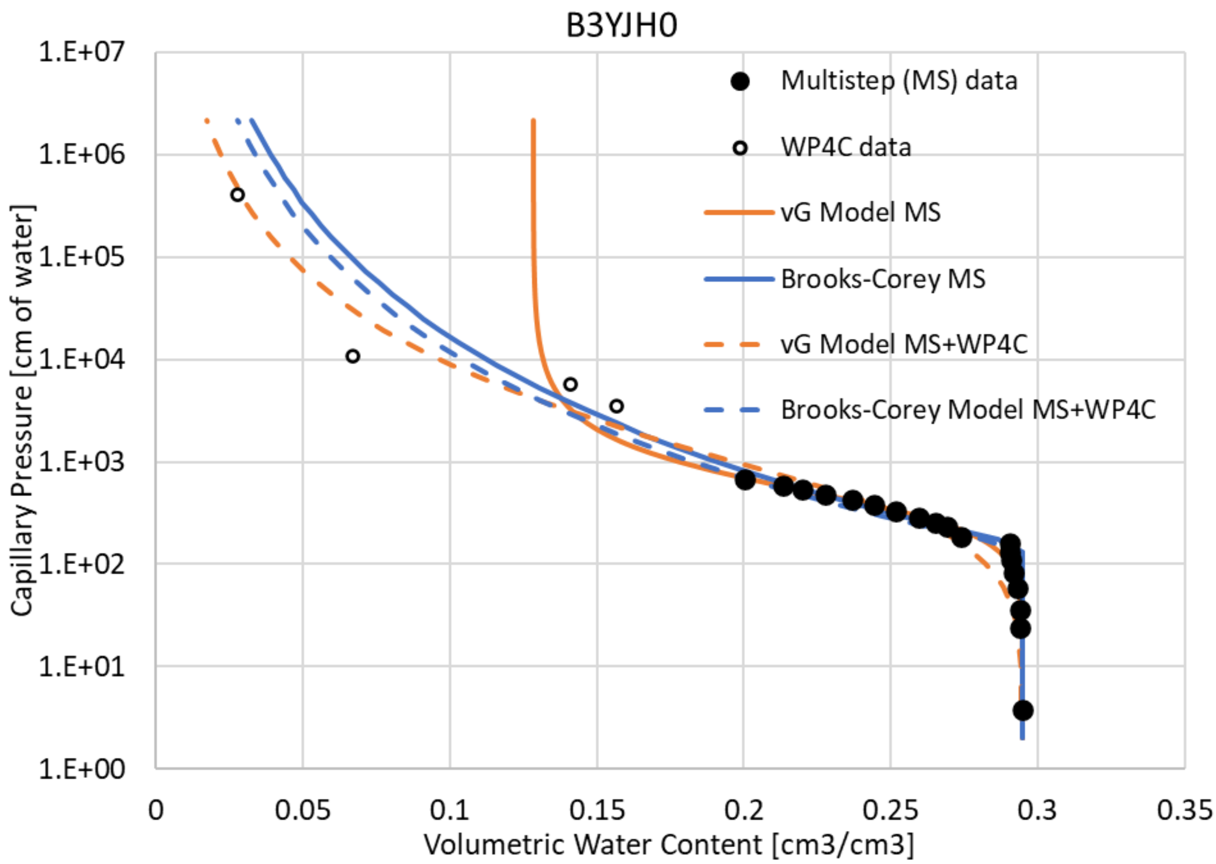

Model fits			
vG			
	alpha (1/cm)	n	theta_r
Multistep (MS)	0.0026	2.2049	0.1284
MS+WP4C	0.0028	1.3383	0.0019
Brooks-Corey			
	hb (cm)	lambda	theta_r
Multistep (MS)	153.2695	0.2303	0.0000
MS+WP4C	142.8235	0.2446	0.0000

D.2 200 East Composites

D.2.1 Composite 2

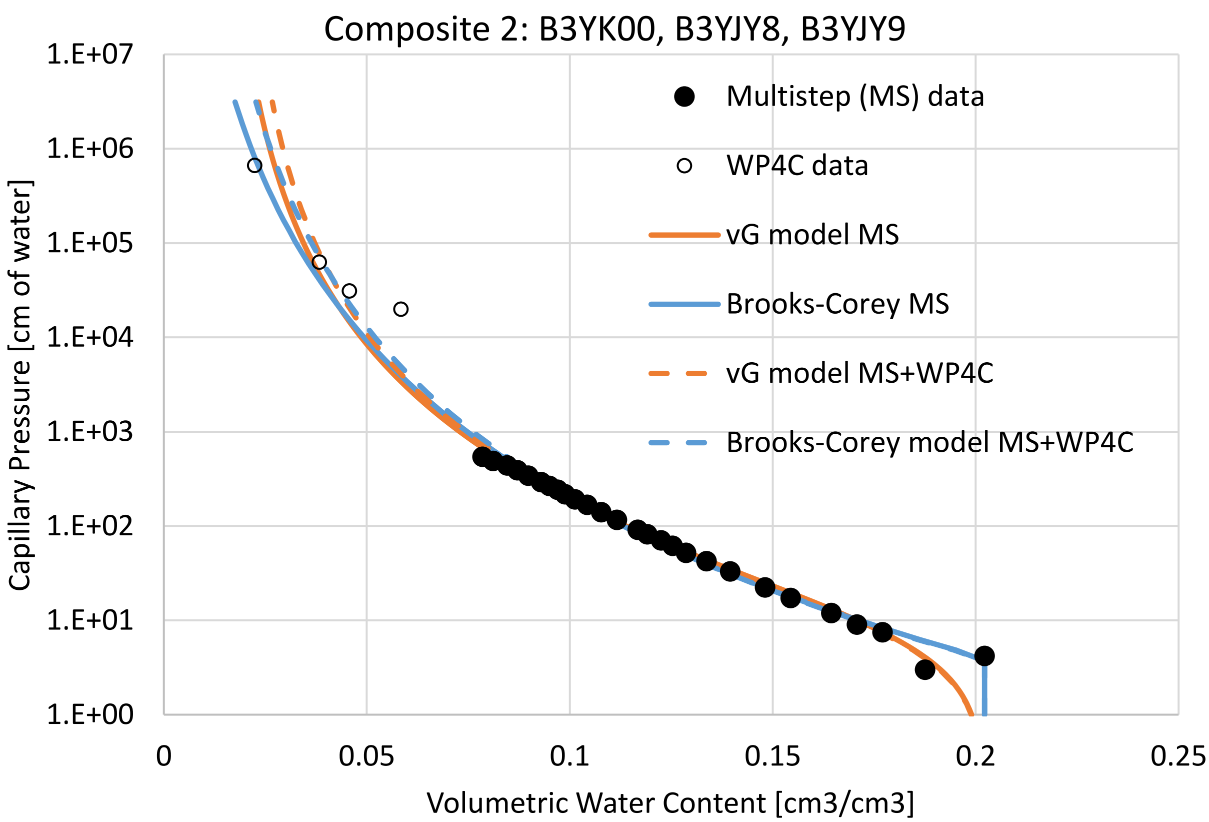

Model fits			
vG			
	alpha (1/cm)	n	theta_r
Multistep (MS)	0.1487	1.2327	0.0143
MS+WP4C	0.1540	1.2366	0.0184
Brooks-Corey			
	hb (cm)	lambda	theta_r
Multistep (MS)	3.9664	0.1800	0.0000
MS+WP4C	3.9223	0.1884	0.0076

D.2.2 Composite 3

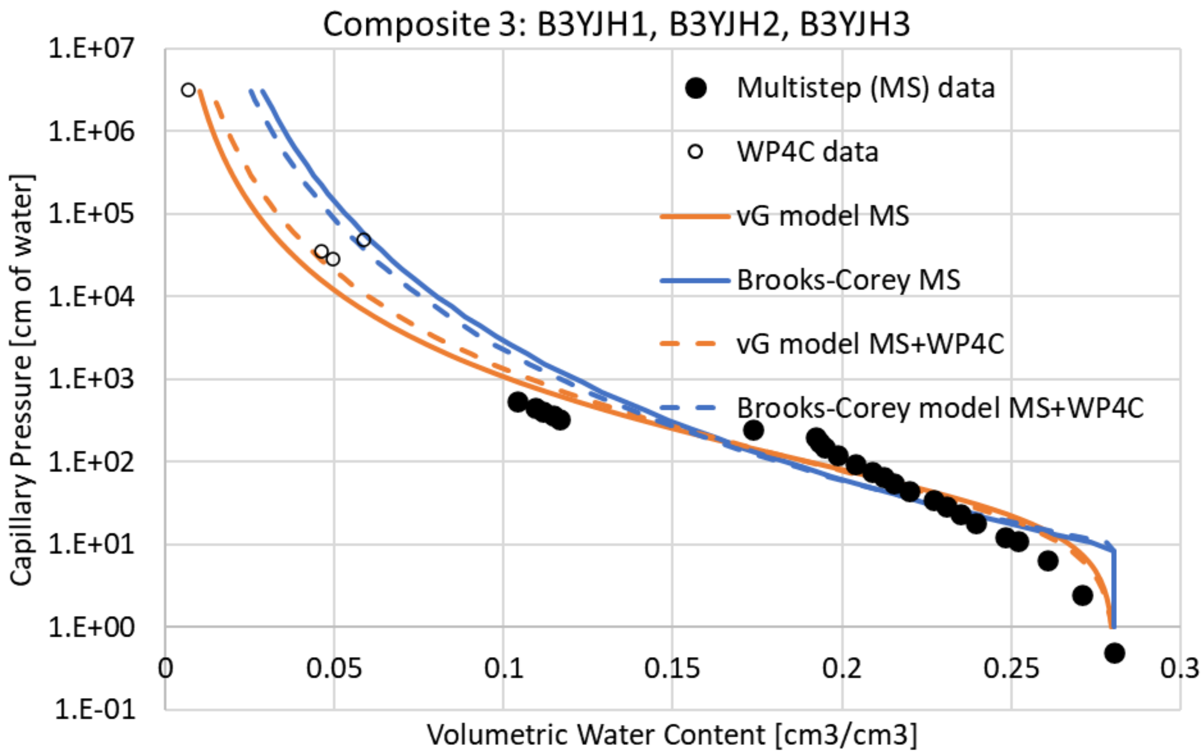

Model fits			
vG			
	alpha (1/cm)	n	theta_r
Multistep (MS)	0.0330	1.2886	0.0000
MS+WP4C	0.0404	1.2580	0.0005
Brooks-Corey			
	hb (cm)	lambda	theta_r
Multistep (MS)	9.2253	0.1789	0.0000
MS+WP4C	10.1324	0.1904	0.0000

D.3 200 West

D.3.1 B488V7-C

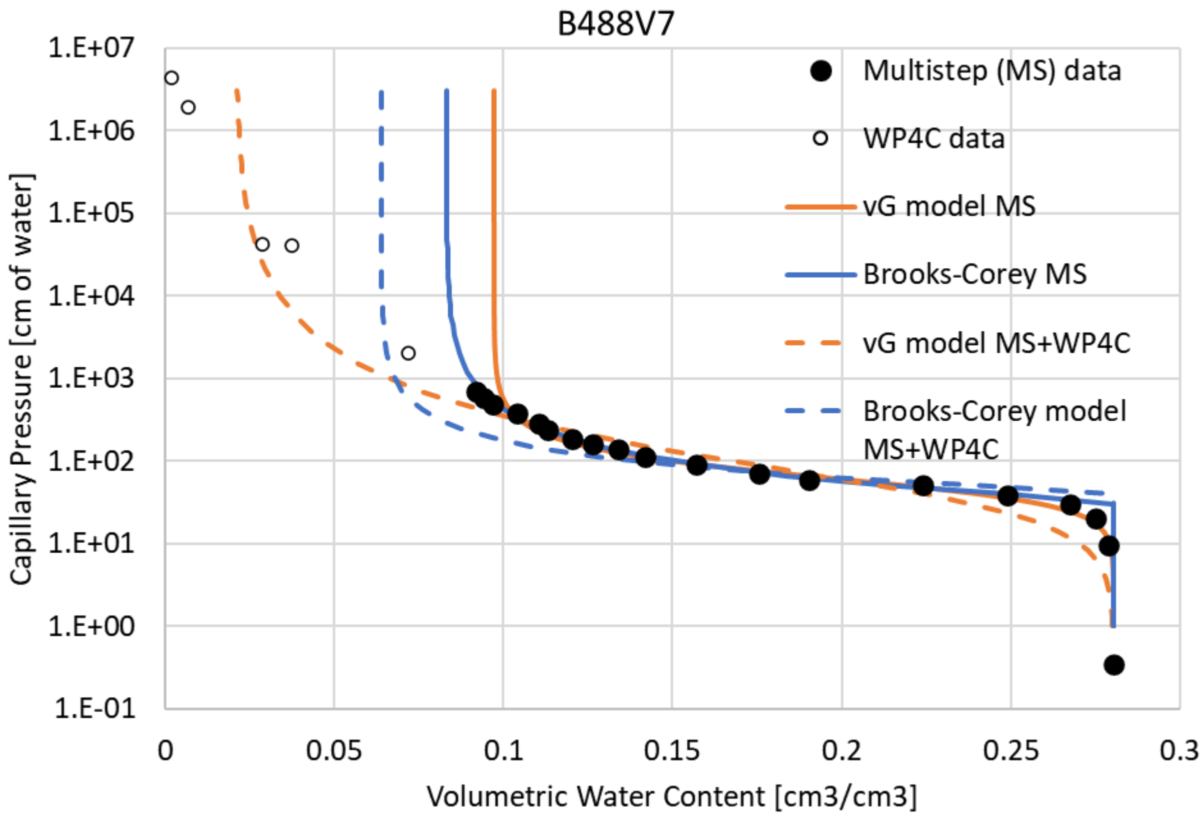

Model fits			
vG			
	alpha (1/cm)	n	theta_r
Multistep (MS)	0.0191	2.7719	0.0971
MS+WP4C	0.0251	1.5378	0.0207
Brooks-Corey			
	hb (cm)	lambda	theta_r
Multistep (MS)	33.0299	0.9652	0.0832
MS+WP4C	43.2639	1.2744	0.0640

D.3.2 B488Y3-G

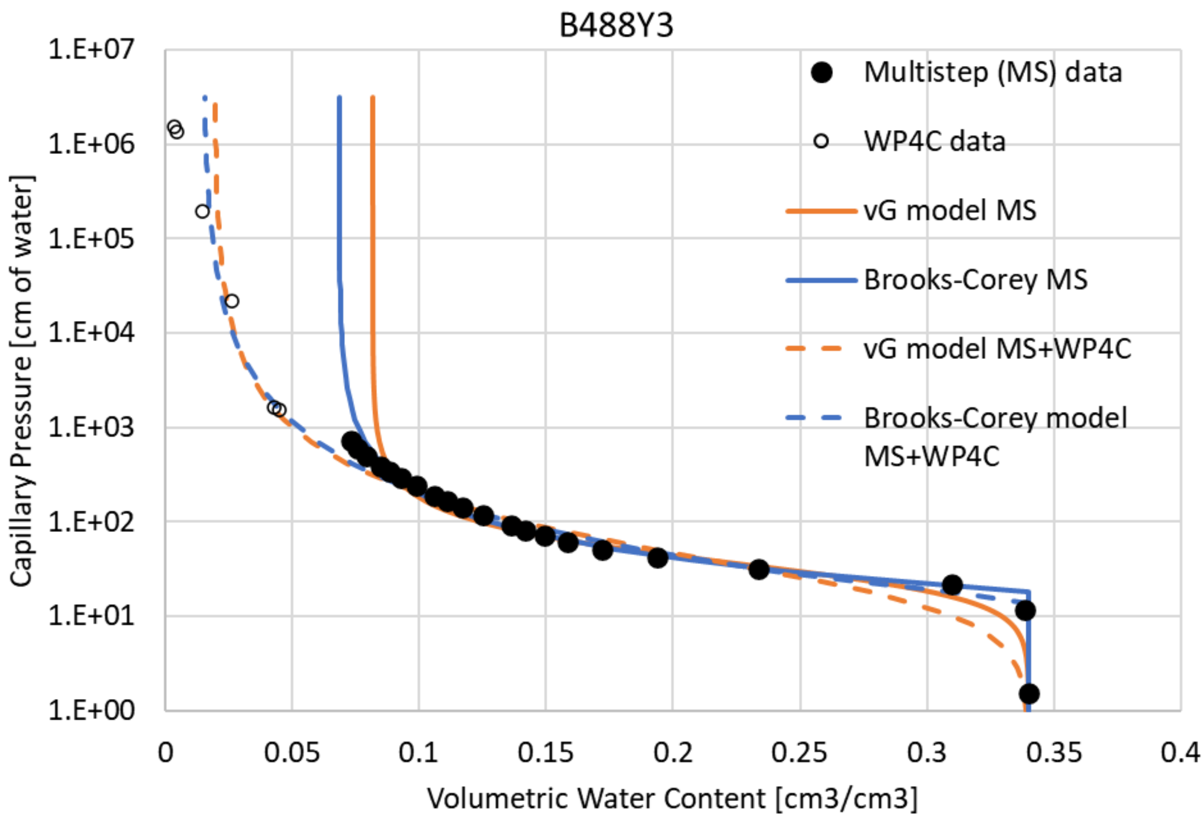

Model fits			
	vG		
	alpha (1/cm)	n	theta_r
Multistep (MS)	0.0342	2.4434	0.0817
MS+WP4C	0.0474	1.6072	0.0194
	Brooks-Corey		
	hb (cm)	lambda	theta_r
Multistep (MS)	18.6873	0.9034	0.0685
MS+WP4C	14.7993	0.5112	0.0149

D.3.3 B488Y4-C

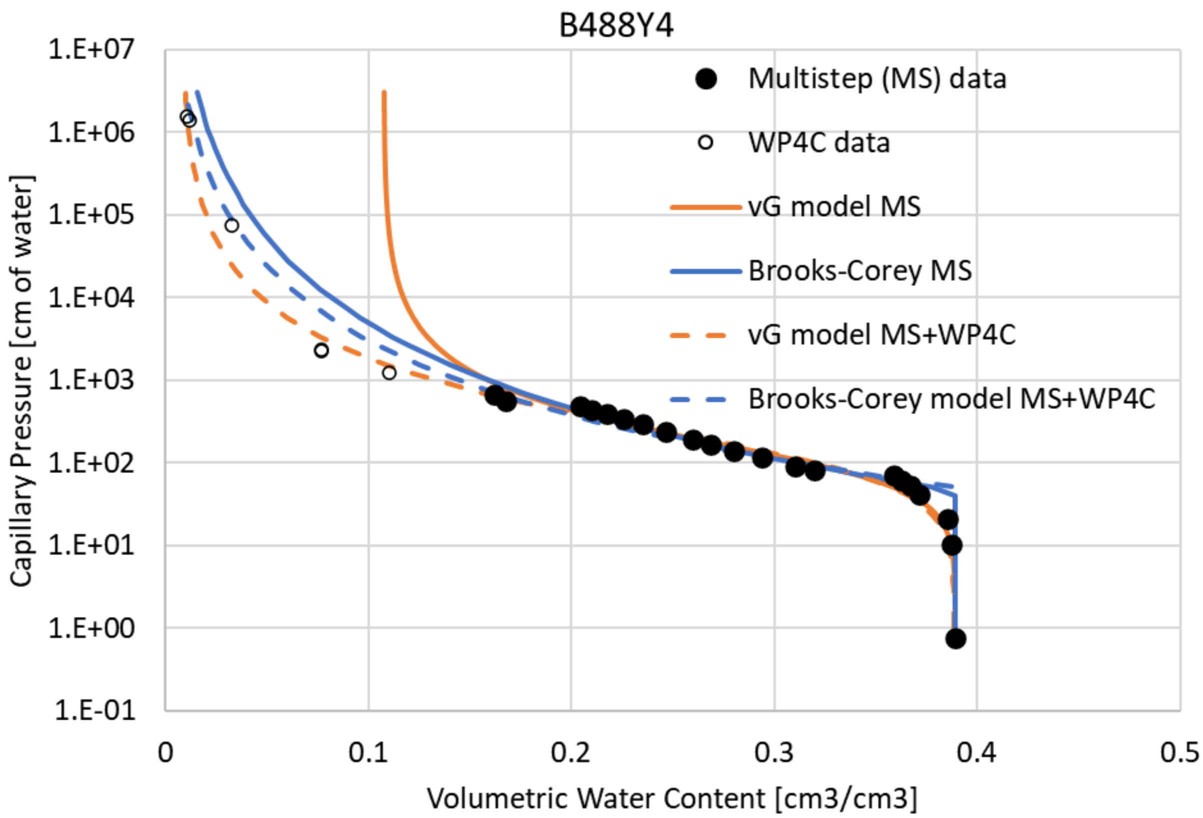

Model fits			
vG			
	alpha (1/cm)	n	theta_r
Multistep (MS)	0.0101	1.7306	0.1078
MS+WP4C	0.0086	1.5080	0.0078
Brooks-Corey			
	hb (cm)	lambda	theta_r
Multistep (MS)	46.0113	0.2898	0.0000
MS+WP4C	51.0470	0.3319	0.0000

D.3.4 B488W5-D

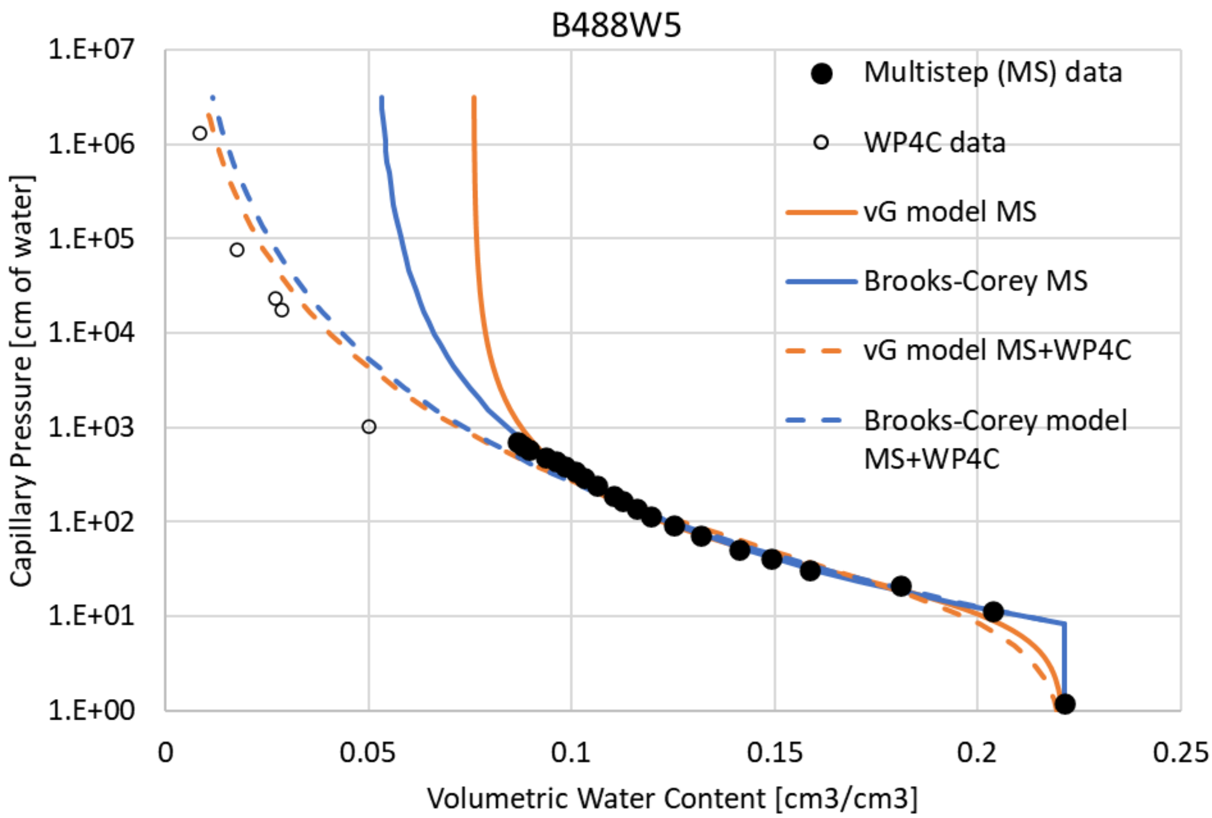

Model fits			
vG			
	alpha (1/cm)	n	theta_r
Multistep (MS)	0.0628	1.6075	0.0759
MS+WP4C	0.0860	1.2513	0.0000
Brooks-Corey			
	hb (cm)	lambda	theta_r
Multistep (MS)	8.3465	0.3421	0.0511
MS+WP4C	8.1284	0.2288	0.0000

D.3.5 B488W7-B

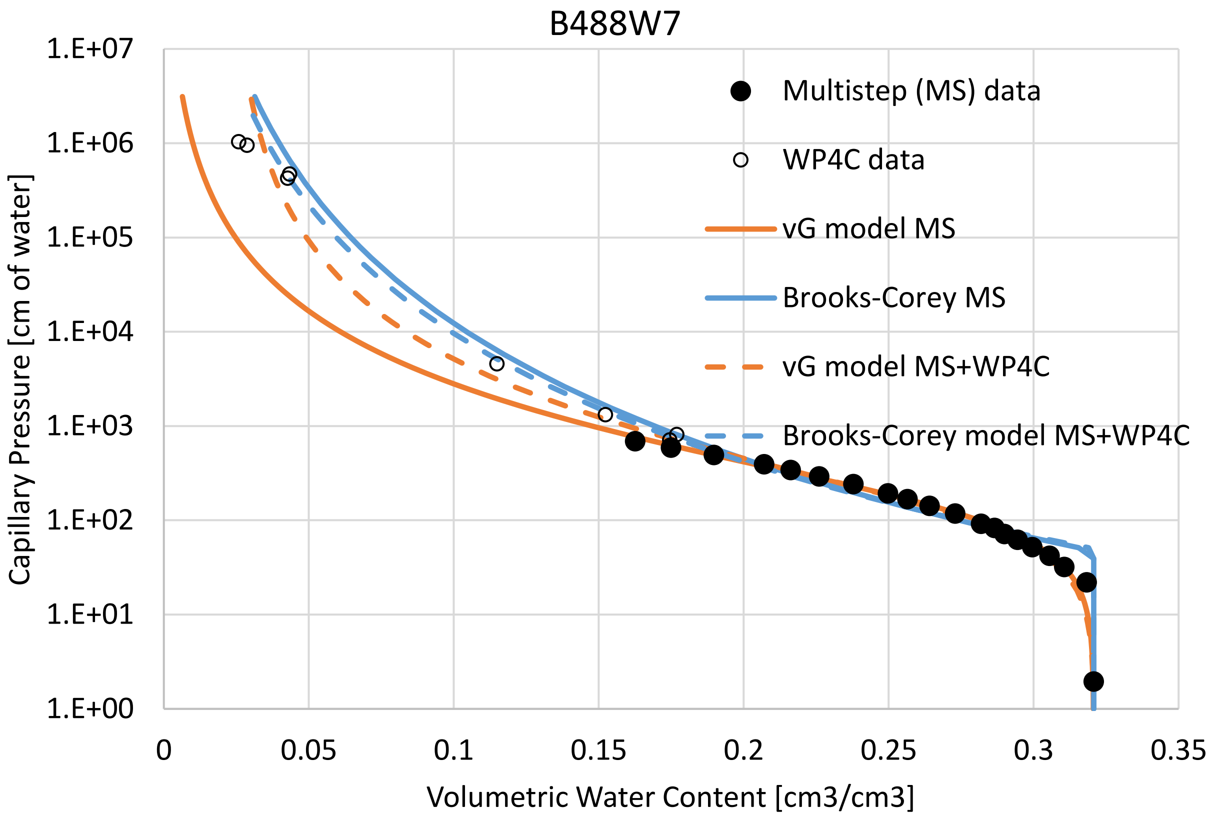

Model fits			
vG			
	alpha (1/cm)	n	theta_r
Multistep (MS)	0.0069	1.3922	0.0000
MS+WP4C	0.0085	1.3557	0.0220
Brooks-Corey			
	hb (cm)	lambda	theta_r
Multistep (MS)	47.3414	0.2095	0.0000
MS+WP4C	49.9149	0.2215	0.0000

D.3.6 B48N72-B

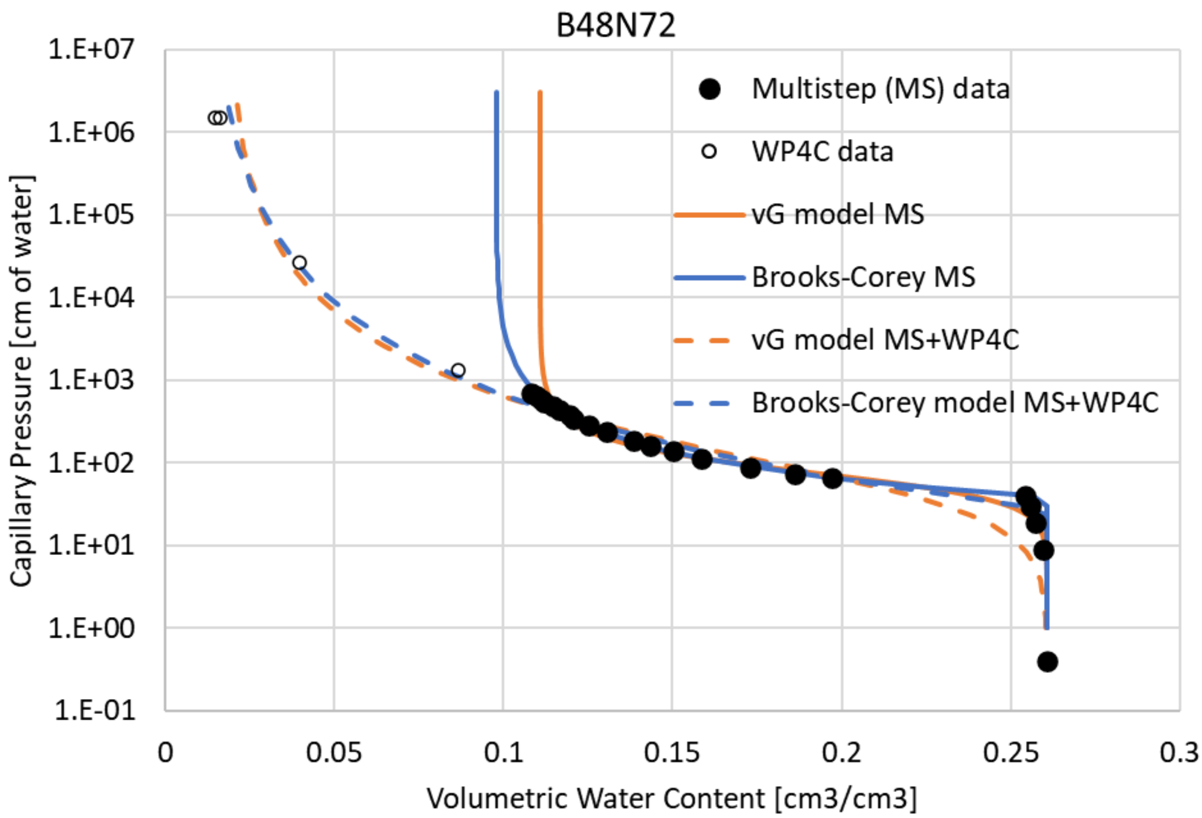

Model fits			
vG			
	alpha (1/cm)	n	theta_r
Multistep (MS)	0.0159	2.7369	0.1110
MS+WP4C	0.0229	1.4030	0.0182
Brooks-Corey			
	hb (cm)	lambda	theta_r
Multistep (MS)	38.2761	0.9026	0.0978
MS+WP4C	27.4785	0.3268	0.0125

D.3.7 B48N73-B

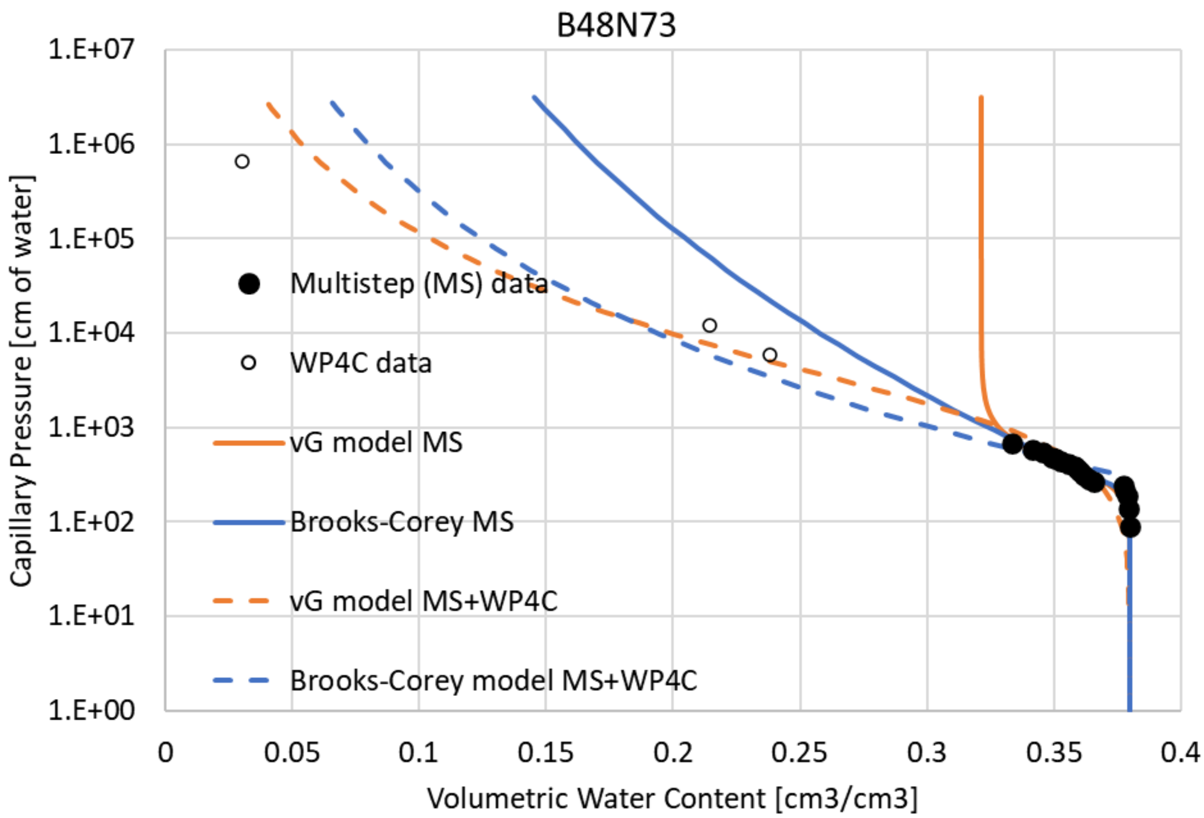

Model fits			
	vG		
	alpha (1/cm)	n	theta_r
Multistep (MS)	0.0026	3.1851	0.3214
MS+WP4C	0.0009	1.2861	0.0000
	Brooks-Corey		
	hb (cm)	lambda	theta_r
Multistep (MS)	202.8454	0.0996	0.0000
MS+WP4C	300.1572	0.1920	0.0000

D.3.8 B48N74-I

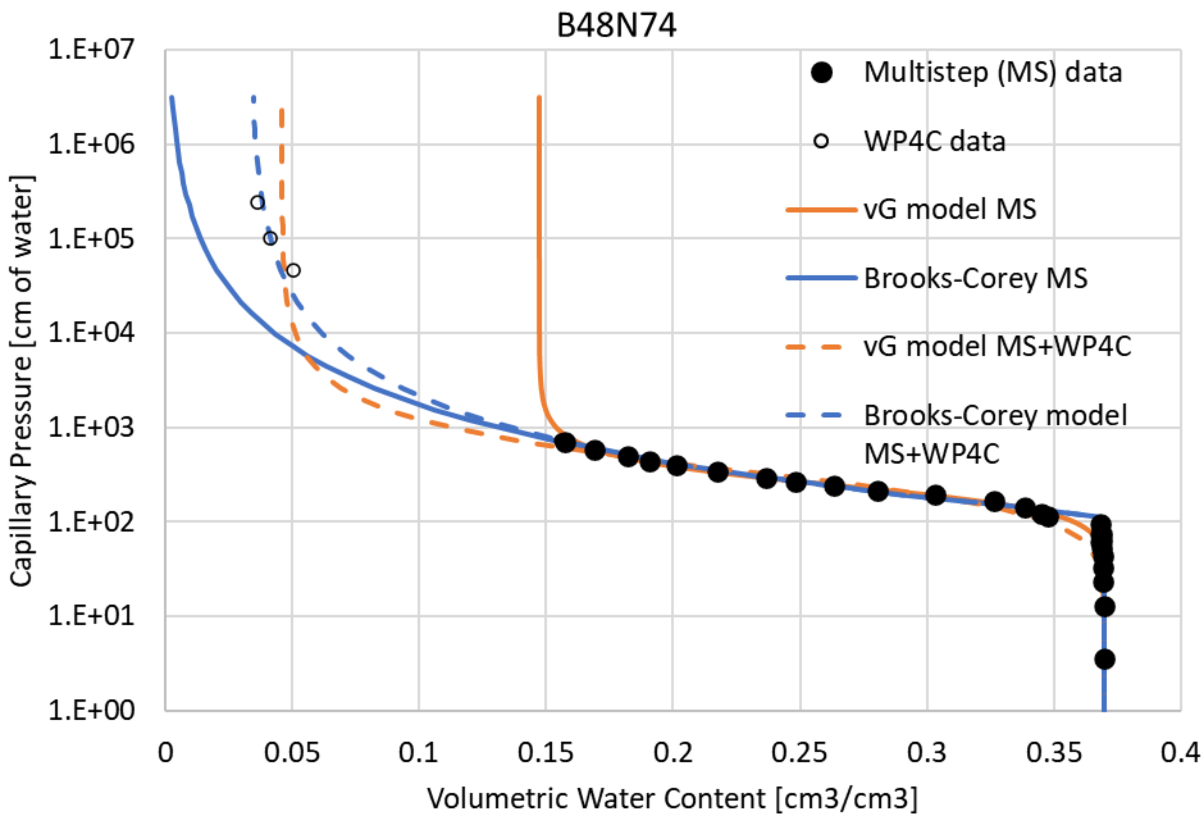

Model fits			
vG			
	alpha (1/cm)	n	theta_r
Multistep (MS)	0.0046	3.2775	0.1472
MS+WP4C	0.0040	2.1185	0.0459
Brooks-Corey			
	hb (cm)	lambda	theta_r
Multistep (MS)	117.7514	0.4855	0.0000
MS+WP4C	118.9426	0.5593	0.0335

D.3.9 B48N76-H

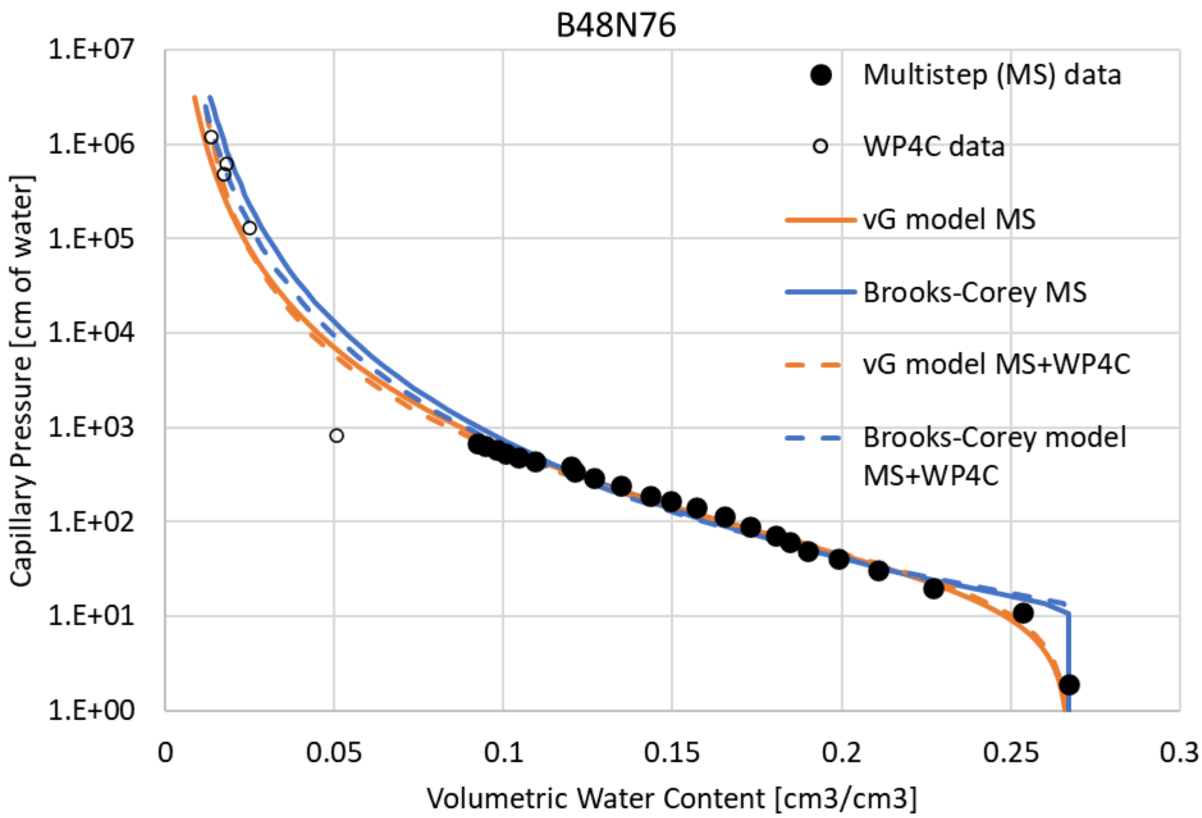

Model fits			
vG			
	alpha (1/cm)	n	theta_r
Multistep (MS)	0.0473	1.2890	0.0000
MS+WP4C	0.0415	1.3238	0.0058
Brooks-Corey			
	hb (cm)	lambda	theta_r
Multistep (MS)	12.3084	0.2407	0.0000
MS+WP4C	13.4616	0.2561	0.0000

D.3.10 B48N79-B

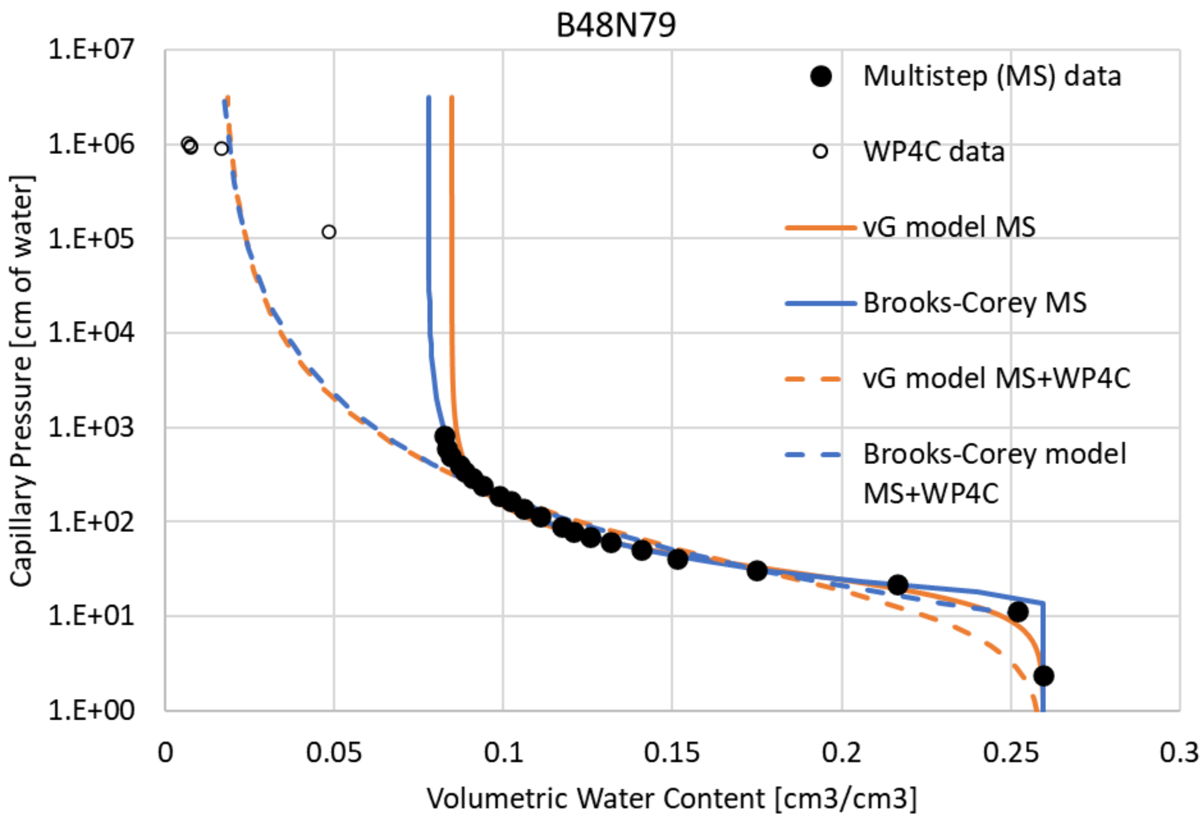

Model fits			
vG			
	alpha (1/cm)	n	theta_r
Multistep (MS)	0.0420	2.3239	0.0846
MS+WP4C	0.0795	1.3914	0.0165
Brooks-Corey			
	hb (cm)	lambda	theta_r
Multistep (MS)	15.8058	0.9009	0.0779
MS+WP4C	9.5535	0.3554	0.0148

D.3.11 B48ND9-B

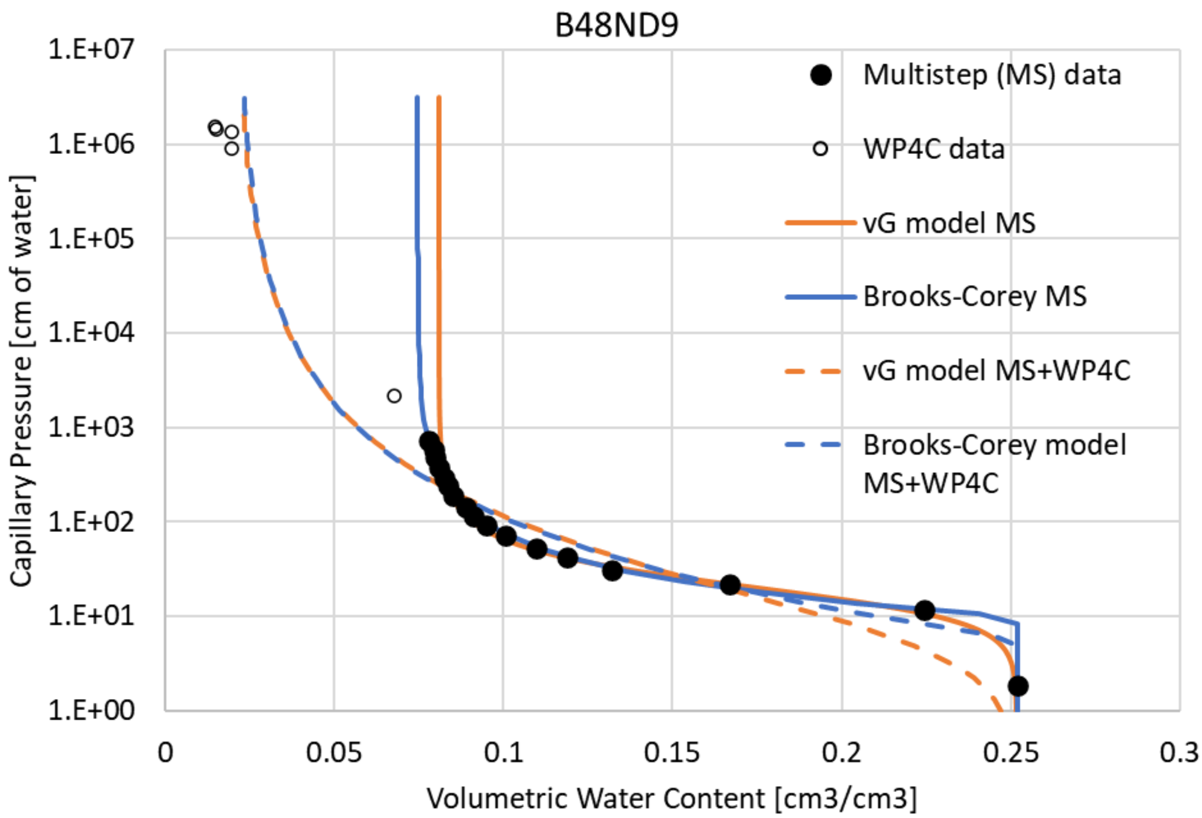

Model fits			
vG			
	alpha (1/cm)	n	theta_r
Multistep (MS)	0.0604	2.5731	0.0808
MS+WP4C	0.1589	1.3662	0.0210
Brooks-Corey			
	hb (cm)	lambda	theta_r
Multistep (MS)	9.9055	0.9475	0.0747
MS+WP4C	5.7536	0.3635	0.0215

D.3.12 B48NF4-C

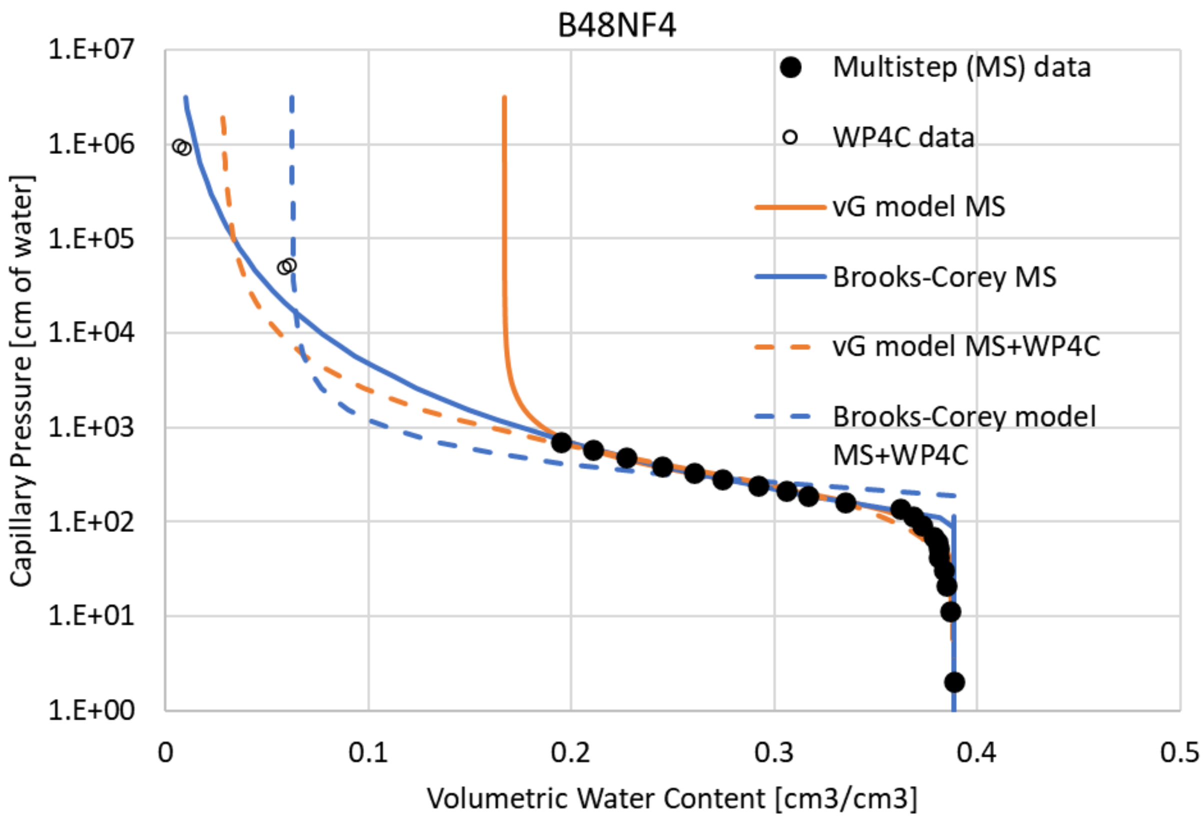

Model fits			
vG			
	alpha (1/cm)	n	theta_r
Multistep (MS)	0.0048	2.5485	0.1672
MS+WP4C	0.0042	1.6826	0.0279
Brooks-Corey			
	hb (cm)	lambda	theta_r
Multistep (MS)	107.2766	0.3581	0.0000
MS+WP4C	198.6818	1.2084	0.0627

D.3.13 B48NH0-H

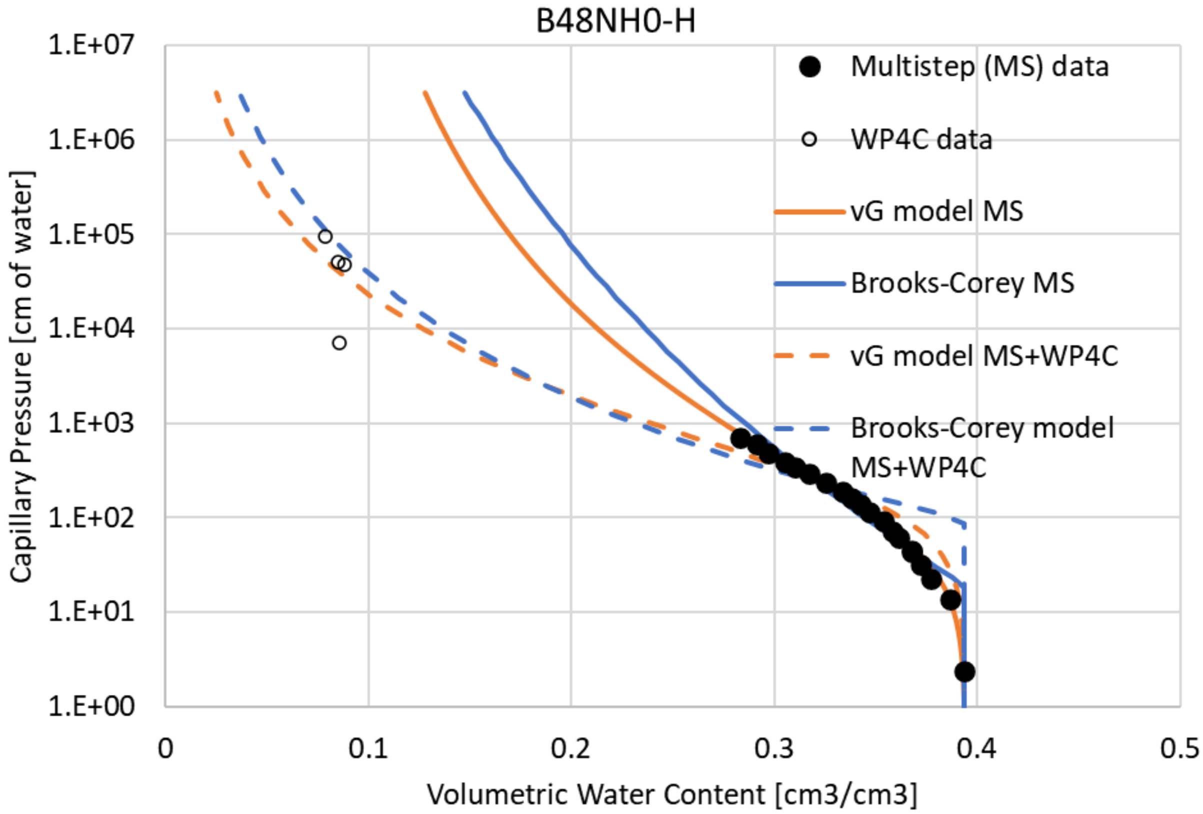

Model fits			
vG			
	alpha (1/cm)	n	theta_r
Multistep (MS)	0.0177	1.1243	0.0000
MS+WP4C	0.0054	1.2839	0.0000
Brooks-Corey			
	hb (cm)	lambda	theta_r
Multistep (MS)	19.4986	0.0818	0.0000
MS+WP4C	97.0913	0.2282	0.0000

D.3.14 B48NH0-I

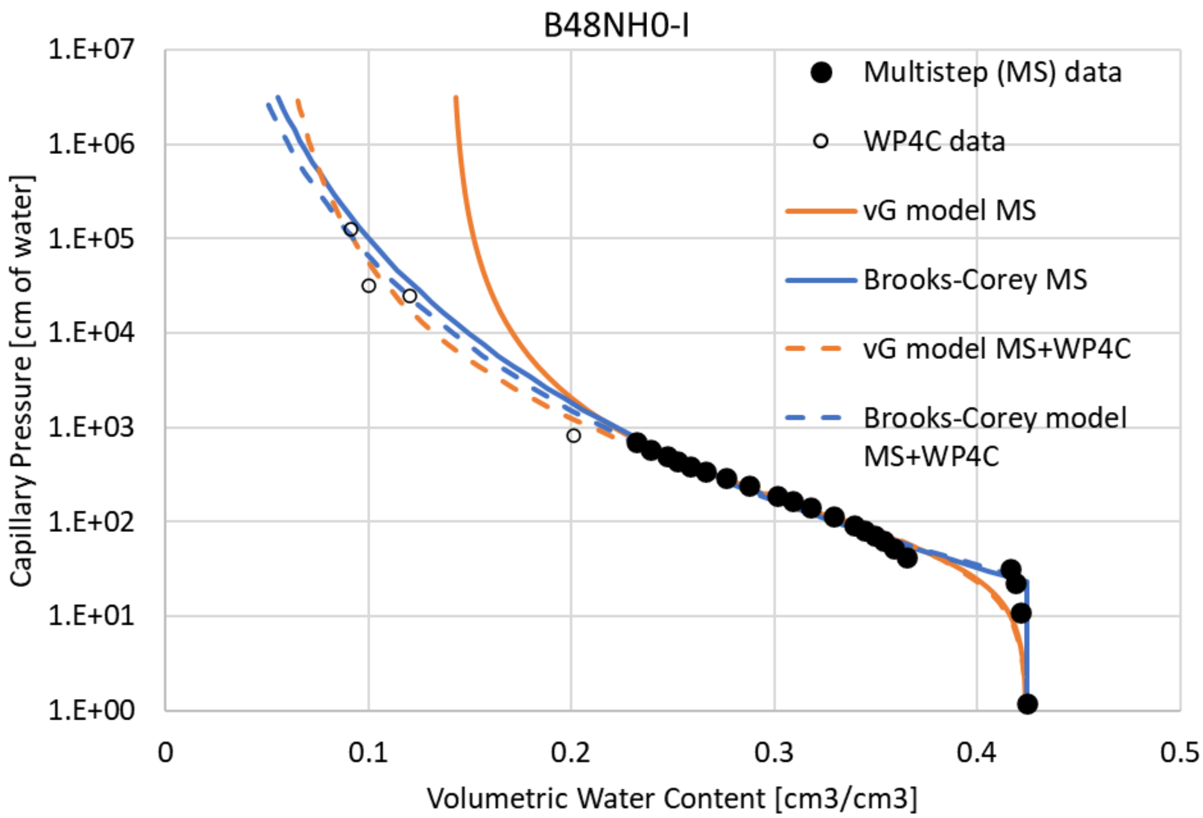

Model fits			
vG			
	alpha (1/cm)	n	theta_r
Multistep (MS)	0.0193	1.4234	0.1405
MS+WP4C	0.0190	1.2867	0.0491
Brooks-Corey			
	hb (cm)	lambda	theta_r
Multistep (MS)	23.3461	0.1724	0.0000
MS+WP4C	25.3171	0.1837	0.0000

Appendix E – Observed and Simulated Aqueous Pressures and Outflow Volumes from Multistep Outflow Experiments

E.1 200 East

E.1.1 B41802

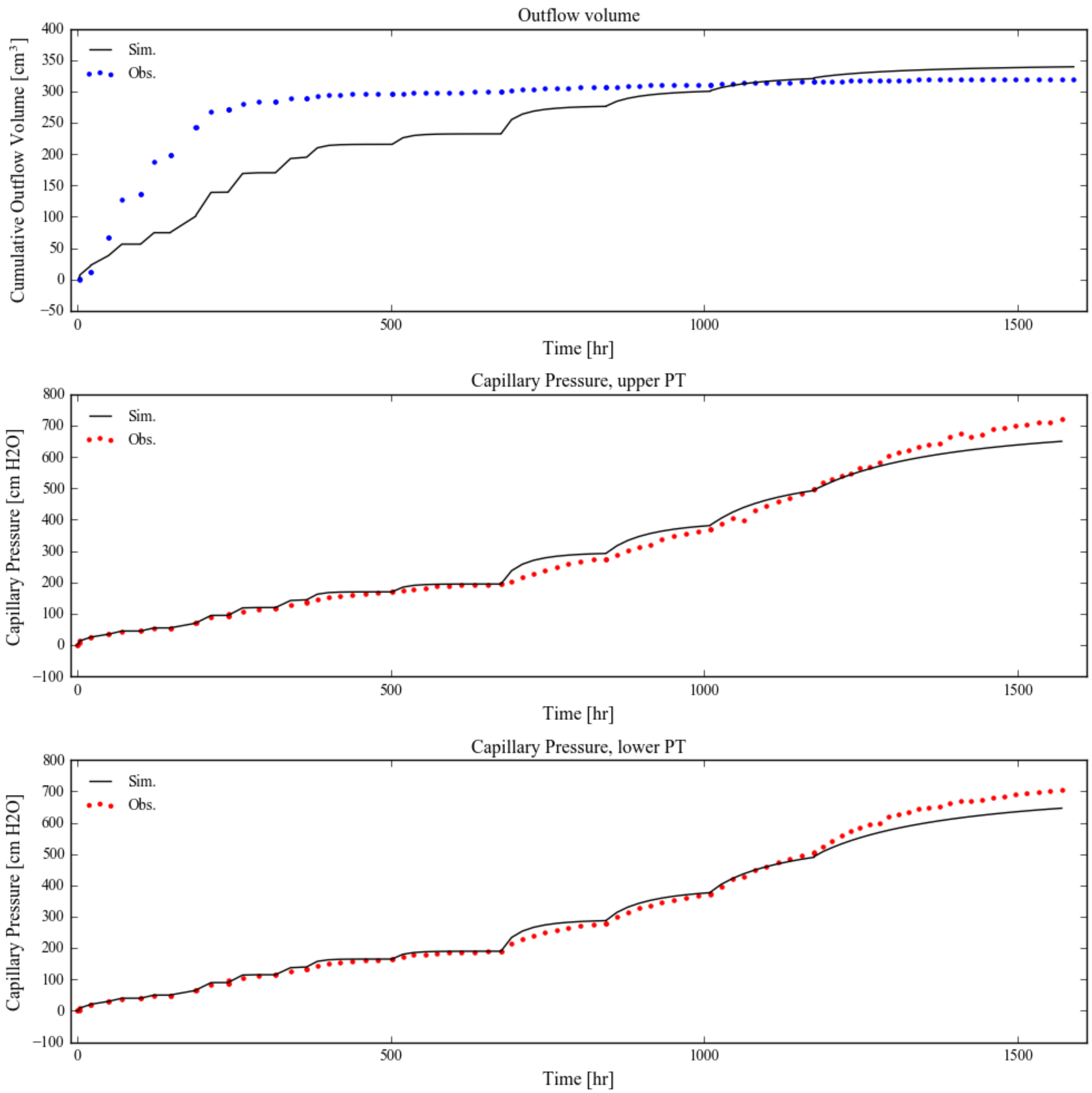

Figure E.1. Simulated and observed cumulative outflow and capillary pressure data for core B41802, using both pressure and outflow data for fitting.

E.1.2 B3YJY6

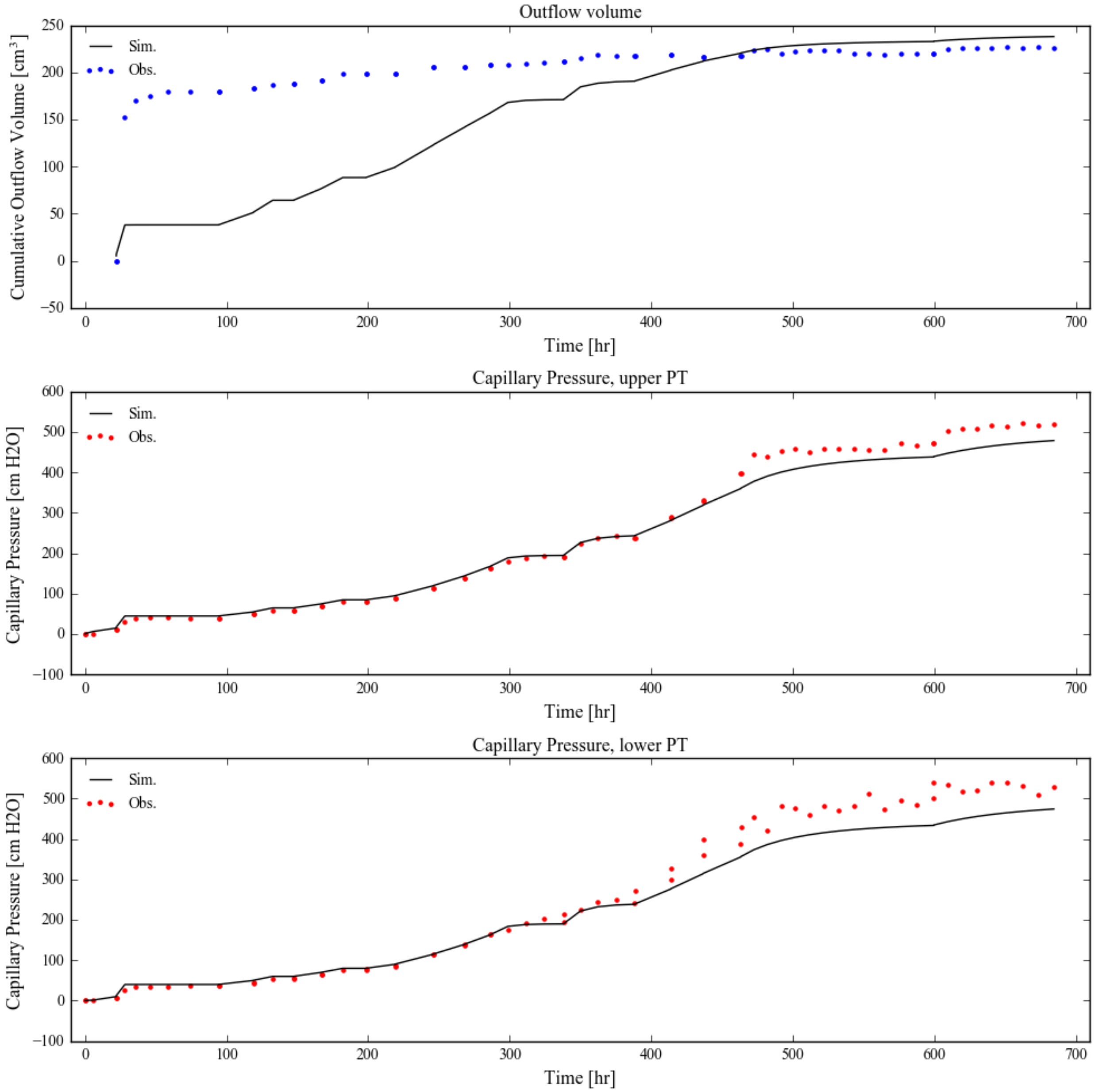

Figure E.2. Simulated and observed cumulative outflow and capillary pressure data for core B3YJY6, using both pressure and outflow data for fitting.

E.1.3 B3YJY7

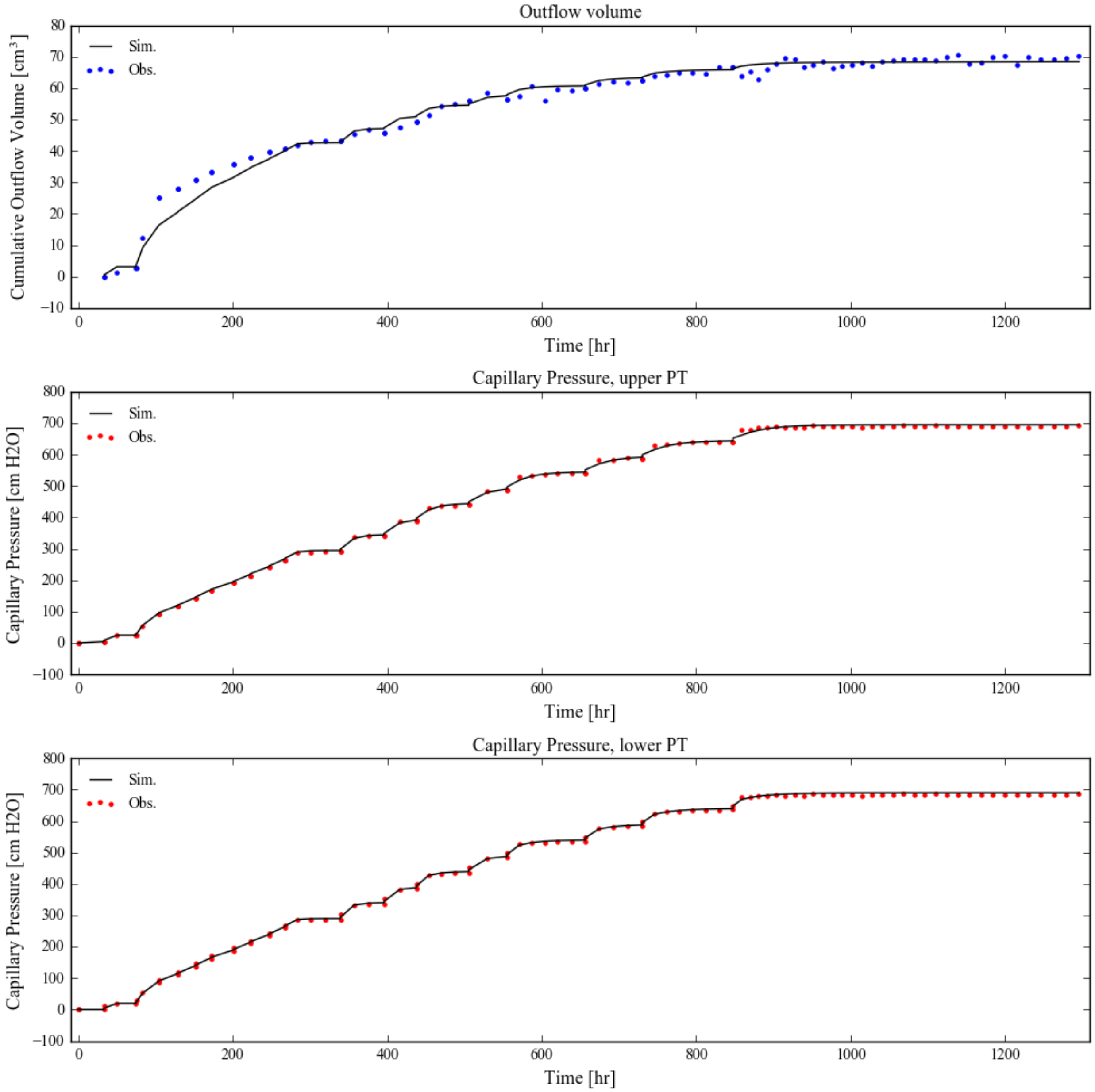

Figure E.3. Simulated and observed cumulative outflow and capillary pressure data for core B3YJY7, using both pressure and outflow data for fitting.

E.1.4 B3YJY5

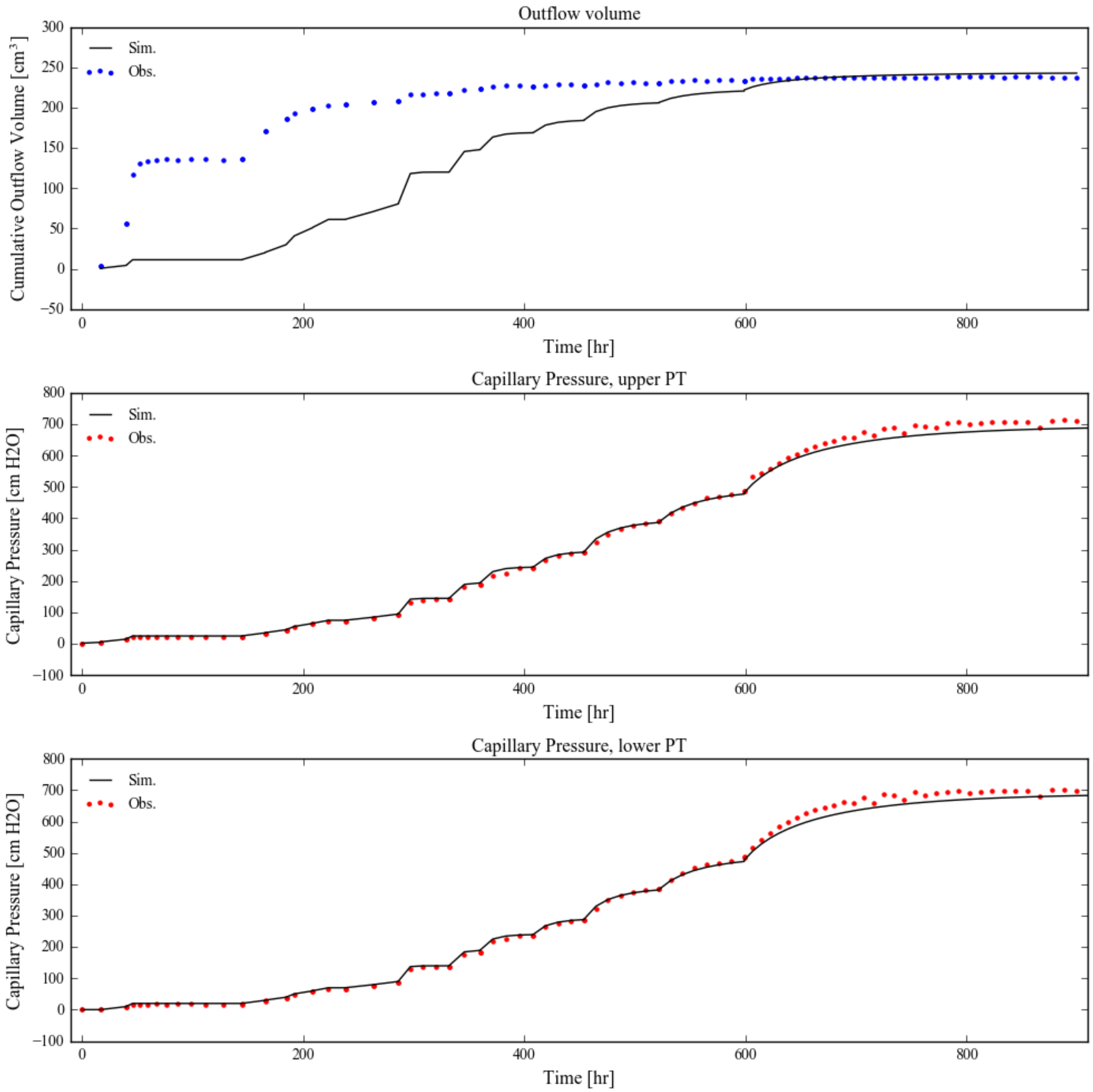

Figure E.4. Simulated and observed cumulative outflow and capillary pressure data for core B3YJY5, using both pressure and outflow data for fitting.

E.1.5 B3YJX2

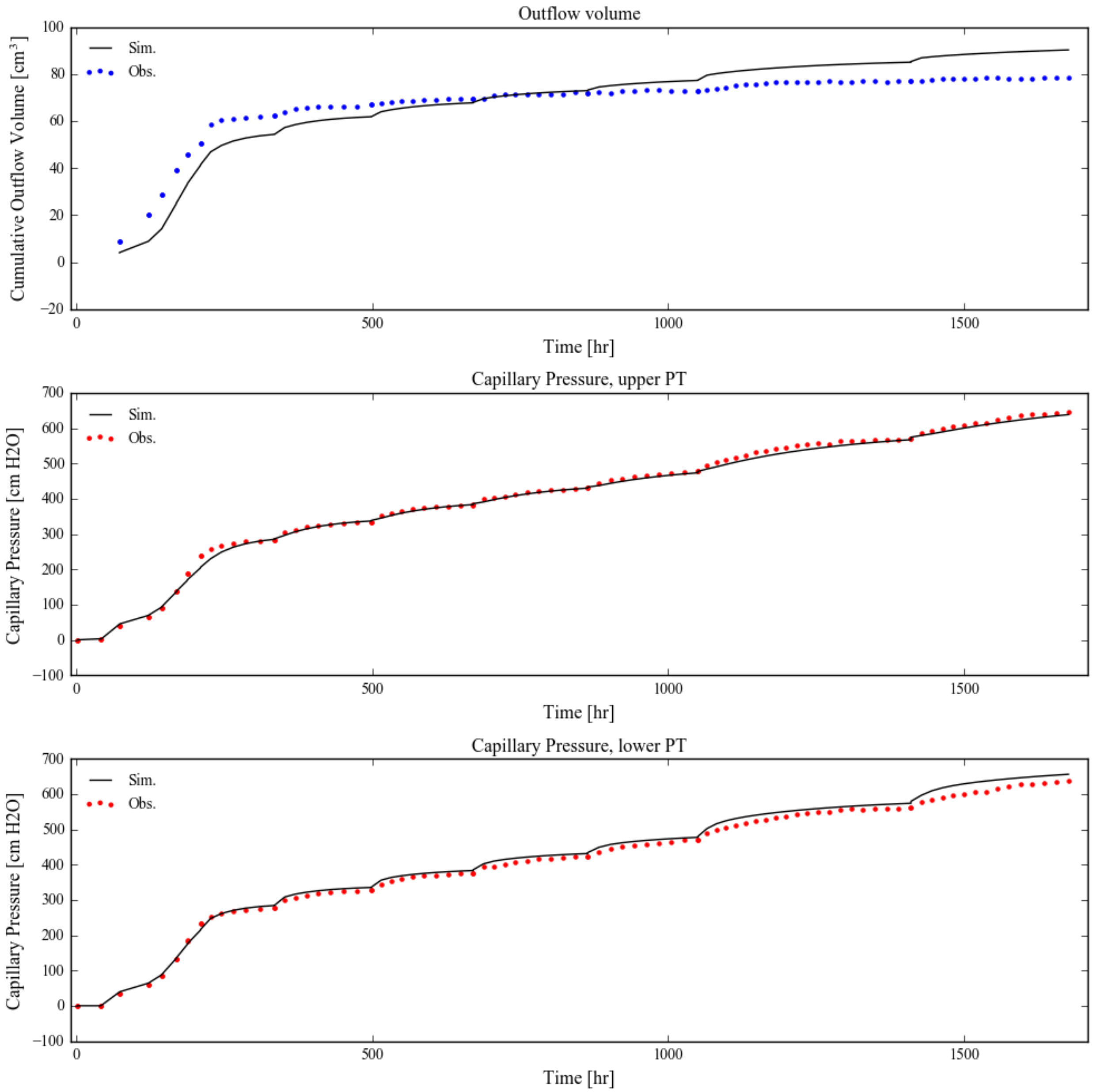

Figure E.5. Simulated and observed cumulative outflow and capillary pressure data for core B3YJX2, using both pressure and outflow data for fitting.

E.1.6 B3YJF9

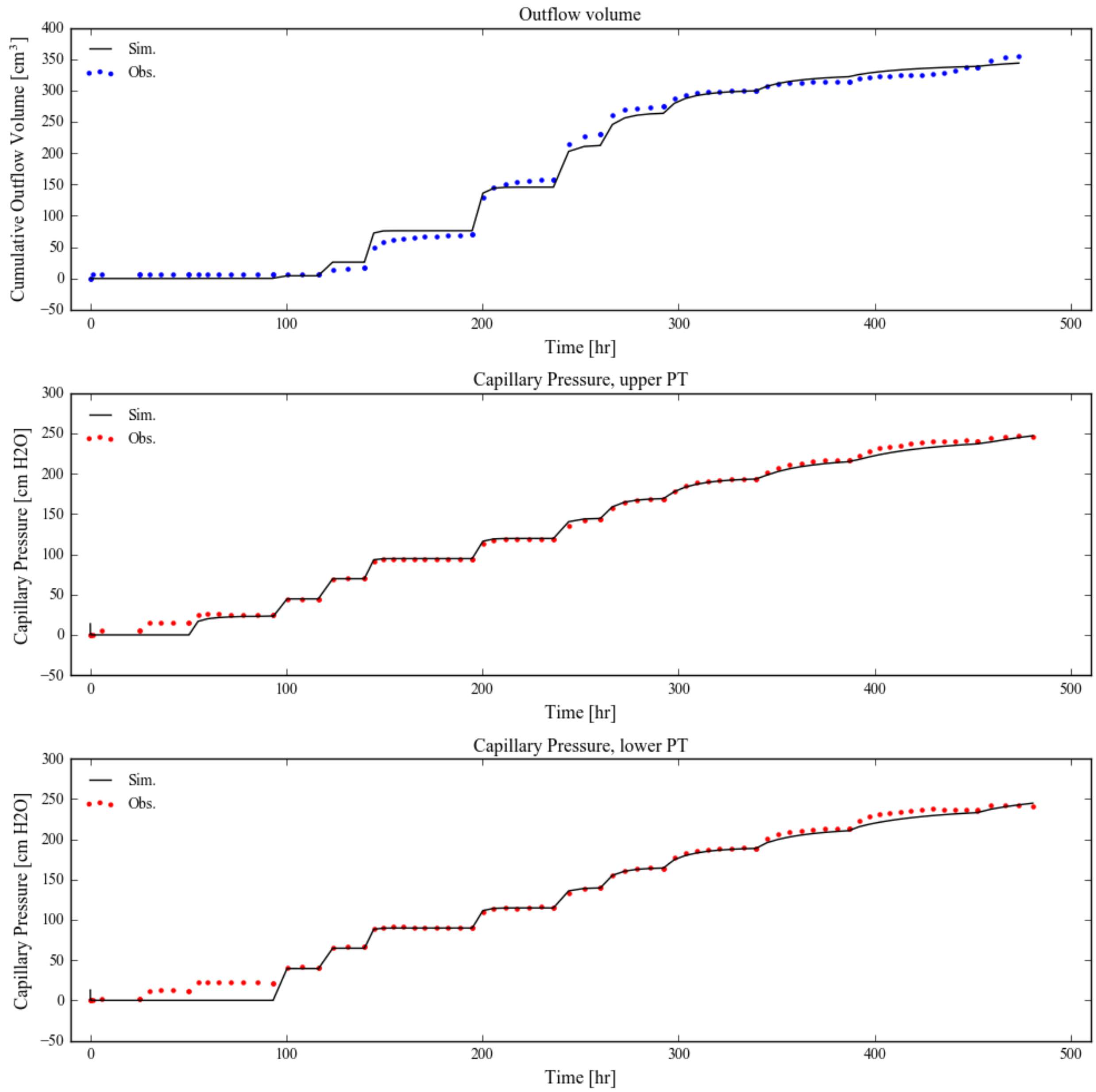

Figure E.6. Simulated and observed cumulative outflow and capillary pressure data for core B3YJF9, using both pressure and outflow data for fitting.

E.1.7 B3YJH0

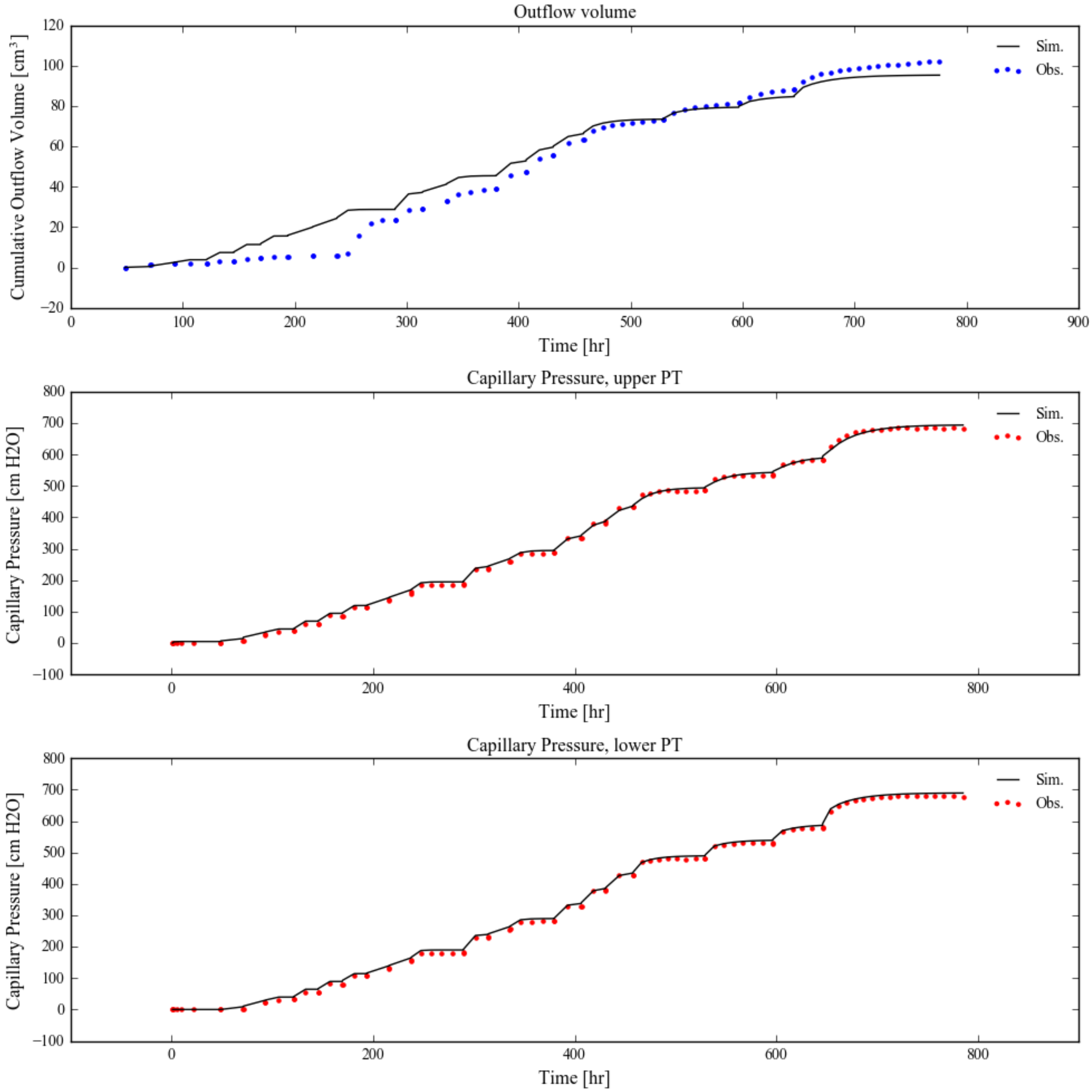

Figure E.7. Simulated and observed cumulative outflow and capillary pressure data for core B3YJH0, using both pressure and outflow data for fitting.

E.2 200 East Composites

E.2.1 Composite 1

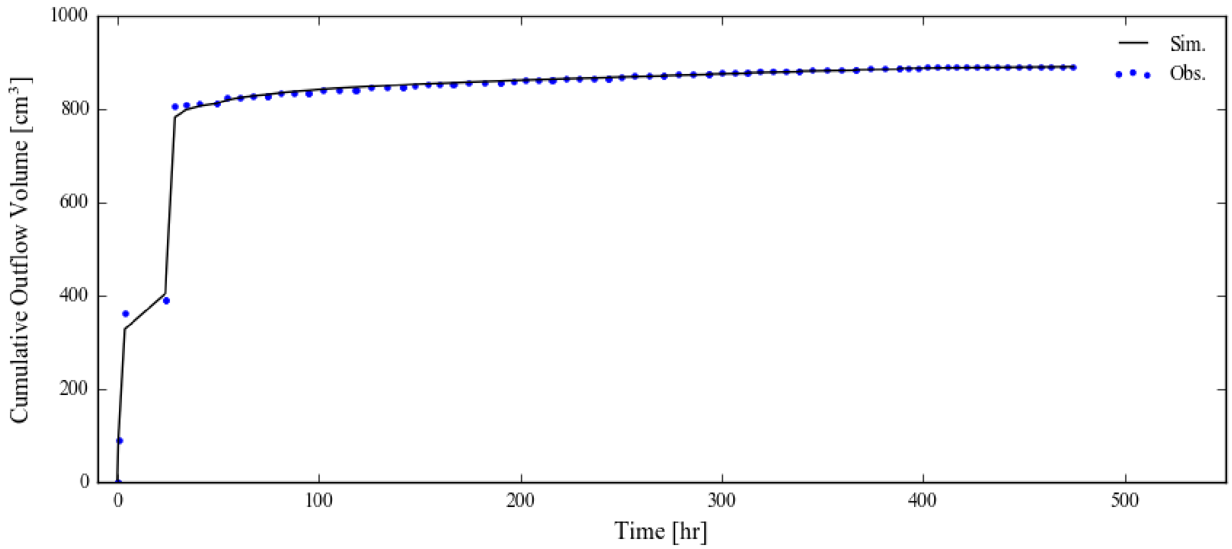

Figure E.8. Simulated and observed cumulative outflow data for Composite 1 column, using only outflow data for fitting.

E.2.2 Composite 2

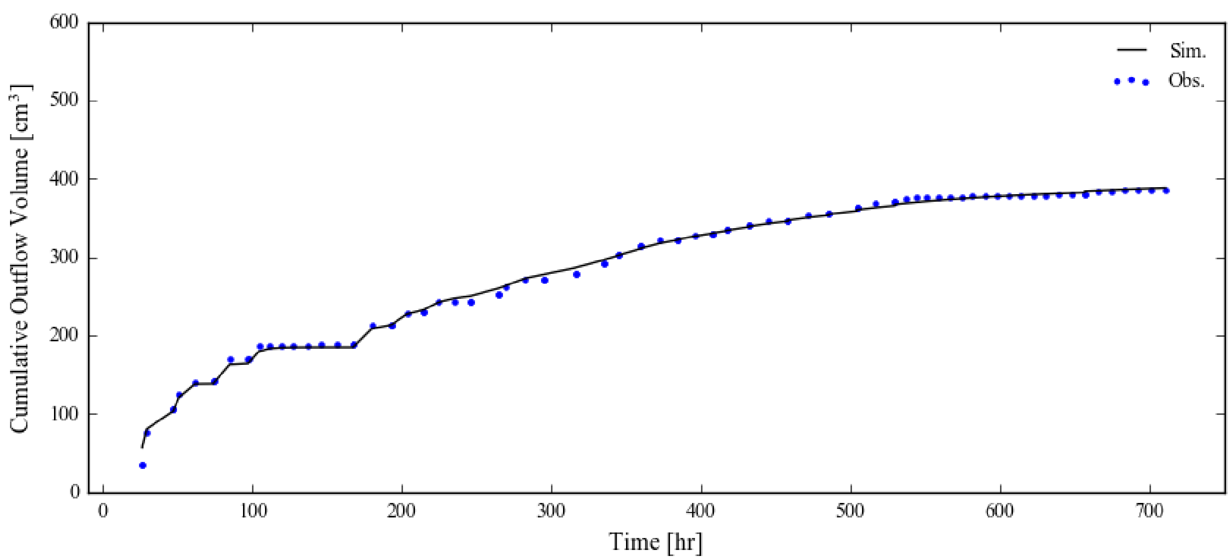

Figure E.9. Simulated and observed cumulative outflow data for Composite 2 column, using only outflow data for fitting.

E.2.3 Composite 3

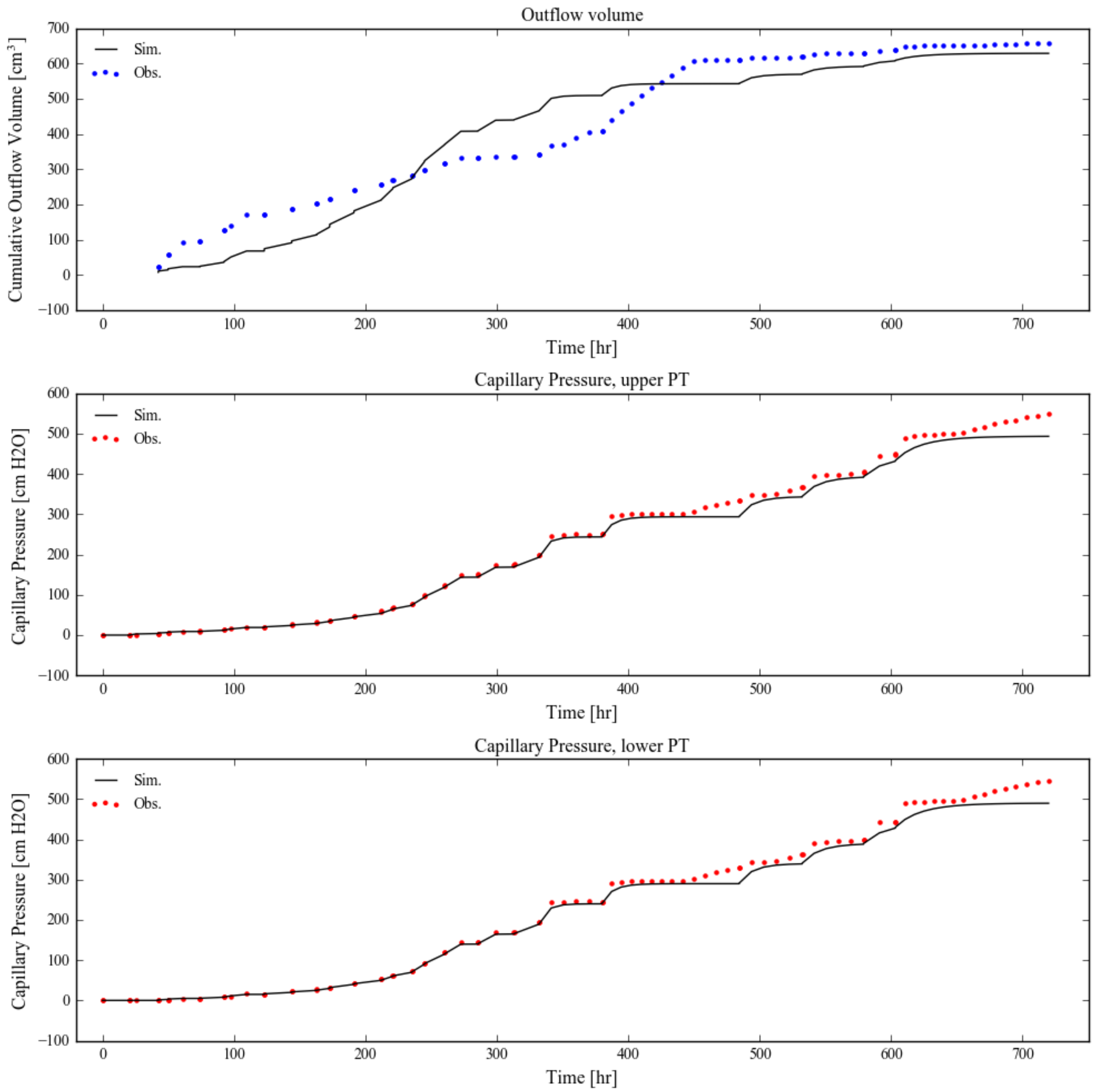

Figure E.10. Simulated and observed cumulative outflow and capillary pressure data for Composite 3 column, using both pressure and outflow data for fitting.

E.3 200 West

E.3.1 B488V7-C

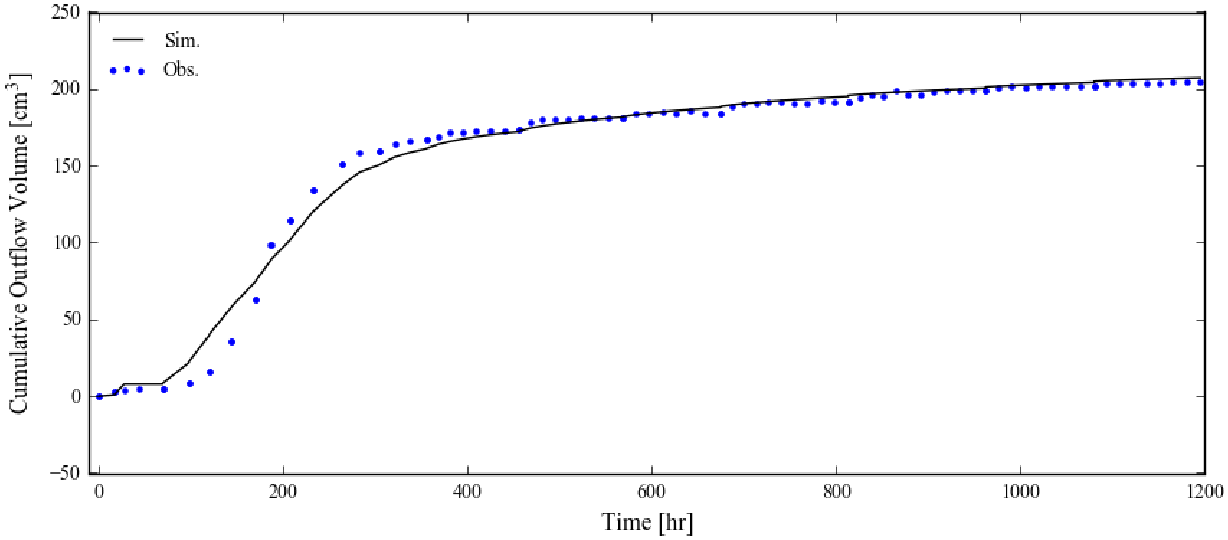

Figure E.11. Simulated and observed cumulative outflow data for core B488V7-C, using only outflow data for fitting.

E.3.2 B488Y3-G

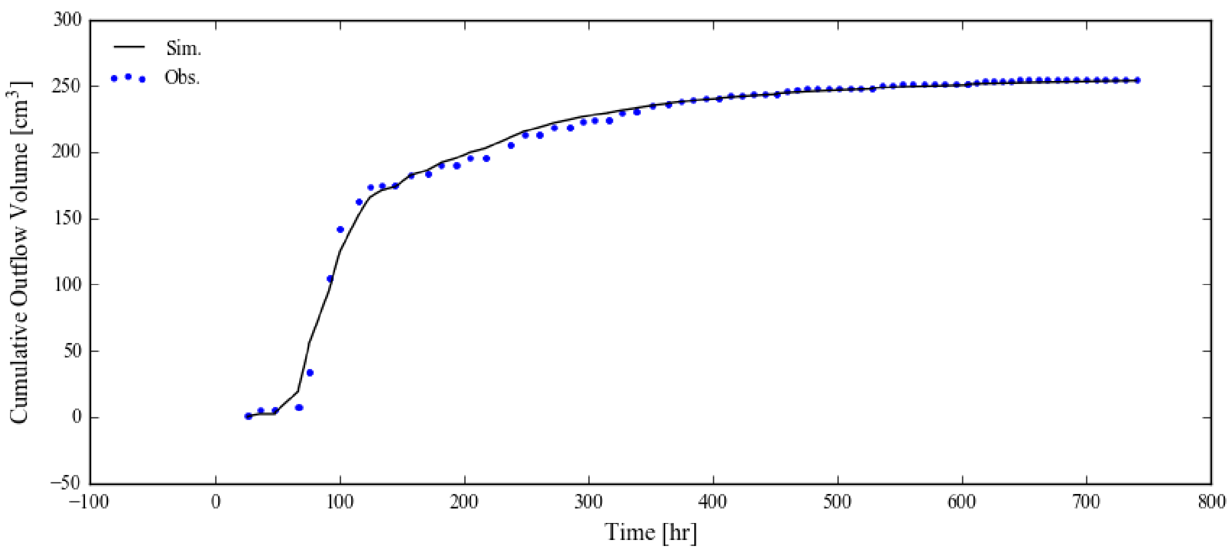

Figure E.12. Simulated and observed cumulative outflow data for core B488Y3, using outflow data only for fitting.

E.3.3 B488Y4-C

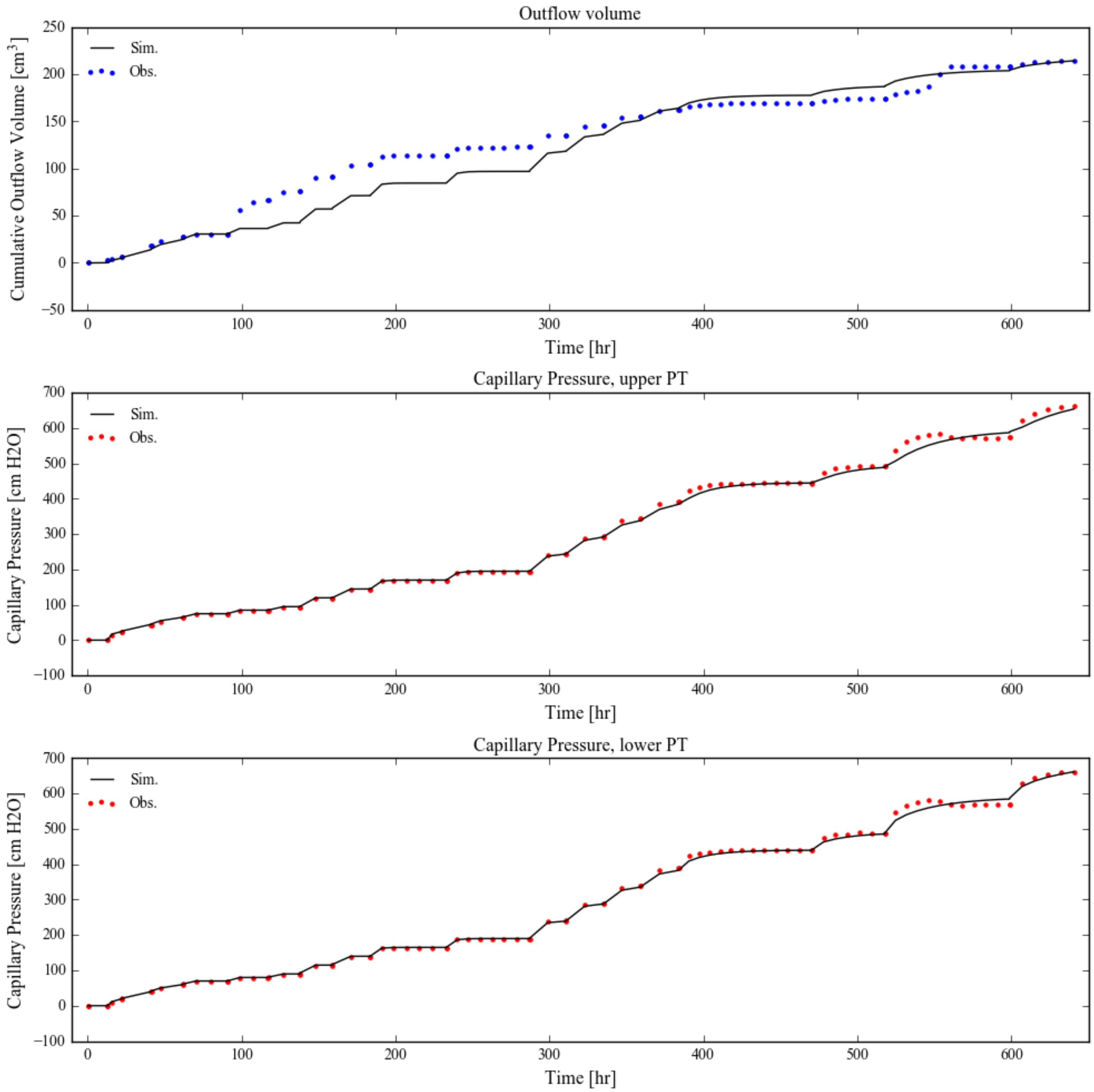

Figure E.13. Simulated and observed cumulative outflow and capillary pressure data for core B488Y4, using both pressure and outflow data for fitting.

E.3.4 B488W5-D

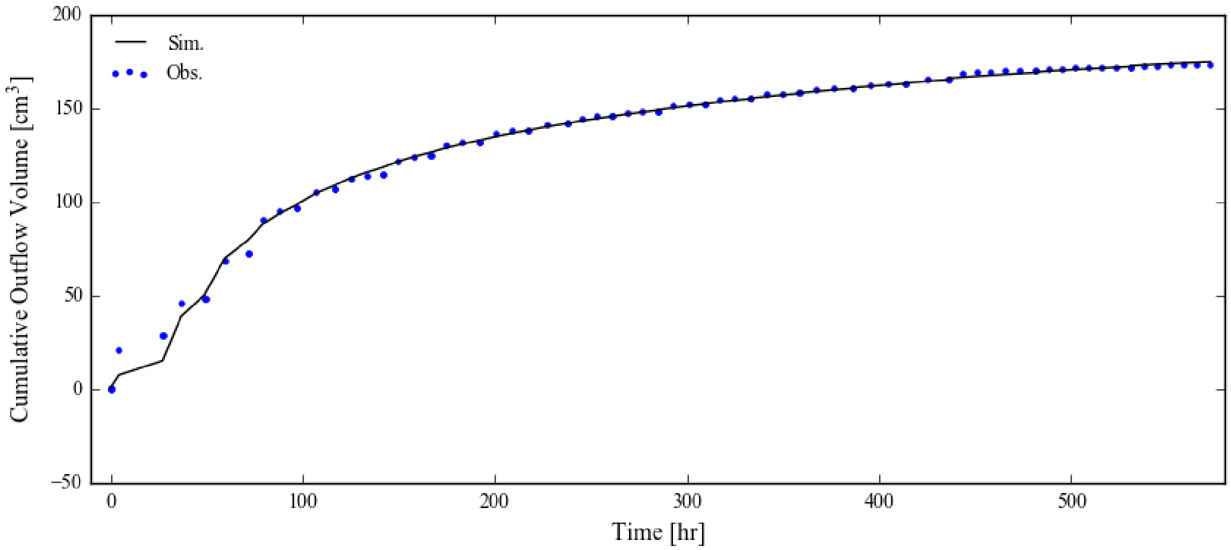

Figure E.14. Simulated and observed cumulative outflow data for core B488W5-D, using outflow data only for fitting.

E.3.5 B488W7-B

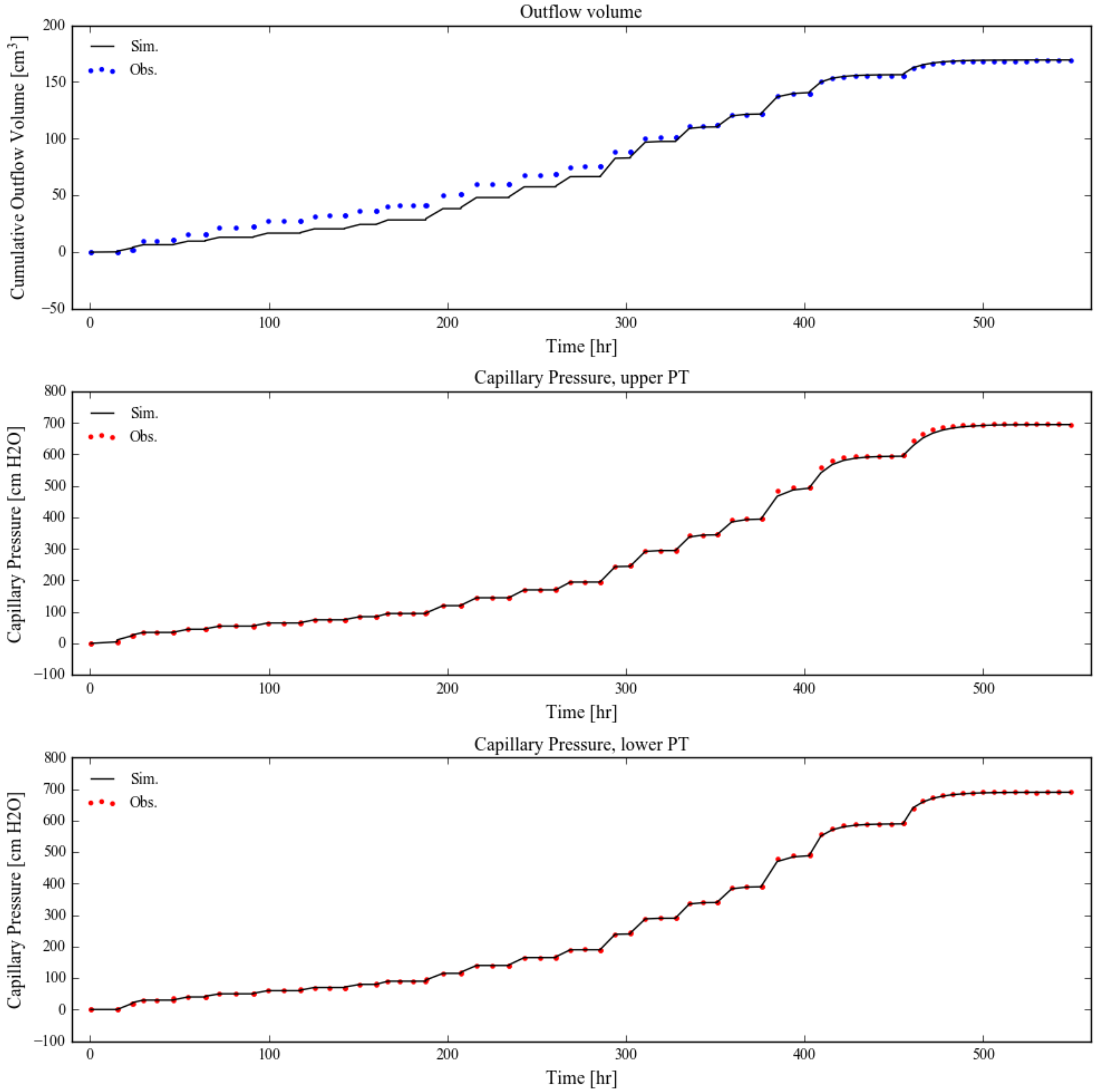

Figure E.15. Simulated and observed cumulative outflow and capillary pressure data for core B488W7-B, using both pressure and outflow data for fitting.

E.3.6 B48N72-B

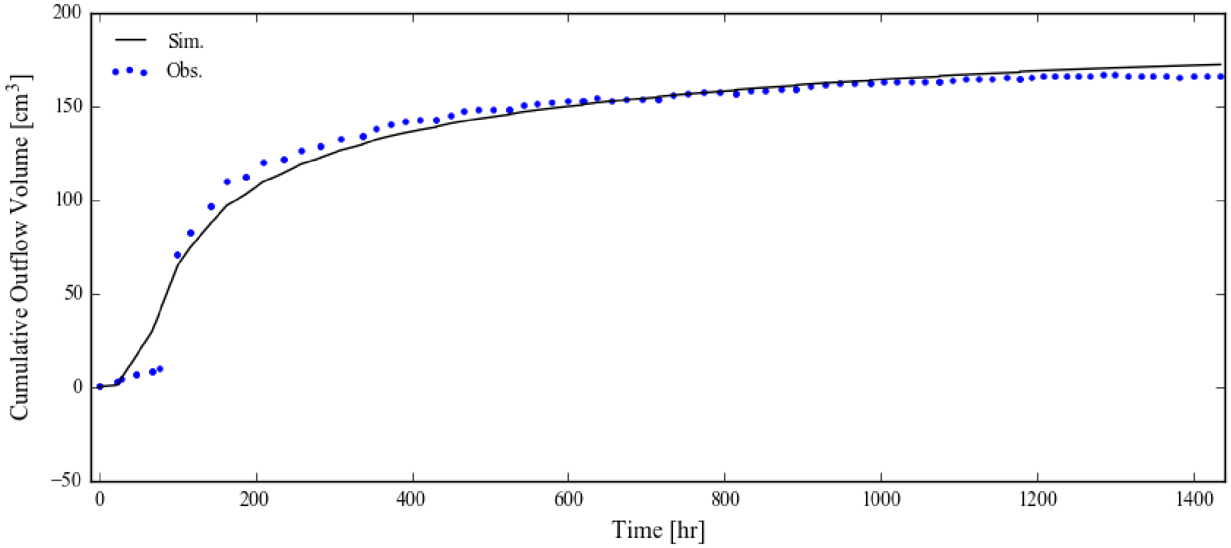

Figure E.16. Simulated and observed cumulative outflow data for core B48N72-B, using outflow data only for fitting.

E.3.7 B48N73-B

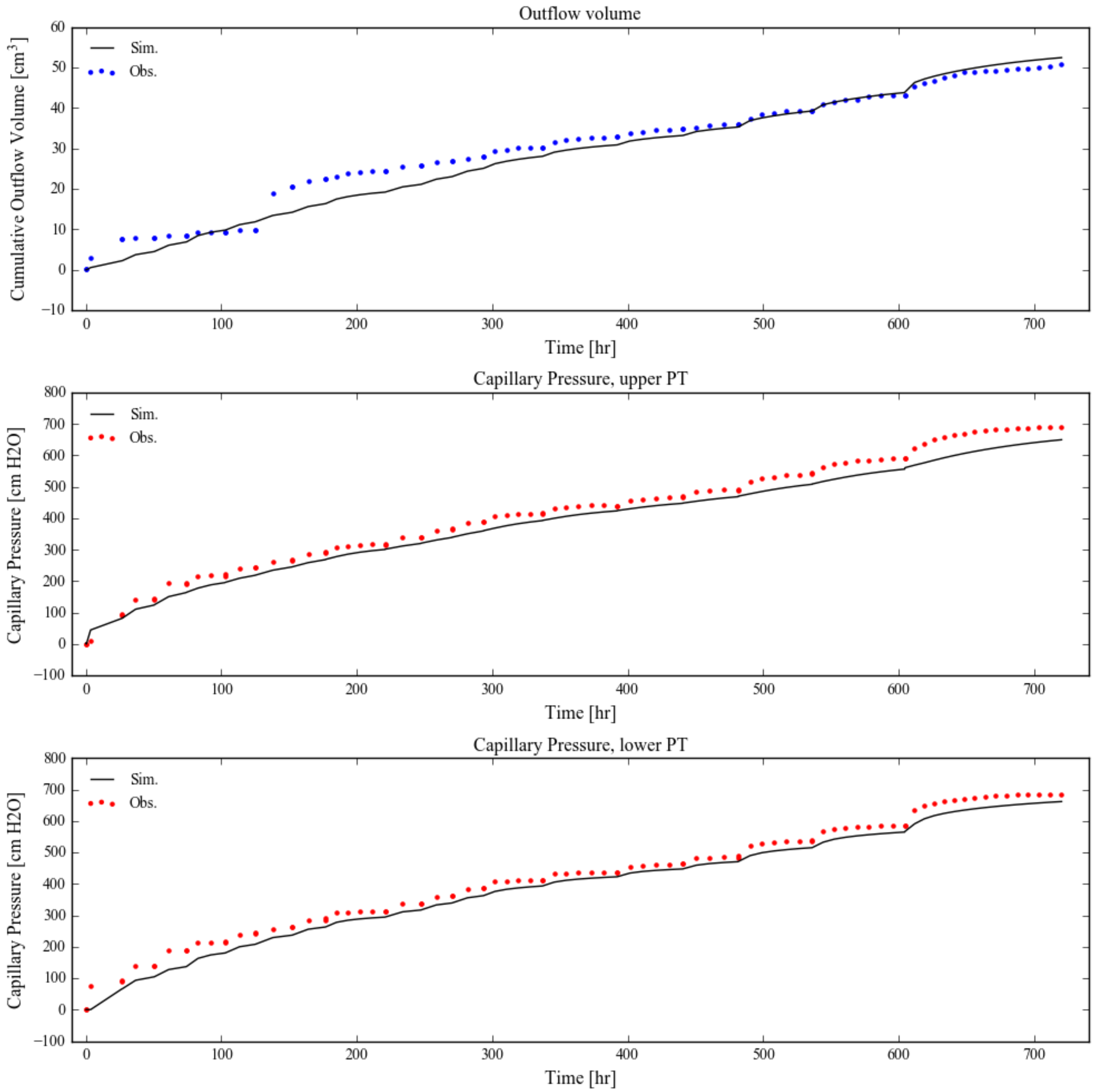

Figure E.17. Simulated and observed cumulative outflow and capillary pressure data for core B48N73-B, using both pressure and outflow data for fitting.

E.3.8 B48N74-I

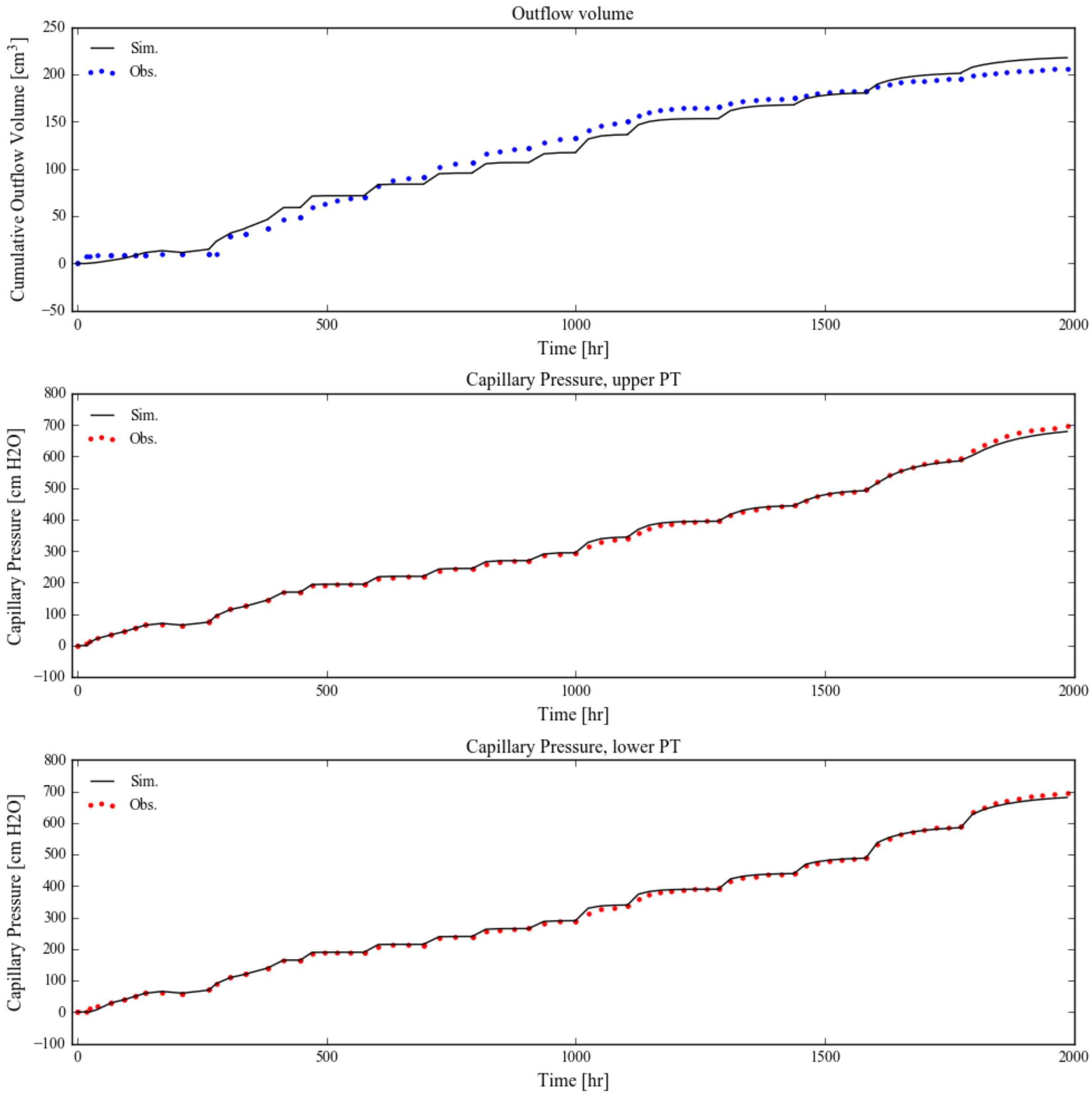

Figure E.18. Simulated and observed cumulative outflow and capillary pressure data for core B48N74-I, using both pressure and outflow data for fitting.

E.3.9 B48N76-H

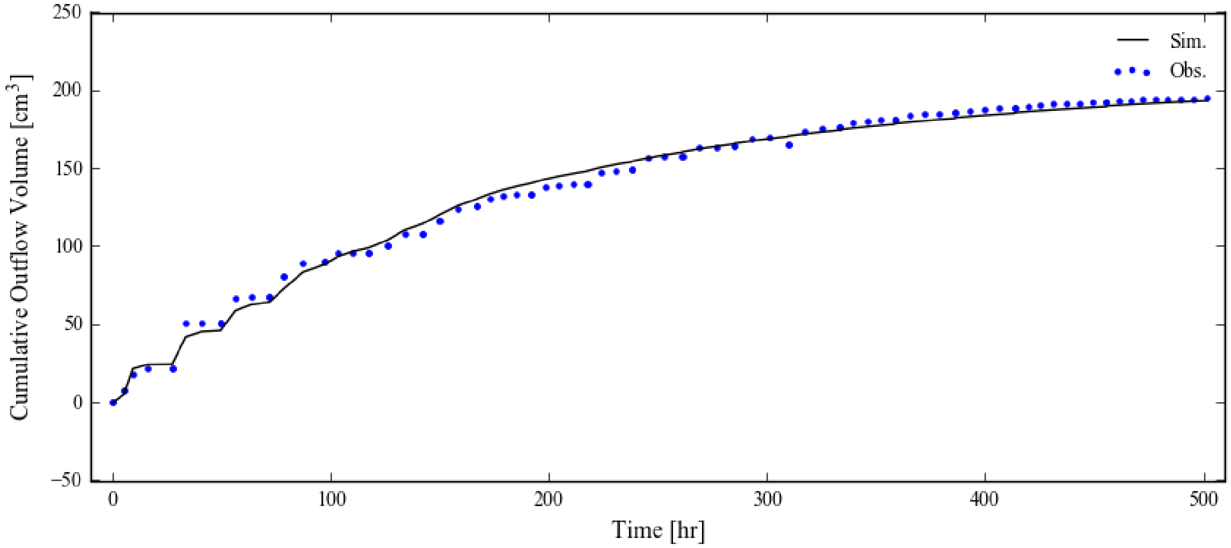

Figure E.19. Simulated and observed cumulative outflow data for core B48N76-H, using outflow data only for fitting.

E.3.10 B48N79-B

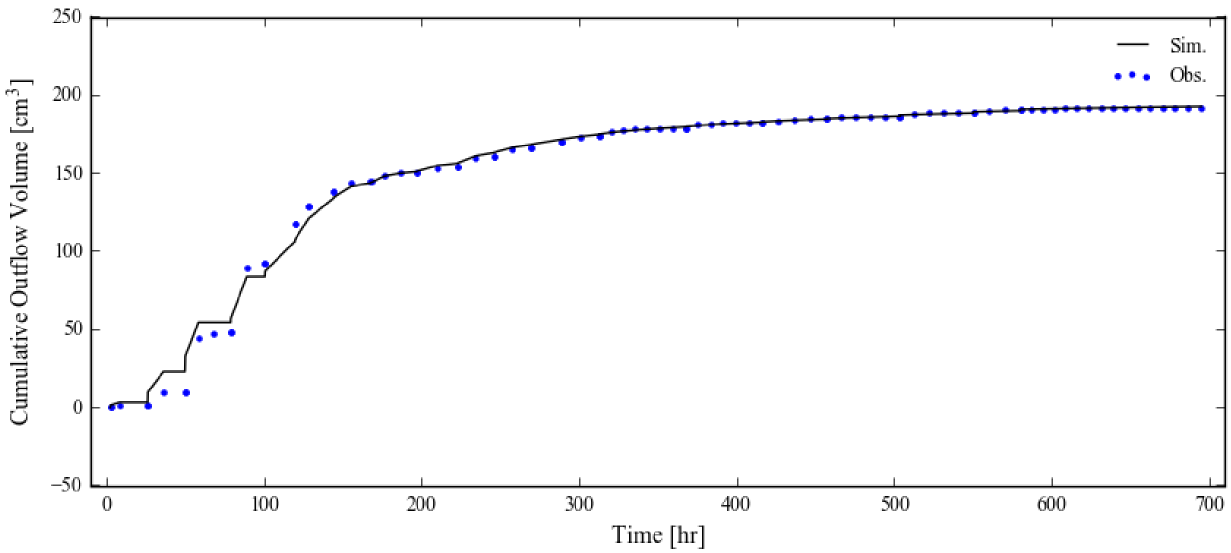

Figure E.20. Simulated and observed cumulative outflow data for core B48N79-B, using outflow data only for fitting.

E.3.11 B48ND9-B

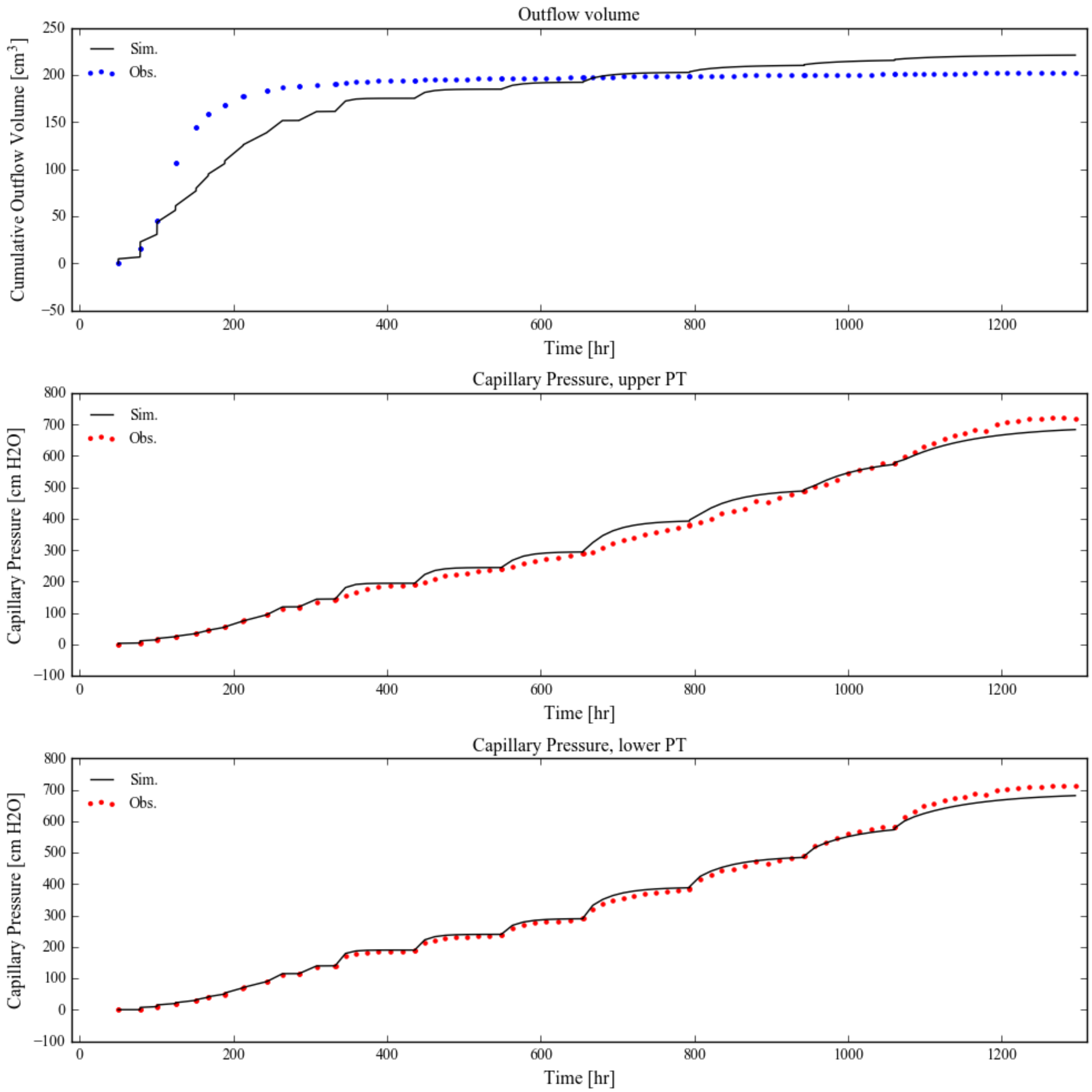

Figure E.21. Simulated and observed cumulative outflow and capillary pressure data for core B48ND9-B, using both pressure and outflow data for fitting.

E.3.12 B48NF4-C

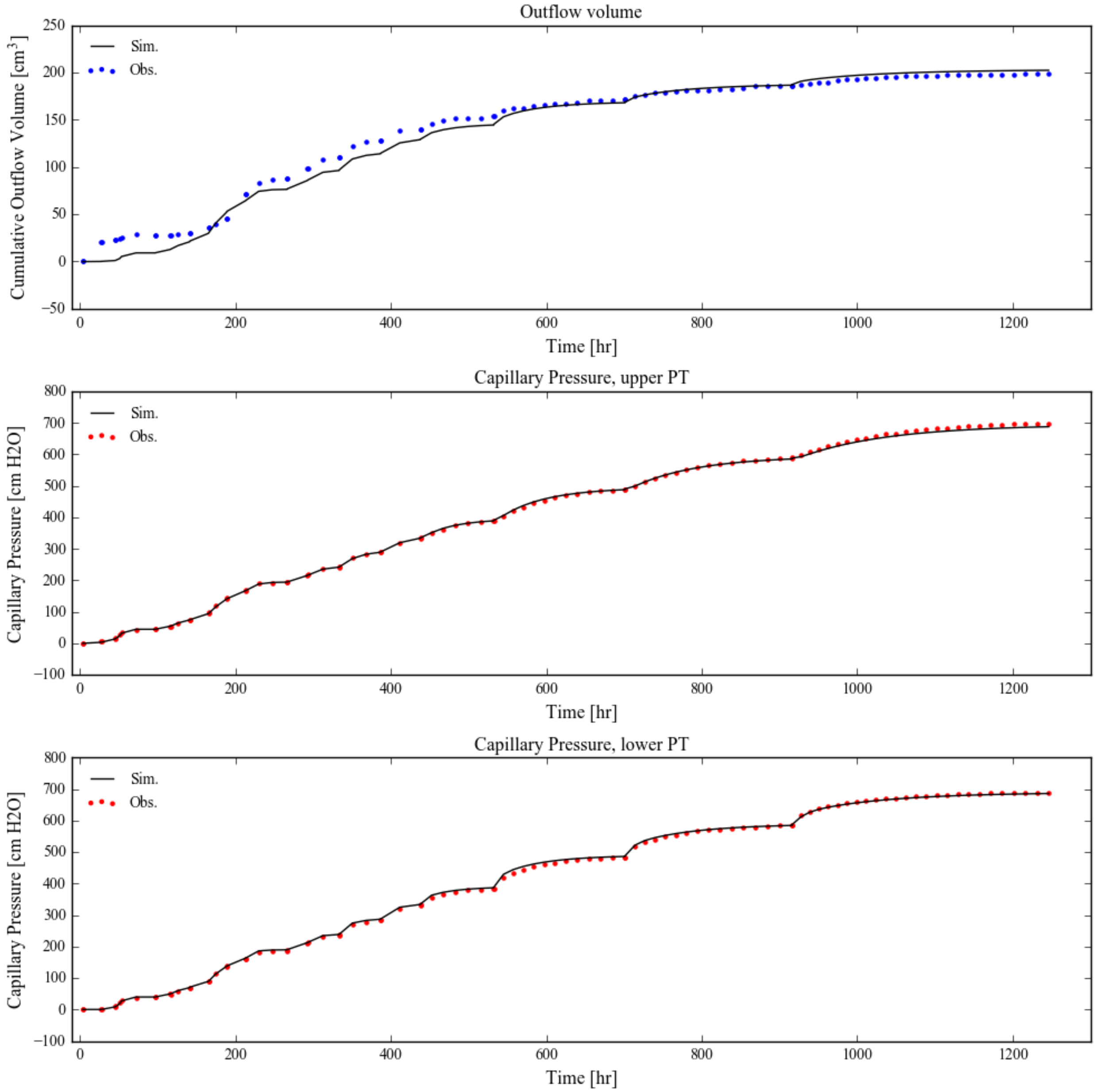

Figure E.22. Simulated and observed cumulative outflow and capillary pressure data for core B48NF4-C, using both pressure and outflow data for fitting.

E.3.13 B48NH0-H

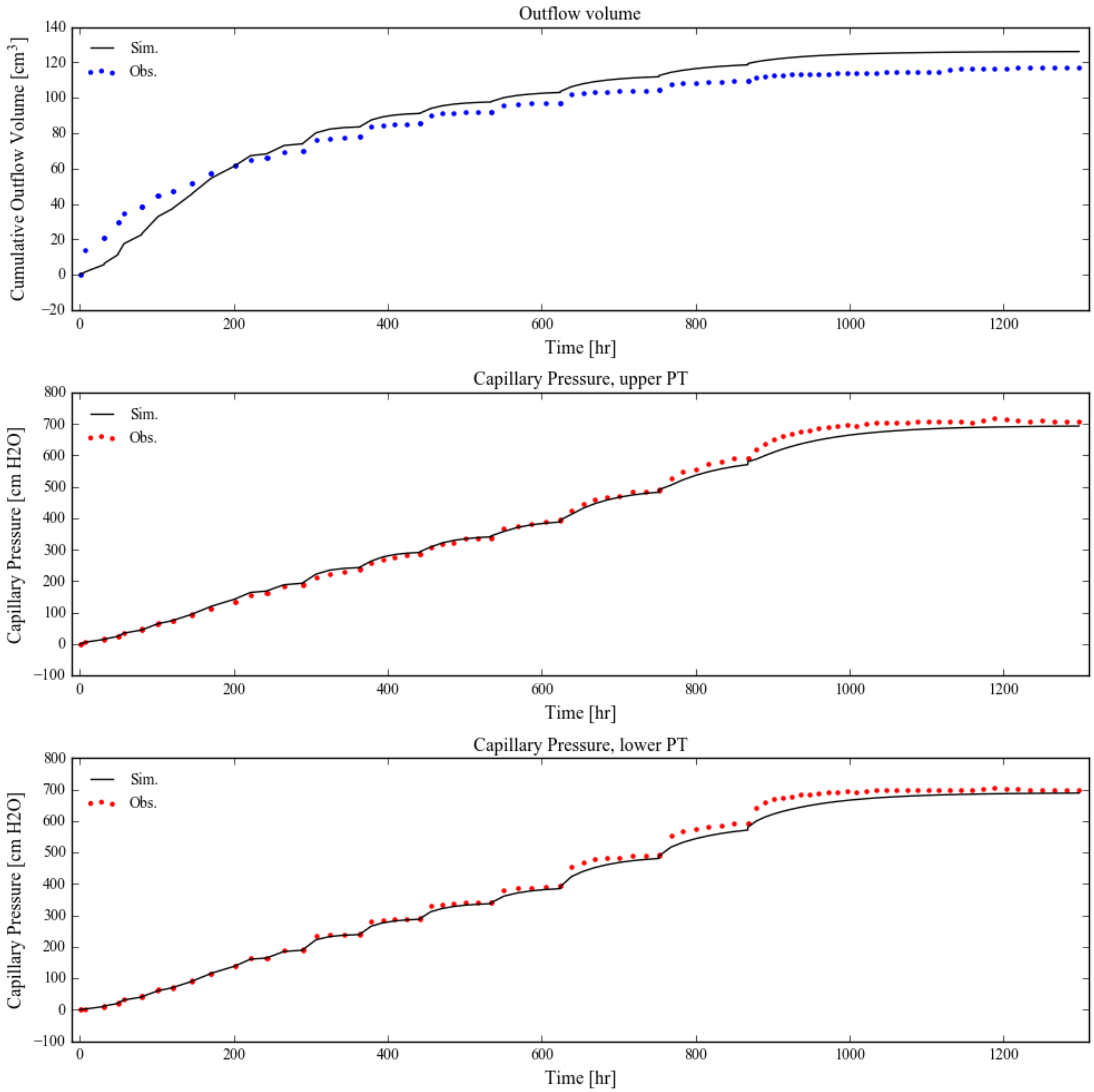

Figure E.23. Simulated and observed cumulative outflow and capillary pressure data for core B48NH0-H, using both pressure and outflow data for fitting.

E.3.14 B48NH0-I

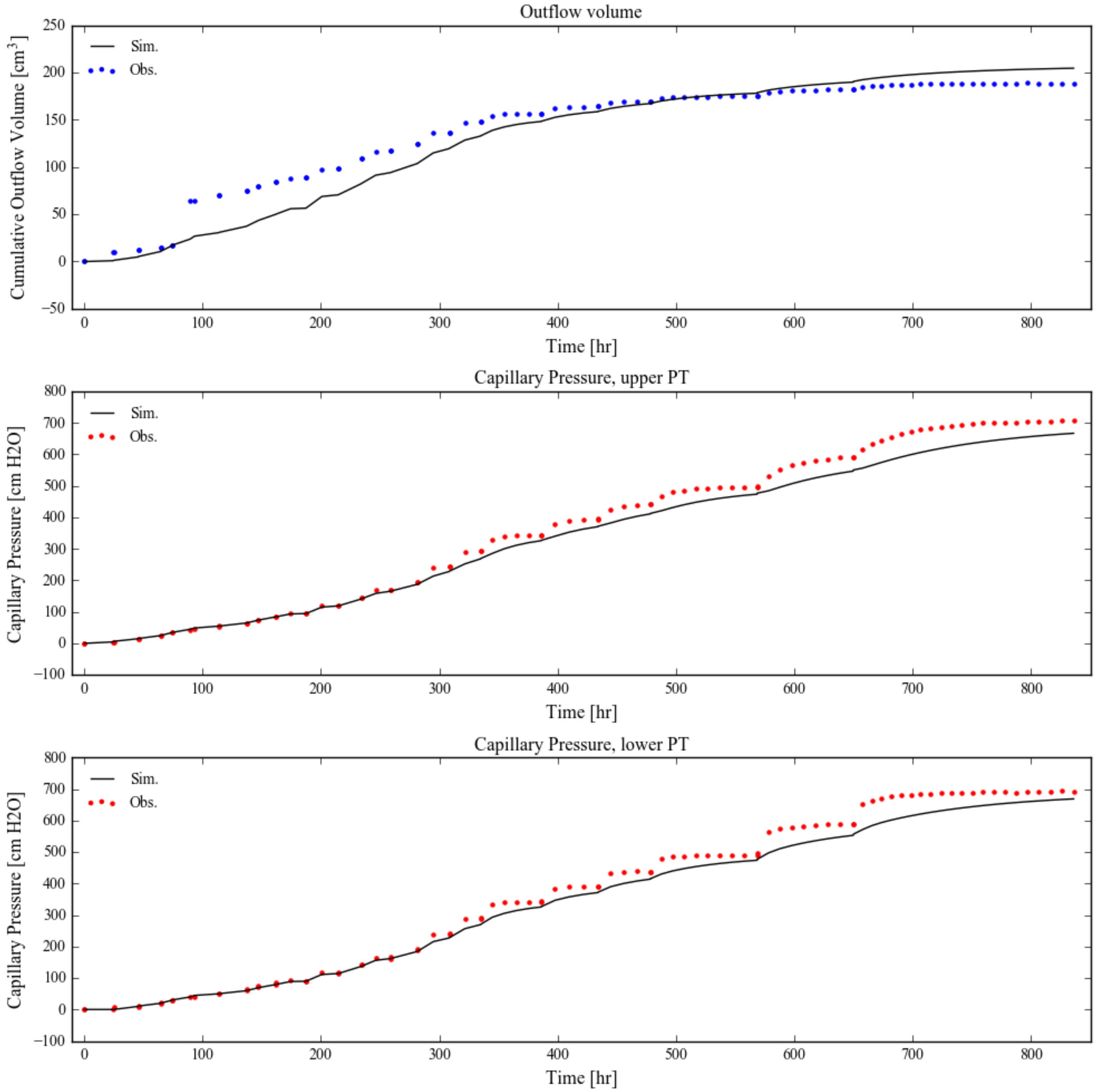

Figure E.24. Simulated and observed cumulative outflow and capillary pressure data for core B48NH0-I, using both pressure and outflow data for fitting.

Appendix F – Summary Tables of Characterization Data Collected on Core Samples

Table F.1. Summary table of characterization data collected on core samples. XCT = X-Ray computed tomography, MP = matric potential, GMC = gravimetric moisture content, PSA = particle size analysis, DBD = dry bulk density, K = hydraulic conductivity (Ksat and multistep outflow data). An 'x' indicates that measurements were performed for the listed data type.

#	Sample ID	Area	Unit	XCT	XCT Evaluation	MP	GMC	PSA	DBD	K
1	B40DC4	200E	CCUg	x	Too coarse for intact core MS	x	x	x	x	
2	B41802	200E	Hf1	x	Suitable for intact core MS	x	x	x	x	x
3	B41806	200E	Hf3	x	Too coarse for intact core MS	x	x	x	x	
4	B41807	200E	Hf3	x	Too coarse for intact core MS	x	x	x		
5	B41809	200E	CCU	x	Too coarse for intact core MS	x	x	x	x	
6	B41868	200E	Hf3	x	Too coarse for intact core MS	x	x	x		
7	B418C0	200E	CCU	x	Too coarse for intact core MS	x	x	x	x	
8	B418C2	200E	CCU	x	Too coarse for intact core MS	x	x	x	x	
9	B3YK00	200E	CCUg	x	Too coarse for intact core MS	x	x	x		
10	B3YJY6	200E	Hf3	x	Suitable for intact core MS			x	x	x
11	B3YJY7	200E	CCU	x	Suitable for intact core MS			x	x	x
12	B3YJY8	200E	CCUg	x	Too coarse for intact core MS	x	x	x		

13	B3YJY9	200E	CCUg	x	Too coarse for intact core MS	x	x	x		
14	B3YJX6	200E	Hf1	x	Workable	x	x	x		
15	B3YJY5	200E	Hf3	x	Workable	x	x	x	x	x
16	B3YJX1	200E	CCU	x	Suitable for intact core MS	x	x	x	x	
17	B3YJX2	200E	CCU	x	Suitable for intact core MS			x	x	x
18	B3YJD8	200E	Hf1	x	Too coarse for intact core MS	x	x	x		
19	B3YJD9	200E	Hf1	x	Too coarse for intact core MS	x	x	x	x	
20	B3YJF9	200E	CCU	x	Suitable for intact core MS			x	x	x
21	B3YJH0	200E	CCUg	x	Suitable for intact core MS			x	x	x
22	B3YJH1	200E	CCUg	x	Workable	x	x	x	x	
23	B3YJH2	200E	CCUg	x	Too coarse for intact core MS	x	x	x	x	
24	B3YJH3	200E	CCUg	x	Workable	x	x	x	x	
25	B3YJF8	200E	Hf3/CCU			x	x	x	x	
26	Composite 1	200E	Hf3					x	x	x
27	Composite 2	200E	CCUg					x	x	x
28	Composite 3	200E	CCUg					x	x	x
29	B344V3-A	200W	Hf1	x	Too coarse and liner not full	x	x	x		
30	B488V7-C	200W	Hf2	x	Suitable for intact core MS	x	x	x	x	x
31	B488Y1-H	200W	CCU/CCUc	x	Too coarse and loosely packed	x	x	x		

32	B488Y3-G	200W	CCUc	x	Workable	x	x	x	x	x
33	B488Y4-C	200W	CCUc	x	Suitable for intact core MS	x	x	x	x	x
34	B488W5-D	200W	Rwie	x	Suitable for intact core MS	x	x	x	x	x
35	B488W7-B	200W	Rwie	x	Workable	x	x	x	x	x
36	B488X2-B	200W	Hf1	x	Too coarse and loosely packed	x	x	x		
37	B48N72-B	200W	Hf2	x	Suitable for intact core MS	x	x	x	x	x
38	B48N73-B	200W	CCU	x	Suitable for intact core MS	x	x	x	x	x
39	B48N74-I	200W	CCU	x	Suitable for intact core MS	x		x	x	x
40	B48N76-H	200W	CCUc	x	Suitable for intact core MS	x	x	x	x	x
41	B48N79-B	200W	Rwie	x	Workable	x	x	x	x	x
42	B48ND9-B	200W	Hf2	x	Suitable for intact core MS	x	x	x	x	x
43	B48ND9-D	200W	Hf2	x	Too coarse intact core MS	x	x	x	x	
44	B48NF4-C	200W	Hf2	x	Suitable for intact core MS	x	x	x	x	x
45	B48NH0-H	200W	CCUc	x	Workable	x	x	x	x	x
46	B48NH0-I	200W	CCUs	x	Workable	x	x	x	x	x
47	B48NH7-C	200W	Rwie	x	Too coarse for intact core MS	x	x	x	x	

Table F.2. Number of core samples analyzed for each characterization data type

Hanford Area	XCT	MP	GMC	PSA	DBD	K
200E	24	20	20	28	21	10
200W	19	19	18	19	16	14
Total	**43**	**39**	**38**	**47**	**37**	**24**

Pacific Northwest National Laboratory

902 Battelle Boulevard
P.O. Box 999
Richland, WA 99354
1-888-375-PNNL (7665)

www.pnnl.gov